AN INVESTIGATION INTO THE SYNAPTIC CONDITIONS AND CELLULAR MECHANISMS UNDERLYING CEREBELLAR SYNAPTIC PLASTICITY

JULIA KATE SUTTON

Doctor of Philosophy

ASTON UNIVERSITY

December 1999

ASTON UNIVERSITY

AN INVESTIGATION INTO THE SYNAPTIC CONDITIONS AND CELLULAR MECHANISMS UNDERLYING CEREBELLAR SYNAPTIC PLASTICITY

Julia Kate Sutton, December 1999, Thesis submitted for the degree of: Doctor of Philosophy

The direction of synaptic plasticity at the connection between parallel fibres (PFs) and Purkinje cells can be modified by PF stimulation alone. Strong activation (Hartell, 1996) or high frequency stimulation (Schreurs and Alkon, 1993) of PFs induced a long-term depression (LTD) of PF-mediated excitatory postsynaptic currents. Brief raised frequency molecular layer stimulation produced a cAMP-dependent long-term potentiation (LTP) of field potential (FP) responses (Salin et al., 1996).

Thin slices of cerebellar vermis were prepared from 14-21 day old male Wistar rats decapitated under Halothane anaesthesia. FPs were recorded from the Purkinje cell layer in response to alternate 0.2Hz activation of stimulating electrodes placed in the molecular layer. In the presence of picrotoxin, FPs displayed two tetrodotoxin-sensitive, negative-going components termed N1 and N2. FPs were graded responses with paired pulse facilitation and were selectively blocked by 10μM 6-cyano-7-nitroquinoxaline-2,3-dione (CNQX) an antagonist at α-amino-3-hydroxy-5-methyl-4-isoxazolepropionate-type ionotropic glutamate receptors (AMPAR) suggesting that they were primarily PF-mediated.

The effects of raised stimulus intensity (RS) and/or increased frequency (IF) activation of the molecular layer on FP responses were examined. In sagittal and transverse slices combined RS and IF molecular layer activation induced a LTD of the N2 component of FP responses. RSIF stimulation produced fewer incidences of LTD in sagittal slices when an inhibitor of nitric oxide synthase (NOS), guanylate cyclase (GC), protein kinase G (PKG) or the $GABA_B$ receptor antagonist CGP62349 was included into the perfusion medium.

Application of a nitric oxide (NO) donor, a cyclic guanosine monophosphate (cGMP) analogue or a phosphodiesterase (PDE) type V inhibitor to prevent cGMP breakdown paired with IF stimulation produced an acute depression.

Raised frequency (RF) molecular layer stimulation produced a slowly emerging LTD of N2 in sagittal slices that was largely blocked in the presence of NOS, cGMP or PKG inhibitors. In transverse slices RF stimulation produced a LTP of the N2 component that was prevented by an inhibitor of protein kinase A or NOS. Inhibition of cGMP-signalling frequently revealed an underlying potentiation suggesting that cGMP activity might mask the effects of cAMP. In sagittal slices RF stimulation resulted in a potentiation of FPs when the cAMP-specific PDE type IV inhibitor rolipram was incorporated into the perfusion medium.

In summary, raised levels of PF stimulation can alter the synaptic efficacy at PF-Purkinje cell synapses. The results provide support for a role of NO/cGMP/PKG signalling in the induction of LTD in the cerebellar cortex and suggest that activation of $GABA_B$ receptors might also be important. The level of cyclic nucleotide-specific PDE activities may be crucial in determining the level of cGMP and cAMP activity and hence the direction of synaptic plasticity.

Hartell, N.A. (1996). Strong activation of parallel fibers produces localized calcium transients and a form of LTD that spreads to distant synapses. Neuron *16*, 601-610.

Salin, P.A., Malenka, R.C., and Nicoll, R.A. (1996). Cyclic-AMP mediates a presynaptic form of LTP at cerebellar parallel fiber synapses. Neuron *16*, 797-803.

Schreurs, B.G. and Alkon, D.L. (1993). Rabbit cerebellar slice analysis of long-term depression and its role in classical conditioning. Brain Res. *631*, 23-240.

Keywords: LTD, LTP, Extracellular, Field potential recording, Phosphodiesterases.

ACKNOWLEDGEMENTS

I would first like to acknowledge my supervisor Dr N A Hartell for giving me technical advice during my PhD, for taking the time to read my PhD thesis and for providing suggestions as to how the work could be improved.

I also wish to thank Mr Steve Wells, Mr Mel Gamble and Mr Alan Richardson for their technical support.

I would like to thank Dr P Ellis of Pfizer Limited for generously supplying UK114-542-27, for providing some information about its properties and for reading chapter 4 which relates to the use of the compound.

I extend my thanks to Mr John Bailey and Professor Ian Martin for giving me the confidence to persevere in the final stages of the project.

And last but not least a big thank you to my family, Miss Fiona Salvage and to Mr James McGough for giving me support and encouragement throughout the challenges of my PhD.

CONTENTS

LIST OF FIGURES

ABBREVIATIONS

AC	Adenylate cyclase
Trans-ACPD	A racemic mixture of 1S,3R- and 1R,3S-1-aminocyclopentane-1,3-dicarboxylic acid
ACSF	Artificial cerebrospinal fluid
5'-AMP	Adenosine-5'-monophosphate
AMPA	α-Amino-3-hydroxy-5-methyl-4-isoxazole-4-propionic acid
AMPAR	α-Amino-3-hydroxy-5-methyl-4-isoxazole-4-propionic acid – type ionotropic glutamate receptor
ATP	Adenosine triphosphate
3-AP	3-acetylpyridine
Baclofen	(+) or (-) β-p-chlorophenyl GABA
BAPTA	Bis(2-aminophenoxy)ethane-N,N,N'N'-tetraacetate
BH_4	Tetrahydrobiopterin
8-Br-cGMP	8-Bromoguanosine cyclic 3'5'-monophosphate sodium salt
BRF	Brief raised frequency
cADPR	Cyclic adenosine diphosphate ribose
cAMP	Cyclic adenosine monophosphate
CNO-4	Acetic acid,2,2'-[[(3,3-diethyl-1-triazenyl)oxy]methyl]-5-nitro-1,2-phenylene]bis(oxy)]bis(oxy)]bis-,N-oxide
CNQX	6-cyano-7-nitroquinoxaline-2,3-dione
CNS	Central nervous system
cGMP	Cyclic guanosine monophosphate
CF	Climbing fibre
CR	Conditioned response
CREB	cAMP response element binding protein
CS	Conditioned stimulus
DAG	Diacylglyerol

DMSO	Dimethylsulphoxide
EBC	Eye blink conditioning
EGTA	Ethylene glycol-bis(β-aminoethyl ether)-N,N,N'N'-tetraacetic acid
EPSC	Excitatory postsynaptic currents
EPSP	Excitatory postsynaptic potentials
FP	Field potential
GABA	γ-aminobutryic acid
$GABA_AR$	γ-aminobutryic acid type A receptor
$GABA_BR$	γ-aminobutryic acid type B receptor
GC	Guanylate cyclase
GFAP	Glial fibrillary acidic protein
5'-GMP	Guanosine-5'-monophosphate
G-protein	Guanine-nucleotide binding protein
GTP	Guanosine triphosphate
H-89	N-[2-bromocinnamyl(amino)ethyl]-5-isoquinolinesulfonamide
IF	Increased frequency
L-NAME	N(G)-nitro-L-arginine methyl ester hydrochloride
IP_3	Inositol triphosphate
LTD	Long term depression
LTP	Long term potentiation
MCPG	α-methyl-4-carboxyphenylglycine
mGluR	Metabotropic glutamate receptor
mGluR1	Metabotropic glutamate receptor type I receptor
7-NI	7-nitroindazole
NADPH	Nicotinamide adenine dinucleotide phosphate
NC	No change
NMDAR	N-methyl-D-aspartate – type ionotropic glutamate receptors
NO	Nitric oxide
NO^+	Nitrosonium ion
NOS	Nitric oxide synthase
ODQ	1H-[1,2,4]Oxadiazolo[4,3-a]quinoxalin-1-one

PDE	Phosphodiesterases
PF	Parallel fibre
PIP_2	Phosphatidylinositolbisphosphate
PKA	Protein kinase A
PKC	Protein kinase C
PKG	Protein kinase G
PLA_2	Phospholipase A_2
PLC	Phospholiipase C
PP	Protein phosphatase
PPR	Paired pulse ratio
PTK	Protein tyrosine kinase
Rolipram	4-[3-(Cyclopentyloxy)-4-methoxyphenyl]-2-pyrrolidinone
RF	Raised frequency
RS	Raised stimulus intensity
RSIF	Raised stimulus intensity and increased frequency
SNAP	S-nitroso-penicillamine
SNP	Sodium nitroprusside
TTX	Tetrodotoxin
UR	Unconditioned response
US	Unconditioned stimulus
VOR	Vestibular occular reflex

CHAPTER 1

GENERAL INTRODUCTION

1.1 THE ANATOMICAL STRUCTURE AND THE CELL POPULATIONS OF THE CEREBELLAR CORTEX

The cerebellum, which derives its name from the Latin word 'little brain', comprises approximately 10% of the total volume of the human brain (Sutton, 1971; Nolte, 1988). It is a mass of nervous tissue that covers most of the posterior surface of the brainstem. The cerebellum receives sensory information and projects it via cerebellar nuclei to sites in the brainstem and thalamus (Nolte, 1988). The cerebellum has an outer cortex composed of grey matter and an inner cortex of white matter. The grey matter consists of neuronal cell bodies, dendrites and glial cells and the white matter contains myelinated nerve fibres (Nolte, 1988).

In mammals the surface of the cerebellum has folds which are known as folia. In the anterior region transverse grooves or fissures extend to the lateral edge of the cerebellum (Voogd and Glickstein, 1998). In sagittal slices the appearance of the cerebellar surface has many cortical ridges. Deep fissures indent the cerebellar surface and smaller fissures indent the walls of these deep fissures. During development the first fissure to appear is the posterolateral fissure, which separates the flocculonodular lobe from the corpus cerebelli. The primary fissure then subdivides the corpus cerebelli into anterior and posterior lobules (Voogd, 1992).

The cerebellum is also divided into longitudinal zones perpendicular to the fissures that cut across the anterior, posterior and flocculonodular lobes. The middle zone is the vermis

which has a large cerebellar hemisphere on either side (Sutton, 1971; Nolte, 1988). There is a shallow groove that contains the paravermal vein which helps to distinguish the division between the central vermis and the two hemispheres (Voogd and Glickstein, 1998).

The cerebellar cortex is made up of three layers, the outer molecular layer, the Purkinje cell layer and the inner granular layer. The outer molecular layer contains inhibitory stellate and basket cells. The neurotransmitter of basket and stellate cells is γ-aminobutyric acid (GABA). These interneurons synapse with the cell body and dendrites of Purkinje cells, respectively (as discussed in, Eccles et al., 1967a; Palay and Chan-Palay, 1974; Nolte, 1988).

The Purkinje cell layer contains Purkinje cells that have large cell bodies, which are spaced, at a distance of two or three diameters apart; their extensive dendritic tree extends into the molecular layer (Sutton, 1971). The granule cell layer contains large numbers of small granule cells and fewer golgi cells (Sutton, 1971). Each granule cell bifurcates and extends two axons known as the parallel fibres (PFs, Eccles et al., 1967a; see also, Palay and Chan-Palay, 1974). During development the actively growing PF axons are found closest to the pial surface of the cerebellum and the more mature ones lie deeper within the molecular layer (Liljelund and Levine, 1998). Studies of PF growth cones have provided evidence that PF axons extend in a straight pathway and give rise to few branches (Liljelund and Levine, 1998). In the molecular layer the cell bodies of Bergmann glia are found in between the dendrites of Purkinje cells (Voogd and Glickstein, 1998). The Purkinje cells receive two distinct excitatory inputs; one is from the axons of granule cells and the other is from the axons of inferior olive neurons known as climbing fibres (CFs). One hundred thousand or more different PFs synapse upon a single Purkinje cell. Each PF may, in turn, terminate on one thousand or more different Purkinje cells (Eccles et al., 1967a; Palay and Chan-Palay, 1974). In contrast, a single CF ends directly on each Purkinje cell and winds around the proximal portion of its dendrites (Eccles et al., 1967a). Mossy fibres originating from vestibular nerves and nuclei, the spinal cord and the cerebral cortex terminate on the dendrites of granule cells therefore they provide an indirect connection to the Purkinje cells (Eccles et al., 1967b; see also, Nolte, 1988).

The cerebellar molecular layer where PFs interact with the Purkinje cell dendrites has a 2-dimensional organisation in which the PFs are orientated in the transverse plane and the dendritic field of Purkinje cells is orientated in the sagittal plane. The unique structure of the cerebellum makes it difficult to prepare cerebellar slices that do not damage either Purkinje cell dendrites or truncate PFs. The inferior olive is composed of subdivisions. The CFs from one of these divisions terminate in the cerebellar cortex in sagittally orientated zones (Oscarsson, 1979). Purkinje cells within a particular sagittal zone project to one cerebellar nucleus which receives inputs from inferior olive axons that terminate as CFs in that zone (Voogd, 1992; Simpson et al., 1996). The sagittal zones can be further divided into microzones (Andersson and Oscarsson, 1978).

A selective chemical lesion of the inferior olive that was produced by the administration of 3-acetylpyridine (3-AP) resulted in ataxia, shaky movement and an unsteady gait in rats (Llinas et al., 1975). This suggested that the inferior olive was important for compensating for abnormalities in motor tasks.

1.2 SYNAPTIC PLASTICITY AND MOTOR LEARNING

In his book that was titled 'The Organisation of Behaviour' which was first published in the 1940s Donald Hebb proposed how the mammalian brain could store memories. He suggested that the association of presynaptic and postsynaptic activity in two neurons could elicit a change such that the synaptic connection between them was strengthened (Hebb, 1949). The idea of Hebbian synapses is widely known and for the last 50 years has been considered as a possible process by which memories could be formed and stored (see for example, Brown et al., 1990; Lechner and Byrne, 1998; Sejnowski, 1999). Synaptic plasticity refers to a change in the strength of transmission at a given synapse. The presence of synaptic plasticity in the cerebellum was theoretically proposed (Marr, 1969; Albus, 1971) and later, discovered in the cerebellum (Ito et al., 1982). A number of groups have tried to establish if long-term synaptic plasticity is the cellular mechanism for memory

formation (see for example, Thompson, 1986; for reviews see, Ito, 1989; Bliss and Collingridge, 1993; Maren and Baudry, 1995; Milner et al., 1998)

In the dentate area of the hippocampus in rabbits, high frequency stimulation of perforant path fibres produced a facilitation of the population responses recorded from granule cells. This phenomenon was termed long term potentiation (LTP, Bliss and Lomo, 1973). Only those inputs that were activated during the tetanus were potentiated and so the LTP was described as being input-specific. The strength of tetanic stimuli had to reach an intensity threshold in order for the LTP to be induced. In addition, the strength of synaptic transmission was only enhanced if both presynaptic and postsynaptic components of the synapse were active at the same time; this form of LTP is termed associative (see Bliss and Collingridge, 1993 for a review).

In 1982 a persistent decrease of the strength of PF to Purkinje cell synaptic transmission was produced by conjunctive stimulation of the PF and CF inputs to Purkinje cells in the rabbit cerebellum which was termed long term depression or LTD (Ito and Kano, 1982). This form of LTD was also described as being input-specific, that is, restricted to only those PFs active at the time of CF stimulation (Ekerot and Kano, 1985).

In the cerebellum simple behavioural models of motor learning such as the vestibular ocular reflex, (VOR, Ito, 1982; DuLac et al., 1995; Lisberger, 1998) and eyeblink conditioning, (EBC, Houk et al., 1996; Milner et al., 1998) have been used to investigate the importance of LTD in motor learning. The VOR and EBC have quite different properties but are both examples of classical conditioning, that is, they are forms of associative learning which require the pairing or 'association' of two stimuli (see, Thompson et al., 1997; as reviewed by, Milner et al., 1998). In classical conditioning the behavioural response to a conditioned stimulus (CS) becomes altered when the CS is followed by the unconditioned stimulus (US). The result of this pairing is an conditioned response (CR) and a modified response to the CS (Lechner and Byrne, 1998). For example in EBC the CS is an auditory tone and the US is an air puff to the eye. After a period of training the tone will trigger an eyeblink as the CR (Houk et al., 1996).

Bergmann glia surround the dendrites and synapses of Purkinje cells and provide both nutritional and structural support (Eccles et al., 1967a; Palay and Chan-Palay, 1974). Glial fibrillary acidic protein (GFAP) is normally found in Bergmann glia (Wagemann et al., 1995). In GFAP mutant mice, impaired EBC and deficient LTD was observed (Shibuki et al., 1996). The VOR is a motor reflex that induces eye movements that compensate for changes in head position to ensure that during head movement the retinal images remain constant. Acquisition of this reflex is a form of motor learning (Ito, 1982). In transgenic mice protein kinase C (PKC) was blocked in Purkinje cells by specific expression of a PKC inhibitory peptide. LTD was prevented and the adaptation of the VOR was impaired in these mice. No behavioural deficits in general eye movements or in motor performance were noted (DeZeeuw et al., 1998). These observations provide strong support for the requirement of PKC-dependent cerebellar LTD in VOR motor learning. Studies have therefore linked LTD to both VOR and EBC providing strong evidence that LTD subserves these behavioural models of motor learning.

The sequence and timing of CS and US is crucial in classical conditioning. The importance of the time interval between stimulation of CF and PF inputs for the induction of LTD has been investigated. Traditionally it was thought that CF activation should precede PF stimulation in order to induce LTD (Ekerot and Kano, 1985). However, it was reported later that activation of PFs and then CFs in a classical conditioning-like order could also produce a brief depression (Schreurs and Alkon, 1993). In another study the most robust LTD was observed with 300 pulses at 1Hz and was still effective at CF-PF delays of 1 second or longer (Karachot et al., 1995). In an extracellular FP recording study the level of LTD that was measured after 600 pairings at 1Hz did not appear to depend on the temporal order of the PF and CF inputs (Chen and Thompson, 1995).

1.3 THE PHOSPHORYLATION OF AMPA RECEPTORS IN LTD

The α-amino-3-hydroxy-5-methyl-4-isoxazolepropionate-type ionotropic glutamate receptors (AMPAR) mediate fast excitatory synaptic currents at PF-Purkinje cell synapses. A decreased sensitivity of these receptors to glutamate is thought to underlie the expression of

LTD (Hemart et al., 1994; Nakazawa et al., 1998). The finding that application of a potent protein phosphatase (PP) inhibitor, calyculin A, to prevent protein dephosphorylation mimicked the LTD produced by conjunctive stimulation of CF and PF inputs to Purkinje cells suggested that a mechanism involving receptor phosphorylation was necessary for the induction of LTD (Ajima and Ito, 1995). The PP1 and PP2 isoforms of PPs were immunohistochemically localised in the rat cerebellum, the PP1γ1 isoform was found to be dominantly expressed at Purkinje cell synapses (Hashikawa et al., 1995). In the cerebellum, G-substrate that is a specific substrate for cGMP-dependent protein kinase G (PKG) was found to be highly concentrated in Purkinje cells (see review by, Nairn et al., 1985). Recent purification and characterisation of G-substrate showed similarities to existing PP1 inhibitors. The messenger RNA for G-substrate was predominantly localised in cerebellar Purkinje cells (Hall et al., 1999). Together these findings suggest that phosphorylation-dependent inhibition of PP1 by G-substrate could function as a pathway by which PKG regulates the activity of PPs.

1.4 ACTIVATION OF IONOTROPIC AND METABOTROPIC GLUTAMATE RECEPTORS IS NECESSARY FOR LTD

It is well established that LTD is accompanied by a decrease in the responsiveness of Purkinje cells to glutamate (Crepel and Krupa, 1988), quisqualate (Kano and Kato, 1987) and α-amino-3-hydroxy-5-methyl-4-isoxazolepropionate (AMPA, Linden et al., 1991). The excitatory amino acid receptors at PF to Purkinje cell synapses were first characterised using a grease-gap technique. Glutamate was found to activate non-N-methyl-D-aspartate-type ionotropic receptors (NMDAR) at these synapses (Garthwaite and Beaumont, 1989). LTD has been produced by conjunctive iontophoretic application of glutamate and depolarisation strong enough to elicit Purkinje cell spiking (Crepel and Krupa, 1988). This finding suggested that glutamate receptor activation in addition to Ca^{2+} influx was necessary for LTD. In acute slices LTD could not be induced if 6-cyano-7-nitroquinoxaline-2,3-dione (CNQX, Honore et al., 1988) an antagonist at AMPAR was bath applied during a pairing protocol of Ca^{2+} spike firing and PF stimulation (Hemart et al., 1995). In Purkinje cell

cultures application of trans-1-aminocyclopentane-1,3-dicarboxylic acid (trans–ACPD) a selective agonist of metabotropic glutamate receptors (mGluRs) paired with the AMPAR agonist AMPA was effective in eliciting LTD (Linden et al., 1991). The selective mGluR antagonist (RS)-3,5-methyl-4-carboxyphenylglycine (MCPG, Eaton et al., 1993) prevented LTD induction by either conjunctive stimulation of CFs and PFs or by pairing PF stimulation with dendritic injections of 8-Bromoguanosine cyclic 3'5'-monophosphate sodium salt (8-Br-cGMP, Hartell, 1994a). Antibodies against mGluR type 1 (mGluR1) also blocked LTD induction (Shigemoto et al., 1994). Mice deficient in metabotropic glutamate type 1 receptors (mGluR1, Conquet et al., 1994; Aiba et al., 1994) or lacking the GluRδ2 subunit (Kashiwabuchi et al., 1995) were found to exhibit severe motor deficits such as locomotor ataxia and impaired LTD. There was no obvious brain abnormality in the GluRδ2 mutant mice. However, instead of the normal single contact by a CF to each Purkinje cell, it was noted that the cells were innervated by more than one CF suggesting that the neuronal circuitry may have been disturbed in these mice. This information suggests that activation of both mGluRs and AMPARs is required for LTD induction.

1.5 LTD REQUIRES AN INFLUX IN POSTSYNAPTIC CALCIUM

The induction of LTD is blocked by iontophoretic application of the Ca^{2+} chelator ethylene glycol-bis(β-aminoethyl ether)-N,N,N'N'-tetraacetic acid (EGTA, Sakurai, 1990; Freeman et al., 1998) or by intracellular dialysis of bis(2-aminophenoxy)ethane-N,N,N'N'-tetraacetate (BAPTA, Konnerth et al., 1992). In addition, inclusion of BAPTA in the intracellular pipette solution was effective in blocking the induction of LTD in mouse cerebellar cultures (Linden and Connor, 1991).

In the cerebellum, the highly Ca^{2+} permeable NMDARs are only transiently expressed in early development (Crepel and Audinat, 1991; Rosemund et al., 1992). A large amount of the GluR2 subunit that confers low Ca^{2+} permeability was found in AMPAR in Purkinje cells (Lambolez et al., 1992). This finding suggested that the stimulation of these receptors was unlikely to contribute directly to changes in intracellular Ca^{2+}. Immunohistochemical studies

have located a high density of high voltage activated P-type Ca^{2+} channels in Purkinje cell dendrites (Usowicz et al., 1992). The stimulation of AMPAR could however, activate Ca^{2+} influx indirectly through voltage-dependent Ca^{2+} channels.

Ca^{2+} can also be released from ryanodine or inositol triphosphate (IP_3)-sensitive intracellular stores. The ryanodine receptor is thought to be important for Ca^{2+}-induced Ca^{2+} release in Purkinje cells (Llano et al., 1994). There is some evidence that the cyclic adenosine diphosphate ribose (cADPR) metabolite interacts with ryanodine receptors and induces Ca^{2+} release from ryanodine-sensitive intracellular stores (Sitsapesan et al., 1995; Willmott et al., 1996). Type 1 IP_3 receptors are predominantly expressed in cerebellar Purkinje cells (Furuichi et al., 1989). LTD could not be induced by a combination of depolarisation and PF stimulation in slices prepared from mice with a disrupted IP_3 receptor type 1 gene and a specific antibody against type 1 IP_3 receptors (Inoue et al., 1998). Additionally uncaging of IP_3 did not induce Ca^{2+} release in these mice. Activation of mGluR1 was recently reported to produce Ca^{2+} transients that required IP_3-mediated Ca^{2+} release from intradendritic stores (Takechi et al., 1998). Together these findings suggest that functional IP_3 receptors are required for the induction of LTD.

Whole cell patch-clamp recording and confocal microscopic imaging were combined to observe the transient and local rise in postsynaptic Ca^{2+} concentration produced by the activation of PF to Purkinje cell synapses (Finch and Augustine, 1998). There was an initial rise in Ca^{2+} that was sensitive to block by the AMPAR antagonist CNQX and a delayed component that was blocked by the mGluR antagonist MCPG. In addition, Ca^{2+} signals that spread only a few micrometers were produced by focal photolysis of caged IP_3 in the dendritic regions of Purkinje cells. This Ca^{2+} release was restricted to individual postsynaptic spines where mGluR (Martin et al., 1992; Gorcs et al., 1993; Baude et al., 1993) and IP_3 receptors (Walton et al., 1991) are known to be located. This data suggests that stimulation of PF to Purkinje cell synapses releases glutamate from presynaptic terminals which activates both AMPAR and mGluR and triggers a Ca^{2+} signal with 2 components (Kasono and Hirano, 1995; Plant et al., 1996; Mikoshiba, 1997; Finch and Augustine, 1998). The initial Ca^{2+} signal arises from influx through voltage gated Ca^{2+} channels activated when

AMPARs depolarise postsynaptic dendrites. The delayed component of the Ca^{2+} signal results from guanine-nucleotide binding protein (G-protein) coupled mGluR activation which produces the second messenger IP_3 which is responsible for mobilization of Ca^{2+} from intracellular stores.

It is now well accepted that the activation of both mGluRs and AMPARs and an increase in postsynaptic Ca^{2+} are the three basic requirements for the induction of LTD at PF-Purkinje cell synapses in acute slices and of glutamate-induced currents in cultured Purkinje cells (as reviewed by Zhuo and Hawkins, 1995; Linden and Connor, 1995a; Daniel et al., 1998).

1.6 THE ROLES OF CF AND PF ACTIVATION IN THE INDUCTION OF LTD

Ca^{2+} transients were detected in response to CF synaptic activation providing direct evidence that CFs might be the source of Ca^{2+} (Ross and Werman, 1987). The requirement for CF activation in LTD can be replaced by depolarisation of the postsynaptic Purkinje cell (Hirano, 1990; Crepel and Jaillard, 1990). LTD induction can also be inhibited by hyperpolarisation of the Purkinje cell during conjunctive PF and CF stimulation (Hirano, 1990). Together these findings suggest that the primary role of CF activation in the induction of LTD is to produce a strong depolarisation of the postsynaptic Purkinje cell and trigger Ca^{2+} influx into the dendritic region through voltage gated ion channels. Inclusion of Fura-2, a fluorescent Ca^{2+} indicator dye in the intracellular pipette solution during whole cell patch-clamp recordings made it possible to observe dramatic increases in the Ca^{2+} signal during CF stimulation, particularly in peripheral Purkinje cell dendrites (Konnerth et al., 1992). In cultures of foetal rat cerebellum, pairing application of glutamate with photolysis of nitr-5 a photolabile Ca^{2+} chelator, produced LTD suggesting that the role of Ca^{2+} influx in the induction of LTD was independent of depolarisation (Kasono and Hirano, 1994).

More recently, the PF input has been implicated as a possible source of Ca^{2+} for LTD. Confocal microscopic imaging revealed that strong activation of PF inputs to Purkinje cells can also trigger localised increases in dendritic Ca^{2+} (Eilers et al., 1995). These Ca^{2+} signals

were sufficiently large to induce LTD (Hartell, 1996b; Eilers and Konnerth, 1997a). In addition either PF stimulation or the uncaging of IP_3 produced Ca^{2+} release signals (Finch and Augustine, 1998). Glutamate from presynaptic terminals was reported to initiate an IP_3-mediated calcium release that was restricted to individual postsynaptic spines on Purkinje cell dendrites (Takechi et al., 1998). These findings indicate that the Ca^{2+} signal induced by PF stimulation is at least in part IP_3-mediated.

Immunohistochemical localisation of nitric oxide synthase (NOS) in the rat brain was the first anatomical study to identify dense staining in the cerebellar molecular layer and granule cell layer. Furthermore this same study suggested that basket cells and PFs which are in close proximity to Purkinje cells dendrites could possibly be a source of nitric oxide (NO) because under high magnification some immunofluorescence for NOS was apparent in these cells (Bredt et al., 1990). Nicotinamide adenine dinucleotide phosphate (NADPH)-diaphorase histochemistry was used to identify cells with a high content of neuronal NOS, the enzyme necessary for the production of NO. This technique revealed the most prominent staining in the molecular layer and the granule cell layer (Southam et al., 1992). Raising the concentration of K^+ in the perfusion medium was found to initiate a rise in cyclic guanosine monophosphate (cGMP) levels in slices of cerebellar vermis. This effect was reduced by the application of an inhibitor of NOS. In slices prepared from rats pre-treated with 3-AP to produce a lesion to the CFs a 50% reduction in the amount of cGMP accumulation was observed (Southam and Garthwaite, 1991). LTD could also be induced when CF stimulation was replaced by bath application of a NO donor (Shibuki and Okada, 1991). Taken together these data suggested that CFs could be the source of NO. However, it has since been reported that neuronal NOS is not expressed in CFs (Vincent, 1996). The messenger RNA encoding NOS was not detected in Purkinje cells (Crepel et al., 1994). NADPH-diaphorase histochemisry did not detect any staining in Purkinje cells (Vincent and Kimura, 1992).

LTD could be induced by replacing PF stimulation with caged release of NO and simultaneously depolarising the Purkinje cell supporting the theory that NO is released from the molecular layer (Lev Ram et al., 1995). Release of NO in the molecular layer following strong stimulation of the white matter was measured using an electrochemical NO probe

(Shibuki and Kimura, 1997). This technique showed that repetitive stimulation elicited an activity-dependent release of NO from the molecular layer (Kimura et al., 1998). In addition to NO release and Ca^{2+} signals PF stimulation has been linked to mGluR activation.

It was thought that activation of both CF and PF inputs to Purkinje cells was necessary for LTD (Ito and Kano, 1982) however, there is now support for an alternative form of LTD induced by PF stimulation alone (DeSchutter, 1995). Strong activation of PFs elicited a Ca^{2+} influx and a non-conjunctive, heterosynaptic form of LTD. The LTD largely occluded the depression induced by conjunctive CF and PF stimulation. At the control site a NO-dependent form of LTD was observed (Hartell, 1996b). Stimulation of PF alone at high frequencies (100Hz) was reported to be sufficient to induce a pronounced long-lasting depression of PF-excitatory postsynaptic potentials (EPSPs, Schreurs and Alkon, 1993).

1.7 THE INVOLVEMENT OF THE NO/cGMP SIGNALLING SYSTEM IN LTD

In addition to the three essential components; activation of AMPAR and mGluR and an increase in postsynaptic Ca^{2+}, the NO/cGMP/PKG cascade has been linked to the induction of LTD (Crepel and Jaillard, 1990; Ito and Karachot, 1992; Daniel et al., 1993; Hartell, 1994a; Hartell, 1994b; Hemart et al., 1995; Zhuo and Hawkins, 1995; Hartell, 1996b; Daniel et al., 1998).

NO is a highly reactive molecule that has been implicated in neuronal signalling (Holscher, 1997). Because NO has a short biological half-life *in vivo* (Kelm and Yoshida, 1996) its effective concentration is controlled by the rate of its formation from L-arginine and the extent of degradation. The calcium-calmodulin dependent enzyme NOS is required for synthesis of NO from its precursor L-arginine (Fukuto and Mayer, 1996). Immunohistochemical localisation of NOS in the rat brain has shown that the strongest staining is in the molecular layer and granule cell layer of the cerebellum whereas the Purkinje cells were unstained (Bredt et al., 1990). The site of action of NO is likely to be confined to the vicinity of its

production site (Kelm and Yoshida, 1996). Activation of the soluble form of guanylate cyclase (GC) is mediated by NO and is responsible for initiating a rise in the intracellular levels of cGMP (Schulz et al., 1991). The existence of a cGMP signalling system in the mammalian central nervous system (CNS) has been known for over 20 years (Ferrendelli, 1978). The cerebellum was found to contain a high cGMP concentration in comparison to the rest of the brain suggesting that this structure was important for cGMP-mediated cellular signalling (Bandle and Guidotti, 1978; Ferrendelli, 1978). Autoradiographic localisation studies identified [^{3}H]-cGMP binding sites in the cerebellar cortex (Bladen et al., 1996). cGMP is thought to activate cGMP-dependent PKG (Wood et al., 1996; Wang and Robinson, 1997).

In cerebellar slices support for the involvement of NO in LTD came from the discovery that induction of LTD was prevented in the presence of inhibitors of NOS (Crepel and Jaillard, 1990; Boxall and Garthwaite, 1996a). Extracellular application of a NO donor such as sodium nitroprusside (SNP) paired with PF stimulation induced LTD (Shibuki and Okada, 1991). Depolarisation paired with caged acetic acid,2,2'-[[(3,3-diethyl-1-triazenyl)oxy]methyl]-5-nitro-1,2-phenylene]bis(oxy)]bis(oxy)]bis-,N-oxide (CNO-4) that releases NO upon photolysis was also sufficient for LTD. Extracellular perfusion of the NO trapping agent haemoglobin or the NOS inhibitor N^{G}-nitro-L-arginine prevented this LTD but intracellular application of either of these compounds did not (Lev Ram et al., 1995). This information suggests that NOS catalyses the production of NO within cells which then exerts its effects at nearby cells. In contrast to the above findings in perforated patch recordings from cultured Purkinje cells, the LTD of glutamate currents was unaffected by NOS inhibitors or NO donors (Linden and Connor, 1992; see also, Linden et al., 1995b) . Also PF-excitatory postsynaptic currents (EPSCs) were reported to be unaffected by bath application of SNP (Glaum et al., 1992). However this data was obtained from only 3 cells and a low concentration (100μM) of SNP was used.

NO-sensitive GCs are thought to be the target of NO (as reviewed by Schulz et al., 1991). Purkinje cells possess abundant GC immunoreactivity (Ariano et al., 1982). Immunofluoresence for guanylate cyclase was also apparent within basket and stellate cells

of the granule cell layer (Ariano et al., 1982). The production of a new potent and specific inhibitor of GC called 1-H-[1,2,4]oxadiazolo[4,3-a]quinoxalin-1-one (ODQ, Garthwaite et al., 1995) has made it possible to investigate the importance of GC in long term decreases in the synaptic efficacy of PF-Purkinje cell synapses. LTD could not be produced by pairing PF stimulation with postsynaptic Ca^{2+} spike firing in the presence of intracellular application of ODQ (Boxall and Garthwaite, 1996a). One approach to investigate the involvement of cGMP in LTD induction has been to apply analogues of cGMP. Bath application of 8-Br-cGMP produced a LTD of PF-excitatory postsynaptic currents (Shibuki and Okada, 1992b; Hartell, 1994a). In contrast, in cerebellar cultures the intracellular application cGMP or 8-CPT-cGMP did not produce a depression of glutamate-evoked currents (Linden et al., 1995b).

Phosphodiesterases (PDEs) catalyze the inactivation of cyclic nucleotides. A number of PDE isozyme families have been identified; cGMP-stimulated, cGMP-inhibited, cGMP-specific, cyclic adenosine monophosphate (cAMP)-specific, Ca^{2+}-calmodulin dependant, light stimulated photoreceptor (cGMP-specific) and rolipram-insensitive (cAMP specific) however, in total greater than 12 isozymes could exist (see reviews by, Beavo, 1988; Thompson, 1991; Conti and Catherine-Jin, 1999). The amount of cGMP activity in a tissue is therefore controlled by both the rate of GC-stimulated formation and the extent of PDE-catalyzed inactivation. Further support for the importance of cGMP signalling in the induction of LTD in cerebellar slices was provided by studies in which cGMP breakdown was prevented by Zaprinast a cGMP-specific PDE inhibitor (Hartell, 1996a). In contrast, in cultured Purkinje cells application of Zaprinast failed to induce LTD (Linden et al., 1995b).

1.8 THE IMPORTANCE OF PROTEIN KINASES IN LTD

cGMP-dependent kinase is concentrated in Purkinje cells within the cerebellum (Walter and Greengard, 1981; as reviewed by, Nairn et al., 1985). In the presence of the PKG inhibitor KT5823 (Nakanishi, 1989), a combined application of 8-Br-cGMP and AMPA could no longer cause a desensitisation of AMPA responses detected by wedge recording in rat cerebellar slices (Ito and Karachot, 1992). Similarly, the LTD induced by application of 8-Br-cGMP or

by conjunctive stimulation of PF and CF inputs to Purkinje cells was prevented in the presence of KT5823 (Hartell, 1994a). Interference with PKG was reported to block the LTD induced by depolarisation paired with either PF stimulation or photorelease of NO (Lev Ram et al., 1997). In contrast, in cerebellar cultures the LTD produced by bath application of cGMP analogues was not prevented by application of KT5823 (Linden et al., 1995b).

In a study using antibodies specific for the C-terminus of mGluR1αR, these receptors were found to co-localise with specific AMPAR subunits in Purkinje cells (Martin et al., 1992). mGluR1 reportedly to couple to phospholipase C (PLC) which cleaves phosphatidylinositol 4,5-bisphosphate (PIP_2) to yield IP_3 and diacylglycerol (DAG, Schoepp and Conn, 1993; Nakanishi, 1994). DAG has been reported to activate PKC (Bramham et al., 1994). Dense PKC-like immunoreactivity was found in the cerebellar molecular layer in rats (Saito et al., 1988). Furthermore, electron microscopic studies confirmed the localisation of type I PKC in Purkinje cells (Kose et al., 1988). Data suggesting that activation of PKC was necessary for the induction of LTD was found in both Purkinje cell cultures and cerebellar slices. Inhibition of PKC by calphostin C (Linden and Connor, 1991) or polymyxin B (Crepel and Jaillard, 1990) was sufficient to prevent LTD. Additionally the application of phorbol esters to activate PKC could mimic LTD in cerebellar slices (Crepel and Krupa, 1988) and in culture (Linden and Connor, 1991). Recently, the specific expression of a PKC inhibitory peptide in Purkinje cells of transgenic mice resulted in a near complete suppression of cerebellar LTD in cultured cells (DeZeeuw et al., 1998).

1.9 CELL SIGNALLING MOLECULES AND RECEPTORS THAT MAY ALSO BE IMPORTANT FOR LTD

Other components have recently been discovered in the cellular mechanism leading to LTD induction. For example, in cerebellar slices application of the protein tyrosine kinase (PTK) inhibitors lavendustin A or herbimycin A blocked the LTD induced by pairing PF stimulation with Ca^{2+} spike activity (Boxall et al., 1996b). The study also suggested that the involvement of PKC in LTD could be dependent on the activity of PTKs. Perhaps PTK inhibits the production of DAG and IP_3 via actions at PLC. Using cultured Purkinje cells, it has been

established that Ca^{2+} dependent-phospholipase A_2 (PLA_2) was required for activation of PKC. PLA_2 was found to be necessary for the LTD produced by pairing iontophoretic glutamate pulses with Purkinje cell depolarisation (Linden, 1995). It was also shown in culture that cytosolic Ca^{2+} required for LTD induction probably involves activation of a Na^{+}-Ca^{2+} exchanger (Linden et al., 1993).

Autoradiographic localisation studies using the GABA analogue β-p-chlorophenyl GABA (baclofen) which has a high affinity for $GABA_B$ receptor ($GABA_BR$) sites showed that the $GABA_B$ Rs were confined almost exclusively to the molecular layer in the cerebellum (Wilkin et al., 1981). In the cerebellar cortex, anatomical (Bowery and Pratt, 1992) and pharmacological studies (Batchelor and Garthwaite, 1992; Vigot and Batini, 1997) suggest both presynaptic and postsynaptic roles for $GABA_BR$ at the PF to Purkinje cell synapse. A slow $GABA_BR$-mediated potential was identified at the synapse between PFs and Purkinje cells in a biplanar cerebellar slice preparation. This finding indicates that there are functional $GABA_BRs$ on Purkinje cells which could contribute to the plasticity at these synapses (Batchelor and Garthwaite, 1992).

1.10 THE cAMP SIGNALLING CASCADE IS IMPORTANT FOR THE INDUCTION OF CEREBELLAR LTP

In addition to postsynaptic LTD a presynaptic form of LTP has been observed in the cerebellar cortex (Salin et al., 1996). This form of LTP was induced in both field potentials (FPs) and PF-EPSCs elicited by brief repetitive PF stimulation. Application of forskolin to directly activate adenylate cyclase (AC) was found to occlude the long lasting enhancement of PF-Purkinje cell synaptic transmission induced by a brief tetanus. Inhibition of protein kinase A (PKA) with Rp-8-CPT-cAMP prevented the generation of LTP (Salin et al., 1996). *In situ* hybridisation localised AC in the granule cell layer of the cerebellum (Matsuoka et al., 1992). This finding suggests that the PFs that synapse with Purkinje cells are a likely source of AC. The mechanism for the LTP at PF-Purkinje cell synapses was investigated using forskolin to elevate cyclic adenosine monophosphate (cAMP) levels by activating AC. cAMP

was reported to act at presynaptic sites downstream from Ca^{2+} entry to enhance the probability of neurotransmitter release and synaptic transmission (Chen and Regehr, 1997). In this paper it was also proposed that the enhancement could be attributed to an increase in the excitability of PFs, in the presynaptic Ca^{2+} influx or in the release of neurotransmitter from vesicles. In another study spike broadening that initiated a longer period of Ca^{2+} release was linked to LTP (Sabatini and Regehr, 1997). Detection of NO with an electrochemical NO probe revealed that repetitive PF stimulation potentiated NO release and this was blocked by inhibition of cAMP-specific PKA with N-[2-bromocinnamyl(amino)ethyl]-5-isoquinolinesulfonamide (H-89, Kimura et al., 1998). Together these findings suggest that the mechanism for LTP at PF-Purkinje cell synapses is a cascade of events involving AC, cAMP and PKA signalling.

1.11 AIMS AND OBJECTIVES

The purpose of this project was:-

i) To evoke field potential (FP) responses by low frequency molecular layer stimulation.

ii) To investigate the synaptic conditions required to induce a LTD that could be detected using extracellular FP recording techniques. A raised stimulus intensity and increased frequency paradigm was used to try to induce LTD. Previously this method of stimulation induced a LTD of PF-EPSPs (Hartell, 1996b).

iii) To elucidate the cellular mechanism required for the induction of the form of LTD that could be detected using an extracellular method.

iv) To study the extent of input specificity of LTD recorded using extracellular methods.

v) If it was possible to induce LTD, to extend the research to examine if LTP could also be induced by certain parameters of molecular layer stimulation and detected in this extracellular system. In FP recording study it was previously reported that a cAMP-mediated form of LTP could be observed in the cerebellar cortex following a brief tetanic stimulation (Salin et al., 1996).

vi) If LTP of FPs evoked by molecular layer activation could be produced, to then observe the extent of input specificity of the LTP and consider which cell signalling molecules might contribute to the cellular mechanism for the LTP

vii) To investigate the possibility that $GABA_BRs$ could modify the incidence or the direction of plasticity in the cerebellum.

viii) Fewer studies of cerebellar synaptic plasticity have been performed in transverse slices than in sagittal slices and so the effect of different parameters of molecular layer activation in the transverse slice preparation was observed also.

FPs reflect the responses of many cells rather than the activity of a single cell. It is possible to manipulate extracellular solutions without disrupting the intracellular environment of cells or penetrating the cell membranes. This makes the technique much less invasive than intracellular recording that can cause cell deterioration due to cell membrane damage or dialysis of the internal contents of the cell by the intracellular pipette solution. The extracellular FP recording technique provides information which when combined with that from whole-cell patch clamp recording gives a fuller understanding of the behaviour of cell populations.

CHAPTER 2

CHARACTERISATION OF FIELD POTENTIAL RESPONSES

2.1 INTRODUCTION

The main objective of the work described in this chapter was to set up an extracellular electrophysiological system for recording FP responses in an *in vitro* cerebellar slice preparation. The first goal was to identify the components of the FP responses evoked by stimulation of the cerebellar molecular layer. The second was to determine as far as possible if the properties of the FPs were consistent with synaptic responses mediated by PF activation. The purpose of setting up this extracellular recording system was ultimately to be able to use the technique to examine various aspects of cerebellar synaptic plasticity and to establish the benefits of using the technique alone or in addition to the whole cell patch-clamp studies performed in our laboratory.

The use of brain slice preparations for electrophysiological recording is an advantage because many of the normal anatomical connections that would be found *in vivo* between the cell populations remain intact (Kano and Konnerth, 1992). This contrasts with the situation in cerebellar cultures where both the cell populations and the synaptic connections between them are likely to be grossly disturbed. If artificial cerebrospinal fluid (ACSF) is continually perfused across the isolated mammalian tissue in the chamber then brain slices can be maintained under good metabolic conditions for long periods while electrical recordings are made (Li and McIlwain, 1957). In brain slice preparations drugs can be washed in and depending on the kinetics of the compound, out of the slice so that responses can be obtained both before and after drug application (Kano and Konnerth, 1992).

The extracellular FP recording method affords a number of benefits over intracellular microelectrode and whole cell patch-clamp techniques. Extracellular recording gives a

picture of the concerted behaviour of a population of cells in contrast to intracellular microelectrode and whole cell patch-clamp recording methods that only consider the response of a single cell. Furthermore, recording outside cells is potentially much less invasive than attempting to record inside where the penetration of the cell membrane can cause cell damage.

For intracellular recording the microelectrodes used to impale cells can potentially damage cell membranes and disturb cells but the intracellular environment is not altered during the recordings. The whole cell patch-clamp recording pipettes are also invasive to the cell membranes and additionally are filled with intracellular pipette solution. There is the opportunity to control the intracellular environment of cells by changing the composition of the internal solution (Hamill et al., 1981; Neher, 1992). However, this intervention can ultimately be a disadvantage because normal cell processes may be disturbed by the fluxes in ion concentration that occur due to diffusion between the patch pipette solution and the cell contents.

The problems resulting from exchange between the cell cytoplasm and the contents of the recording pipette can be overcome by performing the less invasive perforated-patch technique. In this technique a pore-forming antibiotic such as nystatin (Horn and Marty, 1988) or amphotericin B (Rae et al., 1991) is added to the intracellular pipette solution in the recording pipette. The main benefit of this method is that the antibiotic forms tiny channels that are permeable to monovalent ions and not proteins or second messenger molecules. Amphotericin B also causes a decrease in access resistance. In each experiment the final access resistance depends upon the surface area of the membrane that is drawn into the pipette. The bigger the patch of membrane the more scope there is for the insertion of large numbers of channels that will lower the access resistance (Rae et al., 1991). Extracellular recording avoids the two main disadvantages of intracellular microelectrode and whole cell patch-clamp recording techniques. There is little or no disruption to the cell membranes or intracellular environment of the population of cells from which FP responses are recorded.

The basis for detection of FP responses relates to the movement of ions across the membranes of active cells. Ionic movement causes transmembrane currents to be produced that establish current sources and sinks with respect to the extracellular environment. In this context a source is equivalent to a current being injected into the extracellular medium from a cell, conversely a sink represents a current being absorbed from the extracellular medium into the cell. The extracellular currents flowing between sources and sinks gives rise to potential differences that are referred to as FPs (as defined by Nicholson and Freeman, 1974). The changes in the appearance of FP responses that are revealed by depth profiles can be accounted for by the pattern of distribution of current sources and sinks. Current source-density analysis was used to study the amplitude of sources and sinks at a given point in the cerebellum of adult bullfrogs and toads (Nicholson and Freeman, 1974; Nicholson and Llinas, 1975).

The appearance of the FP responses recorded in a particular brain region has a characteristic depth profile. For example, in anaesthetised rabbits the stimulation of the perforant path evoked population responses in the dentate area of the hippocampus. The FPs recorded in the region of perforant path synapses had an initial negative deflection and a superimposed positive-going spike. If the recording electrode was advanced into the cell body layer all the components became reversed. This finding was explained by presynaptic activation of perforant path synapses causing depolarisation of the adjacent dendritic membranes. This activation produced a rise in the extracellular current flow from the cell body layer towards the dendrites resulting in a negative potential in the synaptic region and a positive potential in the cell body region (Bliss and Lomo, 1973).

In the 1960s Eccles *et al.,* interpreted the FP waveforms that were generated in the cerebellar cortex of anaesthetised cats by trans-folial stimulation. The trans-folial method of stimulation was performed to activate purely mossy fibre inputs. This method of stimulation produced FP waveforms that were unusual in appearance with 7 distinct components that were termed P1, N1, P2, N2, P3, N3 and N4. The FP responses were polysynaptic, that is, they represented the synaptic transmission firstly at mossy fibre to granule cell synapses and

secondly at the PF to Purkinje cell synapses. The mode of production of waves N1 to N4 and P1 to P3 was determined to be:

i) The P1 – N1 diphasic spike was attributed to the mossy fibre volley

ii) The P2 wave corresponded to the positivity in the granule cell layer

iii) The delay between the diphasic spike and the N2 potential was consistent with the synaptic delay for excitatory synapses in the CNS therefore it was concluded that the mossy fibre impulses initiated the N2 potential

iv) The N3 potential was detected at depths of 100-200 μm. It was proposed that the activation of Purkinje cells by PF volleys caused negativity in the molecular layer that generated a positive-going wave.

v) At depths of 300-500 μm the N4 potential could be detected. This was related to the propagation of impulses in the Purkinje cell dendrites.

vi) The P3 wave was thought to be the result of either hyperpolarisation of the Purkinje cell body by inhibitory basket cells or due to the inhibitory action of Golgi cells at granule cell dendrites (Eccles et al., 1967b).

In recent studies stimulation of the molecular layer to directly activate PFs was reported to evoke FP waveforms with 4 components which were named P1, N1, P2 and N2. The 'N' referred to a negative-going component and the 'P' to a positive-going component. This is the opposite of the labelling system used by Eccles et al., 1967b where in contrast, the 'N' corresponded to the negativity in the tissue that generated the positive-going component. Molecular layer stimulation caused the excitation of PFs that evoked brief triphasic potentials P1-N1-P2 which were followed by a slow potential wave, N2. The properties of the FPs were fully investigated. The fast component was found to be characteristic of a volley of action potentials propagating along PFs. The slow component related to the synaptic activation of PF to Purkinje cells. The responses were monosynaptic and reflected the synaptic events at the connection between PF and Purkinje cells primarily via AMPARs (Chen and Thompson, 1995; Salin et al., 1996).

The extracellular FP recording technique is potentially a valuable tool for studying the synaptic efficacy at PF to Purkinje cell synapses in the cerebellum. Cerebellar long-term plasticity has already been studied using extracellular FP recording both *in vivo* (Ito et al., 1982; Ito, 1989) and *in vitro* (Chen and Thompson, 1995; Salin et al., 1996). In perforated patch recordings from cultured mouse Purkinje cells a late phase of cerebellar LTD was observed. This late phase was blocked by the inhibition of transcription or translation factors that are essential for protein synthesis (Linden, 1996). It was recently shown to require the activation of the transcription factor cAMP response element-binding protein (CREB, Ahn et al., 1999). It might be possible to maintain stable extracellular FP recordings for periods that are sufficiently long to be able to define slowly emerging changes in synaptic plasticity in addition to any acute effects.

In addition to performing the FP recording technique to identify the synaptic conditions required to induce long-term alterations in synaptic plasticity in an extracellular system, it can also be used to elucidate the cellular mechanisms that contribute to these long-term changes in synaptic efficacy. Inhibitors of key components of intracellular signalling cascades can be bath perfused and their effects on the induction of long-term alterations in synaptic strength can be observed.

The experiments described in this chapter were designed:

i) to reproduce a method of extracellular FP recording comparable to that used by Salin *et al.,* 1996 in an *in vitro* cerebellar slice preparation

ii) to demonstrate how using pharmacological tools such as the neurotoxin tetrodotoxin (TTX) the different components of the FPs were identified and characterised.

iii) to present evidence that the properties of these FP responses were consistent with synaptic responses that are primarily PF-mediated.

2.2 METHODS

2.2.1 SLICE PREPARATION

On a daily basis two litres of ACSF were prepared. The composition of the ACSF in mM was 118 NaCl; 4.7 KCl; 2.5 $CaCl_2.2H_20$; 25 $NaHCO_3$; 1.2 KH_2PO_4; 1.2 $MgSO_4.7H_20$; 11 glucose. Picrotoxin was included in the ACSF at a concentration of 20μM to block inhibitory $GABA_AR$ (Yoon et al., 1993; Qian and Dowling, 1994). To ensure that the picrotoxin was properly dissolved it was sonnicated for 5 minutes in a small volume of distilled water before it was added to the ACSF. Prior to dissection blocks of 3.0% agar that were made up in 0.9% NaCl solution were also prepared. The slice incubation chamber was filled with ACSF, gassed with 95% O_2 and 5% CO_2 to maintain the solution at pH 7.4, and kept at room temperature. A beaker containing ACSF was placed in an icebox filled with crushed ice, chilled to <4 °C and gassed with 95% O_2 and 5% CO_2. A double-sided razor blade (Wilkinson Sword) was broken in half and cleaned in ethanol to remove glue and lubricants. The blade was inserted into the clamp in the Vibroslice chamber (Model 752M, Campden Instruments Limited). Water flow to the Peltier cooling unit (Model 764, Campden Instruments Limited) of the chamber was turned on and the flow rate checked. The power to the cooling unit and cutter was then turned on.

14 – 21 day old male Wistar rats that were bred in house were placed in an anaesthetic box attached to a Boyle's apparatus (Fluotec-3, Cyptane Limited). The rat was deeply anaesthetised using 5 % Fluothane (containing Halothane) and a 3:2 mix of NO_2 and O_2. When corneal and pedal reflexes were absent, the rat was removed from the box and decapitated. The skin overlying the skull was resected. Using scissors, cuts were carefully made along the inter-parietal and parietal skull plates avoiding the cerebellar area. The skull plates were then folded back along the coronal suture. Using a blunt spatula to avoid damage to the cerebellum, it was separated from the rest of the brain and placed in a beaker of ACSF pre-chilled to <4 °C see figure 2.2.1.

The cerebellum was placed on an agar block. Using a blade, the remains of the brain stem were dissected away. Two parasagittal cuts were made, one midway across the paravermis at one side and one at the beginning of the vermis on the other see figure 2.2.1. The cerebellum was then transferred to a pre-glued block (cyanoacrylate, RS components) with the paravermis lying down onto the glue and with the dorsal surface facing towards the blade. The cerebellum was supported from behind by an agar block. The block was quickly placed in the Vibroslice chamber and the tissue covered with chilled ACSF. Where possible the dura overlying the cerebellum was removed using fine forceps to ensure smooth movement of the blade through the tissue when cutting. The blade height was adjusted until it was at an appropriate height to remove the first 'waste' slice. Slices 300 μm thick were cut from the cerebellar vermis in ice cold ACSF solution which was maintained below 4 °C using the Peltier device. The slices were then transferred to an incubation chamber, using the reverse end of a Pasteur pipette. This was repeated until 5-6 slices were obtained or until the paravermis was reached. Slices were kept in a holding chamber for at least 1 hour and then transferred to a submerged chamber. The slice was secured between two nylon nets and perfused with ACSF at a flow rate of 1.5 to 2 ml per minute ready for recording.

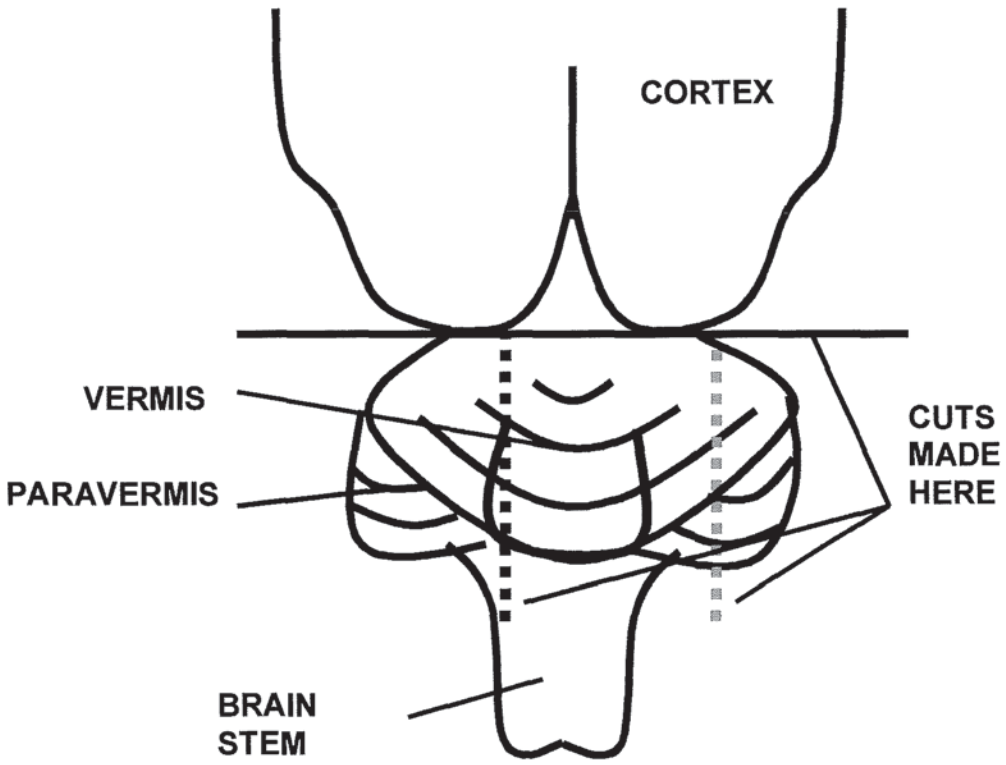

Figure 2.2.1 An illustration of the dorsal view of the cerebellum
The diagram illustrates the position of the cerebellum in relation to the cortex and the brainstem. The black horizontal line indicates where the cerebellum was separated from the cortex. The vertical dotted lines indicate where parasagittal cuts were made midway across the paravermis (grey) at one side and at the beginning of the vermis (black) on the other.

2.2.2 FIELD POTENTIAL RECORDING

Thin walled borosilicate glass capillaries (outside diameter 1.5 mm, inside diameter 1.17 mm; Clark Electromedical) were used to prepare pipettes. A Flaming/Brown micropipette puller (Model P-97, Sutter Instrument Company USA) was used to produce the pipettes for stimulating and recording. The resistances of the pipettes that were made for recording were between 2 and 5 MΩ when filled with ACSF. The recording pipette was secured in the pipette holder with a silver-silver chloride (Ag-AgCl) wire inside. Resistances of the pipettes that were used for stimulating were checked periodically and found to range between 1 and 3 MΩ when filled with ACSF. The stimulating electrodes had two Ag-AgCl wires; one inside and the other wrapped around the outside of the glass pipette.

The slices were viewed using a low power binocular microscope (X40 magnification, Leitz) with the aid of a light source underneath the submerged slice chamber. FP recordings were made from various cerebellar lobules. If possible a region of the lobule where a shiny Purkinje cell layer could be identified was chosen for recording. Recordings were made at room temperature. Two stimulating electrodes were placed opposite the Purkinje cell bodies between the middle of the molecular layer and the pial surface of the slice. The isolated stimulators were set at a pulse width of 0.1 ms and at an intensity of 5V. A recording electrode was lowered into the Purkinje cell layer and slowly advanced into the slice until clear, characteristic extracellular signals were detected in response to alternate 0.2Hz activation of the stimulating electrodes. Optimal FP recordings were obtained by making fine adjustments to the stimulus intensity and the position of the recording and stimulating electrodes see figures 2.2.2 and 2.3.1.

The FP responses were detected by the Ag-AgCl wire inside the recording electrode that was attached to the probe of the amplifier. The responses were amplified by a 2-stage amplification. Firstly with a Duo 773 Electrometer (World Precision Instruments) and secondly with an isolated Bio Preamplifier (Intracel). The final amplification value was between 750 and 850. At 2.5 second intervals the recording electrode resistances were monitored by observing the size of the voltage pulse produced by a repeated test 1 mV

current pulse of 5 ms duration. Changes in the electrode resistance and capacitance were compensated for during the recording with bridge balance and capacitance compensation circuitry on the amplifier. Before being digitised, the analogue signal was filtered with a low pass, 5 KHz filter.

Data were stored and analysed on-line using custom written software (Anderson and Collingridge, 1999). The software was used to trigger the isolated stimulators and to receive the digital signal from the Pico ADC-12 data acquisition board (Pico Technology Ltd. UK). The Picoboard acquired the input analog signal from the recording electrode amplifier and converted it to a digital signal.

Pulse sweeps of 70 ms duration were acquired every 2.5s from alternate stimulating pathways. The frequency of sampling was 10 kHz. At lower sampling frequencies the digital output would not accurately represent the FP response. A diagram of the experimental set-up is shown in Figure 2.2.3.

2.2.3 APPLICATION OF DRUGS

Drugs used for perfusion were 6-cyano-7-nitroquinoxaline (CNQX, Honore et al., 1988, Tocris) and tetrodotoxin (TTX, Catterall, 1992, Sigma). TTX was dissolved directly into the ACSF solution. CNQX was made up as a 10mM stock solution dissolved in dimethylsulphoxide (DMSO, to a final concentration of less than 0.1%) and then diluted in the ACSF solution prior to perfusion.

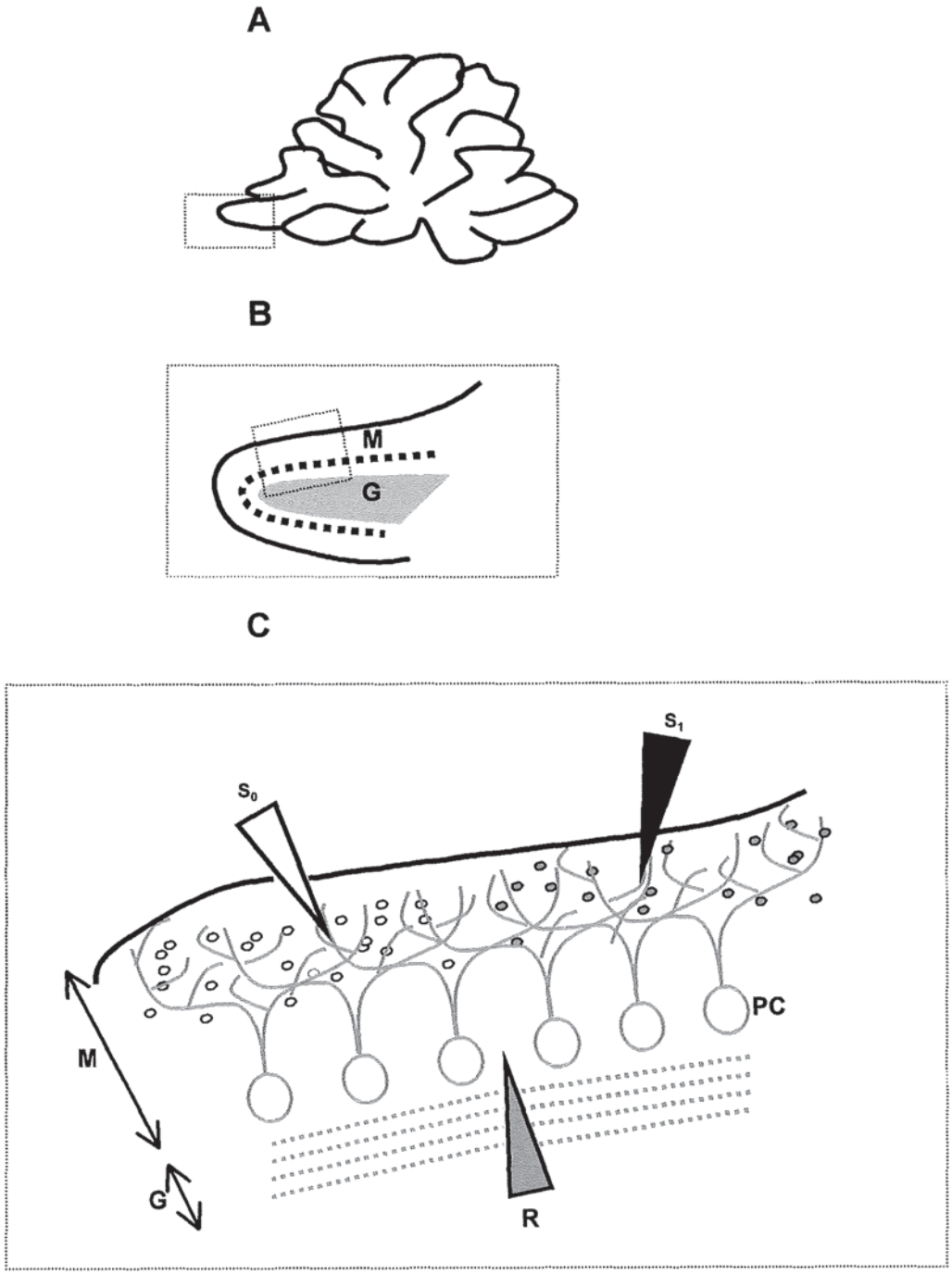

Figure 2.2.2 Field potential recording electrode positions in a sagittal slice of cerebellar vermis

Diagram A represents a sagittal slice of cerebellar vermis. A schematic diagram of the appearance of a cerebellar lobule under a low power binocular microscope is shown in diagram B. The shaded grey area indicates the granule cell layer (G). The molecular layer (M) comprises the Purkinje cell bodies (Purkinje cell layer) which are represented by the dotted black line and their dendrites, which extend towards the pial surface of the slice indicated by the solid black line. Diagram C represents the positioning of the stimulating (black and white) electrodes in the molecular layer (M) between the middle and the pial surface of the slice and the recording (grey) electrode placed in the Purkinje cell layer (PC). The black and grey circles represent PFs innervating the Purkinje cell dendrites in the molecular layer.

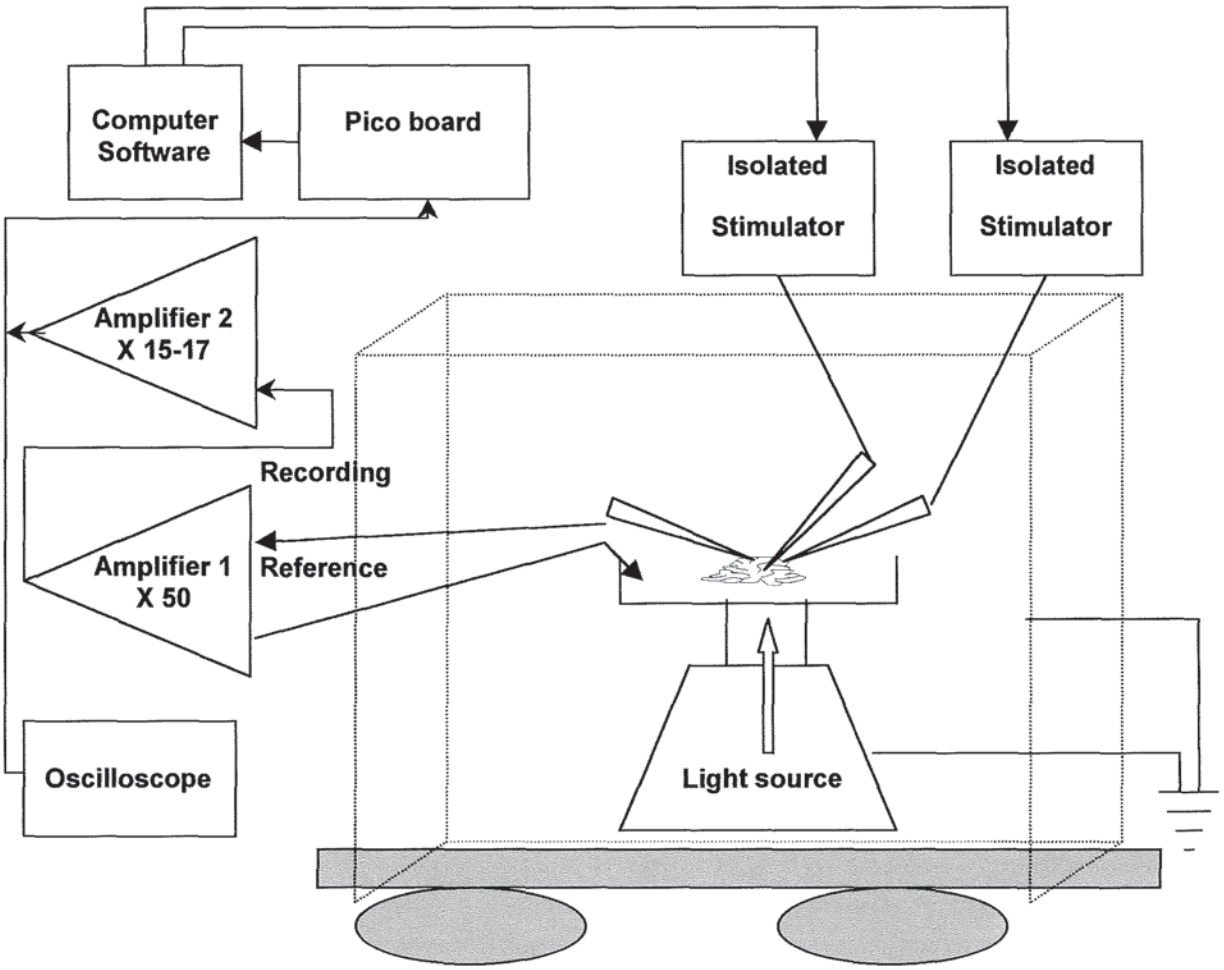

Figure 2.2.3 Experimental set-up
The dotted line indicates the Faraday cage that was made from metal wire netting to shield from sources of electrical noise outside. The grey shaded area represents the vibration isolation system that was made from a heavy metal plate that rested on three part-inflated trailer wheel inner tubes. FP responses were amplified by a two-stage amplification system. The on-line custom written software was used to trigger the isolated stimulators and to capture the signal from the recording electrode amplifier via the Pico ADC-12 data acquisition board.

2.3 RESULTS

2.3.1 APPEARANCE OF FIELD POTENTIAL RESPONSES

The technique of extracellular FP recording was performed in a cerebellar slice preparation. Picrotoxin was incorporated into the ACSF to block the possible inhibitory contribution of $GABA_A$ receptors ($GABA_AR$) to the FP responses. Activation of the molecular layer at a rate of 0.2Hz evoked FP waveforms with four distinct components. Immediately after the stimulus artefact, there was an initial fast triphasic component, P1-N1-P2 followed by a slow negative component, N2 as shown in figure 2.3.1. In some recordings N1 was partially obscured by the stimulus artefact. In the majority of experiments the FP responses had all 4 of the components of the waveform P1, N1, P2 and N2 clearly visible. Recordings were excluded if it was not possible to observe N1 or if a high voltage (above 10V) was required to evoke a response. The stimulus intensity selected for an individual experiment was kept as low as possible and ranged between 2 and 8V.

2.3.2 EFFECT OF INCREASING STIMULUS INTENSITY ON FIELD POTENTIAL RESPONSES

As shown in figure 2.3.2 A-C, at low intensities, FP responses were small but detectable. The amplitudes of N2 and N1 and the slope of the N2 component of FP responses gradually increased as a function of stimulus intensity. In the example shown it was possible to fit a sigmoidal curve to these data. In graph D in figure 2.3.2 the amplitude of N2 was expressed as a percentage of the maximum response between 0 and 40V. At 40V a plateau was not reached but it was noted that the rate of increase in the amplitude of the N2 component began to decline at stimulus intensities above 10V.

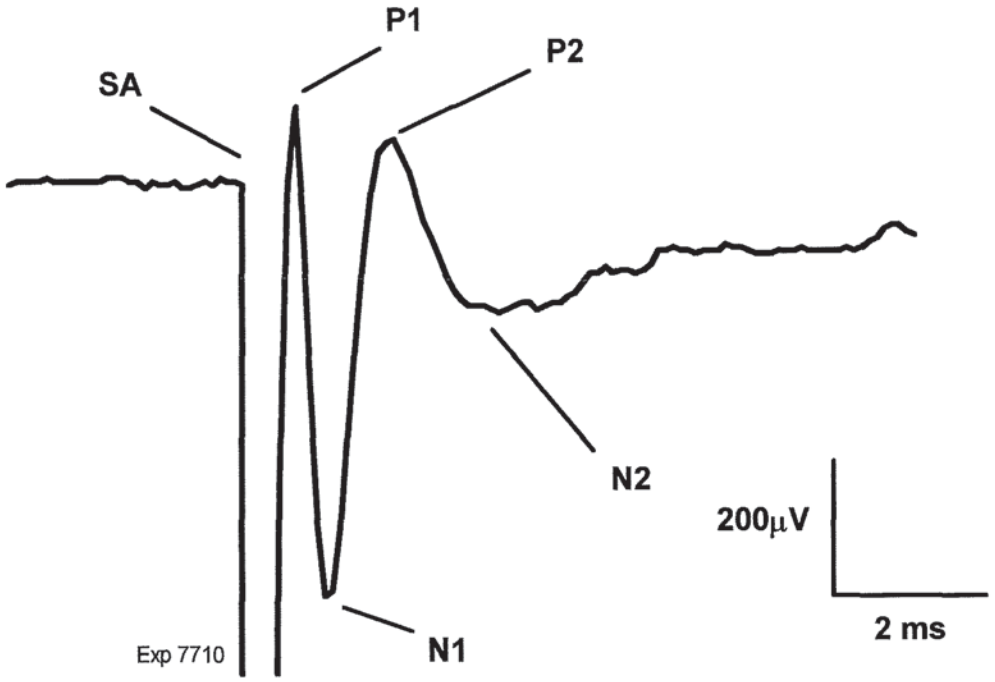

Figure 2.3.1 Appearance of an extracellular field potential response
The trace shown above is an example of the characteristic waveform of FP responses evoked by stimulation of the cerebellar molecular layer. The trace represents the average of 10 responses that were collected at 5s intervals. Immediately after the stimulus artifact (SA) there was a fast triphasic component P1-N1-P2 followed by a slow negative-going component N2. Scale bar 200μV, 2ms.

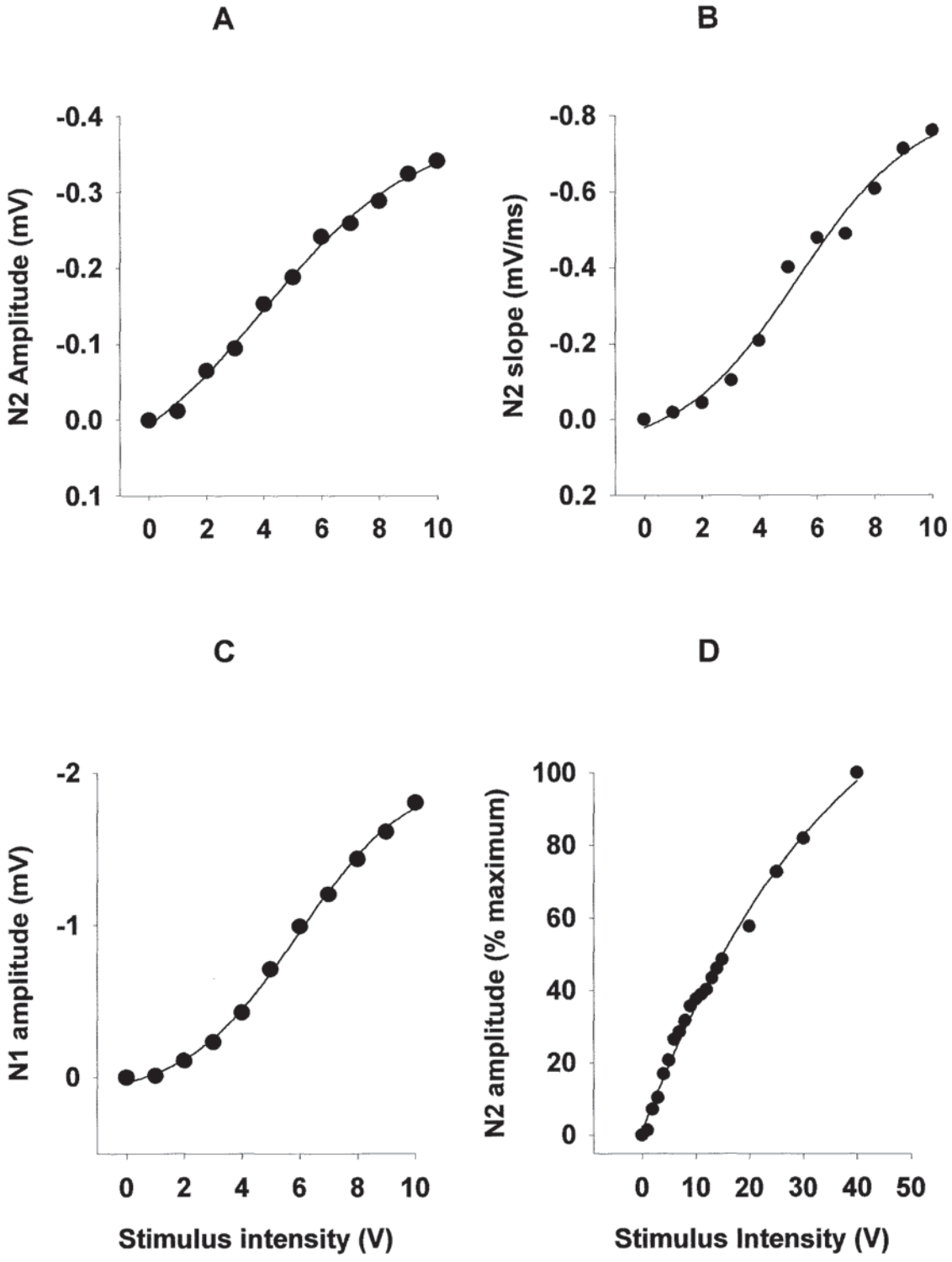

Figure 2.3.2 The graded relationship between the stimulus intensity and the amplitude and slope of field potential responses

Graphs A - C show the graded relationship between the stimulus intensity (0-10V) and the amplitude (mV) of N2, the slope of N2 (mV/ms) and the amplitude of N1 (mV), respectively. Graph D represents the effect of increasing the stimulus intensity between 0 and 40 V on the amplitude expressed as a % of the response at 40V.

2.3.3 PAIRED PULSES REVEAL PAIRED PULSE FACILITATION

The effect of delivering paired pulses at 40ms intervals on the N2 component was recorded. The analogue trace in figure 2.3.3 illustrates the facilitation of the second FP response that was observed when compared to the first response after paired pulse stimulation. This paired pulse facilitation was represented by a paired pulse ratio (PPR) value of greater than 1. The effect of increasing the interval between paired pulses was observed. As shown in the example in figure 2.3.3 the extent of PPF was maximal at a stimulus interval of approximately 40ms. A 40ms interval between paired pulses was therefore chosen for subsequent experiments.

The effect that increasing the stimulus intensity had on the PPR of the amplitude and slope of the N2 component of the FP waveforms was investigated. In the example shown the data suggested that the greatest level of paired pulse facilitation of the N2 amplitude or slope was observed with FPs evoked at very low stimulus intensities see figure 2.3.4. However, if responses were very small both the N2 and N1 components became difficult to measure. For the majority of recordings when the molecular layer was activated at stimulus intensities below 8V it was possible to achieve a FP response with N1 and N2 clearly visible. The absolute amplitude of the N2 component of these waveforms tended to range between 0.2 and 0.4mV. In most cases paired stimuli at 40ms intervals revealed paired pulse facilitation.

Linear regression analysis was performed to determine if there was a degree of association between the absolute amplitude or slope and the corresponding PPR. This analysis produced coefficient of determination (r^2) values of 0.65 $\pm$ 0.11 and 0.56 $\pm$ 0.10 for the amplitude and the slope (N=4), respectively. The r^2 values indicate what percentage of the variability of the data could be explained by the two variables. Even at the smallest r^2 value there was still a tendency to detect a linear relationship between the absolute amplitude or slope and the PPR. The linear relationship shown in figure 2.3.4A had a r^2 value of 0.72 suggesting that 72% of the change in the amplitude of the PPR could be accounted for by the change in the absolute amplitude. As shown in figure 2.3.4C and D a higher PPR of the N2 amplitude and slope, respectively, was observed at lower stimulus intensities.

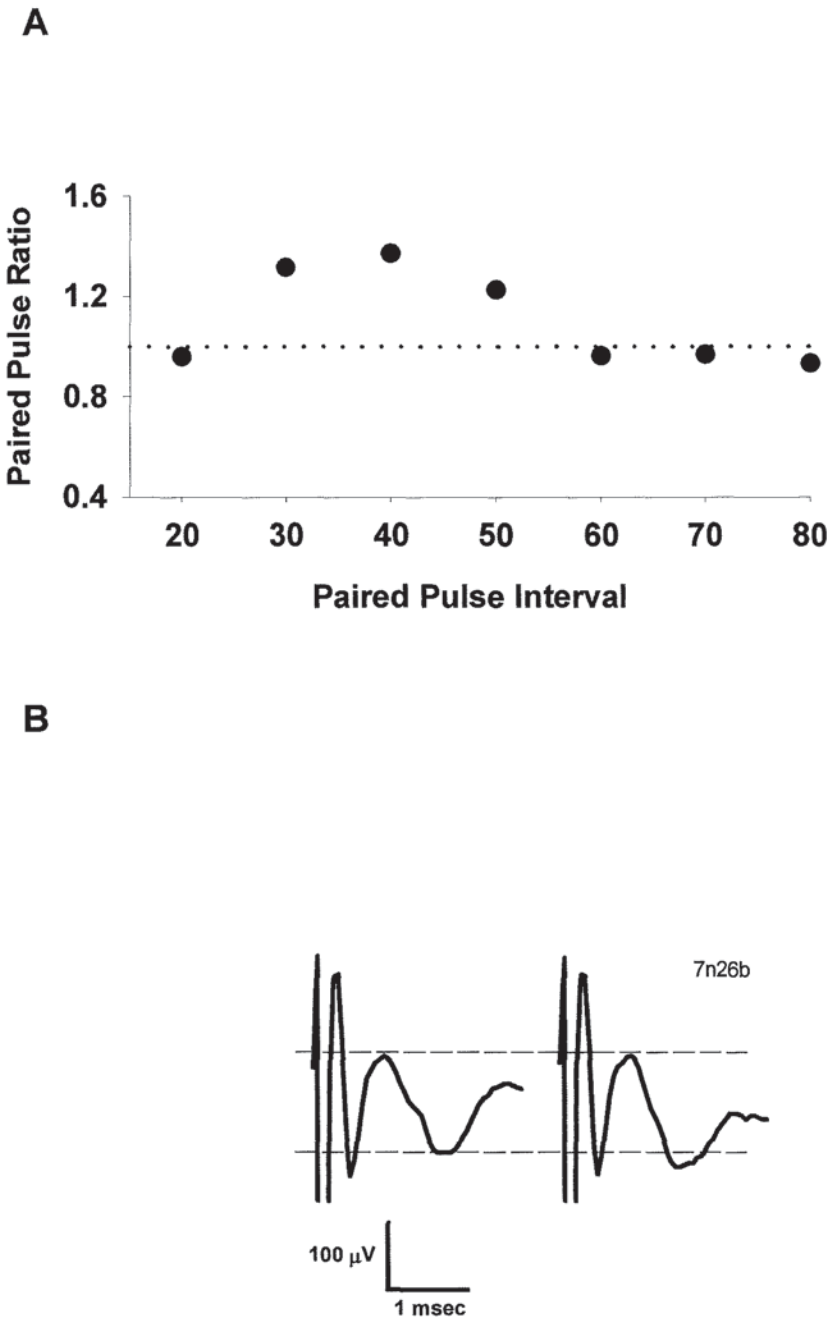

Figure 2.3.3 Paired stimuli reveal paired pulse facilitation
Graph A is an example of the effect of increasing the interval between paired stimuli on the paired pulse ratio. The trace shown in B is an example of the facilitation of the second response that was observed with a paired pulse interval of 40ms. The traces represent the average of 10 responses collected at 5s intervals. Scale bar 100 µV, 1 ms.

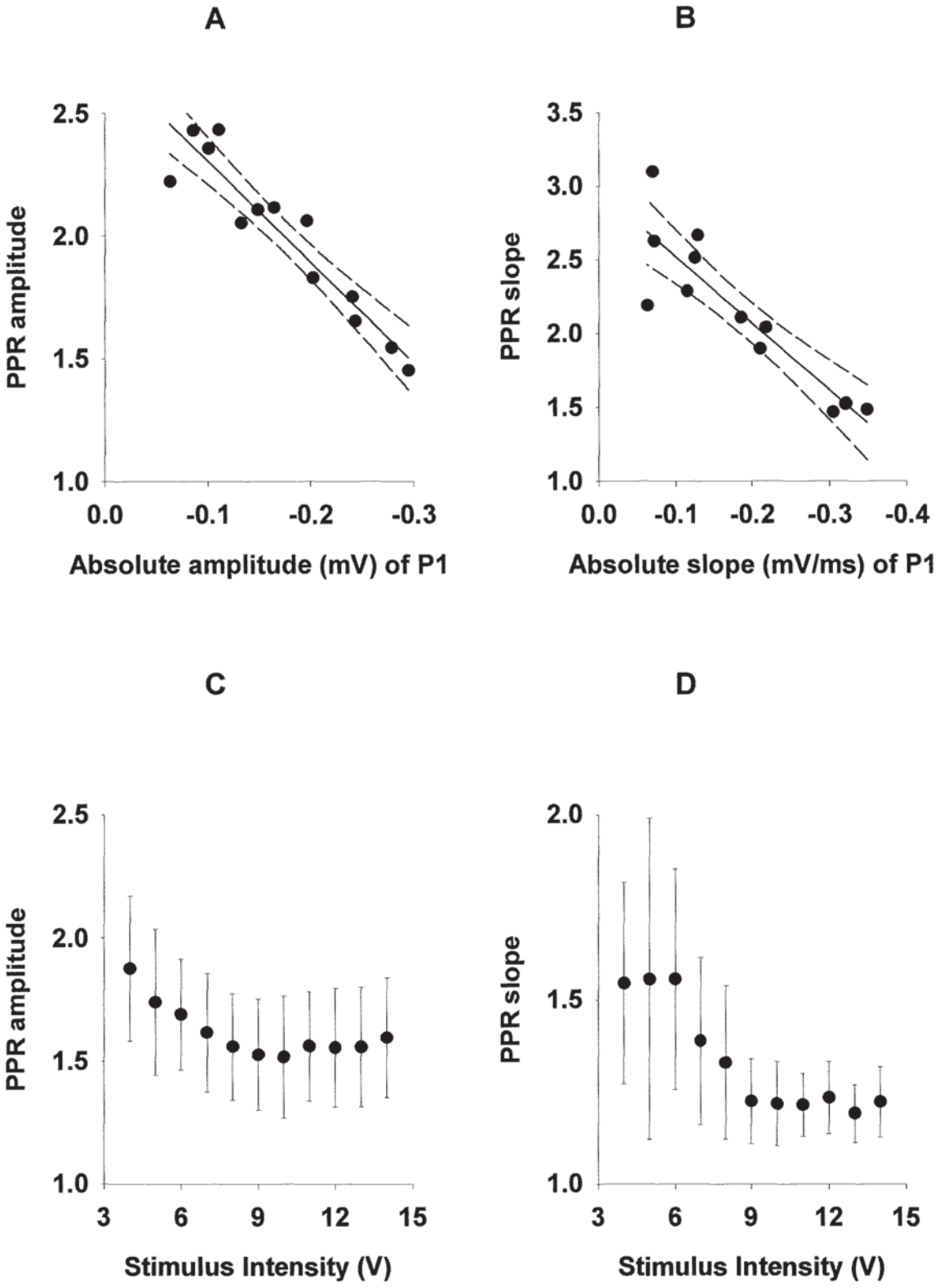

Figure 2.3.4 The relationship between the stimulus intensity or absolute amplitude / slope of field potential responses and the ratio between paired stimuli delivered 40ms apart

As shown in graphs A and B the amplitude of N2 was measured for the first FP response (P1) and then plotted against the ratio of the amplitude or slope of the first and second responses, respectively. Paired stimuli were delivered 40ms apart. Graphs C and D show the change in the amplitude and slope PPR against increasing stimulus intensity. The data in graphs C and D represent the average ± S.E.M of N = 5 FP recordings.

2.3.4 EFFECT OF THE SODIUM CHANNEL BLOCKER TETRODOTOXIN (TTX) OR THE AMPA RECEPTOR ANTAGONIST CNQX

In an attempt to establish which synaptic events contributed to the N2 and N1 components of the FP waveforms the effects of the sodium channel blocker TTX and the AMPAR antagonist CNQX were investigated. Stable baseline responses were recorded for at least 10 minutes before the application of the drugs. Bath perfusion of the sodium channel blocker 0.1 μM TTX for 8 minutes produced a marked blockade of FP responses as shown in figures 2.3.5. Within 5 minutes of the application of TTX the N1 and N2 components of FP responses were no longer visible. At 40 minutes after TTX was washed out the FP responses had partially recovered.

The N2 component but not the N1 component of FPs was selectively blocked by the AMPAR antagonist CNQX. As shown in figure 2.3.6 the bath perfusion of 10μM CNQX markedly reduced the N2 but not the N1 amplitude of the FP waveform. The FP responses fully recovered within 40 minutes of washout. As outlined later in the discussion the fact that the FPs are graded responses with PPF, together with the pharmacology suggests that they are primarily PF-mediated responses. In which case the fast triphasic component P1-N1-P2 represents the PF volley and the N2 component relates to AMPAR-mediated PF to Purkinje cell synaptic transmission.

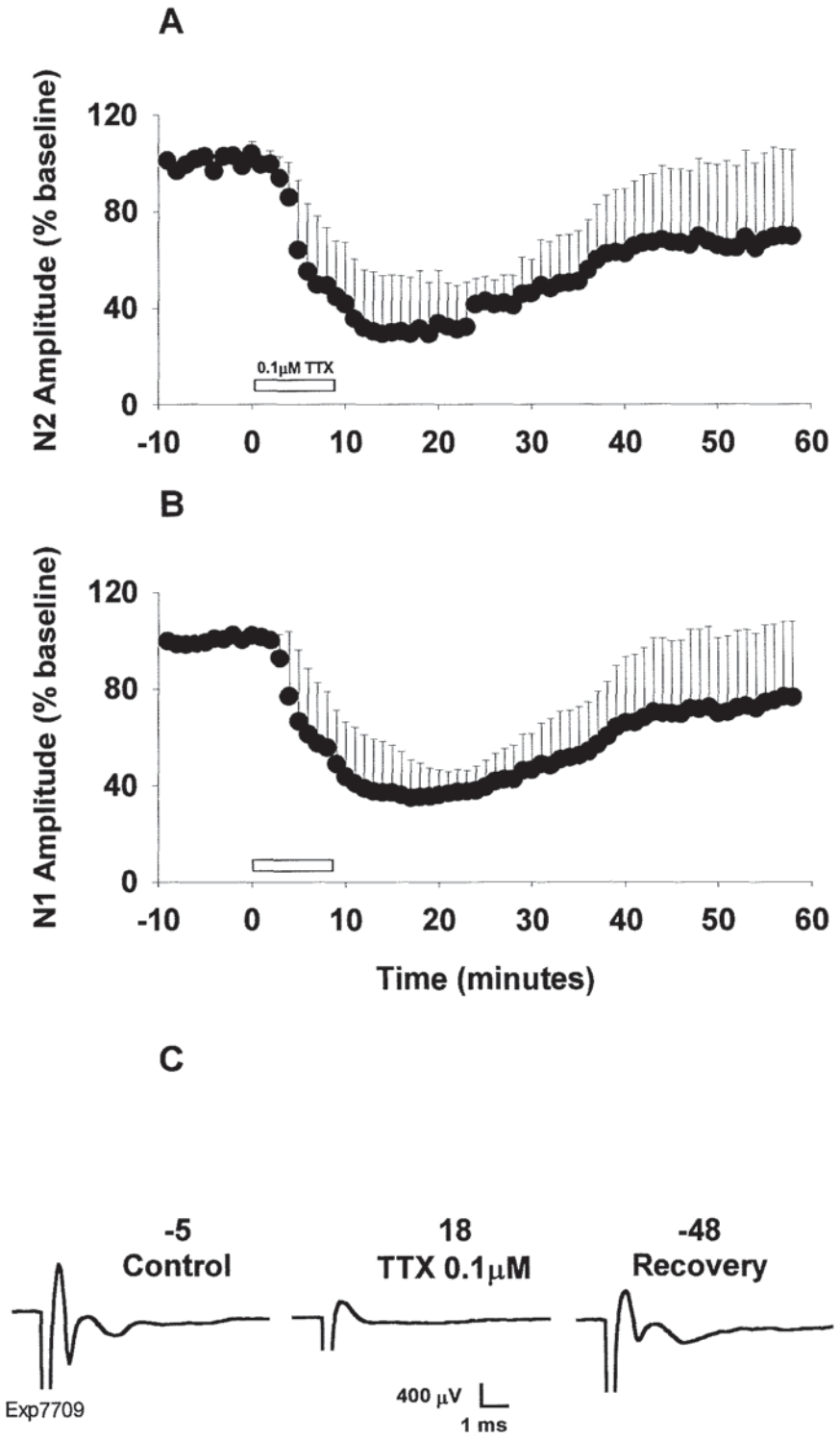

Figure 2.3.5 Effect of the sodium channel blocker TTX on field potential responses
Graphs A and B show the effect of 0.1 μM TTX on the amplitude of the N2 and N1 components of FP responses, respectively. Data represents the mean % of baseline ± S.E.M. of N = 3 recordings. White horizontal bar represents the 8 minute period of drug application. The traces in C from left to right show the control FP response, the effect of 0.1 μM TTX after 10 minutes and the recovery of the FP response 40 minutes after washout of TTX. Scale bar 400 μV, 1 ms.

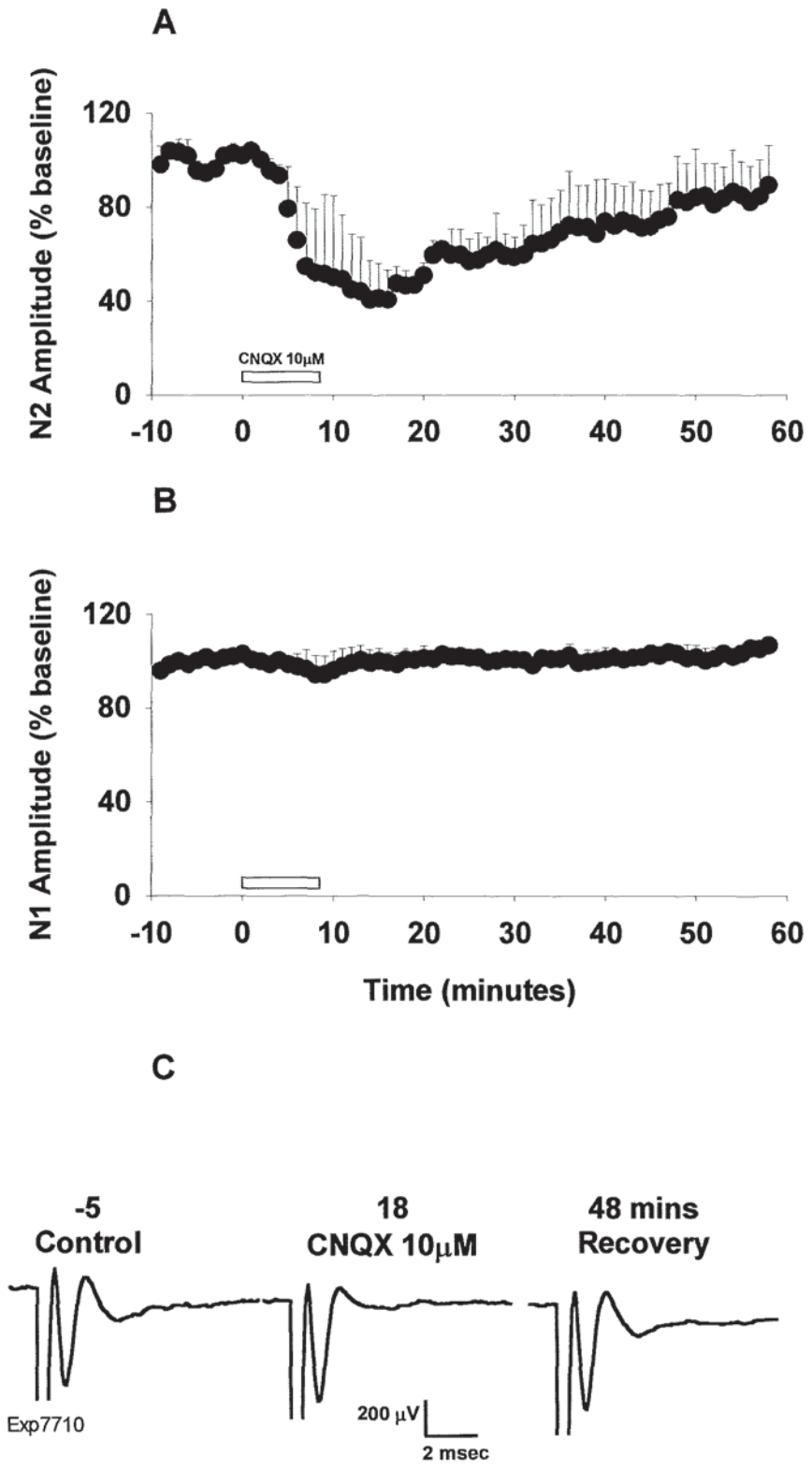

Figure 2.3.6 Effect of the AMPA receptor antagonist CNQX on field potential responses

Graphs A and B show the effect of 10 μM CNQX on the amplitude of the N2 and N1 components of FP responses, respectively. Data represents the mean % of baseline ± S.E.M. of N = 3 recordings. White horizontal bar represents the 8 minute period of drug application. The traces in C left to right show the control FP response, the effect of 10 μM CNQX after 10 minutes and the recovery of the FP response 40 minutes after washout of CNQX. Scale bar 200 μV, 2 ms.

2.4 DISCUSSION

Alternate 0.2Hz activation of two stimulating electrodes in the molecular layer evoked FP waveforms with four distinct components P1, N1, P2 and N2. The FP responses displayed two negative–going components that were termed N1 and N2.

Experiments were undertaken to establish what synaptic events were responsible for the N1 and N2 components of the FP waveforms. A neurotoxin type 1 receptor is located at extracellular sodium ion channel pores. The neurotoxin TTX exerts its effect by tightly binding to the neurotoxin receptor and produces a marked inhibition of ion conductance (Catterall, 1992). Sodium conductance is necessary for the influx of Na^+ that precedes the initiation of action potentials in nerve fibres. TTX was therefore used as a pharmacological tool to identify which component of the FP responses related to Na^+ influx and hence the propagation of action potentials. Both the N1 and the N2 negative-going components of the FP waveforms were sensitive to TTX. The N2 component alone was sensitive to the quinoxalinedione compound CNQX that is a potent competitive antagonist at AMPAR (Honore et al., 1988). These findings suggested that the P1-N1-P2 fast, negative deflection reflected the propagation of action potentials along PFs or the PF volley. Due to the abundance of PF to Purkinje cell synapses (Eccles et al., 1967a) it was expected that PF volleys set up by molecular layer stimulation would powerfully activate the Purkinje cells. The effect of CNQX indicated that the slow negative-going potential termed N2 was AMPAR mediated and represented the synaptic excitation of Purkinje cells by PFs.

This characterisation of FP responses was in agreement with previous descriptions of PF mediated FP responses (Chen and Thompson, 1995; Salin et al., 1996). Electrical molecular layer stimulation triggers the initiation and propagation of action potentials along PFs resulting in presynaptic release of glutamate which then binds to postsynaptic AMPAR.

The paired pulse stimulation method has been used to observe the effect of two stimuli delivered at intervals by a number of groups (see for example, Katz and Miledi, 1968;

Konnerth et al., 1990; Debanne et al., 1996; Salin et al., 1996; Hashimoto and Kuriyama, 1997) on the amplitude of FPs or whole cell EPSCs. Calcium influx through voltage-dependent calcium channels is triggered by the arrival of action potentials at axon terminals. The presence of calcium increases the probability that vesicles located in the axon terminal will fuse with the presynaptic membrane and release neurotransmitter into the synaptic cleft. Under certain conditions a small amount of the calcium that enters the axon terminal may remain for several 100 ms. This residual amount of calcium, although not sufficient to trigger further neurotransmitter release adds to any calcium that enters the terminal during the next action potential (Katz and Miledi, 1968). This causes an increased probability of vesicles fusing with the axon terminal. If the second response is larger than the first when two stimuli are delivered in succession then this is known as paired pulse facilitation. The opposite phenomenon paired pulse depression is thought to relate to a decrease in the amount of action potential evoked neurotransmitter release. In summary then, an alteration in either the probability of neurotransmitter release or the rate of production, uptake or degradation of neurotransmitter molecules might influence the PPR calculated in response to paired stimuli.

The N1 component of FPs provides additional information about the nature of changes in the responses. For example, detecting a change in the PF volley could relate to a change in the number of PFs recruited by molecular layer stimulation or an increase in the excitability of PFs. As shown in figure 2.3.2 there was a graded relationship between the stimulus intensity and the size of the corresponding volley or N1 component. This suggests that raising the stimulus intensity recruits more PFs.

In an intracellular whole cell patch-clamp study the direct activation of the two excitatory inputs to Purkinje cells produced synaptic currents with distinct properties. CF stimulation produced responses that had an all-or-none character and which showed paired pulse depression. In contrast, the second excitatory input, thought to arise from the stimulation of mossy fibres or granule cells, produced a current that was smoothly graded with stimulus strength and underwent paired pulse facilitation (Konnerth et al., 1990). The amplitude of the N1 and N2 components of the FP waveforms evoked by molecular layer stimulation in this study showed a graded relationship with increasing stimulus intensity. In addition paired

pulse stimuli revealed a small amount of paired pulse facilitation. Therefore the FP responses had similar properties to those of the mossy fibre or granule cell-mediated EPSCs described by Konnerth *et al.,* 1990.

This technique of extracellular FP recording has several inherent sources of variation that could affect the size and appearance of the FP responses evoked by molecular layer stimulation. For example:-

i) the slight daily changes in the resistances of the glass electrodes used for recording (2-5 MΩ) and stimulating (1-3 MΩ) can partially account for the range of absolute amplitudes of FPs in response to a given stimulus. The recording electrode resistances of 2-5 MΩ were chosen because with electrodes lower than 1 MΩ it became very difficult to detect FPs.

ii) It is probable that the proximity of the recording electrodes to the Purkinje cell layer from which recordings were made was subject to variation and this could influence the detection of Purkinje cell responses and therefore the absolute amplitude of FP responses.

iii) The depth and positioning of the tips of the stimulating electrodes in the molecular layer will affect the number of activated PFs in contact with the Purkinje cells.

iv) The population responses may represent different numbers of Purkinje cells due to slight variations in the distribution of the Purkinje cells in the cerebellum between one animal and the next.

In one study it was reported that the PF volley could contaminate the slope measurement (Chen and Thompson, 1995) however, we did not find this to be the case. In the majority of experiments it was possible to place cursors accurately to measure both amplitude and slope using custom written software. Occasionally it was possible to detect changes in the slope, which were not reflected in the amplitude. It seemed appropriate to show both N2 amplitude and slope for all experiments unless presentation of both provides no additional information to the reader.

It was intended that the extracellular FP recording technique would be used to determine what synaptic conditions were necessary for induction of LTD or LTP in a cerebellar slice preparation. It was of particular interest to establish if PF activation alone was sufficient for LTD. For this reason it was important to try to identify whether or not these FP responses were PF-mediated. It is possible that this method of molecular layer stimulation could activate CFs in addition to recruiting PFs. Therefore, to determine if there was a significant CF contribution to these FP responses an experiment was designed to observe the responses evoked by molecular layer stimulation in CF deafferented rats. The method that has been widely used for destroying the inferior olive involves administration of intraperitoneal injections of 3-AP to produce lesions of the inferior olive. Niacinamide is also administered to protect the rest of the nervous system from lethal toxicity. Harmaline is given to accelerate the metabolic changes in the nucleus of the inferior olive. The degenerative process takes place within 24 hours and if rats are sacrificed 3 days after injection of 3-AP the destruction of the CFs is complete (Sotelo et al., 1975; Llinas et al., 1975; Vigot et al., 1993; Zagrebelsky et al., 1997). In our FP experiments rats aged between 14-21 days were used. Therefore it was necessary to select immature rats 11-12 days old for the 3-AP treatment. Three days after lesion of the inferior olive they would then be the correct age for FP experiments and therefore could be used for experiments for 1 week after treatment. Unfortunately the immature rats did not survive treatment with 3-AP. It did not seem appropriate to repeat this experiment and so it was not possible to completely eliminate the possibility of a CF input to FPs evoked by molecular layer stimulation.

In summary, stable population responses were recorded from the Purkinje cell layer in response to alternate 0.2Hz activation of two stimulating electrodes placed in the molecular layer. In the presence of picrotoxin, FPs displayed two TTX-sensitive; negative-going components termed N1 and N2. The fast potential wave represented the propagation of action potentials along nerve fibres, the PF volley. The slow potential wave was accounted for by the synaptic actions of PFs at excitatory Purkinje cells. The properties of the N2 component described here are entirely consistent with responses that are primarily PF-mediated since they were graded with stimulus strength, underwent paired pulse facilitation and were selectively blocked by CNQX.

CHAPTER 3

THE SYNAPTIC CONDITIONS REQUIRED FOR THE INDUCTION OF LONG TERM DEPRESSION IN AN EXTRACELLULAR FIELD POTENTIAL MODEL

3.1 INTRODUCTION

The aim of the work described in this chapter was to evaluate whether certain conditions of synaptic activation were capable of inducing LTD that could be measured with extracellular recording techniques. As outlined in the general introduction the coincidence of an influx of Ca^{2+} through voltage gated Ca^{2+} channels and the activation of AMPAR and mGluR leads to a long-lasting attenuation of the transmission at PF to Purkinje cell synapses (Linden et al., 1991; Daniel et al., 1992; Hemart et al., 1994; Hartell, 1994b; Hemart et al., 1995; Hartell, 1996b). Until recently, it was thought that these conditions were met by combined PF and CF activation since separate stimulation of these inputs failed to induce LTD (Ito and Kano, 1982; Ekerot and Kano, 1985; Chen and Thompson, 1995).

There is now evidence to suggest that a form of LTD can be induced by the strong activation of PFs alone (Hartell, 1996b). PF stimulation has been shown to cause a Ca^{2+} influx in localised, small branches of the Purkinje cell dendritic tree following the activation of AMPARs (Eilers et al., 1995; Eilers et al., 1997b).

Antibodies against the mGluR1 subtype of mGluRs that is abundant in cerebellar Purkinje cells blocked the induction of LTD (Shigemoto et al., 1994). To produce LTD PF stimulation can be substituted by iontophoretic application of glutamate or quisqualate to Purkinje cell dendrites combined with CF activation (Kano and Kato, 1987). Similarly, Purkinje cell depolarisation paired with application of glutamate was sufficient to produce LTD in cultured

Purkinje cells (Linden et al., 1991). In addition, LTD of PF-EPSPs that was induced when CF stimulation was replaced with injection of 8-Br-cGMP and paired with 1Hz PF stimulation was blocked in the presence of MCPG. Therefore, there is evidence to suggest that low frequency stimulation of PFs might activate postsynaptic mGluRs.

Increased frequency and intensity PF stimulation might cause sufficient glutamate release to activate voltage gated Ca^{2+} channels, AMPARs as well as mGluRs and therefore alone fulfil the requirements for LTD. Measurements of NO with an electrochemical probe at the surface of the molecular layer of cerebellar slices have shown that repetitive electrical stimulation triggers NO release (Shibuki and Kimura, 1997; Kimura et al., 1998). Based upon immunohistochemical and *in situ* hybridisation studies (Bredt et al., 1990; Vincent and Kimura, 1992; Crepel et al., 1994) the PFs represent a probable source of NO. It was also found that LTD could be induced by replacing PF stimulation with caged release of NO and depolarising the Purkinje cell at the same time (Lev Ram et al., 1995). These pieces of evidence imply that certain parameters of PF stimulation could lead to both NO release and Ca^{2+} influx and together these elements could induce a LTD of PF-EPSCs (Lev Ram et al., 1995).

Based on the above findings it was hypothesised that the activation of the molecular layer at a raised stimulus intensity and increased frequency could alone fulfil the conditions for a form of LTD that could be detected using extracellular recording techniques.

The objectives of this chapter were:-

i) to examine what synaptic conditions were necessary to induce a LTD of FP responses

ii) to consider how the parameters of raised stimulus intensity and increased frequency activation of the molecular layer might influence the events at PF-Purkinje cell synapses

iii) to observe the extent of input specificity of this extracellularly detected form of LTD.

To detect subtle long-term changes in the FP waveforms it was essential to confirm that stable responses could be recorded using this extracellular FP recording system. Therefore the amplitudes and slopes of the N2 component and the amplitudes of the N1 component were carefully monitored for 60 minute periods. The effects of raised stimulus intensity (RS), increased frequency (IF) and combined raised stimulus intensity and increased frequency (RSIF) stimulation of the molecular layer were then investigated.

3.2 METHODS

3.2.1 SLICE PREPARATION

The majority of experiments were performed in sagittal slices that were prepared as described in chapter 2.2.1. In some experiments transverse slices were used that were prepared in the same way but with the following exceptions. Following dissection the cerebellum was placed on an agar block and the remains of the brain stem were dissected away. The vermis was isolated by two parasagittal cuts made on either side. The cerebellum was rolled forward and transferred to a pre-glued block (cyanoacrylate RS components) so that the ventral vermis was lying down onto the glue. 200 μm thick transverse slices were cut from the cerebellar vermis in ACSF maintained below 4°C as shown in figure 3.2.1 and then transferred to an incubation chamber.

3.2.2 FIELD POTENTIAL RECORDING

In both the sagittal and the transverse slices FP responses were obtained according to the methods described in chapter 2.2.2. In transverse slices the FP responses generally had larger PF volleys than those recorded in sagittal slices. A possible explanation for this difference is that in sagittal slices the PFs were truncated during the cutting process whereas in transverse slices the PFs remain more intact. In sagittal slices a smaller volume of PFs would be activated by the same stimulus intensity. Therefore, it is likely that in transverse slices a greater number of uncut PFs are recruited by molecular layer stimulation. An illustration of the positioning of stimulating and recording electrodes in the transverse slice and an example of the appearance of a characteristic FP waveform recorded in a transverse slice are shown in figure 3.2.1.

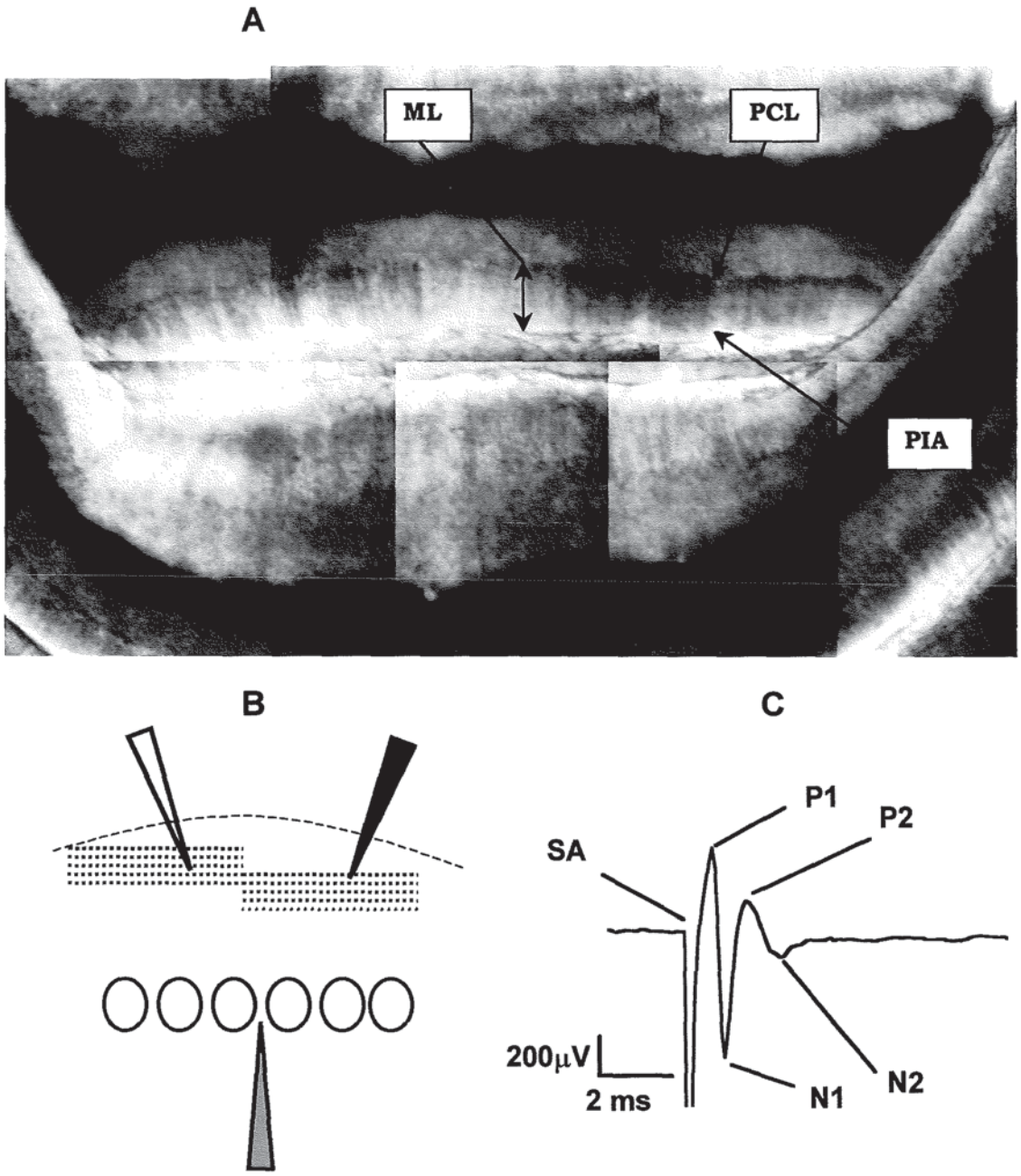

Figure 3.2.1 Field potential responses recorded from transverse slices of cerebellar vermis

A represents a composite bright field image of a transverse slice of cerebellar vermis. The images were taken using a cooled digital CCD camera (Hamamatsu) attached to an upright microscope (Olympus BX50WI) using approximately 20 times overall magnification. The arrows indicate the molecular layer (ML), Purkinje cell layer (PCL) and pial surface (PIA) of the cerebellar slice, respectively.

B is an illustration of the positioning of the stimulating and recording electrodes in the transverse slice. The recording electrode, shaded in grey, was placed in the Purkinje cell layer and the stimulating electrodes shaded in black and white, were placed in the molecular layer midway towards the pial surface of the slice. PFs that innervate the dendritic field of the Purkinje cells are represented by the black dotted lines.

C shows the characteristic appearance of a FP response recorded in a transverse slice. The trace represents the average of 10 FP responses collected at 5s intervals. The stimulus artefact (SA) was followed by a fast triphasic component P1-N1-P2 and a slower negative-going component termed N2. Scale bar 200μV, 2ms.

3.2.3 FLUORESCENCE IMAGING

In a few experiments fluorescence microscopy was used to estimate the distance between the test and control stimulating electrodes. The water-soluble fluorescent indicators, Lucifer yellow and Fura-2, that have distinguishable excitation and emission properties were chosen. The tips of the stimulating electrodes were filled with 2-3μl of fluorescent dye (100 μM Lucifer yellow in one and 200 μM Fura-2 in the other) and back-filled with ACSF. At the end of the experiment the stimulating electrodes were activated for 2 minutes at a high frequency, with 200 ms, -80 V pulses. Due to the ionic nature of the fluorescence indicators, the negative voltage pulse and the negative charge on the dye repelled each other and forced some of the dye to pass out of the pipette tip. In some cases the slices were fixed with a 1 % glutaraldehyde solution and kept in foil covered glass vials in the refrigerator for 24-48 hours before observation. It was possible to locate where each stimulating electrode had been positioned by detecting the two regions of fluorescence at different excitation and emission wavelengths. Standard filter blocks for calcium green and Fura-2 were used. The excitation wavelength used for Lucifer yellow was 427 nm and for Fura-2 a wavelength of 335nm was used. Images of the regions of Lucifer yellow and Fura-2 fluorescence were collected using an upright microscope (Olympus BX50WI) and a digital cooled CCD camera (Hamamatsu). The two separate images of each dye were then merged to produce a composite image. The distance between the peak intensities of the two regions was measured in pixels and then calibrated to give the approximate electrode separation in microns. It was also possible to view the 3-D and 2-D profiles of the fluorescent regions to identify the peak fluorescence intensity for each region see figures 3.3.13 and 3.3.16.

3.3 RESULTS

3.3.1 STABLE FIELD POTENTIAL RESPONSES WERE RECORDED FOR A 60 MINUTE PERIOD

In order to detect long-term changes in the N2 and N1 components of FP responses it was necessary to check that stable responses could be recorded in drug-free ACSF for long periods. The N2 and the N1 components were therefore monitored for an hour or more to confirm that the FP responses were stable. Alternate 0.2Hz activation of the two stimulating electrodes placed in the molecular layer produced extracellular FP responses that were stable for at least 60 minutes as shown in figures 3.3.1 and 3.3.2. There was no obvious change in the N2 or N1 components of FP responses for the duration of the recording. After 40 minutes the average N2 amplitudes in each pathway (% $\pm$ S.E.M) were 102.9 $\pm$ 3.5 and 104.4 $\pm$ 3.3%, respectively showing no significant change when compared to baseline levels (N = 6, Wilcoxon Matched-Pairs test $p>0.05$). The N2 slopes and N1 amplitude were also stable for the duration of the recording and were not significantly different from the baseline level (Wilcoxon Matched-Pairs test $p>0.05$). Paired pulses were delivered at 40 ms intervals in three of the recordings. The PPR remained constant throughout these recordings. The paired pulse stimulation protocol consequently did not appear to alter the stability of the FP responses.

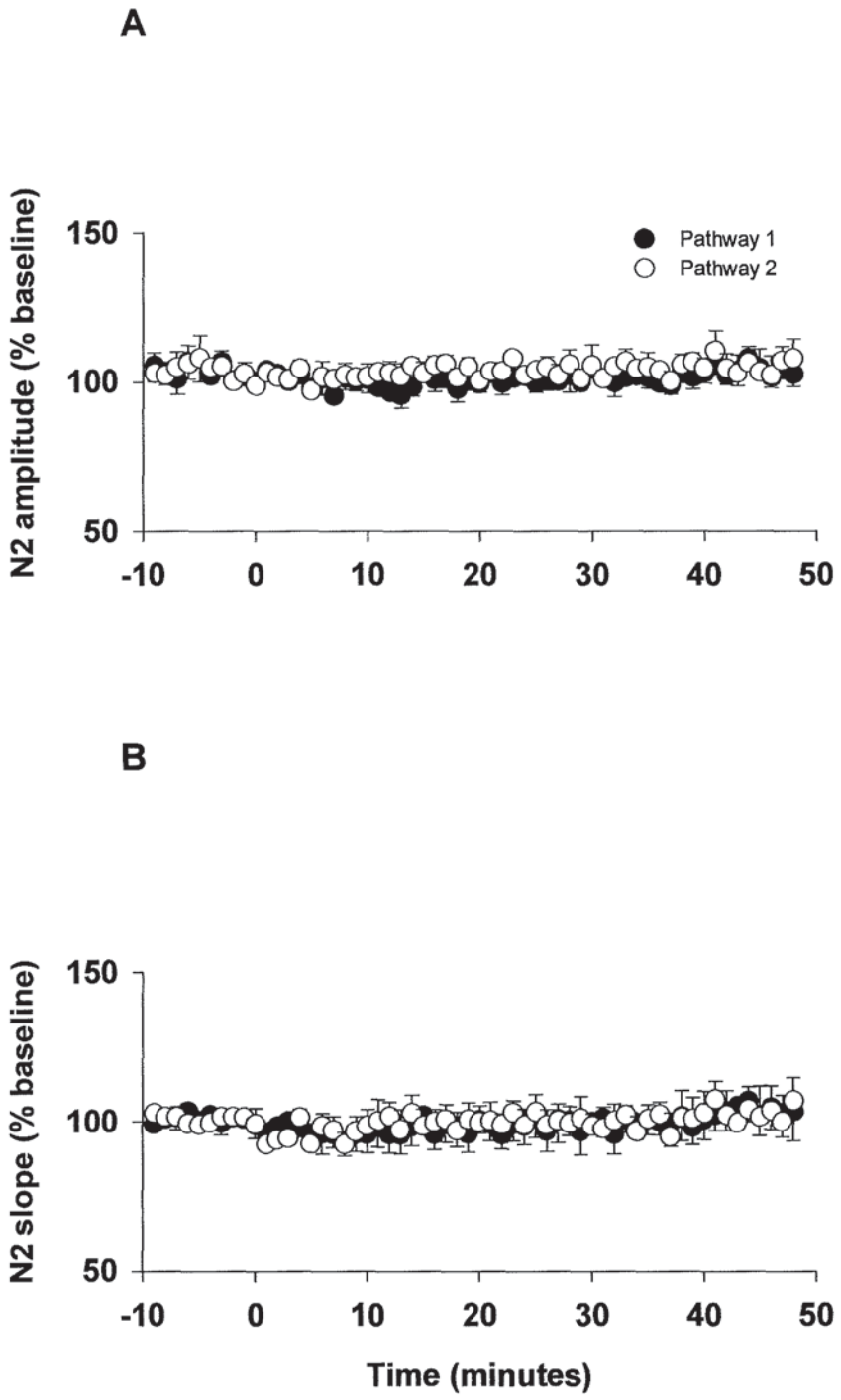

Figure 3.3.1 Stable field potential responses were recorded for a 60 minute period
Graphs A and B illustrate the FP N2 amplitude and slope, respectively. Data are expressed as the mean % ± S.E.M. of 10 responses collected during a 10 minute baseline period. N = 6 paired recordings. Closed circles, pathway 1 (s0); open circles, pathway 2 (s1).

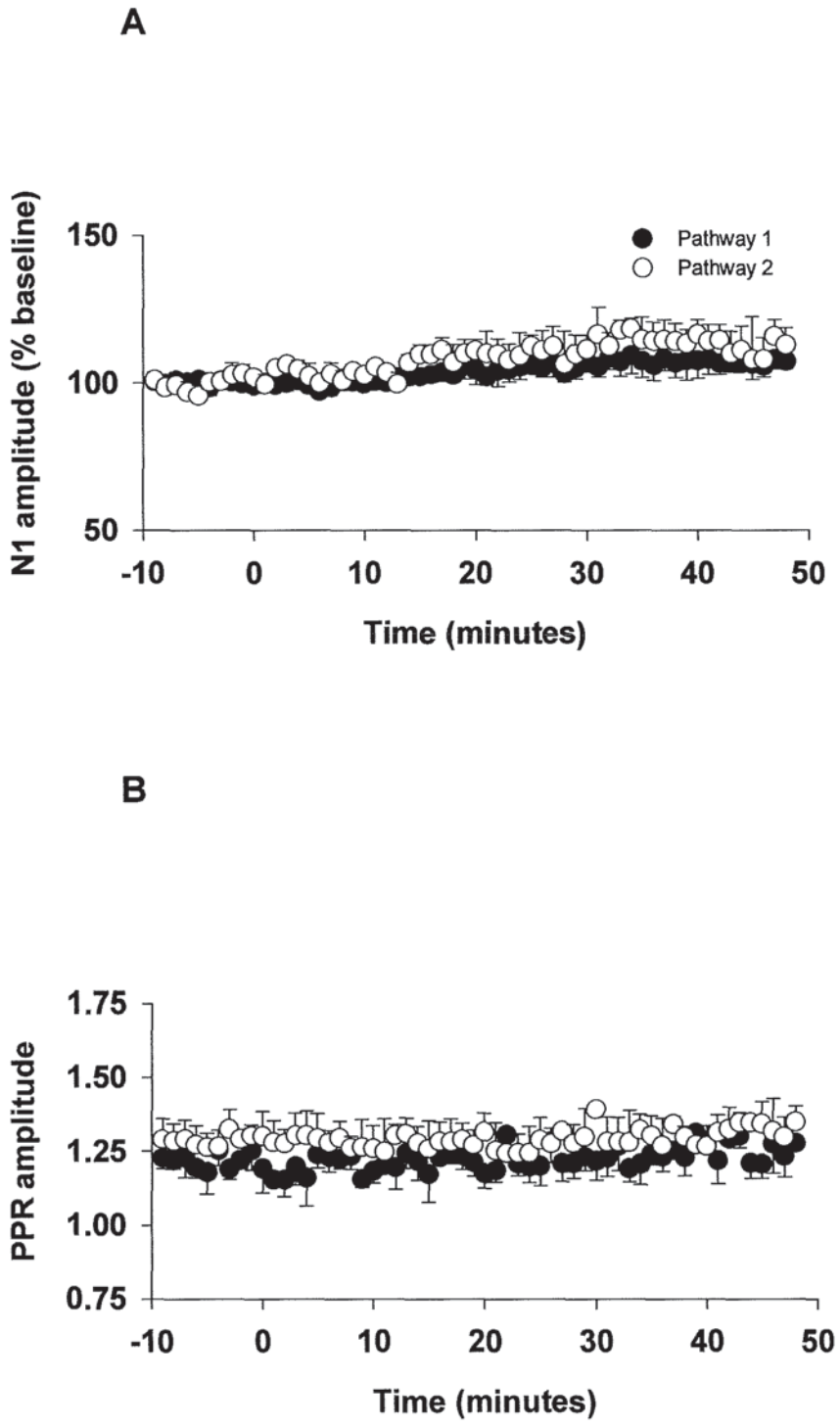

Figure 3.3.2 Stable field potential responses were recorded for a 60 minute period
Graphs A and B illustrate the FP N1 amplitude and amplitude of the PPR, respectively. Data are expressed as the mean % ± S.E.M. of 10 responses collected during a 10 minute baseline period. The amplitude of the PPR data represents N = 3 of the total group of stability recordings in which paired pulses were delivered at 40ms intervals. Closed circles, pathway 1 (s0); open circles, pathway 2 (s1).

3.3.2 EFFECT OF A 5 MINUTE PERIOD OF EITHER INCREASED FREQUENCY (IF) OR RAISED INTENSITY (RS) STIMULATION ON FIELD POTENTIAL RESPONSES

The effect of changing the parameters of molecular layer stimulation for 5 minutes on the appearance of the N2 and N1 components of FP responses was examined. The frequency of molecular layer stimulation was increased from 0.2 to 1Hz for 5 minutes (IF) in the test pathway as shown in figure 3.3.4. Stimulation to the control pathway was stopped during this period. During the IF stimulation period the test pathway N2 amplitude, slope and the N1 amplitude were briefly reduced. The data were grouped according to the incidence of changes in synaptic efficacy in the amplitude of the N2 component 35 minutes after stimulation. The three groups were designated:-

i) LTD if the amplitude or slope was less than or equal to 80%.

ii) LTP if the amplitude was greater than or equal to 120% and

iii) No change (NC) if the amplitude was between 81 and 119%.

35 minutes after stimulation was resumed at 0.2Hz there was no change evident in the test N2 amplitude in 4 recordings and in 1 recording the FP underwent LTP as shown in the pie chart in figure 3.3.3. For the pooled data, there was no significant difference between the test and control N2 amplitudes 103.4 $\pm$ 11.4 and 112.4 $\pm$ 8.0% of baseline levels, respectively (N = 5, Wilcoxon Matched-Pairs test $p>0.05$). Although the control pathway was not activated at 1Hz the amplitudes of both N1 and N2 appeared to increase slightly after IF stimulation to the test pathway. The N1 amplitude reached 115.7 $\pm$ 11.4% of the baseline level 35 minutes after IF stimulation.

In six recordings the stimulus intensity to the test pathway was raised for 5 minutes (RS) to increase the N2 amplitude or slope to at least 50% above the baseline level as shown in figure 3.3.5. Stimulation to the control pathway was stopped during this period. 35 minutes after stimulation was resumed at 0.2Hz LTD was induced in the test N2 in only 1 out of six separate recordings. In the remaining 5 cases the amplitude of the N2 component was reduced but not below the 80% cut off level and therefore these 5 recordings were classed

as undergoing no change (Figure 3.3.3). The tendency for the test pathway to decrease was more prominent in the slope measurement of the N2 component. However, there was no significant difference between the test and control average N2 amplitudes which were 94.2 ± 5.7 and 88.0 ± 10.9% of the baseline level, respectively (N = 6, Wilcoxon Matched-Pairs test $p>0.05$) after 35 minutes. Little or no change in the N1 amplitude in either pathway was observed over the duration of the recordings.

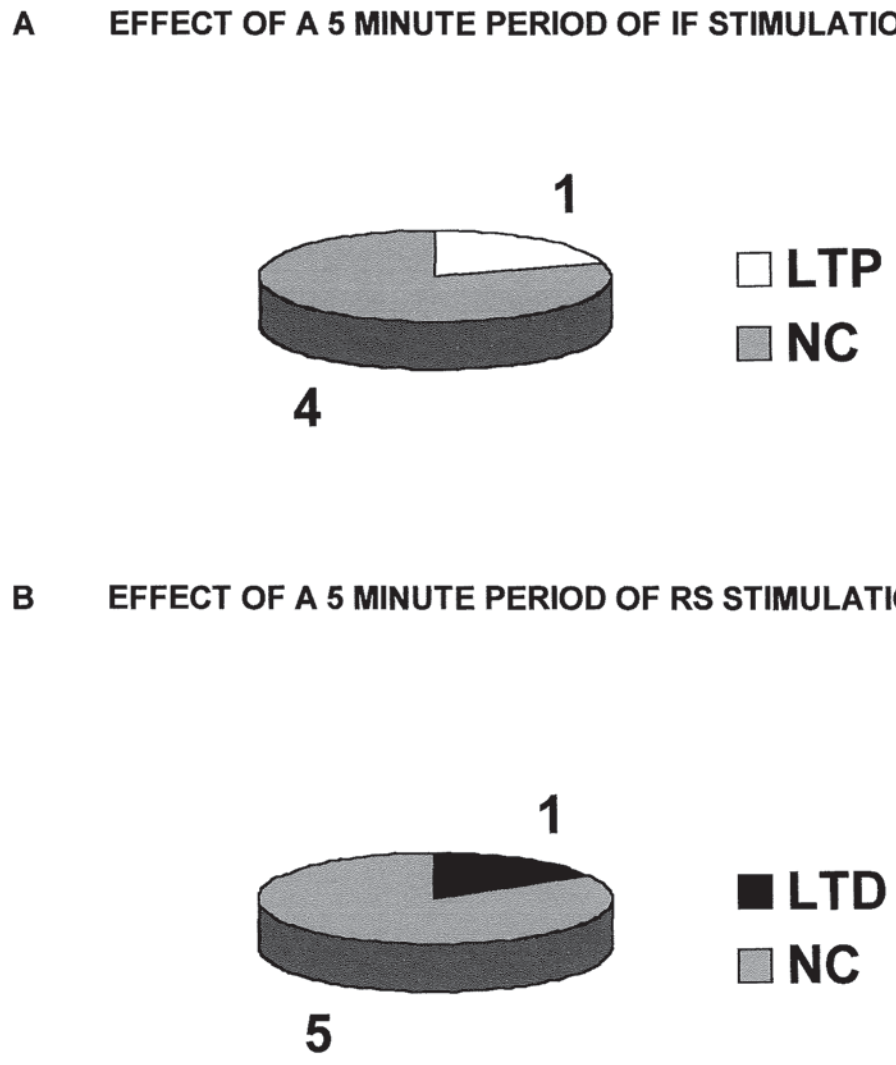

Figure 3.3.3 Effect of a 5 minute period of increased frequency (IF) or raised stimulus intensity (RS) stimulation
Pie charts A and B illustrate the incidence of LTD, LTP and no change (NC) in the amplitude of the N2 component of FPs as measured 35 minutes after IF or RS stimulation, respectively.

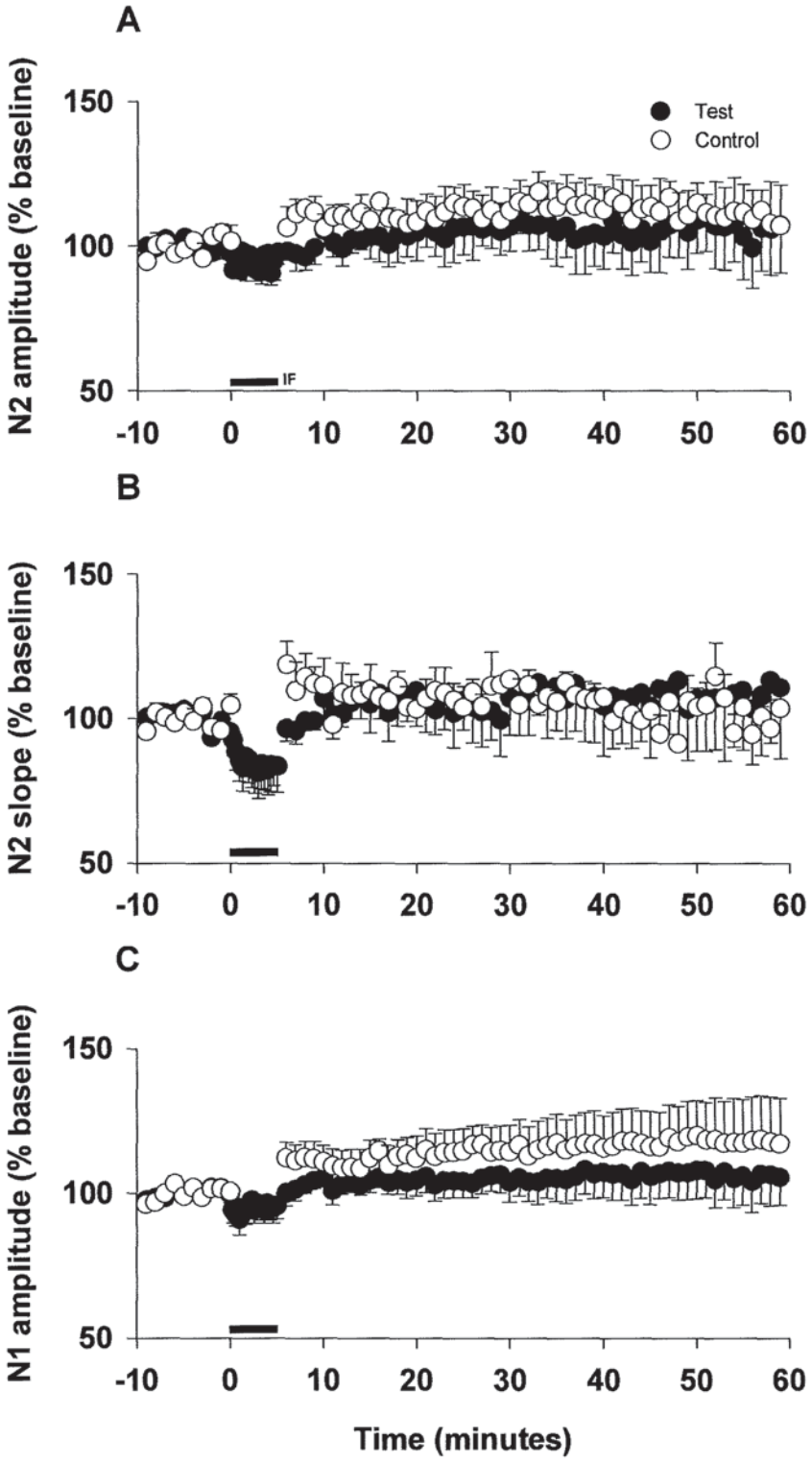

Figure 3.3.4 Effects of a 5 minute period of increased frequency stimulation (0.2 to 1Hz) on field potential responses

Graphs A – C illustrate the FP N2 amplitude, slope and N1 amplitude, respectively. Data are expressed as the mean % ± S.E.M. of 10 responses collected during a 10 minute baseline period. N = 5 paired recordings. Closed circles, test pathway stimulated at 1Hz for 5 minutes; open circles, control pathway. Horizontal black bar indicates the period of increased frequency stimulation.

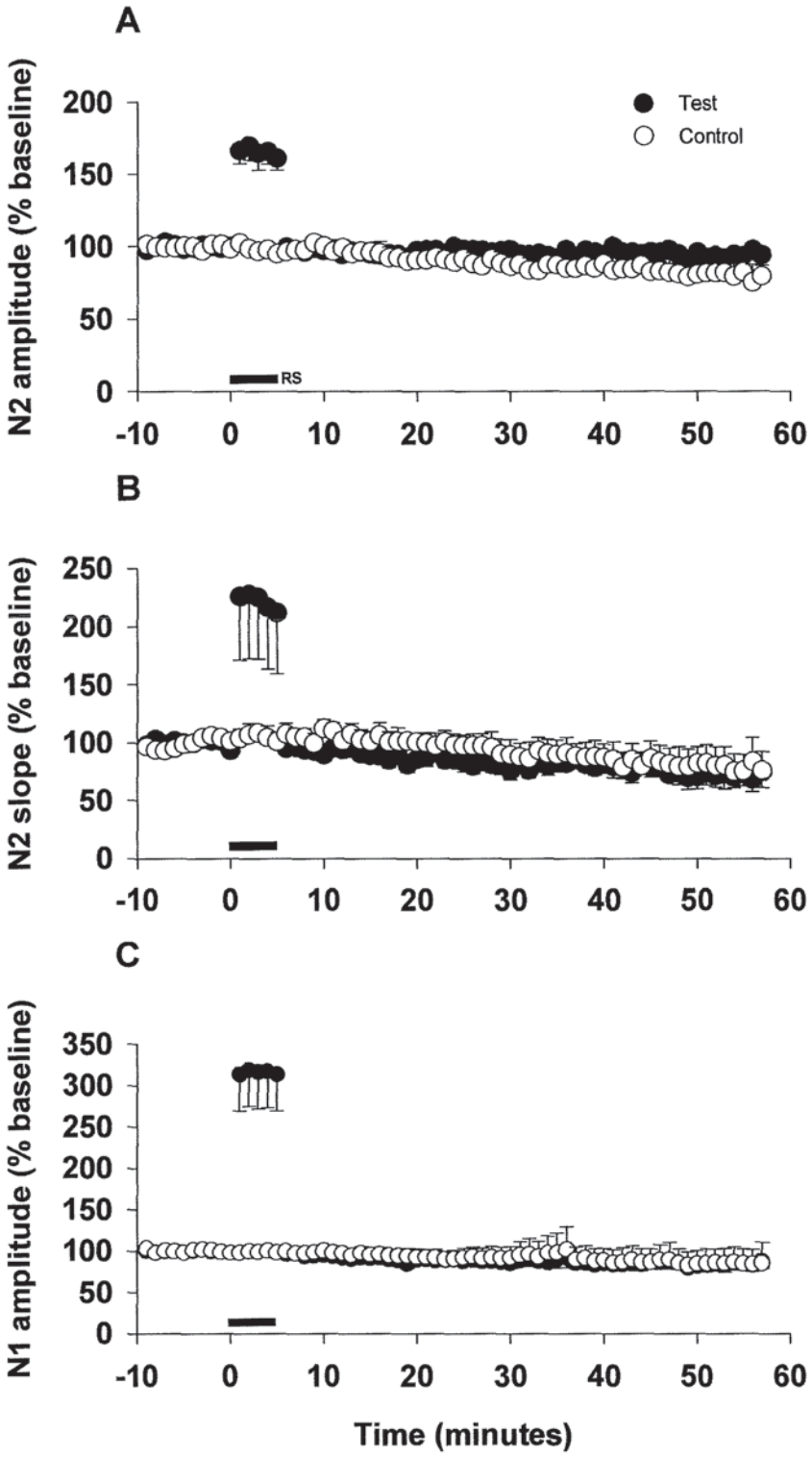

Figure 3.3.5 Effects of a 5 minute period of raised intensity stimulation on field potential responses

Graphs A – C are as shown in figure 3.3.4. N = 6 paired recordings. Closed circles, test pathway stimulated at raised stimulus intensity for 5 minutes; open circles, control pathway. Horizontal black bar indicates the period of raised stimulus intensity.

3.3.3 EFFECT OF PAIRING RAISED STIMULUS INTENSITY AND INCREASED FREQUENCY (RSIF) STIMULATION FOR 5 MINUTES ON FIELD POTENTIAL RESPONSES IN SAGITTAL SLICES

In sagittal slices the RS and IF parameters of stimulation were, alone, not sufficient to induce a robust LTD of FP responses. Therefore in the next set of experiments the effect of combining the two parameters was examined. In 18 recordings the effect of activating the molecular layer at a raised stimulus intensity and increased frequency (RSIF) for 5 minutes was observed. Stimulation to the control pathway was again stopped during this period. The experiments were sorted into groups according to the test pathway N2 amplitude measured 35 minutes after the RSIF stimulation period using the criteria outlined in section 3.3.2. The justification for grouping data in this way was that it was then possible to look at the paired test and control data to determine the level of input specificity when plasticity did occur. In the test pathway an input-specific LTD was induced in 9/18 of the recordings, 4 recordings displayed LTP and in the remaining 5 cases there was no obvious change.

Figures 3.3.6 and 3.3.7a show the group of data in which an input-specific LTD was observed. See also the example traces in figure 3.3.7b. Immediately after the RSIF stimulation, both the amplitudes and the slopes of the test pathway N2 component fell below baseline levels. A Wilcoxon Matched-Pairs test was performed to determine the level of significance between the test and control pathways. The depression of the amplitude of N2 reached levels of 73.6 $\pm$ 7.1% within 35 minutes of stimulation which was significantly different to the control pathway which was 125.0 $\pm$ 19.8% of the baseline level ($N = 9$, $p<0.01$). In the control pathway 35 minutes after stimulation LTP was observed in 3 recordings and in the remaining 6 cases there was no change relative to baseline levels. Little or no change was noted in the amplitude of N1 in either the test or control pathway for the remainder of the recording. The RSIF stimulation paradigm caused a transient reduction in the amplitude of the PPR similar to that observed following IF stimulation. There was a suggestion that the amplitude of the PPR but not the slope of the PPR increased after RSIF stimulation, but this was not significant. In the control pathway, both the amplitude and slope of the PPR remained stable for the duration of the recording.

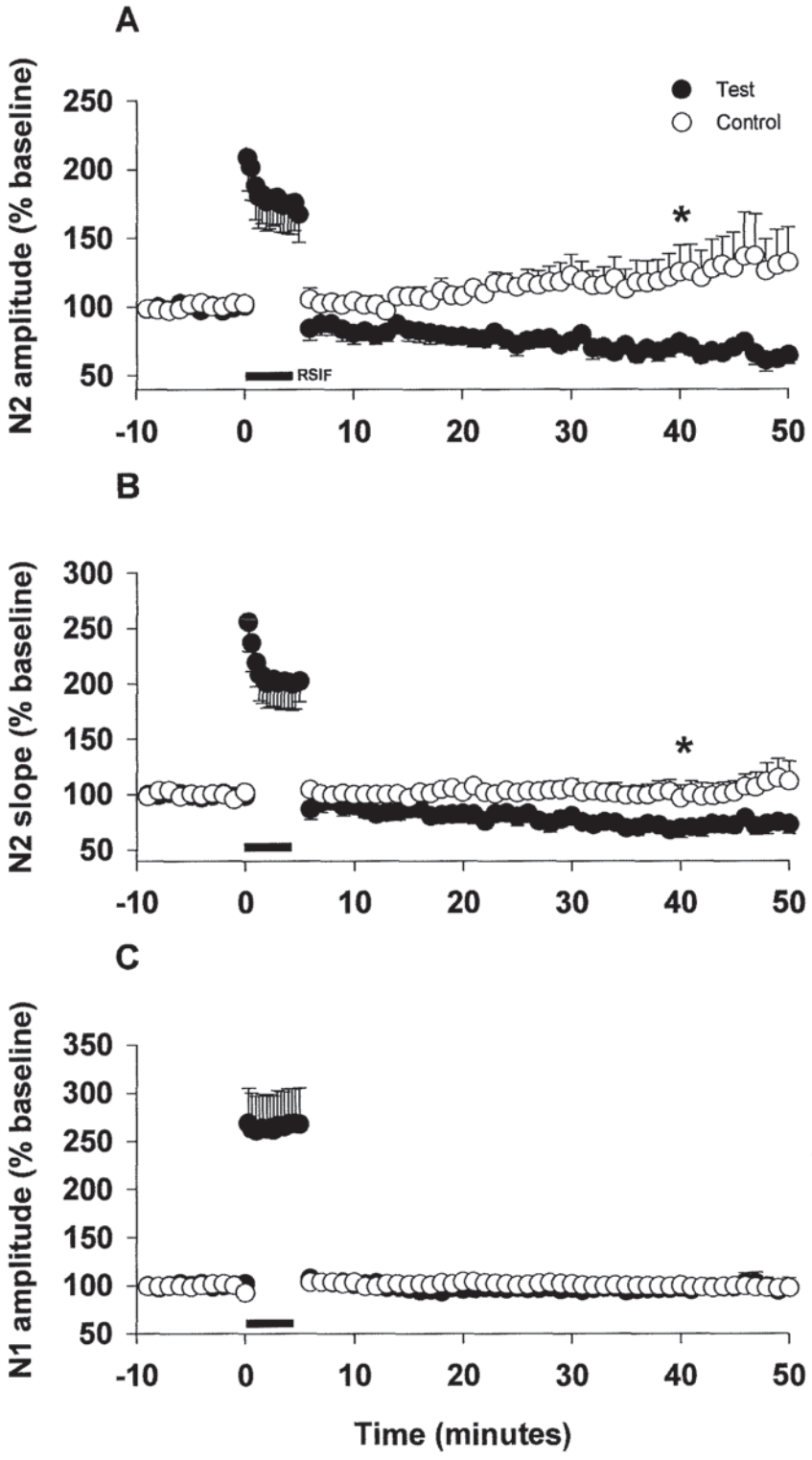

Figure 3.3.6 Graphs show the group of data in which an input-specific long term depression was observed following a 5 minute period of RSIF stimulation

Graphs A - C illustrate the FP N2 amplitude, N2 slope and N1 amplitude, respectively. Data are expressed as the mean % + S.E.M. of 10 responses collected during a 10 minute baseline period. N = 9 paired recordings. Closed circles, test pathway stimulated at RSIF for 5 minutes; open circles, control pathway. Horizontal black bar indicates the period of RSIF stimulation. Asterisks indicate where a significant difference was observed between test and control pathways (Wilcoxon Matched-Pairs test $p<0.05$).

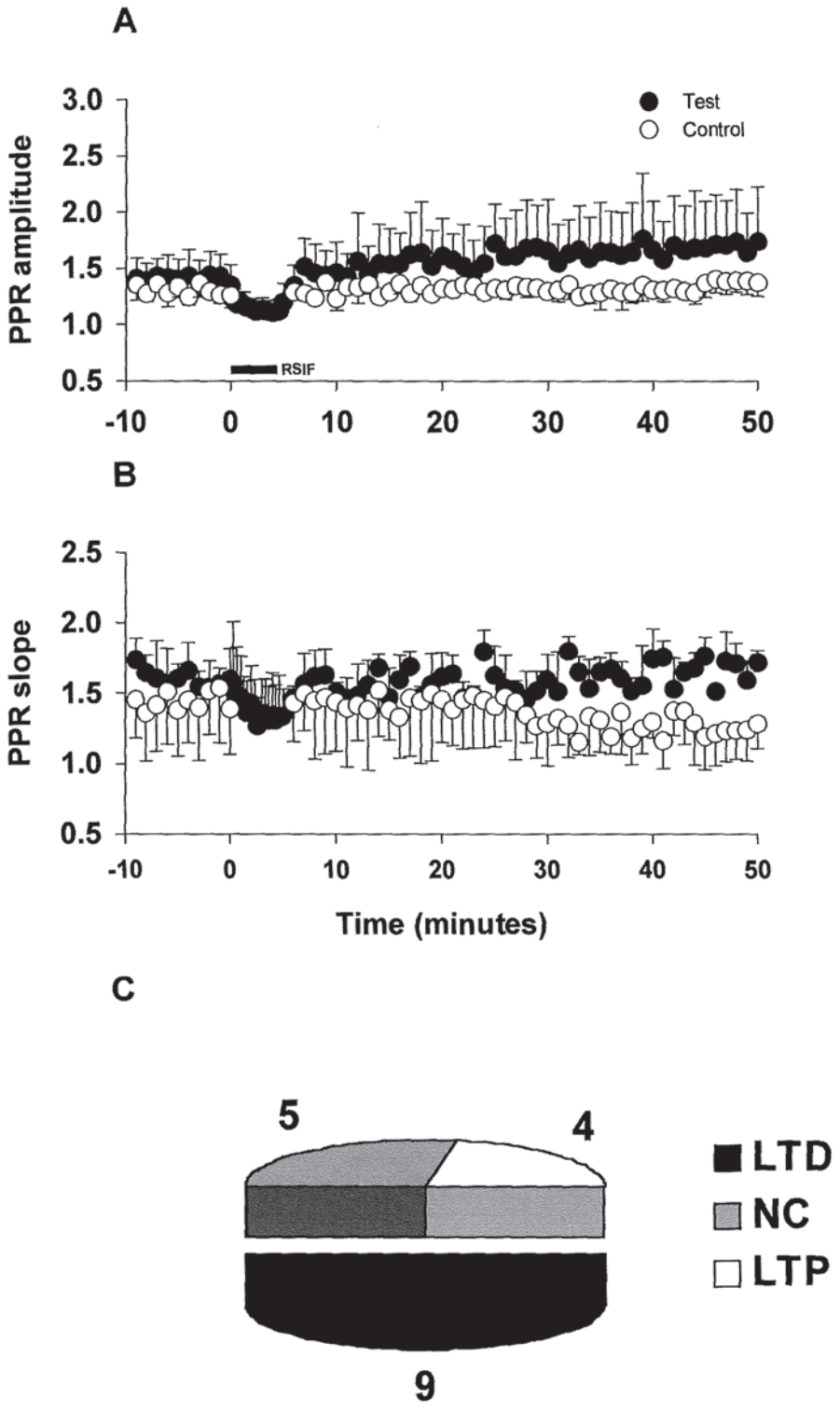

Figure 3.3.7a Graphs shows the group of data in which an input-specific long term depression was observed following a 5 minute period of RSIF stimulation, pie chart represents the incidence of synaptic change for the whole set of data as measured 35 minutes after RSIF stimulation

Graphs A and B illustrate the amplitude and slope of the PPR, respectively. Data are expressed as the mean % ± S.E.M. of 10 responses collected during a 10 minute baseline period. N = 9 paired recordings. Closed circles, test pathway stimulated at RSIF for 5 minutes; open circles, control pathway. Horizontal black bar indicates the period of RSIF stimulation. Pie chart C represents the incidence of LTD, LTP and no change in the test N2 amplitude measured 35 minutes after stimulation for the whole set of data (18 experiments).

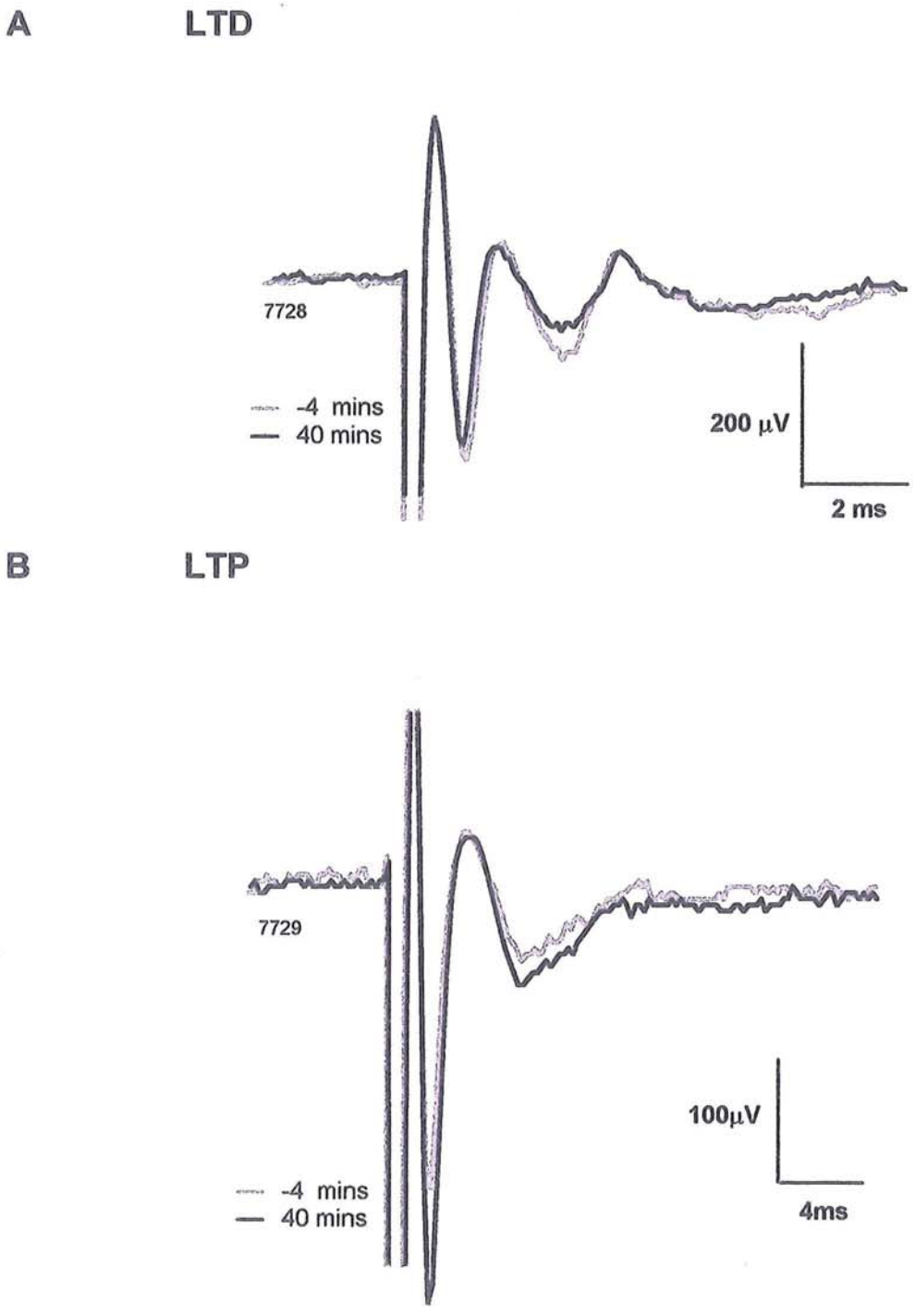

Figure 3.3.7b Effect of RSIF stimulation on field potential responses
Panels A and B, respectively show examples of where LTD or LTP were induced within 40 minutes of RSIF stimulation. The baseline FP response is plotted in grey and the appearance of the FP response 40 minutes after RSIF stimulation is shown in black. Panel A scale bar 200μV, 2ms. Panel B scale bar 100μV, 4ms.

Figure 3.3.8 shows the average of the group of 4 recordings in which a LTP reaching levels of 123.2 ± 12.5% of the baseline level was observed in the test pathway N2 amplitude 35 minutes after RSIF stimulation. See also example traces in figure 3.3.7b. In 3 recordings the LTP in the test pathway was input-specific but in one case the control pathway was also potentiated. After stimulation, the amplitude of N1 increased slightly in the test pathway, indicating that the LTP observed in this group could be due to an increased number of PFs recruited by molecular layer stimulation. The amplitude of N1 showed little or no change for the duration of the recording in the control pathway. PPR data was not collected for these 4 experiments.

Figures 3.3.9 and 3.3.10 illustrate the 5 recordings in which no change was observed in either test or control pathways following RSIF stimulation of the test pathway. The N2 amplitude, slope and N1 amplitude showed no significant change from baseline levels when the stimulation was resumed at 0.2Hz. 35 minutes after stimulation, the N2 amplitudes of the test and control pathways were 98.1 ± 3.4 and 88.1 ± 1.7% of the baseline level N = 5, respectively. RSIF stimulation caused a decrease in the amplitude of the PPR in the test pathway; this did not completely recover after stimulation. In the control pathway the amplitude of the PPR showed no obvious change for the duration of the recording.

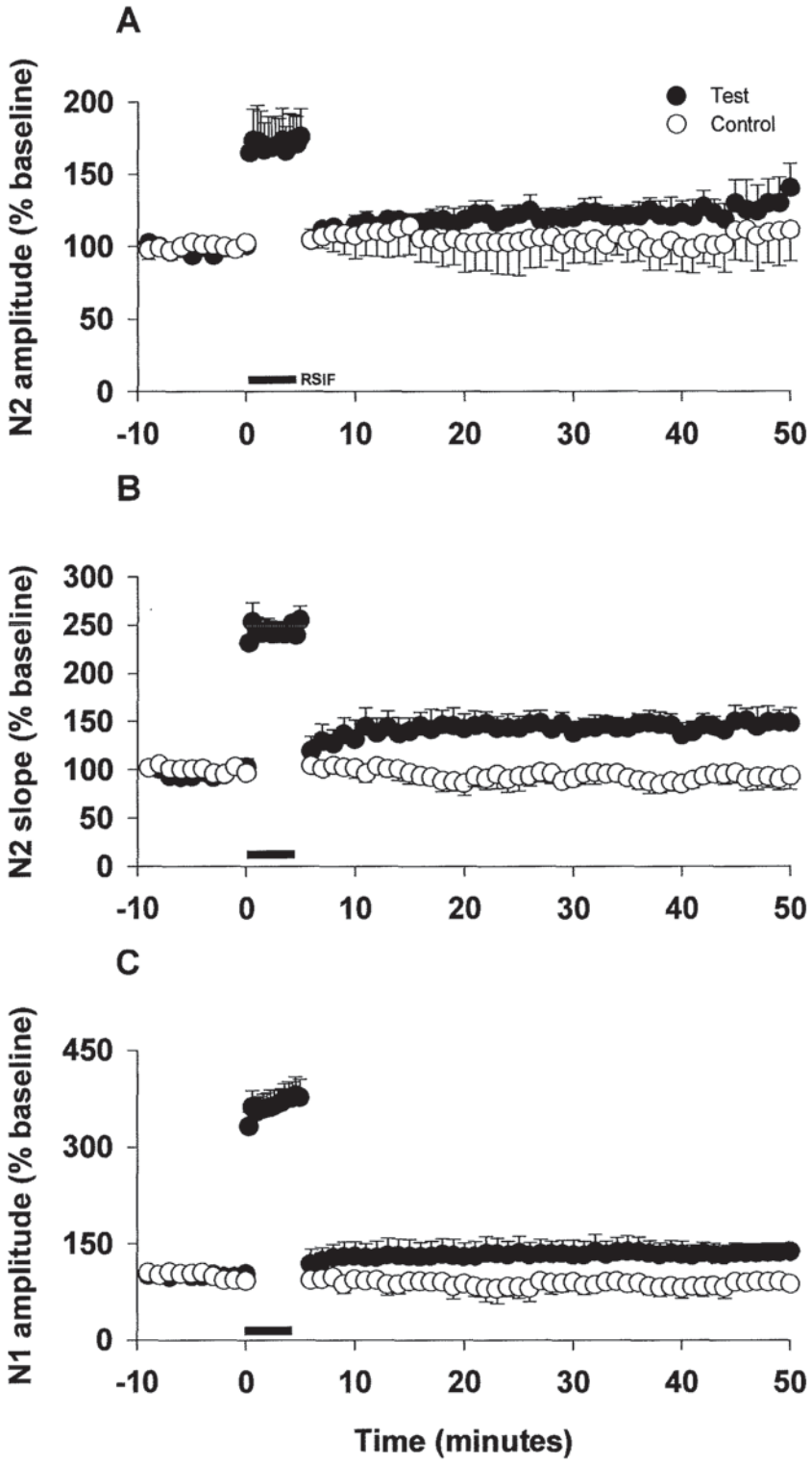

Figure 3.3.8 Graphs show the group of data in which long term potentiation was observed following a 5 minute period of RSIF stimulation
Graphs A – C are as shown in figure 3.3.6. N = 4 paired recordings.

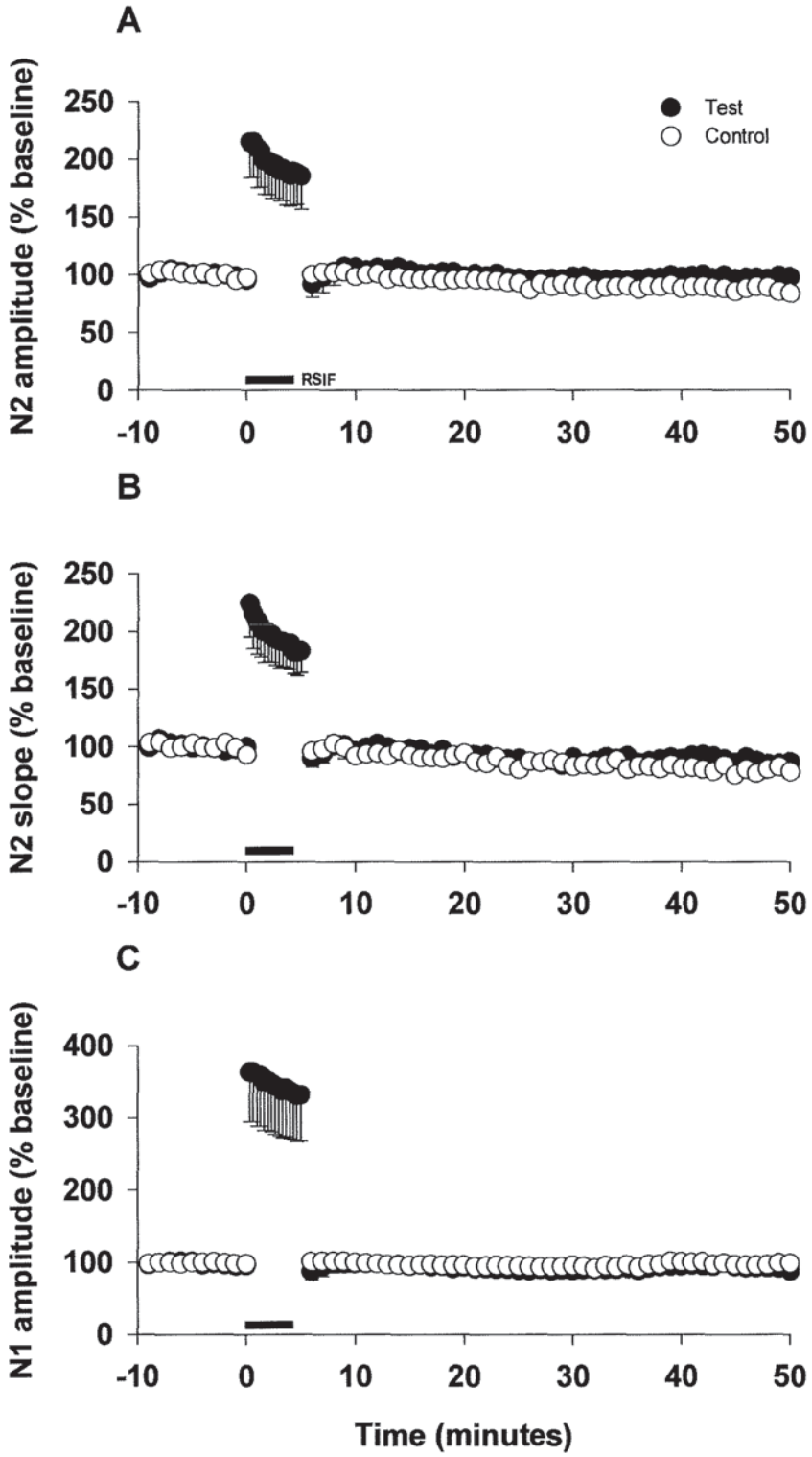

Figure 3.3.9 Graphs show the group of data in which no change was observed following a 5 minute period of RSIF stimulation

Graphs A - C are as shown in figure 3.3.6. N = 5 paired recordings.

A

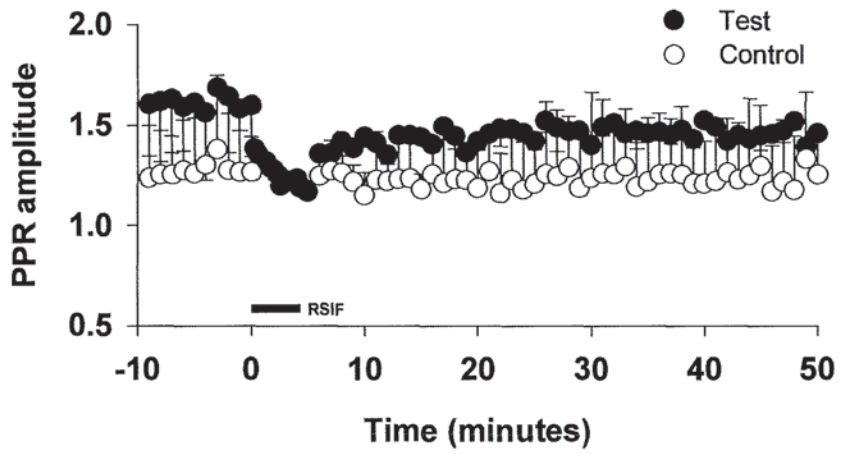

B

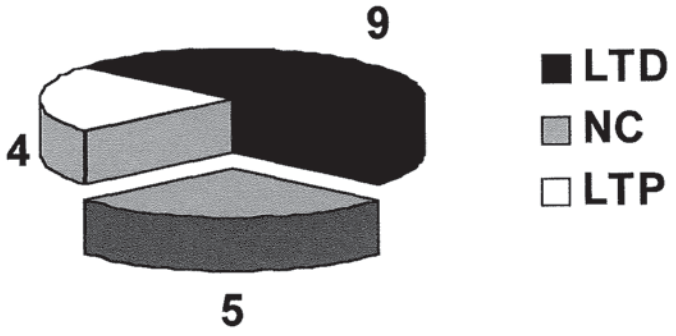

Figure 3.3.10 Graph shows the group of data in which no change was observed following a 5 minute period of RSIF stimulation, pie chart represents the incidence of synaptic change for the whole set of data as measured 35 minutes after RSIF stimulation

Graph A and pie chart B are as shown in figure 3.3.7. N = 5 paired recordings.

When the stimulus intensity was raised, the stimulus voltage was increased until the amplitude of the N2 component increased to at least 50% above the baseline level. It is possible that the baseline responses before stimulation or the level of raised intensity stimulation was, in some way, different between the RS and RSIF experiments and could explain the different incidences of LTD, LTP and no change. Bar charts were constructed for the RSIF and RF experiments and the groups of recordings in which LTD, LTP or no change were observed 35 minutes after RSIF stimulation. Single factor analysis of variance (ANOVA) tests were then performed to compare: i) the mean $\pm$ S.E.M baseline amplitude or slope of the N2 component measured 5 minutes before stimulation and ii) the % increase in the the amplitude and slope of the N2 component at the start of stimulation.

No significant difference was found in either the size of the N2 responses at baseline (see figure 3.3.11) or in the % increase in the N2 component at the start of stimulation between the RS and RSIF experiments (Single factor ANOVA, $p>0.05$). Equally, neither the baseline level as measured 5 minutes before RSIF stimulation nor the % increase in N2 at the start of RSIF stimulation see figure 3.3.12 were significantly different among the recordings in which LTD, LTP and no change were observed (Single factor ANOVA, $p>0.05$). Therefore we suspect that the incidence of LTD, LTP and no change 35 minutes after RS or RSIF stimulation did not directly relate to a particular starting amplitude or slope of the N2 responses or to differences in the level of raised intensity stimulation during the RS or RSIF paradigms.

In four experiments the stimulating electrodes used to activate the molecular layer to evoke FP recordings were filled with either Lucifer yellow or Fura-2. At the end of the experiment the stimulating electrodes were activated for 2 minutes at a high frequency to encourage fluorescent dye to pass out of the tip of the electrodes. An upright microscope and a digital cooled CCD camera were used to collect images of the two regions of fluorescence in the sagittal slices of cerebellar vermis. The 2-D and 3-D profiles of the fluorescent regions were then used to estimate the distance between the stimulating electrodes. The distance between the electrodes was found to range between 40 and 100μm. An example is shown in figure 3.3.13.

A **Amplitude of N2 responses recorded at baseline measured 5 minutes before stimulation**

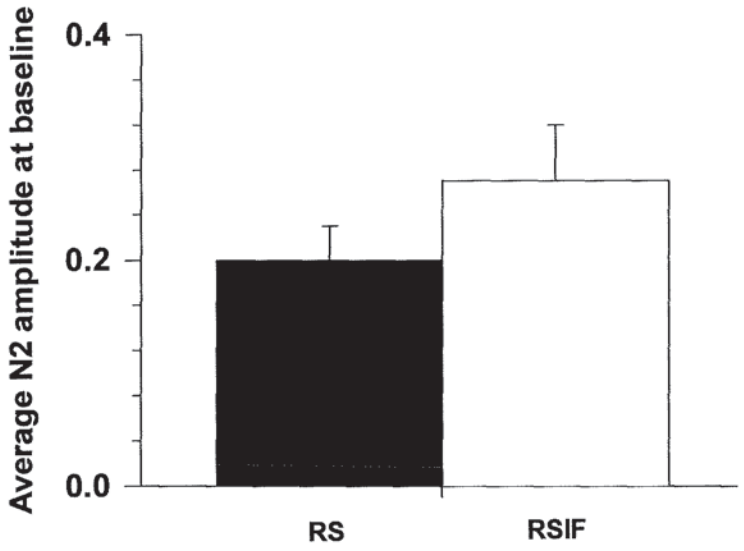

B **Slope of N2 responses recorded at baseline measured 5 minutes before stimulation**

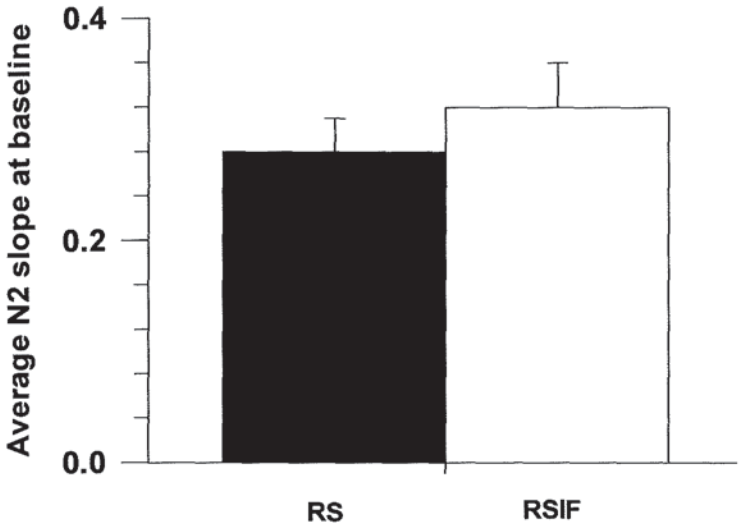

Figure 3.3.11 A comparison between the mean absolute amplitude (mV) or slope (mV/ms) of N2 at baseline as measured 5 minutes before RS or RSIF stimulation

Bar charts A and B show the mean absolute amplitude (mV) or slope (mV/ms) of N2 at baseline as measured 5 minutes before RS or RSIF stimulation, respectively. Black bars show N = 6 experiments in which RS stimulation was applied for 5 minutes; White bars represent N = 18 recordings in which RSIF stimulation was applied for 5 minutes. Single factor analysis of variance tests did not detect any difference between these groups.

A **% increase in the amplitude of N2 responses recorded at the start of RSIF stimulation**

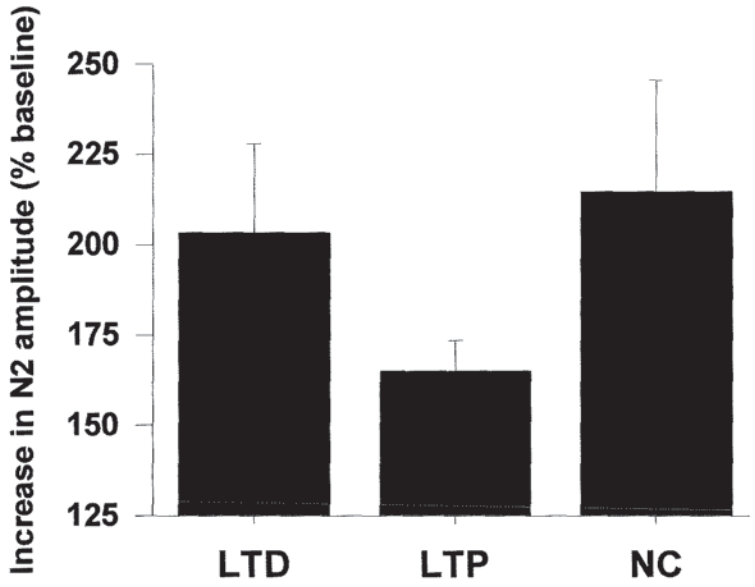

B **% increase in the slope of N2 responses recorded at the start of RSIF stimulation**

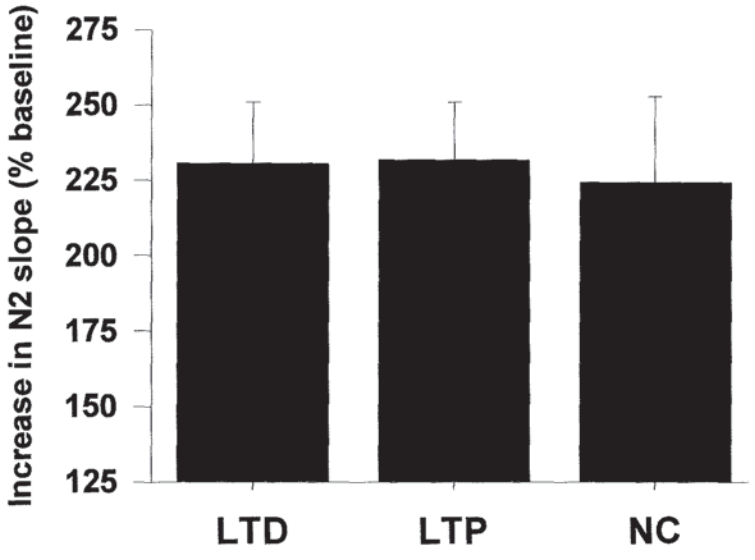

Figure 3.3.12 A comparison between the % increase in the N2 amplitude or slope at the start of RSIF stimulation

Bar charts A and B show the % N2 amplitude and slope, respectively at the start of stimulation. From left to right, black bars represent the recordings in which LTD (N = 9), LTP (N = 4) and no change (N = 5), respectively were detected at 35 minutes after RSIF stimulation.

A

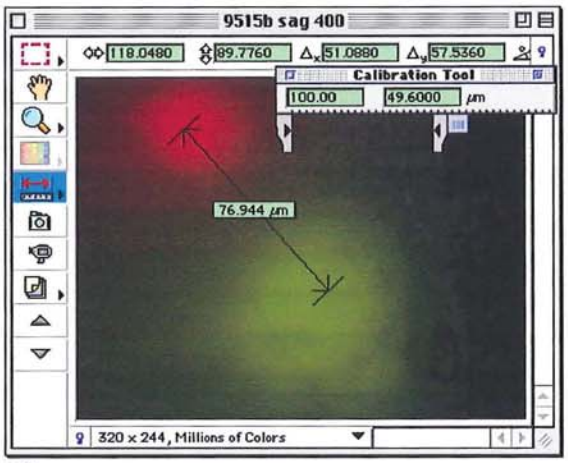

B

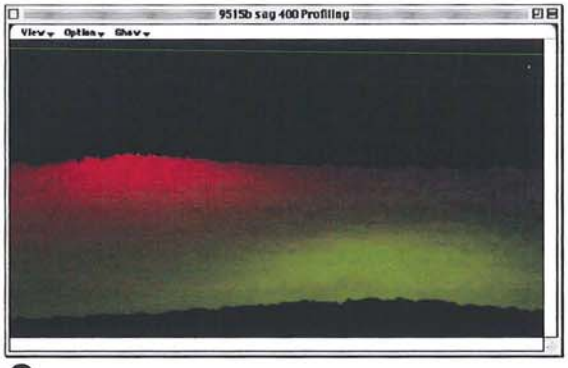

C

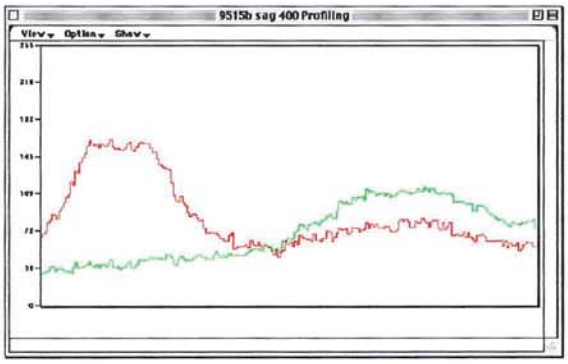

Figure 3.3.13 Fluorescent imaging of the stimulating electrode positions in sagittal slices

Panel A displays a composite image of the stimulating electrode positions collected using a digital cooled CCD camera at x 400 magnification. To increase the brightness of the images 4 x 4 binning was used. The Lucifer Yellow fluorescence is shown in green and the Fura-2 fluorescence is shown in red. Panel B represents the 3-D profile of the fluorescent regions. The 2-D profile shown in panel C was used to observe the peak fluorescence intensity for Lucifer Yellow and Fura-2 as this was likely to be the source of the dye and therefore the site of the electrode tips.

3.3.4 EFFECT OF RAISED STIMULUS INTENSITY AND INCREASED FREQUENCY (RSIF) STIMULATION FOR 5 MINUTES IN TRANSVERSE SLICES

The effect of RSIF stimulation in transverse slices of cerebellar vermis was also studied. In sagittal slices the PFs are truncated during the cutting process whereas in transverse slices the PFs remain relatively intact. Consequently it was anticipated that the nature of the synaptic connections and therefore the effect of molecular layer activation on the transmission between Purkinje cells and parallel fibres might differ. Moreover, this orientation allows PFs to be activated at some distance from the recording site, which might reduce the likelihood of direct activation of PCs or CFs. As shown in figures 3.3.14 and 3.3.15 RSIF stimulation induced an activity-dependent form of LTD when measuring the N2 amplitude in 4 out of 6 recordings and in all 6 recordings when measuring the slope of N2 within 35 minutes of RSIF stimulation. In those recordings in which LTD was apparent the amplitude and the slope of the test pathway N2 component fell below baseline levels immediately after RSIF stimulation. A Wilcoxon Matched-Pairs test was performed to determine the level of significance between the test and control pathways. The depression of the amplitude of N2 reached levels of 74.3 $\pm$ 12.4% within 35 minutes of stimulation which was not significantly different from that in the control pathway which was 114.0 $\pm$ 25.1% ($p>0.05$). However, the difference between the N2 slope in the test and control pathways (59.3 $\pm$ 6.7 and 98.1 $\pm$ 23.6%, respectively) did achieve significance (Wilcoxon Matched-Pairs test $p<0.05$). RSIF caused a marked but transient reduction in the amplitude of the PPR that gradually returned to pre-stimulation levels. After stimulation there was a decrease in the amplitude of N1. These observations indicated that there could be presynaptic events taking place during the stimulation period and suggested that the LTD induced in transverse slices could have a presynaptic component. With respect to the control pathway in 2 recordings the N2 and N1 amplitudes increased. In 2 other cases a depression was observed and in the remaining 2 cases there was no change after stimulation of the test pathway. There was no marked change in the amplitude PPR in the control pathway over the duration of the recording. As shown in the example in figure 3.3.16 the 2-D and 3-D profiles of fluorescent images were used to approximate the distance between the stimulating electrodes that were placed in the molecular layer in transverse slices of

cerebellar vermis for FP recording. The distance between the electrodes was found to range between 15 and 50μm. However, it should be noted that because of the different orientation of the fibres within the slice this does not reflect the distance between pathways at the recording site.

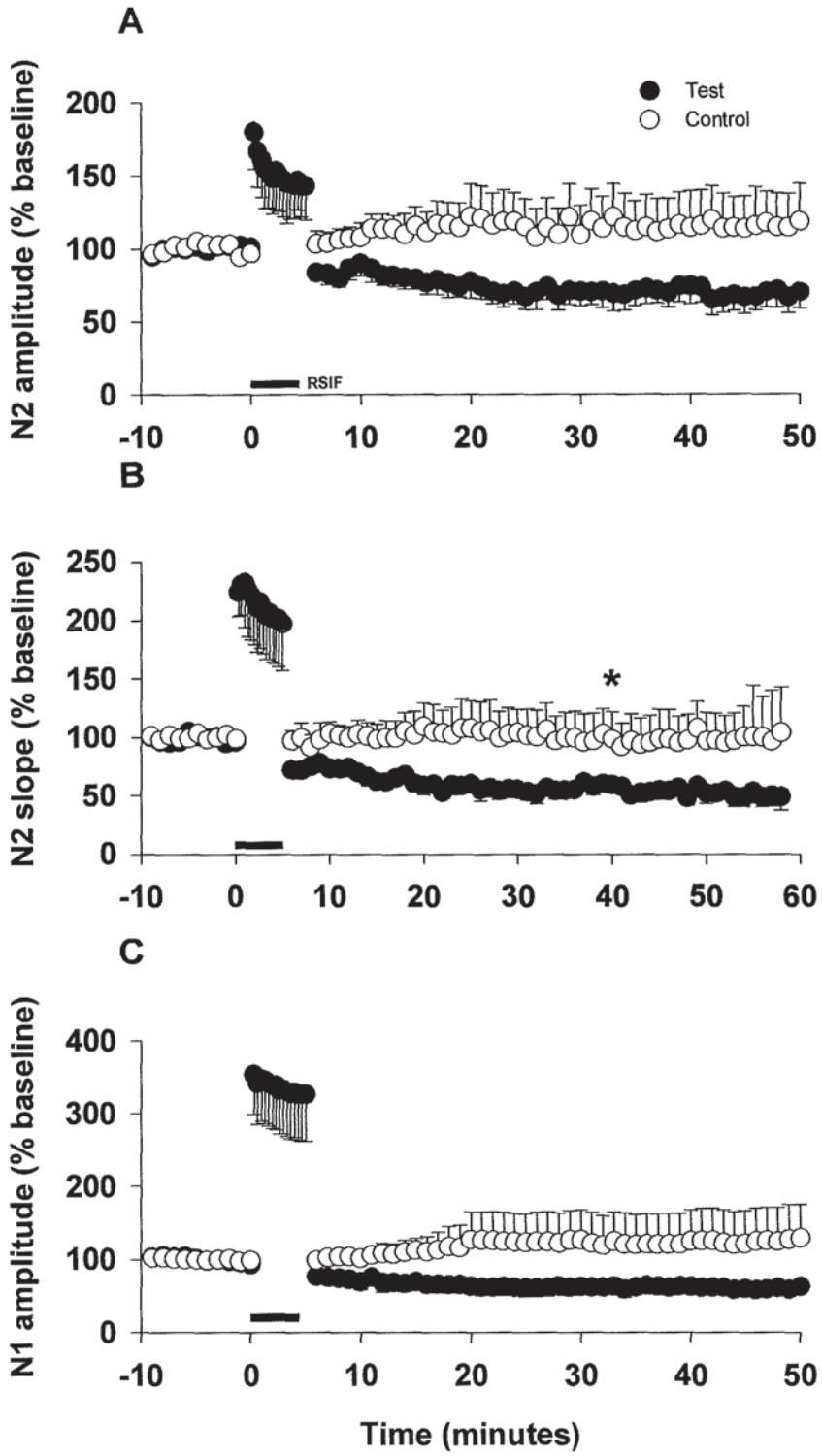

Figure 3.3.14 Effects of a 5 minute period of RSIF stimulation on field potential responses evoked in transverse slices

Graphs A – C are as shown in figure 3.3.6. N = 6 paired recordings. Asterisk indicates where a significant difference was observed between test and control pathways (Wilcoxon Matched-Pairs test $p<0.05$).

A

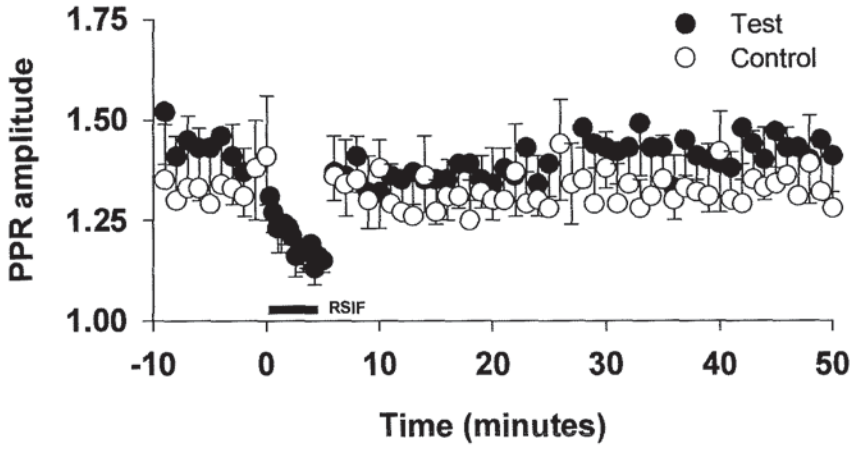

B

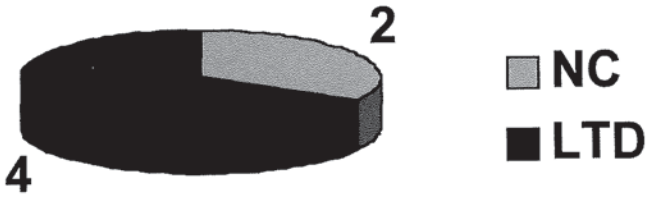

Figure 3.3.15 Effects of a 5 minute period of RSIF stimulation on field potential responses evoked in transverse slices

Graphs A and pie chart B are as shown in figure 3.3.10. N = 6 paired recordings.

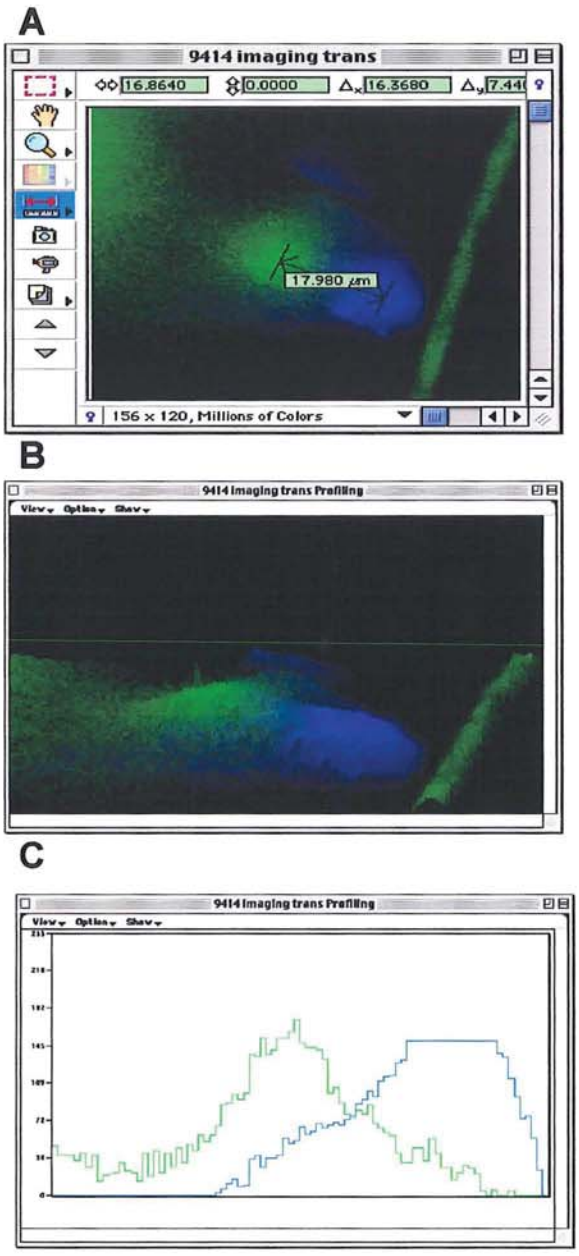

Figure 3.3.16 Fluorescent imaging of the stimulating electrode positions in transverse slices

Panels A – C are as described in figure 3.3.13. The Lucifer Yellow fluorescence is shown in green the Fura-2 fluorescence is shown in blue.

3.4 DISCUSSION

The experiments in this chapter were designed to examine the synaptic requirements for the induction of a form of LTD that could be detected using extracellular FP recording in slices of cerebellar vermis. It was possible to demonstrate that stable FP responses could be followed for at least 60 minutes. The effects of altering the parameters of molecular layer stimulation were observed. In sagittal slices, after a 10 minute period of baseline recording, raising the intensity of molecular layer stimulation for 5 minutes resulted in 1 incidence of LTD in 6 experiments. Increasing the frequency of activation from 0.2Hz to 1Hz was not sufficient to induce LTD however there was 1 occurrence of LTP out of 6 recordings. From these experiments it was concluded that with only 1 exception neither RS nor IF stimulation provided the conditions for a LTD of the N2 component of FPs. In saggital slices, after a 10 minute baseline period, combining the parameters of raised stimulus intensity and increased frequency stimulation for 5 minutes produced an input-specific LTD of the N2 component of extracellular FP responses in 50% of cases. There was no obvious change in the amplitude of N1. The data was grouped according to the incidence of LTD, LTP and no change of the test N2 amplitude 35 minutes after stimulation. This allowed the response of the control pathway to be studied when LTD, LTP or no change was observed in the test pathway. The finding that the extent of PPF decreased transiently during RSIF stimulation suggested that there could have been a decrease in the probability of neurotransmitter release for the duration of the stimulation. The depression did not appear to be associated with either a long-term change in N1 or in the PPR. Therefore a presynaptic mechanism is unlikely to underlie the LTD observed in these FPs but during RSIF stimulation some depletion of transmitter may have occured.

As summarised in figure 3.4.1 RS and IF may independently initiate changes at the synapse between PFs and Purkinje cells. Although these events alone were not sufficient to induce LTD when the 2 parameters were joined together the concerted actions of RS and IF activation of the molecular layer produced an LTD of FPs in 50% of cases

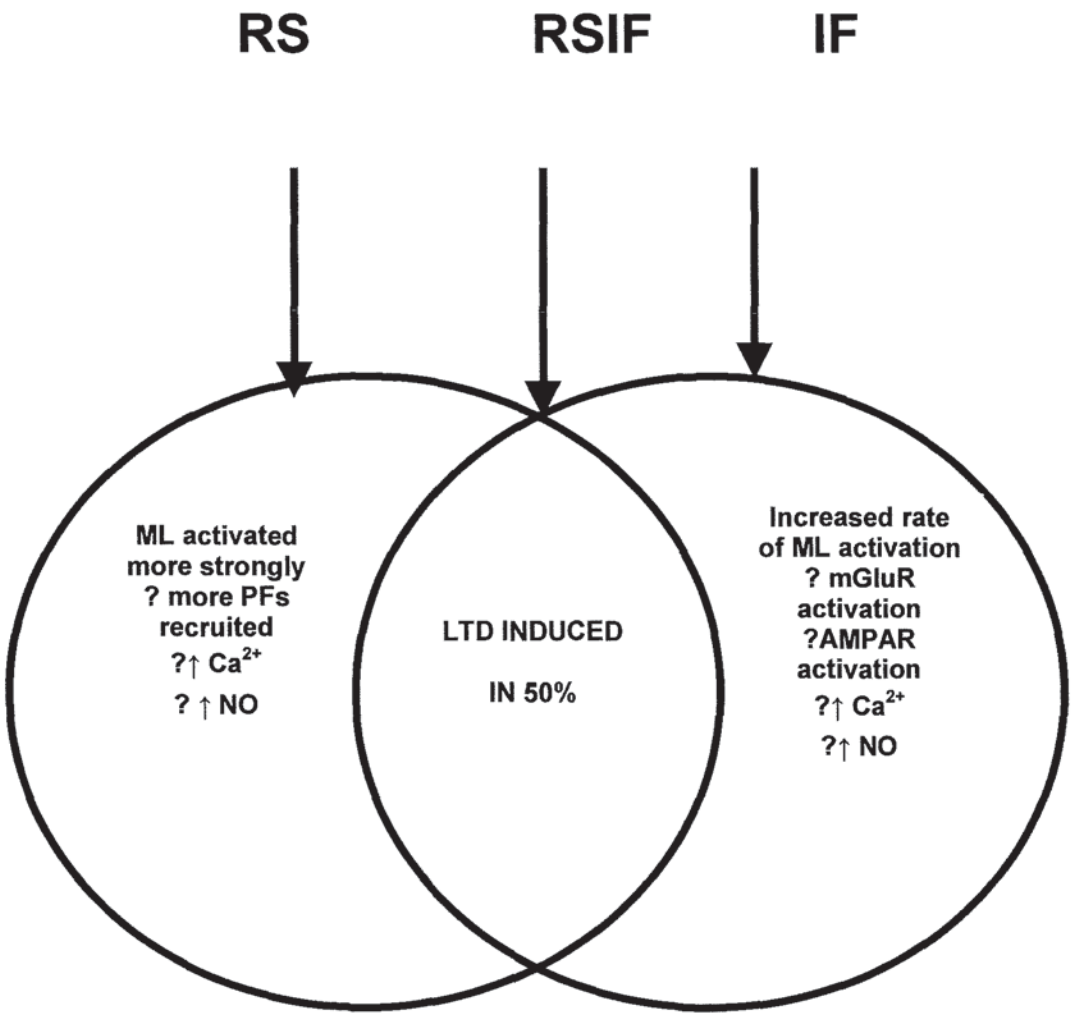

Figure 3.4.1 Illustration of the synaptic events that could be produced by a 5 minute period of RS or IF activation of the cerebellar molecular layer in sagittal slices
The diagram represents the possible events that could be initiated at the synapse between PFs and Purkinje cells by a 5 minute period (from left to right) of RS or IF stimulation, respectively. The intersection illustrates that when the two parameters were combined, RSIF stimulation for 5 minutes produced LTD in 50% of FP recordings.

In the study by Eilers *et al.,* 1995 when PFs were activated with short bursts of stimuli at a frequency of 1Hz and at an increased stimulus intensity elevations in Ca^{2+} could be detected. This finding suggests that either RS or IF could potentially elicit an increase in the postsynaptic Ca^{2+} concentration. It was anticipated that during RS stimulation more PFs would be recruited. Therefore, presumably the likelihood of crossing the threshold of activation for voltage-gated Ca^{2+} channels to open is enhanced. Repetitive PF stimulation at 10Hz was found to evoke NO release which was detected by an electrochemical probe in the experiments by (Kimura et al., 1998). Therefore IF stimulation might well cause an increase in the level of Ca^{2+} influx and NO release. RS activation could also promote the entry of presynaptic Ca^{2+} and augment the release of NO from the molecular layer. The additive effect of the synaptic events produced by RS and IF activation of the molecular layer produced an attenuation of FP responses in 50% of recordings.

The fact that the depression was only apparent in 50% of FPs indicates that the ability to induce LTD was very sensitive to the conditions under which the experiments were performed. As discussed in chapter 2 in section 2.4 extracellular FP recording has a number of inherent sources of variation. These include the level of stimulation, the position of the stimulating and recording electrodes and the size of the N2 and N1 components of the FP responses. However, the results from single factor analysis of variance (ANOVA) comparisons suggested that the different incidences of LTD, LTP and no change between the RS and RSIF experiments were unlikely to be accounted for by differences in:-

i) the amplitude or slope of N2 responses at baseline prior to stimulation or

ii) the level of raised intensity stimulation at the start of the RS or RSIF paradigms.

The fluorescence imaging of the stimulating electrode tip positions in sagittal slices in figure 3.3.13 indicated that the typical electrode separation during FP recordings ranged between 40 and 100μm. As shown in figure 3.4.2 the two stimulating electrodes s0 and s1 could potentially activate the same, overlapping, or distinct PF presynaptic inputs to Purkinje cell dendrites. If the stimulating electrodes s0 and s1 activate the same PFs then the same Purkinje cell population will be activated by either electrode. If overlapping PF inputs are

activated then the FP responses will represent either the same or partially overlapping Purkinje cell populations. Each stimulating electrode might activate separate PFs and in this case the FP responses could represent either the same, partially overlapping or distinct Purkinje cell populations. It is not possible to be certain which of these combinations is correct. However, the input-specific LTD that was induced by RSIF stimulation in sagittal slices in 50% of cases demonstrated that there is a considerable degree of separation between the two stimulating electrodes. Due to the numerous contacts between PFs and the dendritic tree of Purkinje cells it is probable that each electrode will stimulate PF inputs which activate some of the same Purkinje cells. The FP responses evoked by the stimulation of s0 and s1 might therefore represent a Purkinje cell population that has some individual Purkinje cell responses in common.

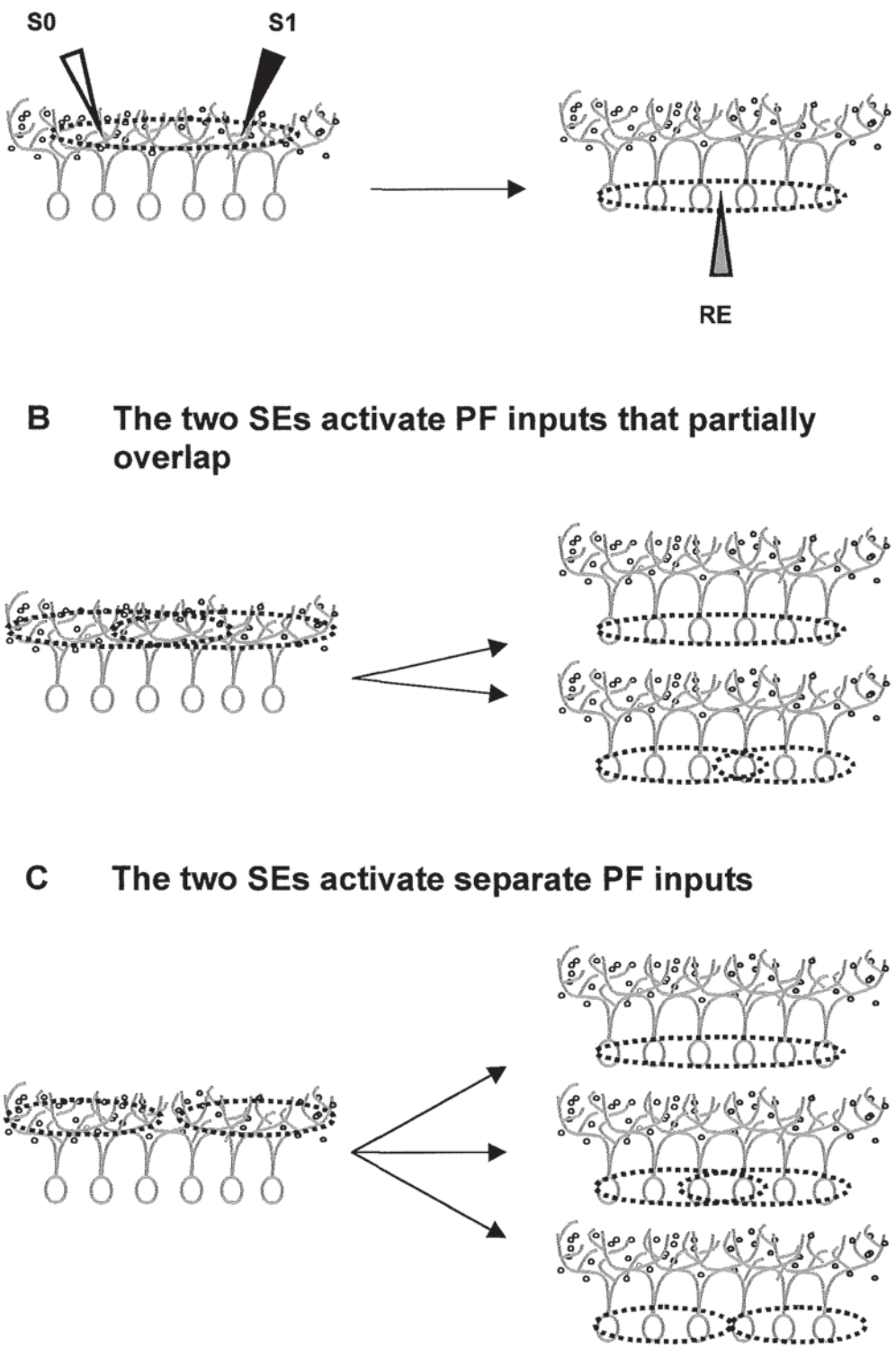

Figure 3.4.2 Molecular layer stimulation activates PF inputs to Purkinje cells
Diagrams A – C on the left hand side show the three possible ways that the stimulating electrodes (s0 and s1) in the cerebellar molecular layer could activate PF inputs to Purkinje cells. The diagrams on the right hand side suggest the extent to which adjacent Purkinje cells might be activated by the stimulating electrodes activating either the same (A), overlapping (B), or distinct (C) PF presynaptic inputs to the dendritic field of Purkinje cells. For simplicity the stimulating electrodes shown in black and white and the recording electrode shown in grey are only shown on the top diagram.

The transverse slices are cut in the plane of the PFs leaving them more intact than in sagittal slices in which PFs are truncated during the cutting process (Garthwaite and Batchelor, 1996). In sagittal slices it is possible that stimulation of the molecular layer activates CFs or even the Purkinje cells directly. In transverse slices the situation is less clear and we are unsure how the PFs terminate in the region of the Purkinje cell dendrites. In this orientation it is more probable that molecular layer stimulation yields a more 'pure' PF input. It is interesting to note therefore that in transverse slices of cerebellar vermis the RSIF stimulation method produced a higher incidence of LTD than in sagittal slices. The slope of the N2 component of all 6 recordings clearly displayed LTD. The extent of input specificity following RSIF stimulation was slightly reduced in transverse slices. In 2 cases when there was a LTD in the test pathway there was also some degree of depression in the N2 component in the control site that was not stimulated. This may have been due to pathway overlap that is less easy to control in transverse slices. This model was only used towards the end of this investigation. In future studies it would be interesting to investigate more fully the LTD produced by RSIF in the transverse slice preparation, since it appeared to induce LTD more reliably.

Simultaneous recordings from three interconnected hippocampal neurons in culture showed that LTD was accompanied by a retrograde spread of the depression by propagation to adjacent presynaptic and postsynaptic neurons (Fitzsimonds et al., 1997). The idea that LTD may spread over distance was assessed using a superfusion technique with a spatial resolution of 30μm. Synapses in close proximity to the site of induction were also potentiated but distant synapses were not affected. These results suggested that input specificity was not observed at distances less than 70μm (Engert and Bonhoeffer, 1997). Together these studies challenge the assumption that LTD and LTP are spatially restricted. The extent of input specificity following RSIF stimulation was reduced in transverse slices. This is likely to be due to overlap between the PFs activated by the stimulating electrodes in the molecular layer due to the short distance between PF beams in slices cut in this orientation. As shown in the image in figure 3.3.16 the distance between stimulating electrodes placed in the molecular layer was estimated to range between 15 and 50μm.

Even if the separation between the stimulating electrodes had been 70 μm or greater there probably would still be overlap between PF beams.

In summary, in sagittal slices IF or RS stimulation alone were insufficient to produce LTD but when joined together they tipped the balance in favour of an input-specific LTD in 50% of FP responses. In the remaining cases there was an almost equal occurrence of LTP or no change. In transverse slices an activity dependent LTD could be induced by RSIF stimulation but the extent of input specificity was reduced. These findings illustrate that LTD can be produced and that with this extracellular technique, as with previous studies (Ekerot and Kano, 1985; Linden, 1994a) LTD tends to be input-specific.

CHAPTER 4

TO EXAMINE THE CELLULAR MECHANISMS REQUIRED FOR THE INDUCTION OF LONG TERM DEPRESSION IN AN EXTRACELLULAR FIELD POTENTIAL MODEL

4.1 INTRODUCTION

The goal of this chapter was to examine if the NO/cGMP/PKG signalling cascade was important for the induction of LTD recorded using an extracellular technique as described in chapter 3. It was anticipated that if the cGMP signalling cascade contributed to the cellular mechanism underlying the decrease in synaptic efficacy at the PF-Purkinje cell synapse the inhibition of NOS, GC or PKG might prevent the induction of LTD. The extent and the incidence of LTD was therefore compared with that apparent in the absence of inhibitors. The majority of experiments were performed in sagittal slices but in a few cases the RSIF stimulation method was also applied to transverse slices of cerebellar vermis. In a separate set of experiments applications of a NO donor, a membrane permeable analogue of cGMP or an inhibitor of type V cGMP-specific PDEs were paired with IF stimulation. The aim of these experiments was to find out if one aspect of the RSIF stimulation could be replaced by raising the level of NO or cGMP. Figure 4.1.1 indicates how the compounds that were bath-applied during these experiments interfere or interact with the cGMP-signalling cascade.

As outlined in the general introduction in section 1.7 several lines of experimental evidence support roles for NO/cGMP/PKG signalling in the induction of LTD. For example, it was discovered that extracellular application of the NO donor SNP, when paired with white matter stimulation was sufficient for LTD (Shibuki and Okada, 1991). The expression of a long-term attenuation of PF-mediated EPSCs was observed following bath application of the NO donors SNP or S-nitroso-penicillamine (SNAP, Blond et al., 1997). In addition bath

application of NO donors including SNP was found to cause a clear LTD of PF-mediated EPSPs recorded from cerebellar slices (Daniel et al., 1993). It was reported that the caged compound CNO-4, that releases NO upon photolysis, produced a LTD of EPSCs when paired with depolarisation. This finding was further investigated by repeating the paradigm in the presence of either the NO scavenger myoglobin or the NOS inhibitor, N^G-nitro-L-arginine in either the intracellular pipette solution or the extracellular medium. Extracellular application of either of these compounds prevented the induction of LTD (Lev Ram et al., 1995). This suggests a transcellular action of NO that is; the production of NO occurs inside cells via NOS and then exerts its action at adjacent cells. It is important to mention that not all studies support the postulated role of NO in LTD. For example, in perforated patch recordings from cultured Purkinje cells the LTD of glutamate currents was unaffected by either the NOS inhibitor N^G-nitro-L-arginine or the NO donor SNP (Linden and Connor, 1992). In cerebellar slices it was reported that a 15 minute application of SNP was not sufficient to induce a LTD of PF-mediated responses (Glaum et al., 1992).

NO triggers an accumulation of cGMP via stimulation of the soluble GC enzyme (Schulz et al., 1991). Antibodies against soluble GC suggested that the enzyme is associated with the cell body and the primary dendritic tree of Purkinje cells in the rat cerebellum (Ariano et al., 1982). Consistent with the immunohistochemical localisation of soluble GC that was described above, *in situ* hybridisation studies have since provided direct evidence that GC mRNA is highly expressed in Purkinje cells (Matsuoka et al., 1992). Intracellular application of ODQ a potent and selective inhibitor of GC (Garthwaite et al., 1995) blocked the induction of LTD by pairing PF stimulation with postsynaptic Ca^{2+} spike firing (Boxall and Garthwaite, 1996a). A LTD of PF-EPSPs was induced by bath application of the membrane-permeable cGMP analogue, 8-Br-cGMP (Daniel et al., 1993; Hartell, 1994a). Inhibition of type V cGMP specific PDEs to prevent the breakdown of cGMP led to a robust depression of PF to Purkinje cell synaptic responses (Hartell, 1996a). In contrast, in whole cell patch-clamp recordings from cultured Purkinje cells the intracellular application of analogues of cGMP, the inhibition of GC or of type V cGMP-specific PDEs did not induce a LTD of glutamate currents (Linden et al., 1995b).

As described in the general introduction, the LTD of AMPA-selective glutamate receptors is thought to be mediated by the regulation of the level of protein phosphorylation by protein kinases and phosphatases (Ito and Karachot, 1992). KT5823 inhibits the cGMP-dependent protein kinase PKG by competing for the adenosine triphosphate (ATP) binding site (Kase et al., 1987). The LTD induced by the application of 8-Br-cGMP or by the conjunctive stimulation of PF and CF inputs was prevented in the presence of KT5823 (Hartell, 1994a). Inhibitors of PKG: Rp-8Br-PET-cGMPs (Butt et al., 1995), KT5823 and Gly-Arg-Thr-Gly-Arg-Arg-Asn-(D-Ala)-Ile-NH_2 (PKGI) a novel pseudosubstrate peptide blocked LTD induction by a paradigm of depolarisation paired with either PF stimulation or photorelease of NO (Lev Ram et al., 1997).

It is widely accepted that LTD requires an influx of Ca^{2+} through voltage-gated calcium channels and the activation of both AMPAR and $mGluR_1$ (see for example, Linden et al., 1991; Daniel et al., 1992; Hemart et al., 1994; Hartell, 1994b; Linden, 1994b; Hemart et al., 1995; Zhuo and Hawkins, 1995; Linden and Connor, 1995a; Hartell, 1996b; Daniel et al., 1998). As discussed briefly in this introduction and more extensively in the general introduction there is also substantial evidence for the involvement of NO/cGMP/PKG signalling in the induction of LTD (as discussed in, Hartell, 1994a; Hemart et al., 1995; Lev Ram et al., 1995; Hartell, 1996a; Hartell, 1996b; Lev Ram et al., 1997; Daniel et al., 1998). In sagittal slices when the molecular layer was activated at a RS and IF in the absence of inhibitors, a LTD of the N2 component was induced in the test pathway in 50% of FP recordings as described in chapter 3. The depression of the FP response was input-specific that is; it was confined to the test pathway and did not spread to the control site. In transverse slices in drug-free ACSF an activity-dependant form of LTD could also be induced by RSIF stimulation. In this chapter the possible involvement of cGMP intracellular signalling in the induction of LTD was investigated using extracellular FP recording techniques.

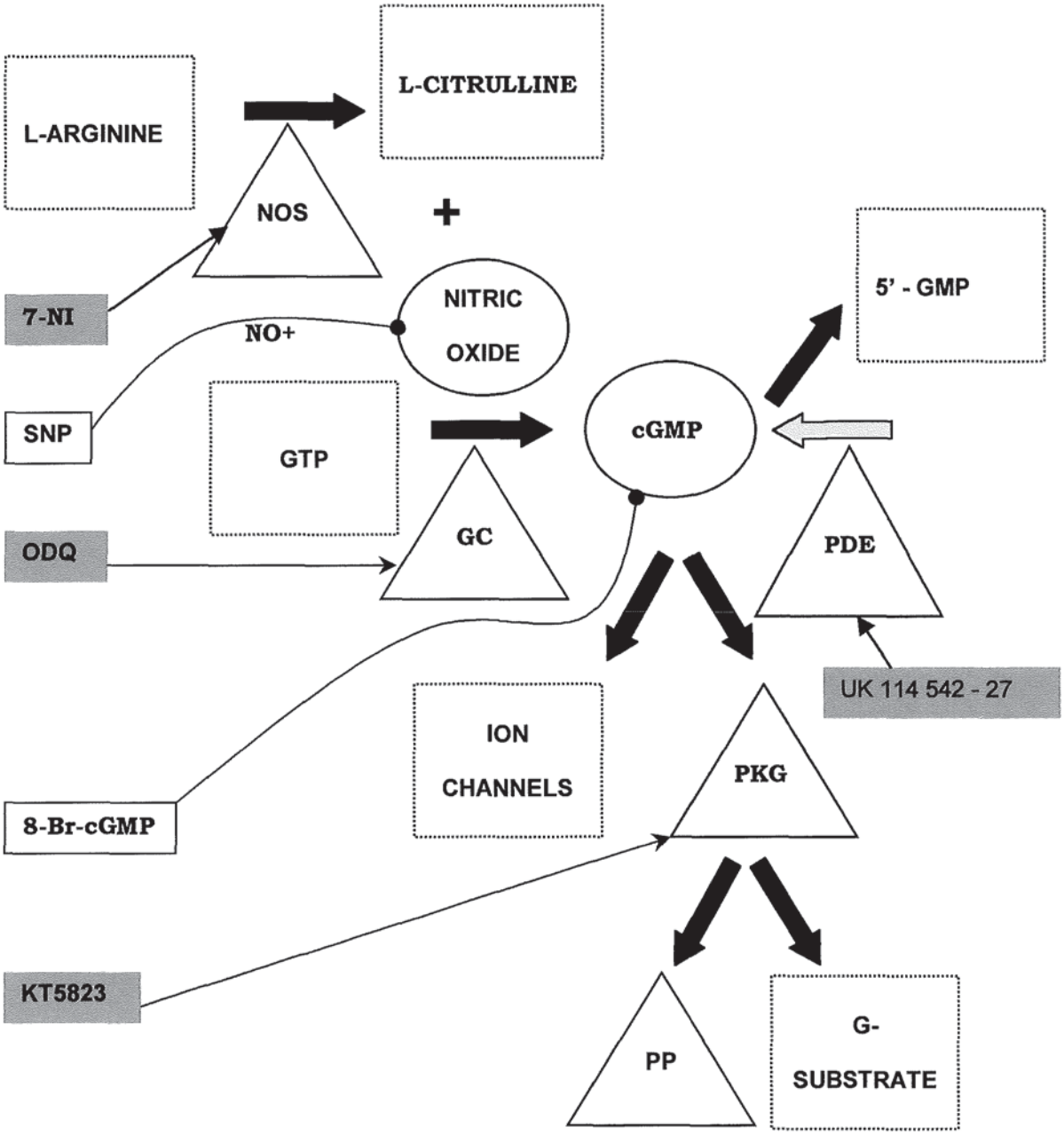

Figure 4.1.1 An illustration of the key components in the cGMP cell signalling cascade
Nitric oxide (NO) and L-citrulline are formed from the conversion of L-arginine by NO synthase (NOS). cGMP is formed from guanosine triphosphate (GTP) by the NO-dependant soluble guanylate cyclase enzyme (GC) and degraded into guanosine monophosphate (5'–GMP) by cGMP-specific type V phosphodiesterases (PDE). cGMP stimulates protein kinase G (PKG) which activates G-substrate. G-substrate regulates the level of protein phosphorylation by inhibiting protein phosphates (PP). The grey boxes and narrow line arrows show the site of action of the compounds 7-NI, ODQ, KT5823 and UK 114 542–27 that were used to inhibit NOS, GC, PKG and cGMP-specific PDEs, respectively. The small white boxes and lines with solid circles at the end show the site of action of the NO donor SNP and the membrane-permeable cGMP analogue 8-Br-cGMP.

4.2 METHODS

4.2.1 SLICE PREPARATION

The majority of recordings were made in sagittal slices that were prepared as described in chapter 2.2.1. In a few experiments transverse slices were used that were prepared using the method as outlined in chapter 3.2.1.

4.2.2 FIELD POTENTIAL RECORDING

In sagittal and transverse slices the FP responses were obtained using the same method as described in chapter 2.2.2.

4.2.3 APPLICATION OF DRUGS

Drugs used for perfusion were 7-Nitroindazole (7-NI, Moore and Handy, 1997, Sigma) 1H-[1,2,4], Oxadiazolo [4,3-a] quinoxalin-1-one (ODQ, Calbiochem, Garthwaite et al., 1995), KT5823 (Calbiochem, Nakanishi, 1989), sodium nitroprusside dihydrate (SNP, Butler et al., 1995, Sigma) 8-Bromoguanosine cyclic 3', 5'-monophosphate sodium salt (8-Br-cGMP; Sigma) and UK 114 542–27 mesylate salt (Pfizer Limited). 7-NI, ODQ, and KT5823 were made up as stock solutions of 50mM, 20mM and 500μM respectively, dissolved in DMSO and then diluted in the ACSF solution prior to perfusion to a final concentration of less than 0.1% DMSO. Care was necessary during the preparation of SNP because the compound was sensitive to oxygen. Concentrated stock solutions were made by dissolving SNP in a small measured volume of distilled water bubbled with nitrogen gas and then added into the ACSF solution prior to perfusion. 8-Br-cGMP and UK 114 542-27 were made up as concentrated stock solutions of 500mM and 100mM respectively, dissolved in a minimal amount of distilled water and then added to the ACSF prior to perfusion.

4.3 RESULTS

4.3.1 EFFECT OF RAISED STIMULUS INTENSITY AND INCREASED FREQUENCY STIMULATION FOR 5 MINUTES IN SAGITTAL SLICES OF CEREBELLAR VERMIS IN THE PRESENCE OF INHIBITORS OF NITRIC OXIDE SYNTHASE, GUANYLATE CYCLASE OR PROTEIN KINASE G

In the preceding chapter a form of LTD was observed in 50% of FP recordings in response to a five minute period of combined RS and IF activation of the cerebellar molecular layer. The purpose of the next set of experiments was to determine if inhibition of NOS, GC or PKG could alter the incidence or the extent of LTD induced by the RSIF stimulation paradigm in either sagittal or transverse slices.

In sagittal slices the NOS inhibitor 7-NI, was bath perfused at a concentration of 5μM for at least 10 minutes prior to the period of RSIF stimulation. *In vitro*, 7-NI binds to the haem prosthetic group of neuronal NOS and this causes disruption of the movement of electrons through the NOS enzyme and therefore prevents the formation of NO (Moore and Handy, 1997). The effect of RSIF stimulation in the presence of 7-NI is shown in figures 4.3.1 and 4.3.2. After 35 minutes there was no significant difference between the N2 amplitude of FPs recorded in the test pathway that was activated by RSIF stimulation and in the control pathway that was not stimulated, 100.3 $\pm$ 4.9 and 90.2 $\pm$ 3.4% of baseline levels, respectively (N=6, Wilcoxon Matched-Pairs test, $p>0.05$). A slight depression emerged in the control pathway that was most evident in measurements of the N2 slope. This depression was not significantly different from that in the test pathway (N=6, Wilcoxon Matched-Pairs test, $p>0.05$). During RSIF stimulation there was a transient reduction in the amplitude of the PPR in the test pathway. An increase in N1 and a reduction of the amplitude of the PPR was noted after RSIF stimulation in the test pathway. The amplitude of the PPR gradually returned to baseline levels after stimulation. No obvious long-term changes were noted in N1 or in the amplitude of the PPR in the control pathway for the duration of the experiment. The amplitude of N1 in the test pathway reached 116.3 $\pm$ 10.9

compared to 99.1 ± 6.1% of baseline levels in the control pathway but there was not a significant difference between the two (N = 6, Wilcoxon Matched-Pairs test $p>0.05$). These results indicate that obstructing the formation of NO by inhibition of the enzyme necessary for its production might have prevented the occurrence of the LTD that was previously observed in 50% of the FP responses recorded in drug-free ACSF following RSIF stimulation. The observation that there was an increase in the N2 and N1 components in the test pathway suggests that inhibition of NOS might unmask an underlying potentiation.

An important biological action of NO is the stimulation of soluble GC that acts on GTP to produce cGMP (Schulz et al., 1991). To investigate whether cGMP was required for the induction of LTD in this preparation, 10μM ODQ was added to the ACSF for at least 10 minutes prior to the RSIF stimulation. The results of these experiments are shown in figures 4.3.3 and 4.3.4. In the test pathway, the N2 amplitude increased after stimulation and was accompanied by an increase in N1. In two cases, 35 minutes after stimulation, this increase in the test pathway N2 amplitude was large enough to be classed as LTP. However, in the remaining 5 recordings there was no change. 35 minutes after stimulation, the test and control pathway N2 amplitudes were not significantly different reaching 105.7 ± 7.3 (N=7) and 91.6 ± 7.7% (N = 6) of baseline levels, respectively (Wilcoxon Matched-Pairs test, $p<0.05$). As with previously described experiments the test period produced a brief reduction in the amplitude of the PPR but the ratio returned to baseline levels after stimulation. Little or no change was observed in N1 or in the amplitude of the PPR in the control pathway after stimulation. The difference between the amplitude of N1 in the test and control pathways did not achieve significance (Wilcoxon Matched-Pairs test $p>0.05$). These results suggest that GC could be involved in the pathway by which RSIF stimulation can lead to a long-term decrease in the N2 component of 50% of FP responses.

RSIF stimulation failed to induce a LTD in the test pathway N2 component in the presence of the PKG inhibitor KT5823 as shown in figures 4.3.5 and 4.3.6. 35 minutes after RSIF stimulation there was no change in the N2 amplitude in the test pathway in 2 recordings and in the remaining 4 recordings the FP response became potentiated. Similar observations were made in the slope of the N2 component of FPs. N2 amplitudes in the test and control

pathways were not significantly different 35 minutes after RSIF stimulation, 116.1 ± 8.0 and 105.3 ± 11.2% of baseline levels, respectively (N=6, Wilcoxon Matched-Pairs test, $p>0.05$). In the test pathway an increase in N1 was observed in those recordings in which the amplitude of the N2 component of FPs was potentiated after RSIF stimulation. The LTP of the test pathway N1 component was significantly different when compared to the control pathway (Wilcoxon Matched-Pairs test, $p<0.05$). The amplitude of N1 in the control pathway was stable throughout the experiment. There was no obvious change in the amplitude of the PPR in either pathway after stimulation. One possible interpretation of these results is that RSIF stimulation could trigger the activation of PKG via NO and cGMP in order to induce a form of LTD in 50% of FPs.

It was not appropriate to perform a statistical comparison between groups of data obtained in the absence and in the presence of inhibitors of the NO/GC/PKG signalling cascade because we were unable to produce a consistent LTD of FP responses. Therefore, pie charts were constructed to illustrate the relative incidences of LTD in the absence and in the presence of these inhibitors (Figure 4.3.7). It is apparent from these charts that in the presence of NOS, GC or PKG inhibitors in the test pathway LTD was never observed. Although this might suggest that NO/cGMP and PKG are necessary for this form of LTD, it is also possible that the stimulating conditions were, in some way, different between experiments performed in the absence or presence of inhibitors. Bar charts were constructed to compare the mean ± S.E.M absolute amplitude and slope values between the experiments during i) baseline stimulation and ii) at the start of RS or RSIF stimulation. Single factor analysis of variance (ANOVA) tests were performed to compare baseline and raised levels of both the amplitude and the slope in drug-free ACSF and in the presence of inhibitors. No significant difference was found between the baseline amplitude of N2 between the groups of data illustrated in figure 4.3.8 (Single factor ANOVA test, $P>0.05$). In the case of the baseline N2 slope values, there were differences amongst the five groups which did achieve significance (Single factor ANOVA test, $P<0.05$). However, the raised level of the amplitude or slope of the N2 component was not significantly different in the five sets of data (Single factor ANOVA test, $P>0.05$) suggesting that regardless of the starting baseline level, during raised stimulation all experiments were treated in the same way.

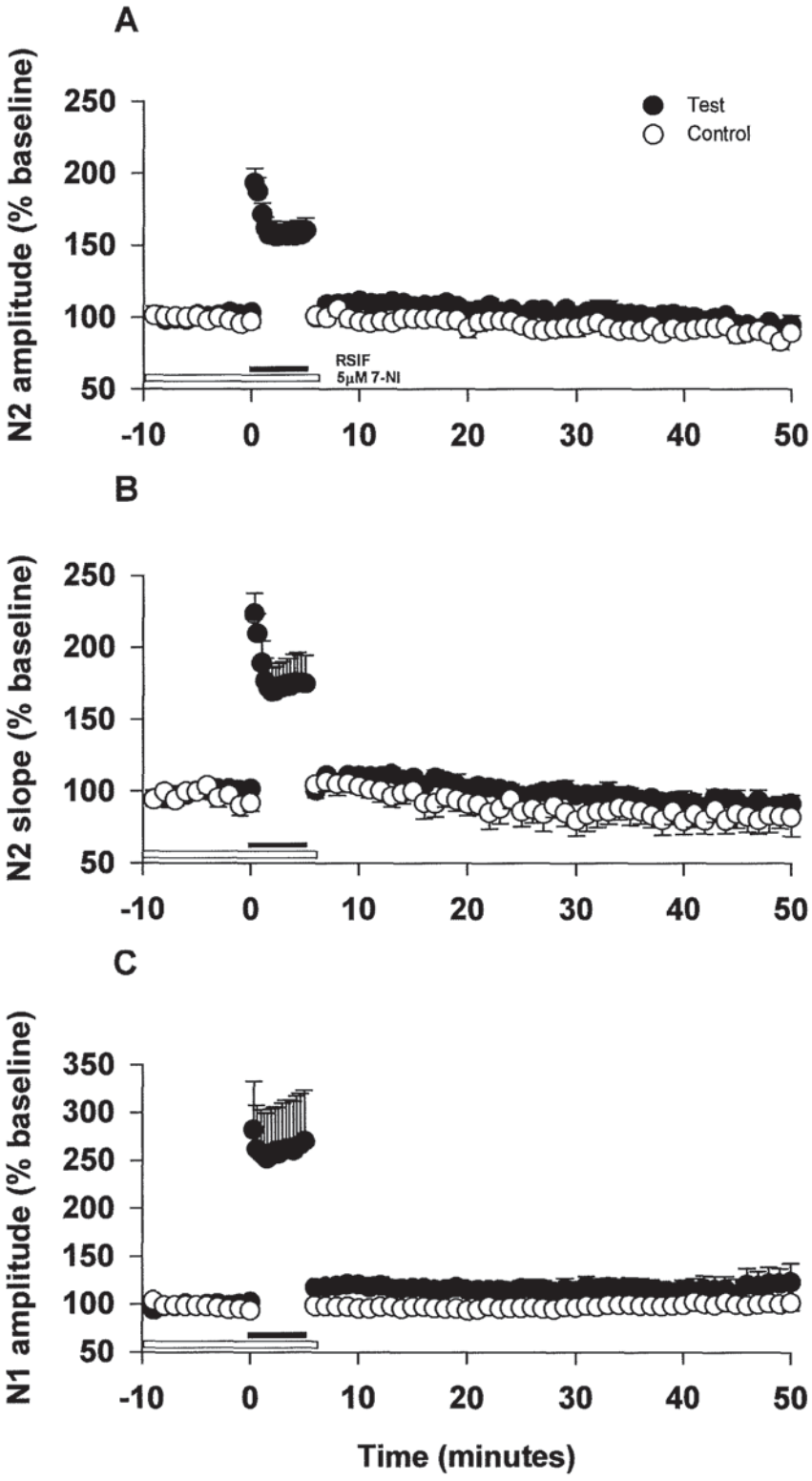

Figure 4.3.1 Effects of a 5 minute period of RSIF stimulation on field potential responses in the presence of 5μM 7-NI

Graphs A - C illustrate the FP N2 amplitude, N2 slope and N1 amplitude, respectively. Data are expressed as the mean % ± S.E.M. of 10 responses collected during a 10 minute baseline period. N = 6 paired recordings. Closed circles, test pathway that underwent RSIF stimulation for 5 minutes; open circles, control pathway. Horizontal black bar indicates the period of RSIF stimulation. Horizontal white bar represents the application of 5μM 7-NI.

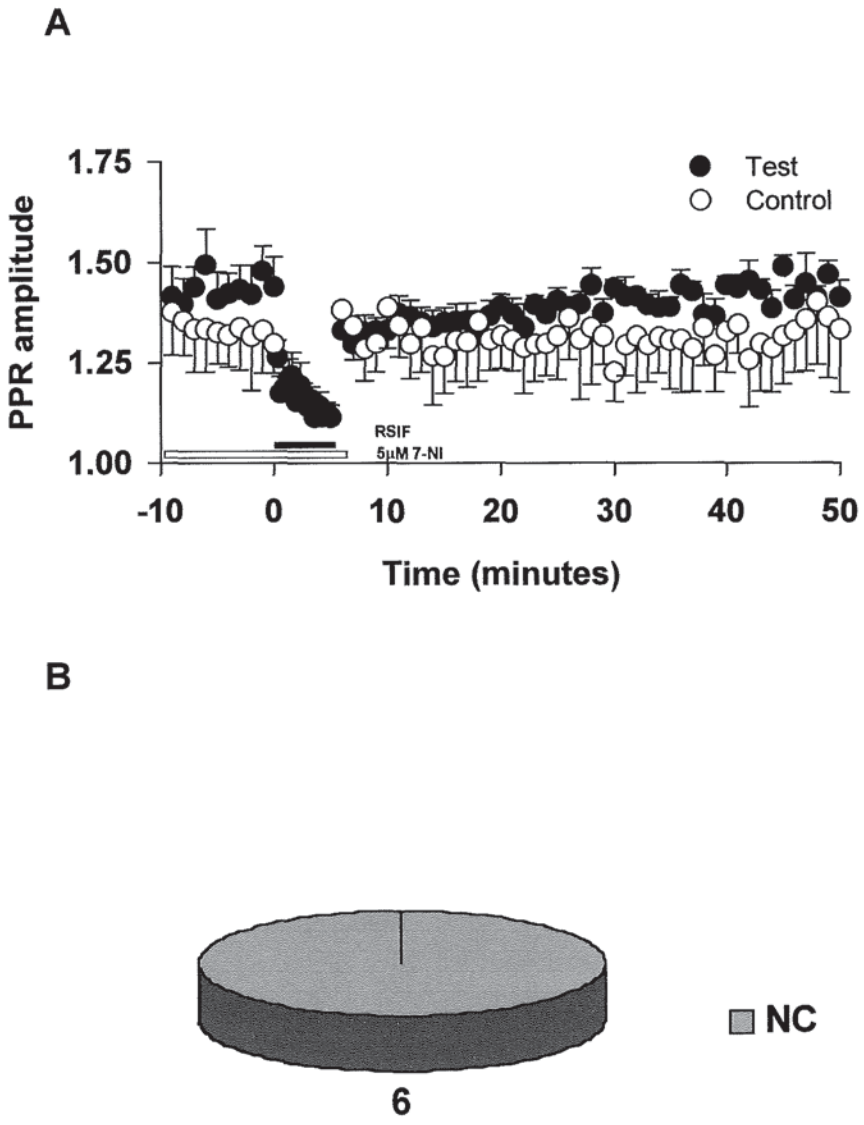

Figure 4.3.2 Effects of a 5 minute period RSIF stimulation on field potential responses in the presence of 5μM 7-NI

Graph A illustrates the amplitude of the PPR. Data are expressed as the mean % ± S.E.M. of 10 responses collected during a 10 minute baseline period. N = 6 paired recordings. Closed circles, test pathway that underwent RSIF stimulation for 5 minutes; open circles, control pathway. Horizontal black bar indicates the period of RSIF stimulation. Horizontal white bar represents the application of 5μM 7-NI. Pie chart B shows the incidence of LTD, LTP and no change in the test pathway amplitude measured 35 minutes after stimulation.

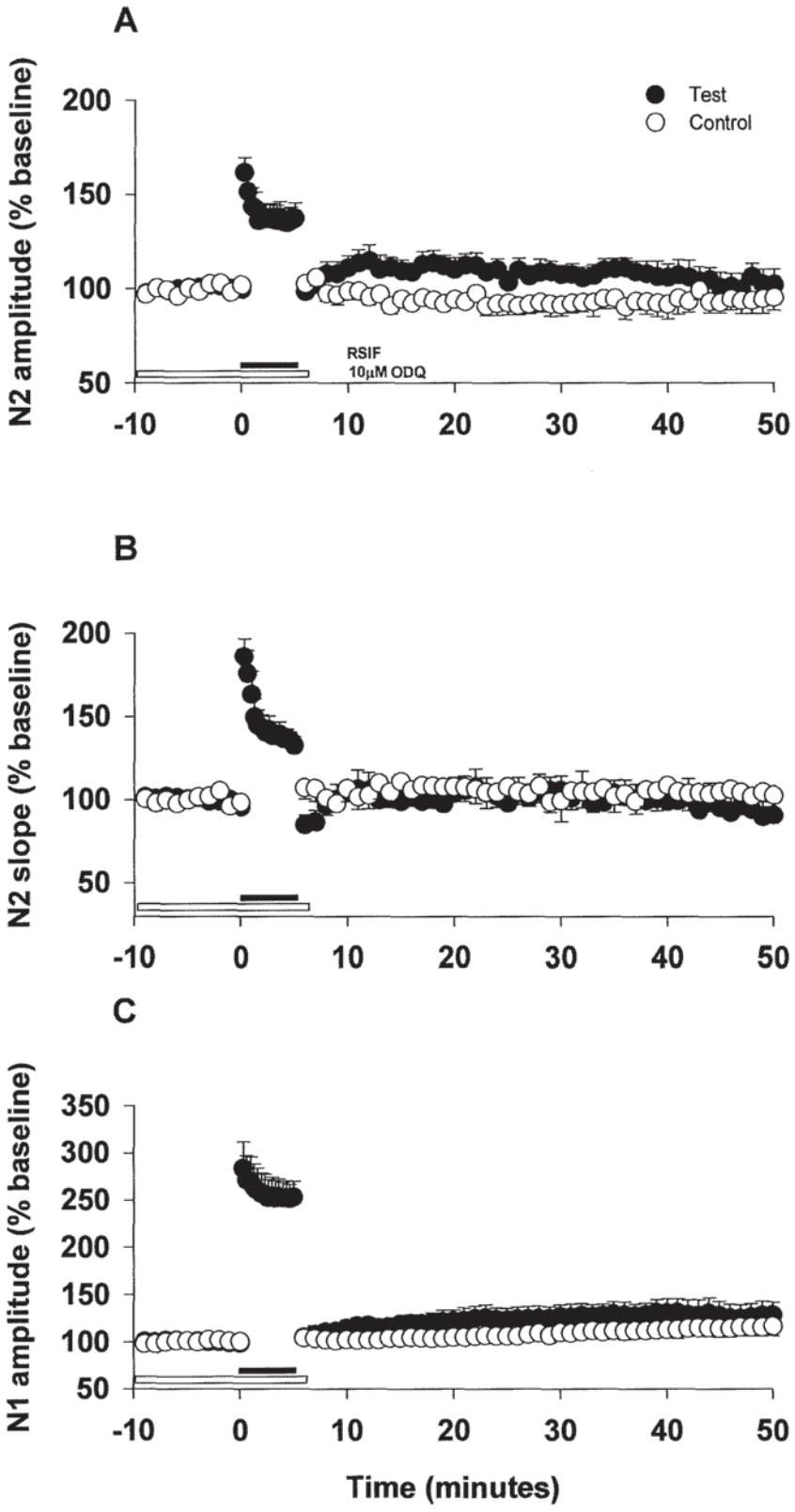

Figure 4.3.3 Effects of a 5 minute period of RSIF stimulation on field potential responses in the presence of 10μM ODQ

Graph A – C are as shown in figure 4.3.1. N = 5 paired recordings (7 pathways 1Hz, 6 pathways 0.2Hz). Horizontal white bar represents the application of 10μM ODQ.

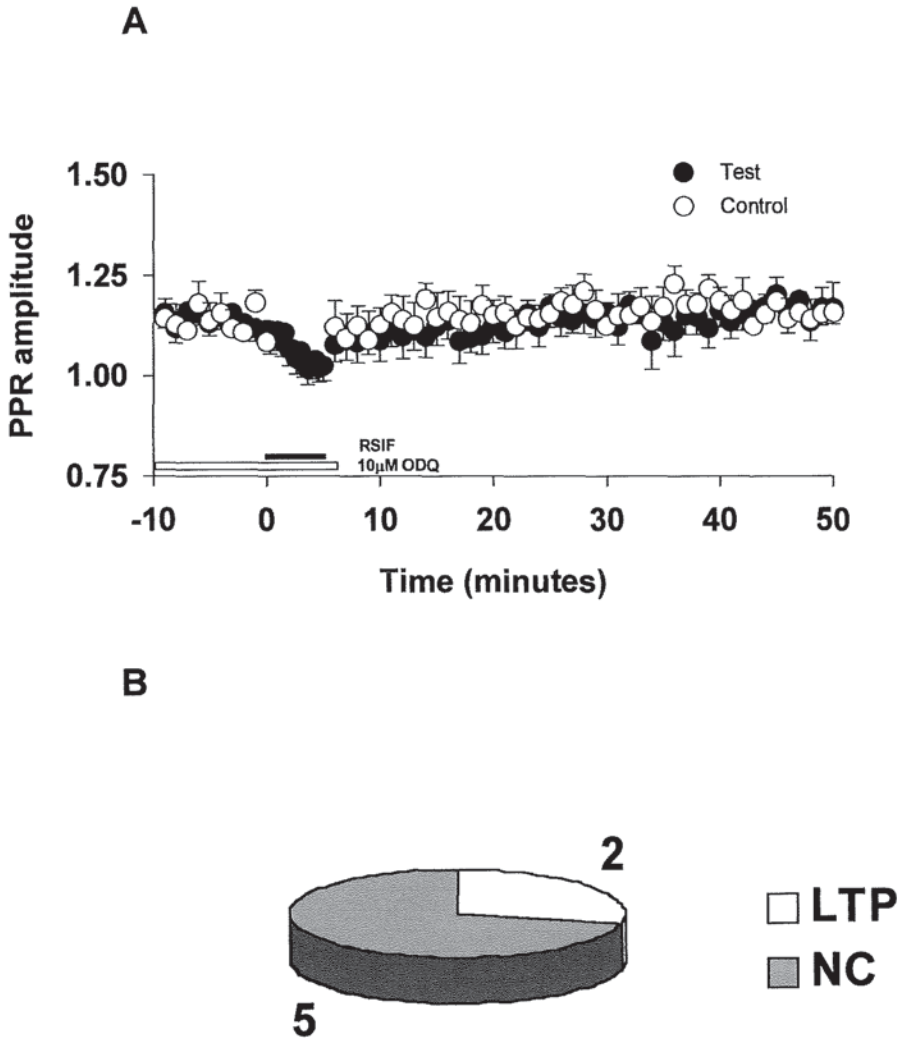

Figure 4.3.4 Effects of a 5 minute period of RSIF stimulation on field potential responses in the presence of 10μM ODQ

Graph A and pie chart B are as shown in figure 4.3.2. N = 5 paired recordings (7 pathways 1Hz, 6 pathways 0.2Hz). Horizontal white bar represents the application of 10μM ODQ.

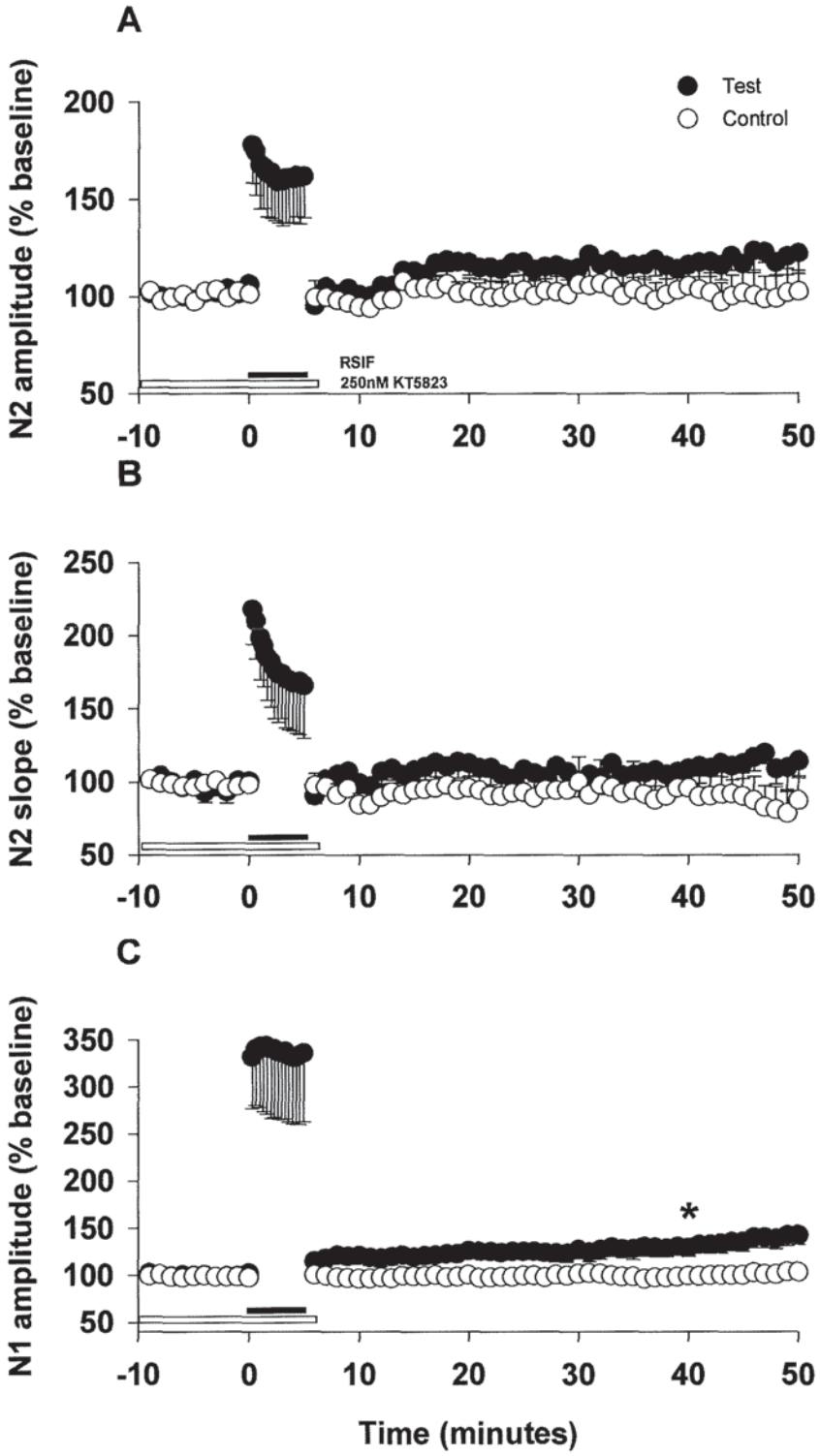

Figure 4.3.5 Effects of a 5 minute period of RSIF stimulation on field potential responses in the presence of 250nM KT5823

Graphs A – C are as shown in figure 4.3.1. N = 6 paired recordings. Horizontal white bar represents the application of 250nM KT5823. Asterisk indicates where a significant difference was found between the test and control pathways at 35 minutes after stimulation (Wilcoxon Matched-Pairs test $p<0.05$).

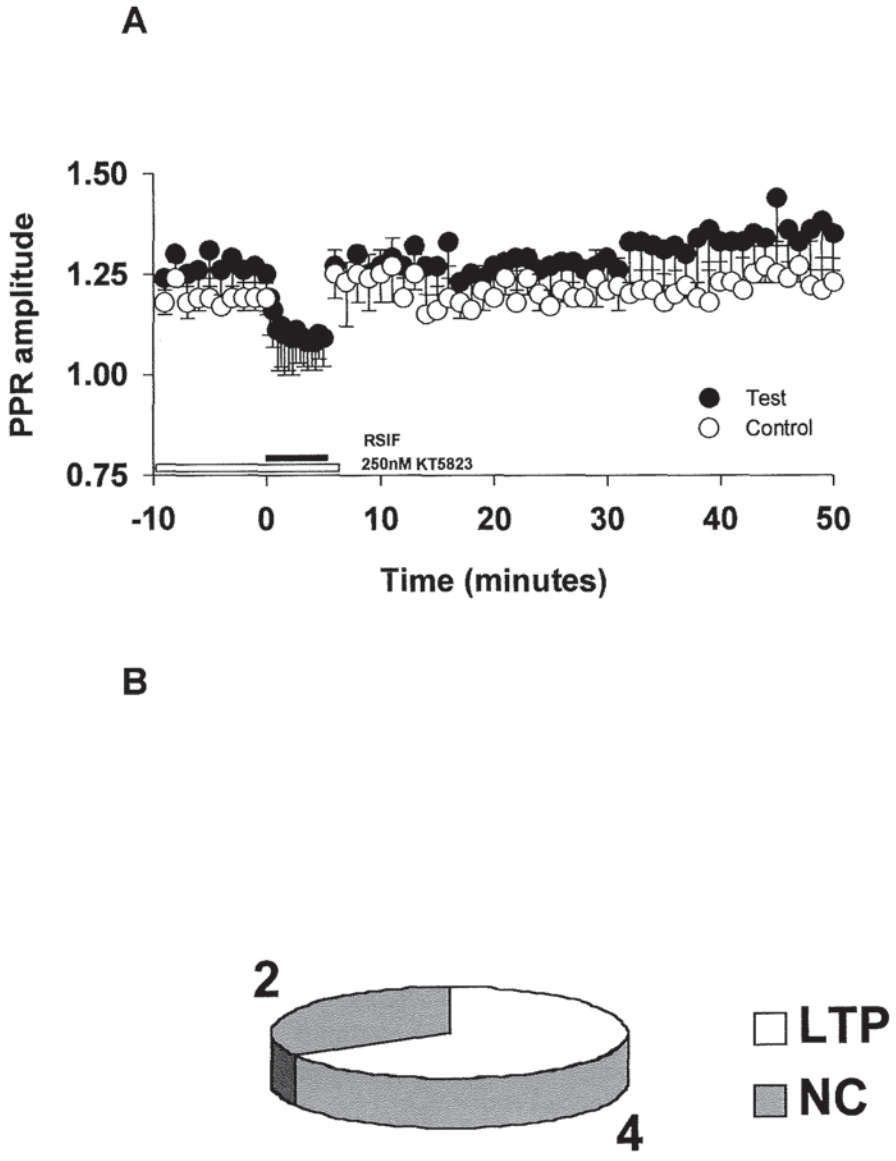

Figure 4.3.6 Effects of a 5 minute period of RSIF stimulation on field potential responses in the presence of 250nM KT5823

Graph A and pie chart B are as shown in figure 4.3.2. N = 6 paired recordings. Horizontal white bar represents the application of 250nM KT5823.

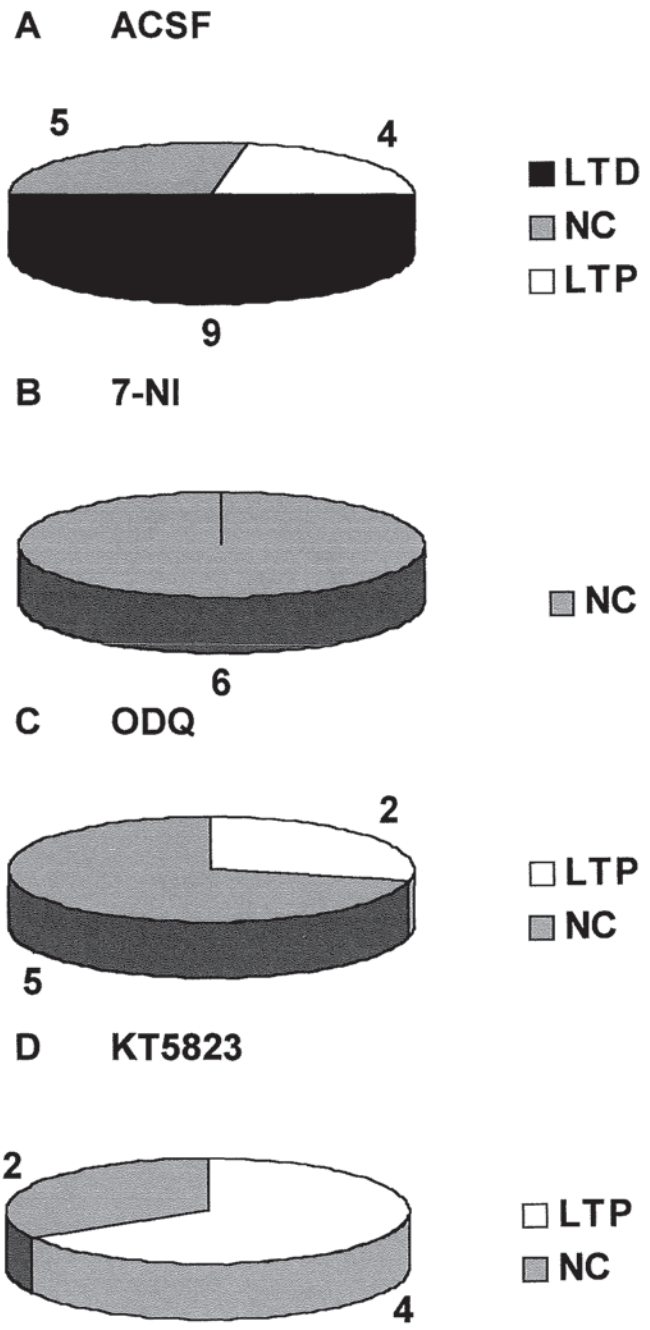

Figure 4.3.7 Effects of RSIF stimulation under control conditions or in the presence of inhibitors of nitric oxide synthase (5μM 7-NI), guanylate cyclase (10μM ODQ) or protein kinase G (250nM KT5823)

Pie charts represent the incidence of LTD, LTP and no change in the test pathway N2 amplitude measured 35 minutes after the stimulation period. Pie charts A – D show the effect of RSIF stimulation alone and in the presence of 5μM 7-NI, 10μM ODQ or 250nM KT5823, respectively.

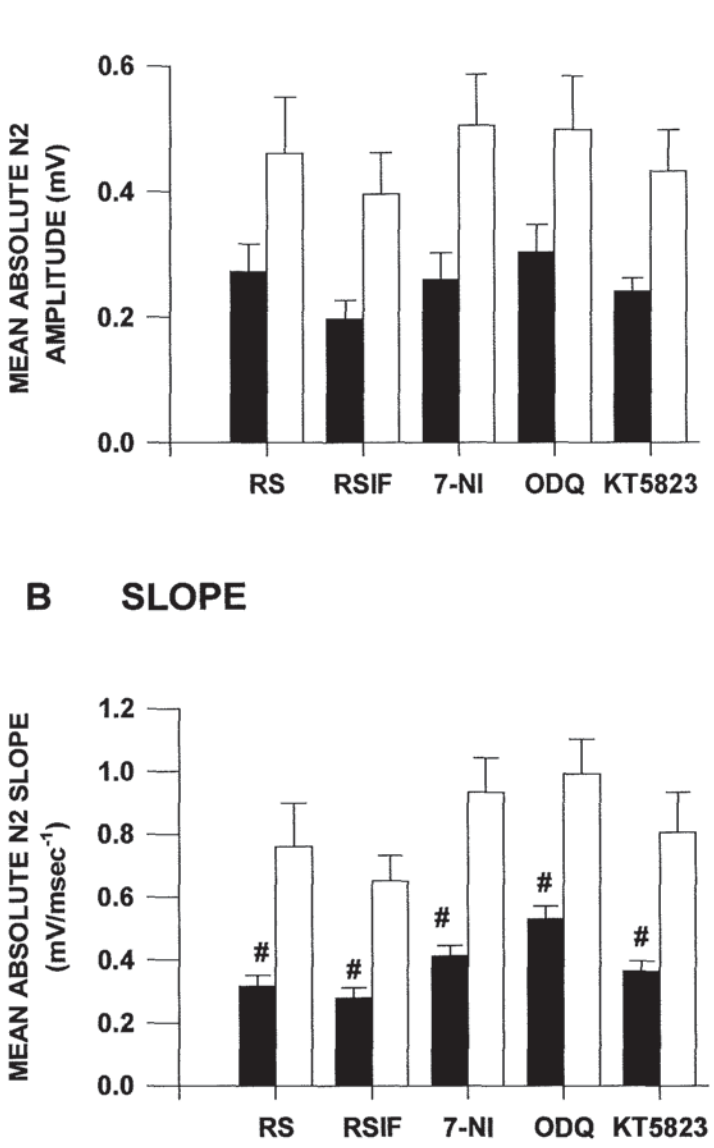

Figure 4.3.8 Bar charts to show the average absolute amplitude and slope values during the baseline control period and at the start of the 5 minute period of raised intensity stimulation

Bar charts A and B show the average absolute amplitude (mV) and slope (mV / ms^{-1}) respectively, during baseline stimulation (black) and at the start of stimulation (white). From left to right; raised stimulus intensity alone, raised stimulus intensity and frequency (RSIF) alone, or RSIF in the presence of 5μM 7-NI, 10μM ODQ or 250nM KT5823, respectively. To compare the baseline and raised levels of both the amplitude and the slope in drug-free ACSF and in the presence of inhibitors, single factor ANOVA tests were performed. '#' indicates where a significant difference was found between the baseline N2 slope values among the five groups ($p<0.05$).

4.3.2 EFFECT OF RAISED STIMULUS INTENSITY AND INCREASED FREQUENCY STIMULATION FOR 5 MINUTES ON EXTRACELLULAR FIELD POTENTIAL RESPONSES IN TRANSVERSE SLICES OF CEREBELLAR VERMIS IN THE PRESENCE OF AN INHIBITOR OF NITRIC OXIDE SYNTHASE

To determine if the inhibition of NOS could alter the induction or extent of LTD, the RSIF stimulation paradigm was repeated in the presence of 5μM 7-NI in transverse slices. In 5 recordings no change was observed compared to the baseline level but in the remaining 2 cases a LTD of the test pathway N2 amplitude and slope emerged after stimulation. As shown in figures 4.3.9 and 4.3.10 the pooled test and control pathway N2 amplitudes were not significantly different 35 minutes after stimulation 92.7 $\pm$ 6.4 and 93.2 $\pm$ 10.6% of baseline levels, respectively (N=7, Wilcoxon Matched-Pairs test $p>0.05$). During stimulation the amplitude of the PPR in the test pathway was transiently reduced. In the test pathway there was a slight increase in the amplitude of N1 but no long-term change in the amplitude of the PPR after RSIF stimulation. In the control pathway there was no obvious change in N1 or the amplitude of the PPR for the duration of the recording. In transverse slices the incidence of LTD in the absence of inhibitors was high, therefore, it was more appropriate to pool the data together. Consequently, a Mann-Whitney U test was performed to compare the amplitude and slope of N2 and the amplitude of N1 35 minutes after RSIF stimulation in drug-free ACSF to the results in the presence of 7-NI to inhibit NOS. Both the slope of N2 and the amplitude of N1 were found to be significantly different between the two sets of experiments ($p<0.05$).

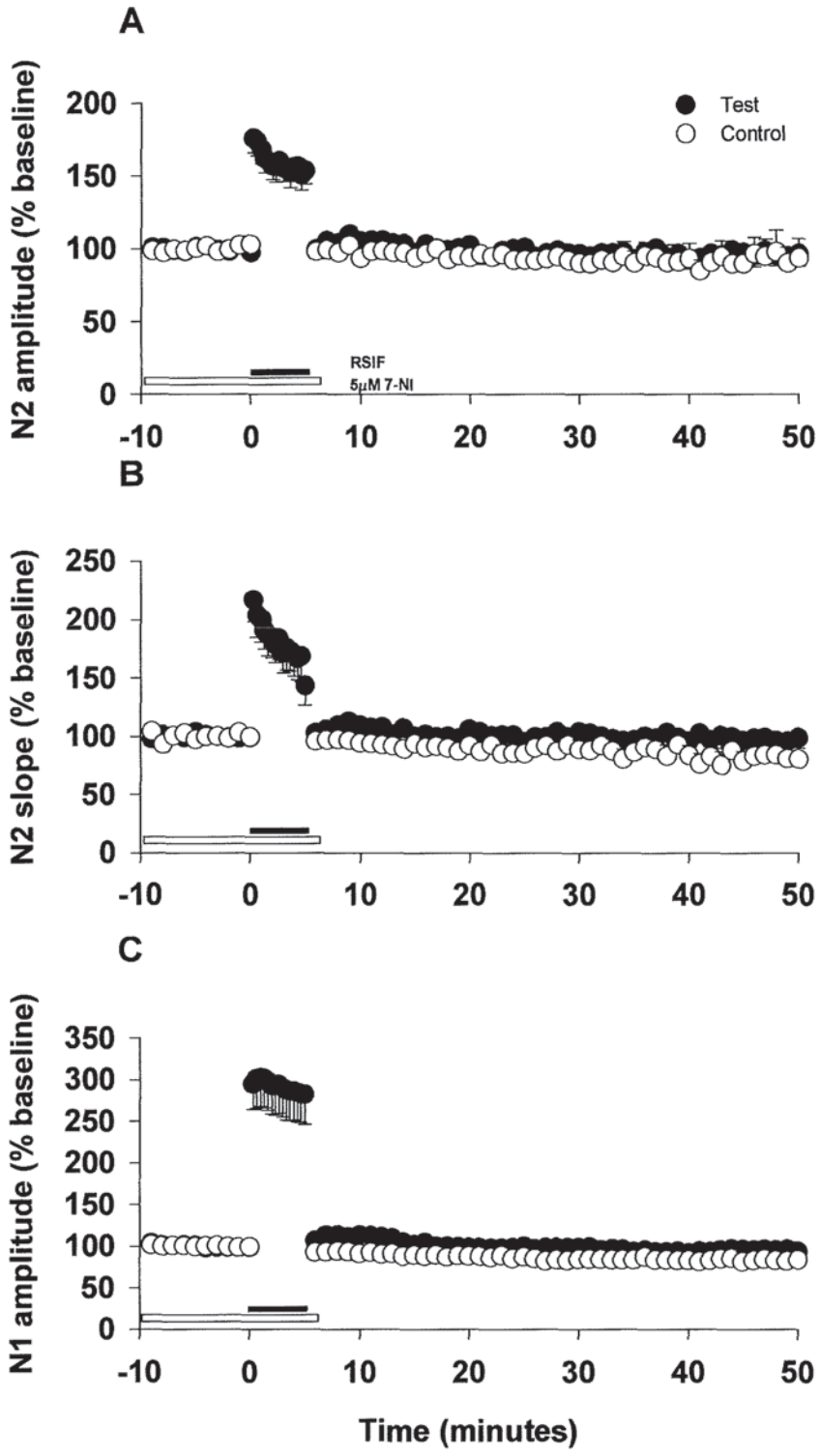

Figure 4.3.9 Effects of a 5 minute period of RSIF stimulation on field potential responses evoked in transverse slices in the presence of 5μM 7-NI
Graphs A –C are as shown in figure 4.3.1. N = 7 paired recordings.

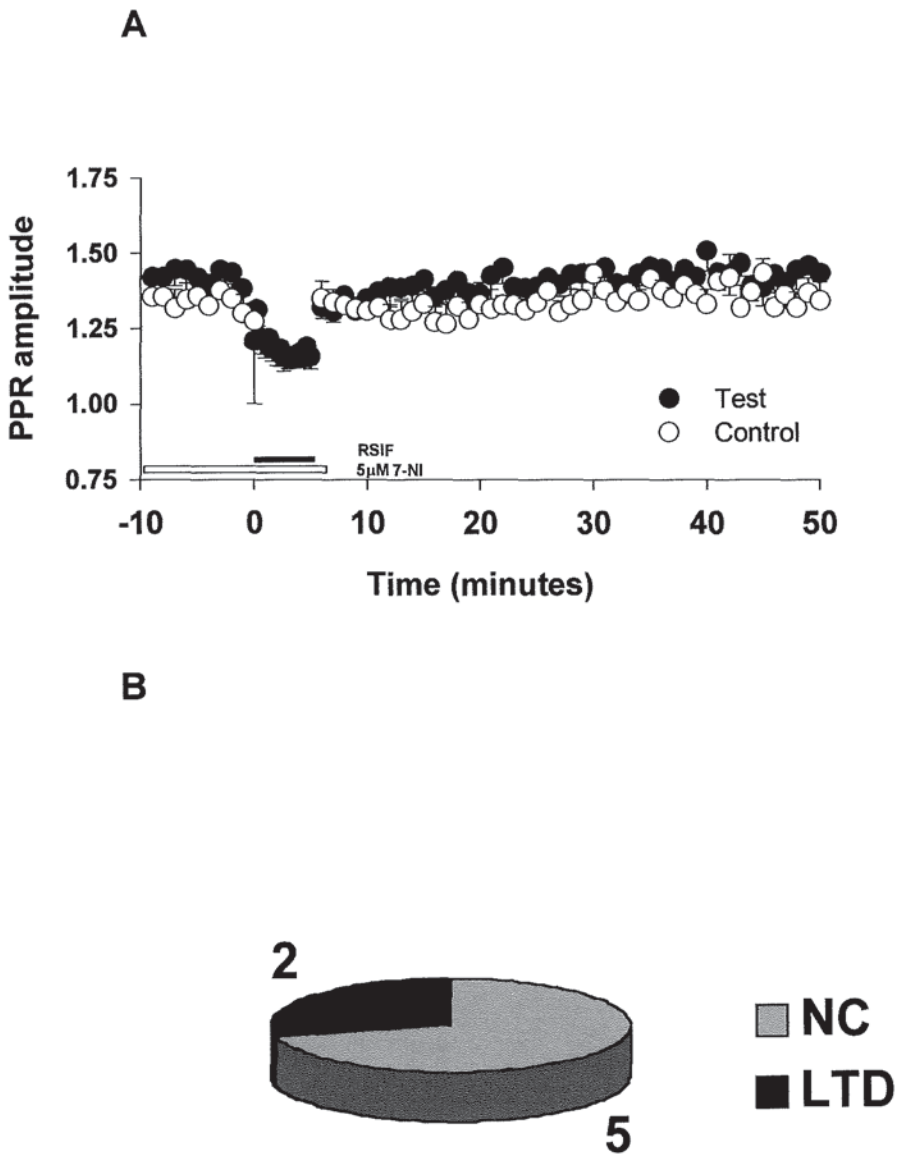

Figure 4.3.10 Effects of a 5 minute period of RSIF stimulation on field potential responses evoked in transverse slices in the presence of 5μM 7-NI
Graph A and pie chart B are as shown in figure 4.3.2. N = 7 paired recordings.

4.3.3 THE EFFECT OF INCREASED FREQUENCY STIMULATION FOR 5 MINUTES ON EXTRACELLULAR FIELD POTENTIAL RESPONSES IN SAGITTAL SLICES OF CEREBELLAR VERMIS IN THE PRESENCE OF A NITRIC OXIDE DONOR, A MEMBRANE PERMEABLE cGMP ANALOGUE OR A cGMP-SPECIFIC TYPE V PHOSPHODIESTERASE INHIBITOR

In this group of experiments the increased frequency stimulation was combined with the application of either a NO donor, an analogue of cGMP or a type V-specific PDE inhibitor. The aim of this was to determine if LTD could be induced under conditions where NO or cGMP were raised.

Increasing the frequency of the test pathway stimulation from 0.2Hz to 1Hz for a period of 5 minutes had little or no effect on FPs as shown in figure 3.3.4 in chapter 3. Figures 4.3.11 and 4.3.12 illustrate the effects of bath perfusion of the NO donor SNP at a concentration of 5mM for 5 minutes followed by a further 5 minutes paired with IF stimulation. The IF stimulation produced a marked, transient depression of the N2 and N1 components of FP responses. An acute effect was seen in the test pathway which was apparent almost immediately after the beginning of the IF stimulation period. One minute after stimulation the N2 amplitude in the test pathway was significantly different from that in the IF experiments recorded in the absence of SNP 74.7 $\pm$ 4.4 (N = 9) and 98.1 $\pm$ 2.9% (N = 5) of baseline levels, respectively (Mann-Whitney U test $p<0.01$). Within 25 minutes of the end of the 1Hz stimulation period a long-lasting depression of the test pathway N2 component was seen in 4 recordings. Of the remaining 4 recordings, responses gradually returned to baseline levels and in one experiment the FP response was potentiated. At 1 or 25 minutes after stimulation of the test pathway, the test and control pathways were not significantly different (Wilcoxon Matched-Pairs test $p>0.05$). Although measurement of the amplitude of the N2 component suggested that less than 50% of recordings showed a long-term effect at 35 minutes after IF stimulation, the slope of the N2 component indicated that 6 out of the total of 9 recordings underwent depression at this time. The test pathway N1 component was depressed during IF stimulation but within 10 minutes it returned to pre-stimulation levels. In the test pathway the amplitude of the PPR was slightly reduced during stimulation and slowly increased after

the IF stimulation period. The N2 components of FP responses in the control pathway, which was not stimulated, were also slightly reduced after stimulation. This suggested that in the absence of IF stimulation this pathway was influenced to a small extent by the application of SNP. In the control pathway there was no obvious change in N1. A transient increase in the amplitude of the PPR was noted after stimulation in both pathways.

The membrane permeable cGMP analogue 8-Br-cGMP was bath perfused at a concentration of 500μM for 5 minutes and then for a further 5 minutes application was combined with IF stimulation. As shown in figures 4.3.13 and 4.3.14 8-Br-cGMP paired with IF stimulation produced similar effects to those of SNP. In the test pathway a pronounced depression of the N2 and N1 components of FPs was observed within 1 minute of the start of the IF stimulation period. One minute after stimulation the N2 amplitude was significantly different from that compared to the control IF experiments recorded in the absence of 8-Br-cGMP 70.7 $\pm$ 6.4 (N = 6) and 98.1 $\pm$ 2.9% (N = 5) of baseline levels, respectively (Mann-Whitney U test $p<0.05$). Within 25 minutes a long lasting depression of the test pathway N2 amplitude was seen in 1 recording. In the remaining 5 recordings, responses returned to baseline levels. In the test pathway the measurement of the FP slope of N2 revealed that a significant proportion of FPs were depressed 25 minutes after stimulation when compared to the control pathway 71.8 $\pm$ 8.2 and 89.5 $\pm$ 7.0% of baseline levels, respectively (N = 6, Wilcoxon Matched-Pairs test $p<0.05$). Before the start of the IF stimulation period there was some evidence that the N2 and N1 components were reduced simply by application of 8-Br-cGMP alone. In addition the N2 components of FPs in the control pathway that was not stimulated were slightly reduced after stimulation. This suggested that even in the absence of IF stimulation 8-Br-cGMP produced some depression of synaptic transmission. This was similar to the effects of SNP that were noted on the FP responses in the control site. In the test pathway the N1 component was markedly reduced during IF stimulation and responses did not return to baseline levels after stimulation. There was also a gradual decrease in the N1 amplitude in the control pathway as the experiment progressed. There was a slight decrease in the amplitude of the PPR in the test pathway during stimulation. However, no obvious long-term changes were observed in either pathway.

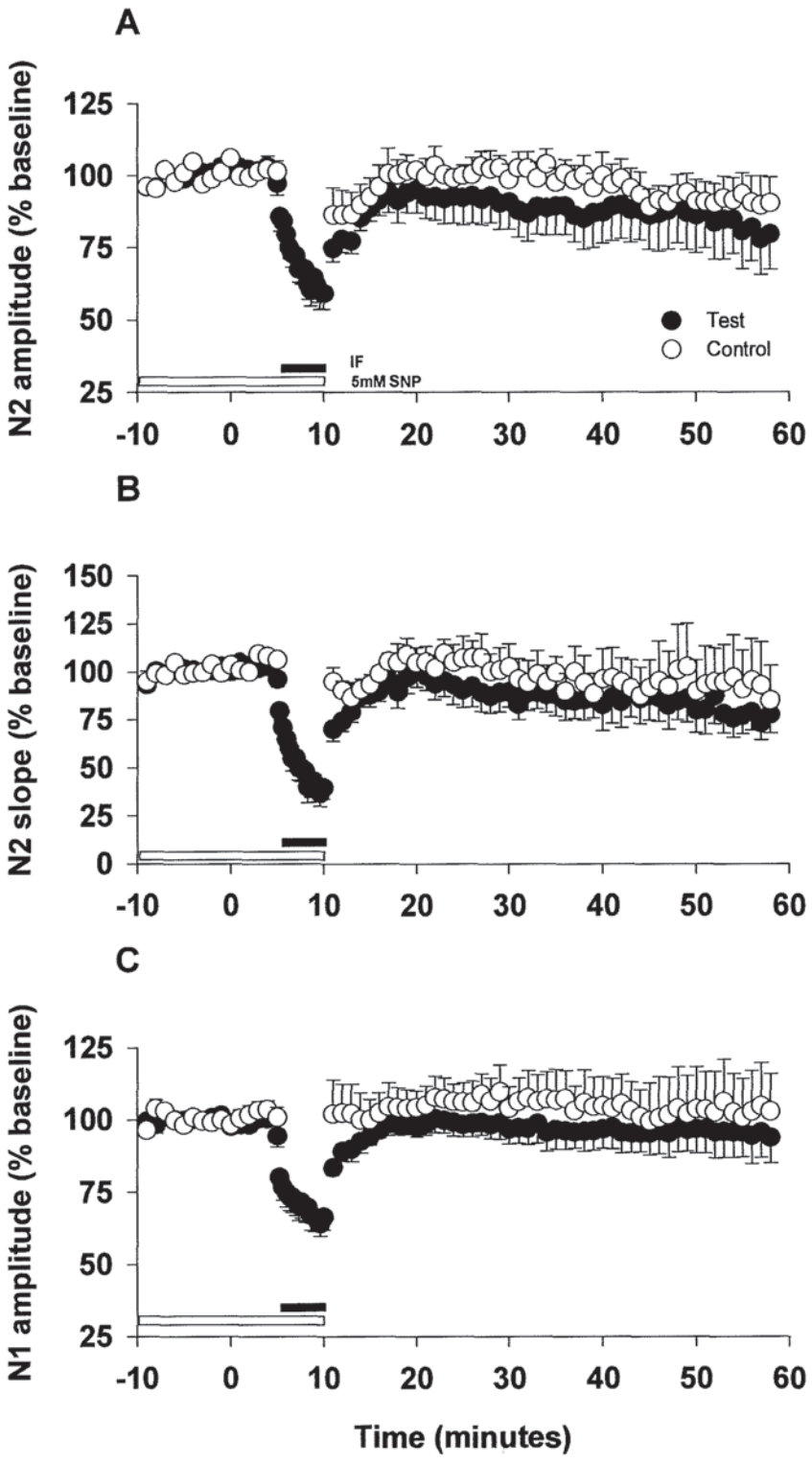

Figure 4.3.11 Effects of increased frequency stimulation (0.2 to 1Hz) on field potential responses in the presence of 5mM SNP

Graphs A - C illustrate the FP N2 amplitude, N2 slope and N1 amplitude, respectively. Data are expressed as the mean % ± S.E.M. of 10 responses collected during a 10 minute control period. N = 6 paired recordings (9 pathways 1Hz, 6 pathways 0.2Hz). Closed circles, test pathway stimulated at 1Hz for 5 minutes; open circles, control pathway. Horizontal black bar indicates the period of IF stimulation. Horizontal white bar represents the application of 5mM SNP.

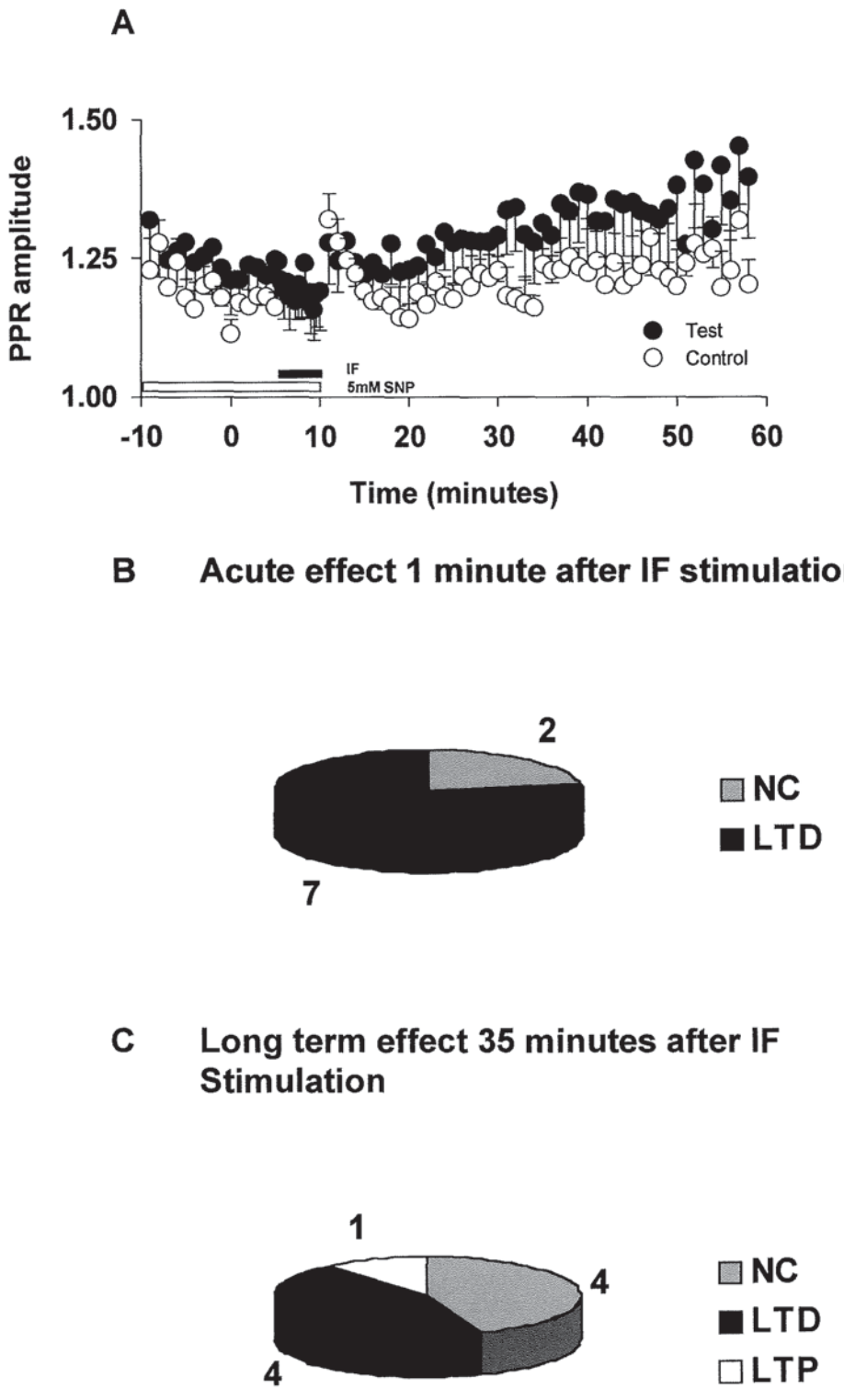

Figure 4.3.12 Effects of a 5 minute period of increased frequency stimulation on field potential responses in the presence of 5mM SNP

Graph A illustrates the amplitude of the PPR. Data are expressed as the mean % ± S.E.M. of 10 responses collected during a 10 minute baseline period. N = 6 paired recordings (9 pathways 1Hz, 6 pathways 0.2Hz). Closed circles, test pathway stimulated at 1Hz for 5 minutes; open circles, control pathway. Horizontal black bar indicates the period of increased frequency stimulation. Horizontal white bar represents the application of 5mM SNP. Pie charts B and C respectively show the incidence of LTD, LTP and no change in the test pathway N2 amplitude measured at 1 and 25 minutes after stimulation.

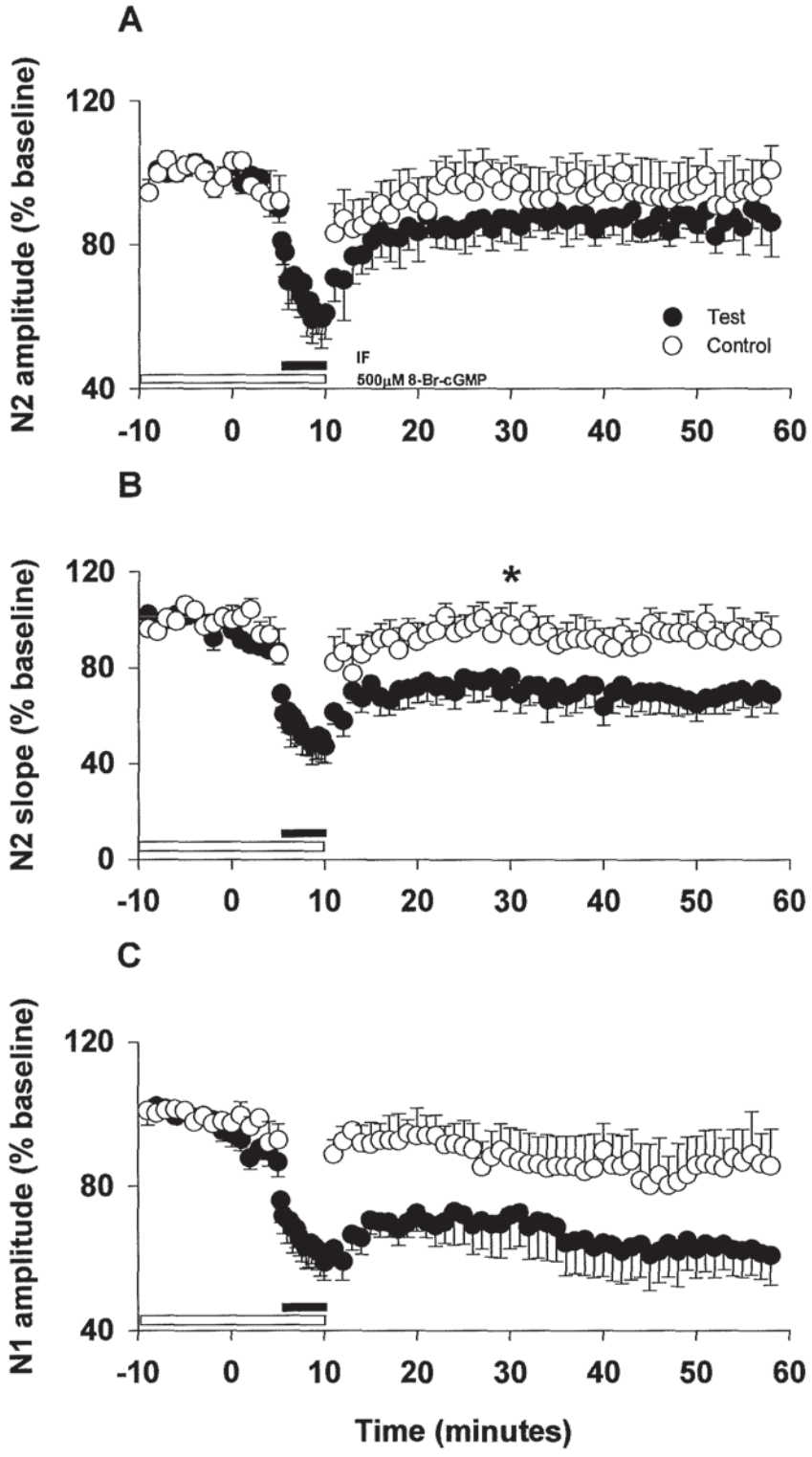

Figure 4.3.13 Effects of a 5 minute period of increased frequency stimulation on field potential responses in the presence of 500μM 8-Br-cGMP

Graphs A - C are as shown in figure 4.3.11. N = 6 paired recordings. Horizontal white bar represents the application of 500μM 8-Br-cGMP. N1 represents only 3 paired recordings (5 pathways 1Hz, 4 pathways 0.2Hz). Asterisk indicates where a significant difference was observed between test and control pathways (Wilcoxon Matched-Pairs test $p<0.05$).

A

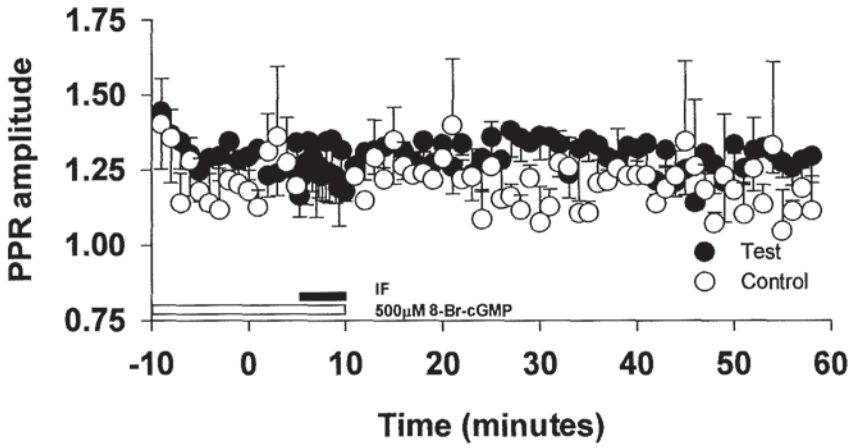

B Acute effect 1 minute after IF stimulation

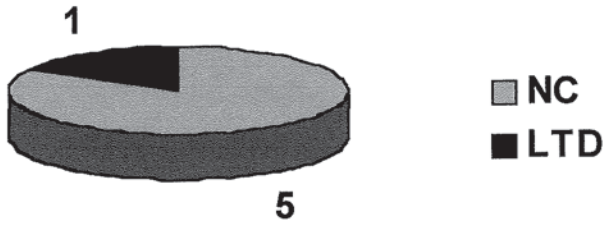

C Long term effect 35 minutes after IF stimulation

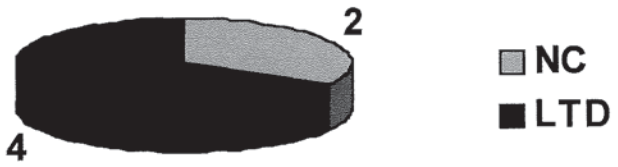

Figure 4.3.14 Effects of a 5 minute period of increased frequency stimulation on field potential responses in the presence of 500μM 8-Br-cGMP

Graph A and pie charts B and C are as shown in figure 4.3.12. The amplitude of the PPR represents 3 paired recordings. Horizontal white bar represents the application of 500μM 8-Br-cGMP.

The effects of IF stimulation in the presence of 10nM of the type V cGMP-specific PDE inhibitor UK114 542-27 are shown in figures 4.3.15 and 4.3.16. UK114 542-27 has a Ki value against type I PDEs of 93nM and of 1.7nM against type V PDEs (P Ellis, Pfizer Limited, personal communication). Therefore, we assume that bath perfusion of a concentration of 10nM of UK114 542-27 would be relatively specific for type V PDEs. During stimulation there was an acute depression of the N2 component of FPs that was coincident with a transient decrease in the amplitude of N1 and the amplitude of the PPR in the test pathway. Immediately after stimulation in the test pathway a depression of the N2 amplitude was observed in only 1 recording but within 25 minutes a long-lasting depression emerged in 4 out of the total group of 7 experiments. This depression was significantly different when compared to IF stimulation in drug-free ACSF. The mean amplitudes of the N2 components were 82.3 $\pm$ 3.9 (N = 7) and 98.1 $\pm$ 2.9% (N = 5) of baseline levels, respectively (Mann-Whitney U test $p<0.05$). The slope of the N2 component showed a slightly different picture as 4 out of the total group of 7 recordings were depressed within 1 minute of IF activation. The majority of the recordings (6 out of the total of 7 experiments) were depressed 25 minutes after cessation of the stimulation period and reached an average depression of 74.4 $\pm$ 4.5 of the baseline level. In the test pathway after stimulation the N1 component rapidly returned to baseline levels and the amplitude of the PPR recovered to pre-stimulation levels within 20 minutes. In the control pathway that was not stimulated, there was no obvious change in the amplitude or slope of the N2 response or the amplitude of the PPR for the duration of these experiments. However after stimulation in the test pathway an increase in the amplitude of N1 was apparent in several recordings.

Inhibition of NOS blocked the induction of LTD by IF stimulation in the presence of 10nM UK114 542-27 as shown in figures 4.3.17 and 4.3.18. 25 minutes after IF stimulation the N2 and N1 components of FP responses in the presence of both 5μM 7-NI and 10nM UK114 542-27 were significantly different from those in the presence of UK114 542-27 alone. The N2 amplitudes were 98.8 $\pm$ 5.2 (N = 6) and 82.3 $\pm$ 3.9% (N = 7) of baseline levels, respectively and the N1 amplitudes were 113.7 $\pm$ 5.4 and 98.8 $\pm$ 4.3% of baseline levels, respectively (Mann-Whitney U test $p<0.05$). The reduction in the N2 and N1 components of FPs and of the amplitude of the PPR was less prominent during IF in the presence of UK114

542-27 and 7-NI than in the presence of UK114 542-27 alone. Interestingly there was a clear increase in the N2 and N1 components after IF stimulation in the presence of UK114 542-27 and 7-NI. This small enhancement of the FP in the presence of the NOS inhibitor was similar to the increase in the N2 and N1 components that was observed after RSIF stimulation also in the presence of 7-NI. This observation raises the possibility that inhibition of components of cGMP signalling can unmask an underlying potentiation of possibly presynaptic origin.

Bar charts were constructed to look at the N2 amplitude and slope of FPs in the test pathway measured at 1 and 25 minutes after cessation of IF stimulation. At these time points Mann Whitney U Tests were performed to compare the FP responses recorded in drug-free ACSF to those responses measured in the presence of applications of SNP, 8-Br-cGMP and UK114 542-27 alone or in combination with 7-NI (Figure 4.3.19). The bar charts illustrate that a significant difference was observed between both the N2 amplitude and slope as measured 1 minute after the end of IF stimulation in the presence of SNP or 8-Br-cGMP when compared to the values in drug-free ACSF ($p<0.05$). However, no significant differences were found in the N2 component recorded at 25 minutes after molecular layer IF activation with the exception of the N2 slope recorded in the presence of 8-Br-cGMP ($p>0.05$). The effects of UK 114 542-27 were most prominent at 25 minutes after the cessation of IF molecular layer activation. The amplitude and slope values of N2 were both significantly different to those recorded in drug-free ACSF at this time point ($p<0.05$). In addition, 7-NI significantly blocked the depression induced by UK 114 542-27 paired with IF stimulation ($p<0.05$).

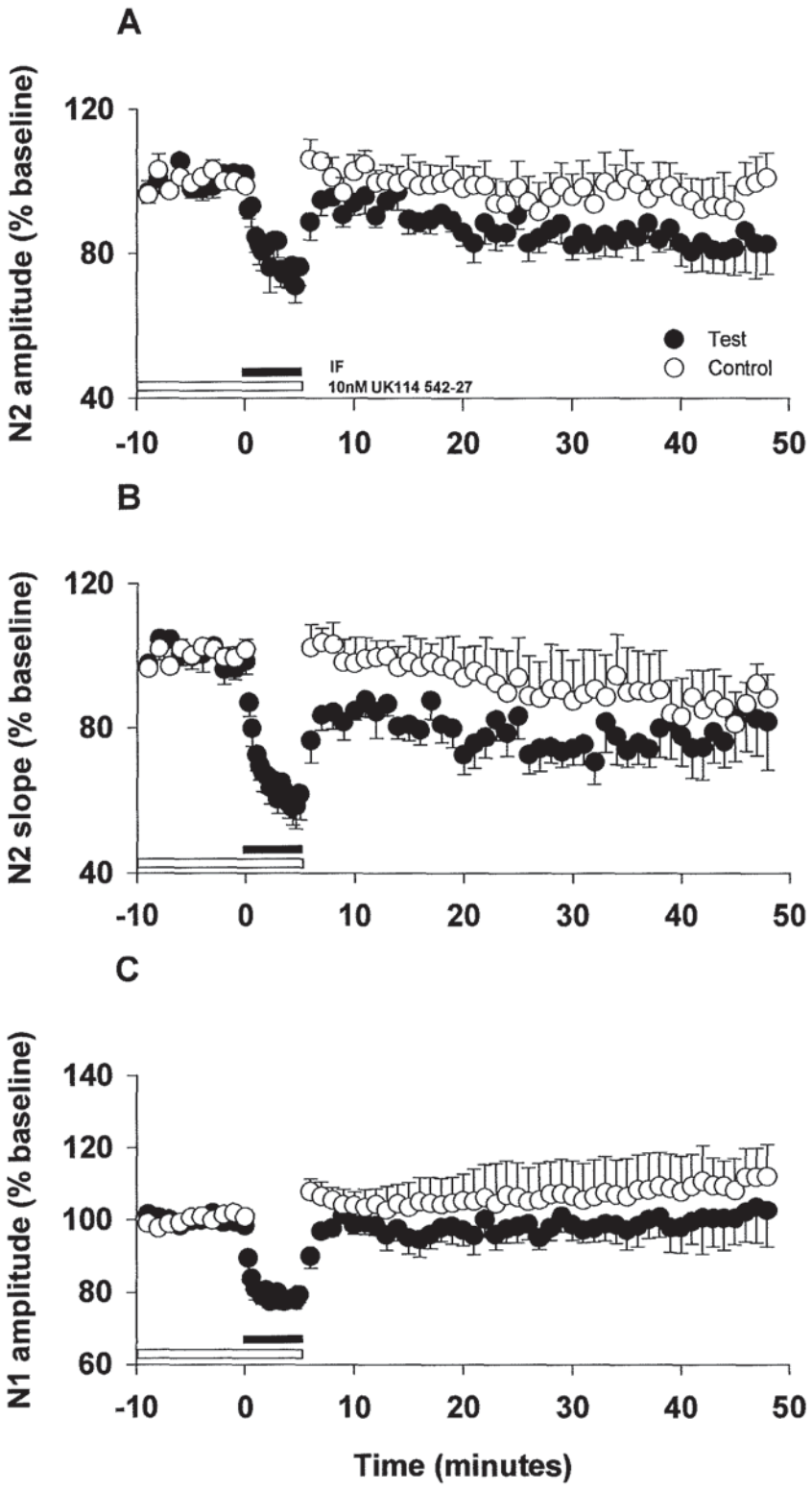

Figure 4.3.15 Effects of a 5 minute period of increased frequency stimulation on field potential responses in the presence of 10nM UK114 542-27

Graphs A – C are as shown in figure 4.3.11. N = 6 paired recordings (7 pathways 1Hz, 6 pathways, 0.2Hz). Horizontal white bar represents the application of 10nM UK114 542-27.

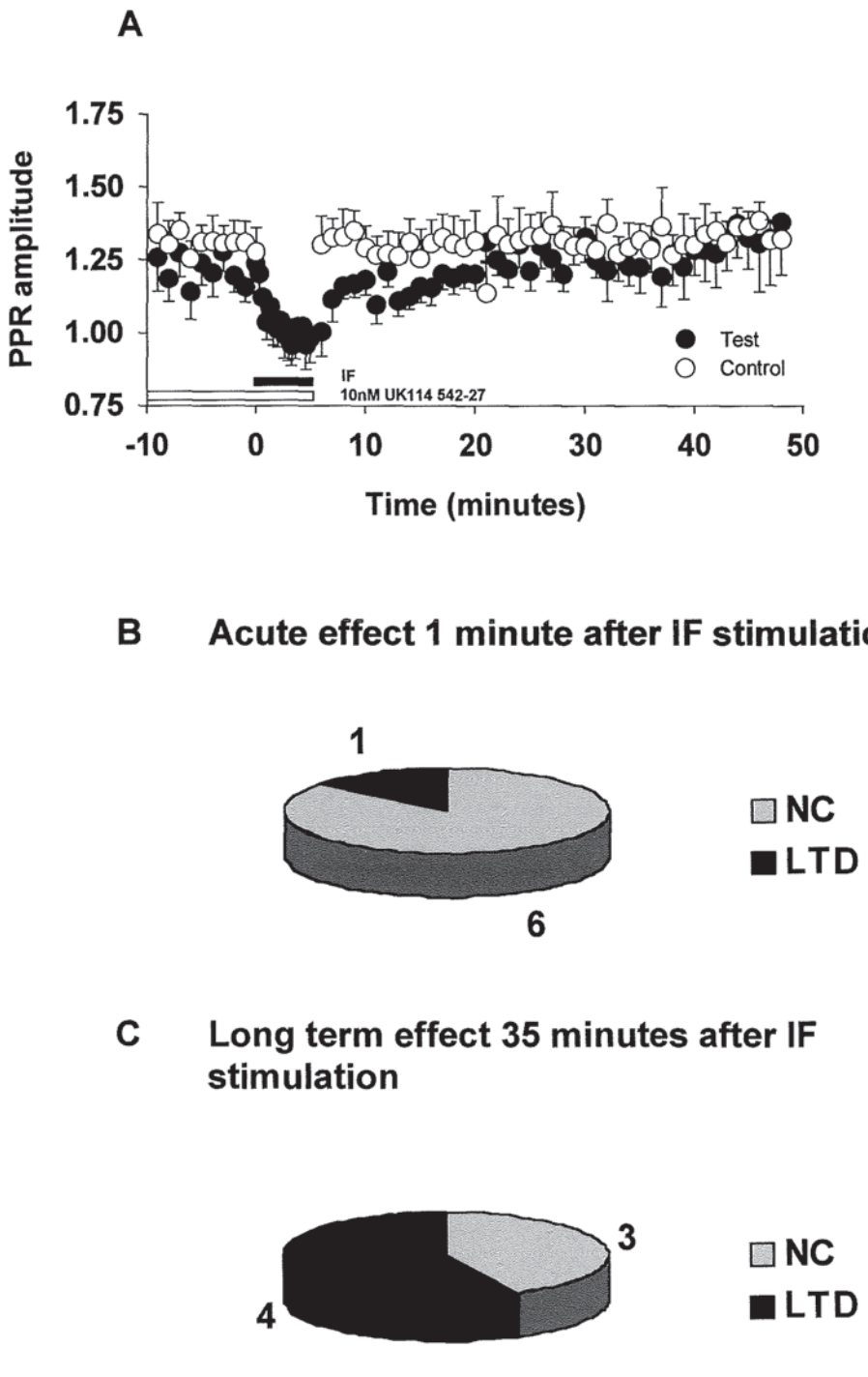

Figure 4.3.16 Effects of a 5 minute period of increased frequency stimulation on field potential responses in the presence of 10nM UK114 542-27

Graph A and pie charts B and C are as shown in figure 4.3.12. N = 6 paired recordings (7 pathways 1Hz, 6 pathways, 0.2Hz). Horizontal white bar represents the application of 10nM UK114 542-27.

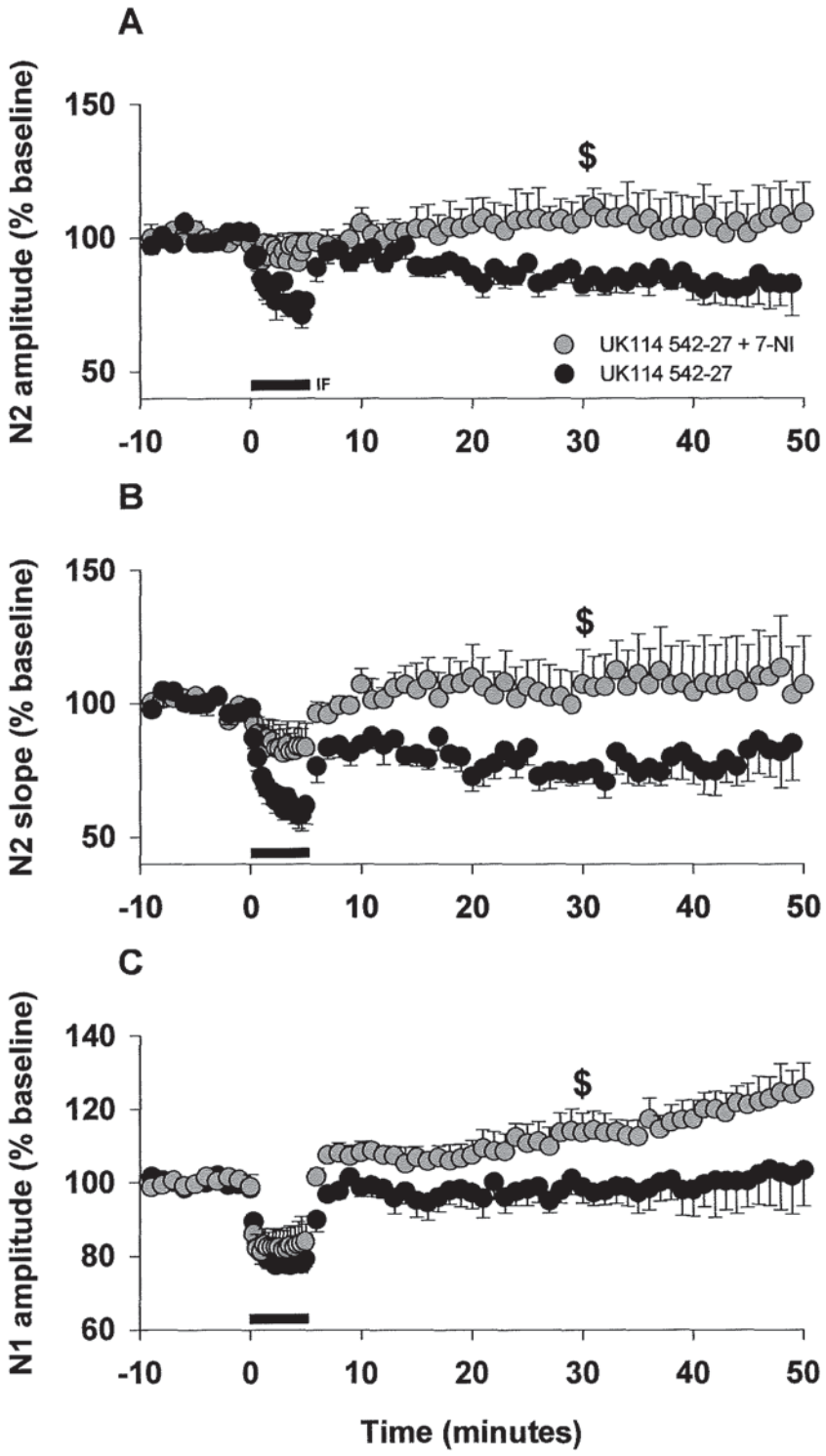

Figure 4.3.17 A comparison of the effects of a 5 minute period of increased frequency stimulation on field potential responses in the presence of 10nM UK114 542-27 alone or in combination with 7 -NI

Graphs A–C are as shown in figure 4.3.11. Each pathway was stimulated at 1Hz for 5 minutes. Black circles, pathway stimulated in the presence of UK114 542-27 (N = 7); grey circles, pathway stimulated in the presence of both UK114 542-27 and 7-NI (N = 6). Dollar signs ($) indicate where a significant difference was observed between the pathways in the absence and presence of 7NI (Mann-Whitney U test, $p<0.05$).

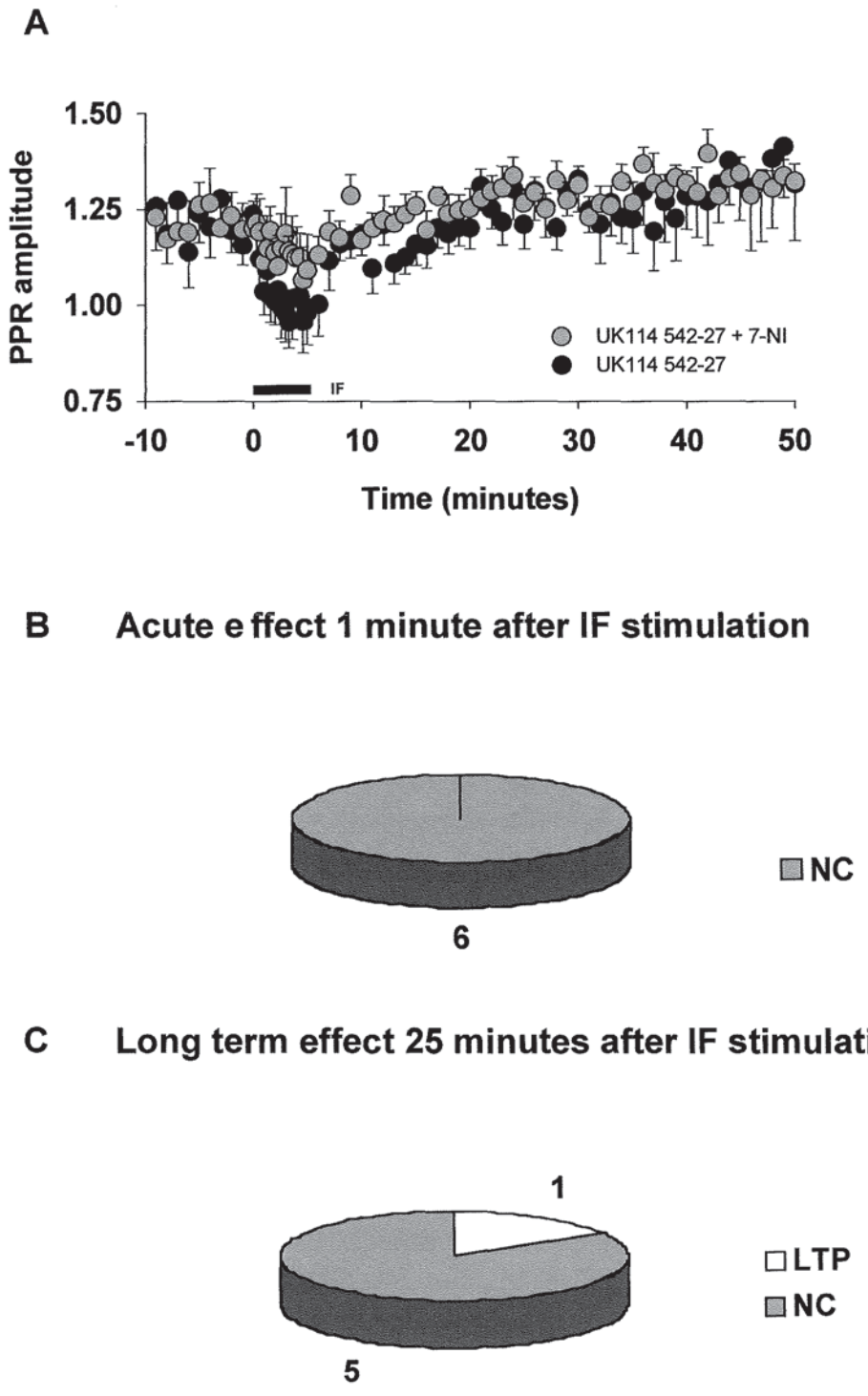

Figure 4.3.18 A comparison of the effects of a 5 minute period of increased frequency stimulation on field potential responses in the presence of 10nM UK114 542-27 alone or in combination with 5μM 7 -NI

Graph A and pie charts B and C are as shown in figure 4.3.12. Each pathway was stimulated at 1Hz for 5 minutes. Black circles, pathway stimulated in the presence of UK114 542-27 (N = 7); grey circles, pathway stimulated in the presence of both UK114 542-27 and 7-NI (N = 6).

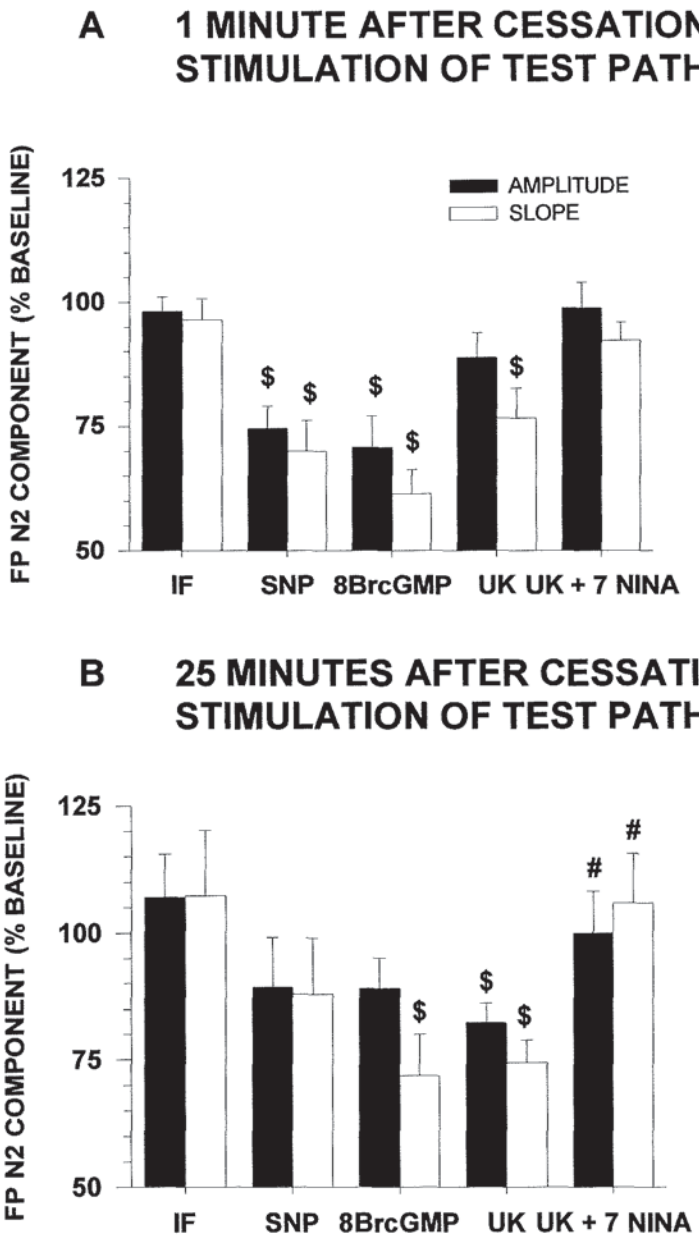

Figure 4.3.19 Effects of a 5 minute period of 1Hz stimulation alone, or in the presence of a NO donor (SNP), a cGMP analogue (8-Br-cGMP) or a phosphodiesterase type IV inhibitor (UK 114 542-27) alone or in combination with a NOS inhibitor (7-NI)

Bar charts A and B represent the test pathway N2 amplitude (black) and slope (white) at 1 and 25 minutes, respectively after the IF stimulation period. From left to right IF stimulation in drug-free ACSF, IF stimulation paired with application of 5mM SNP (N = 9), 500μM 8-Br-cGMP (N = 6), UK114 542-27 (N = 7) or UK114 542-27 in combination with 5μM 7-NI (N = 6). Dollar signs ($) indicate where a significant difference in the amplitude of the N2 component was observed following IF stimulation in drug-free ACSF when compared to IF stimulation in the presence of SNP, 8-Br-cGMP or UK 114 542-27 (Mann Whitney U Test $P<0.05$). Hash Marks (#) show where a significant difference in the amplitude of N2 was found following IF stimulation in the presence of both UK 114 542-27 and 7-NI when compared to IF stimulation in the presence of UK 114 542-27 alone.

4.4 DISCUSSION

Raising the stimulus intensity and increasing the frequency of molecular layer stimulation in sagittal slices provided the conditions necessary to induce an input-specific form of LTD of extracellular FP responses in 50% of recordings as described in chapter 3. This extracellular model was used to examine the possible contributions of NOS, NO, GC, cGMP, type V cGMP-specific PDEs and PKG to the LTD of FP responses. Two different approaches were used. In sagittal slices RSIF stimulation was repeated in the presence of the inhibitors 7-NI, ODQ and KT5823 to investigate whether inhibition of NOS, GC and PKG enzymes affected the extent or the incidence of the induction of LTD. In transverse slices RSIF stimulation was repeated in the presence of 7-NI. The inhibitors were applied for 10 to 20 minutes before stimulation, during stimulation and for only a short period after cessation of the RSIF paradigm. These experiments concentrated on the possible involvement of NOS, GC or PKG in the induction of LTD, less emphasis was placed on the importance of the cGMP cell signalling cascade for the maintenance of LTD. In future if these experiments were repeated it would be interesting to see what would happen if the inhibitors were applied for the duration of the experiment instead. In striatal coronal slices, pre-incubation with N(G)-nitro-L-arginine methyl ester hydrochloride (L-NAME, Moore and Handy, 1997), an inhibitor of NOS was sufficient to prevent the induction of LTD by low frequency stimulation paired with intracellular application of the type 1 and type V PDE inhibitor Zaprinast. In this study it was also noted that NOS inhibitors could not reverse Zaprinast-induced LTD once it was established suggesting that the NO/cGMP pathway might be necessary for the induction of LTD but not its maintenance (Calabresi et al., 1999).

In sagittal slices, five minutes IF stimulation was combined with applications of a donor of NO, a membrane permeable analogue of cGMP or an inhibitor of type V cGMP specific PDEs. This method was designed to determine if stimulation of the molecular layer at a raised frequency paired with an increase in the level of available NO or cGMP could fulfil the conditions required for the induction of LTD.

In sagittal slices the inhibition of NOS, GC or PKG appeared to reduce the incidence of LTD evoked by RSIF stimulation. Interestingly, under these conditions a slight LTP was observed in some recordings. In those recordings in which a potentiation of the N2 amplitude or slope was observed there was an associated increase in N1. This indicated that the facilitation of the N2 component of FP responses could be accounted for by an increase in the number of PFs recruited by stimulation of the molecular layer. 7-NI is an inhibitor of calcium-dependent neuronal NOS. It antagonises both the cofactor tetrahydrobiopterin (BH_4) and its substrate L-arginine (Babbedge et al., 1993; Moore and Handy, 1997). Therefore, inhibition of NOS by 7-NI prevents the sequential oxidation of the substrate L-arginine to NO and L-citrulline. A major function of NO is to activate soluble GC (Schulz et al., 1991). ODQ does not chemically inactivate NO but it inhibits NOS-sensitive GC (Garthwaite et al., 1995) and consequently blocks the intracellular rise of cGMP triggered by GC without affecting NOS activity. The effects of cGMP, which are elicited through a pathway involving the activation of PKG are inhibited by the compound KT5823 which competes for the ATP binding site on PKG (Kase et al., 1987; Nakanishi, 1989). Based on the observation that in drug-free ACSF RSIF stimulation can produce an input-specific LTD of the N2 component in 50% of FP recordings, it is likely that NOS, GC and PKG contribute to the LTD observed in this preparation, because in the presence of inhibitors of this cascade fewer incidences of LTD were observed. In addition, under control conditions, in transverse slices a LTD of the amplitude of the N2 component of FPs was induced in 4 out of 6 recordings by a 5 minute period of RSIF stimulation as described in chapter 3. The presence of 5μM 7-NI during RSIF stimulation reduced the number of recordings in which a LTD of the N2 component was seen 35 minutes after stimulation. Furthermore, these experiments suggested that disruption of the cGMP signalling cascade could reveal an underlying potentiation.

Pairing 1Hz stimulation with bath perfusion of the NO donor SNP produced a pronounced depression of the N2 and N1 components of FP responses 1 minute after cessation of IF stimulation in the test pathway. This acute effect was followed by an input-specific LTD in 4 recordings 25 minutes after stimulation and the washout of SNP. These findings were consistent with reports which showed that 10mM SNP produced an acute and large depressant effect that was followed by a persistent depression of PF-mediated EPSCs after

washout of the compound (Blond et al., 1997). NO donors produce NO or NO related oxides such as the nitrosonium ion (NO^+) when applied to biological systems (Butler et al., 1995). SNP is relatively stable as a pure compound but it has the disadvantage of being sensitive to exposure to oxygen and therefore has to be prepared in distilled water bubbled with nitrogen gas. In an aqueous solution the half life of NO was determined to be less than 10 seconds *in vitro* (Alberts et al., 1994). During bath perfusion of SNP the elevated level of NO^+ paired with IF stimulation produced a more pronounced depression of the N2 and N1 components of FP responses than after washout. Under conditions of raised NO^+ the amplitude of the PPR was reduced during the period of IF stimulation. The amplitude of N1 was markedly decreased during the pairing of application of SNP with IF stimulation, but rapidly recovered when stimulation was resumed at 0.2Hz and SNP was washed out. This data suggested that in agreement with (Blond et al., 1997) the acute depressant effect of SNP was presynaptically mediated whereas the LTD induced in 4 cases after washout of the NO donor was probably a postsynaptic effect.

An acute depression of the N2 and N1 components of FP responses was induced by pairing 1Hz molecular layer stimulation with bath perfusion of the membrane permeable cGMP analogue 8-Br-cGMP. 25 minutes after stimulation, the mean test pathway N2 responses were depressed when compared to the baseline level. This was more evident from measurements of N2 slope than amplitude. The long-term decrease of the N2 component was input-specific and accompanied by a sustained decrease in the amplitude of N1 but no obvious change in the PPR. The decrease in N1 might suggest a presynaptic site of action for the effects of 8-Br-cGMP. These results are in part consistent with previous reports in which injection of 8-Br-cGMP into the dendrites of Purkinje cells produced a robust depression of PF-mediated excitatory postsynaptic potentials (EPSPs, Hartell, 1994a). A combination of PF stimulation and bath perfusion of 8-Br-cGMP was similarly reported to induce a LTD of PF-EPSPs (Shibuki and Okada, 1992a).

IF stimulation in the presence of the type V cGMP-specific PDE inhibitor UK 114 542-27 also led to an acute depression of the N2 and N1 components of FP responses. Input-specific LTD of the N2 component of FP responses was apparent in 4 recordings within 25 minutes

of cessation of IF stimulation. These data were in agreement with the finding that PF stimulation induced LTD in the presence of Zaprinast, a less specific inhibitor of cGMP-specific PDEs (Hartell, 1996a) in whole cell patch-clamp recordings. When IF stimulation paired with application of UK114 542-27 was repeated in the presence of the NOS inhibitor 7-NI, LTD was prevented and a potentiation emerged. Thus, these data support the possibility that LTD can mask LTP under certain conditions.

Applications of SNP or 8-Br-cGMP paired with IF stimulation produced an input-specific depression of FP responses. Since IF stimulation alone was not sufficient to induce LTD this observation suggests that IF stimulation combines with NO/cGMP to produce LTD. In the presence of the type V PDE inhibitor UK114 542-27 IF stimulation also induced a depression that was specific to the test pathway which was activated at 1Hz for 5 minutes. This observation might suggest that IF stimulation triggered cGMP production but only in the pathway that was stimulated. However, the fact that 8-Br-cGMP paired with IF stimulation also produced LTD indicates that IF activation might serve to provide another requirement for LTD such as mGluR activation. This is a possibility since the LTD of PF-EPSPs that was induced by intracellular injection of Zaprinast or 8-Br-cGMP was blocked by MCPG (Hartell, 1996a). In a striatal coronal slice preparation low frequency stimulation paired with application of Zaprinast was reported to induce LTD, this depression was no longer apparent if activation of the test pathway was stopped during application of the cGMP-specific PDE inhibitor (Calabresi et al., 1999).

Important roles for NO (Crepel and Jaillard, 1990; Shibuki and Okada, 1991; Daniel et al., 1993; Lev Ram et al., 1995), NO-sensitive GC (Boxall and Garthwaite, 1996a), cGMP (Daniel et al., 1993; Hartell, 1994a; Hartell, 1996a; Lev Ram et al., 1997) and PKG (Crepel and Jaillard, 1990; Ito and Karachot, 1992) in the induction of LTD have been proposed by a number of groups. In addition LTD can be produced by pairing PF-stimulation with application of either a NO donor (Blond et al., 1997) or an inhibitor of type V cGMP-specific PDEs (Hartell, 1996a). In agreement, the data presented here strongly suggests that the cellular mechanism for the LTD induced in sagittal slices by RSIF stimulation could require the activation of NOS, GC and PKG and a cascade of events involving NO, cGMP and PKG

as shown in figure 4.1.1. The induction of LTD is also thought to require activation of AMPAR and mGluR and a postsynaptic calcium influx.

Moreover the experiments in this chapter have raised the possibility that inhibiting key components of the cGMP signalling cascade can uncover a potentiation. The data suggests that there could be an interaction between cGMP-mediated postsynaptic depression and cAMP-mediated presynaptic potentiation at PF to Purkinje cell synapses. In the cerebellar cortex LTD and LTP could interact via a mechanism that involves the specific PDEs responsible for the degradation of cGMP and cAMP.

CHAPTER 5

RAISED FREQUENCY MOLECULAR LAYER STIMULATION INDUCES CHANGES IN THE DIRECTION OF SYNAPTIC PLASTICITY

5.1 INTRODUCTION

The aim of this chapter was to study the effect of raised frequency molecular layer stimulation on FPs that had properties consistent with PF-mediated responses. In the cerebellar cortex, raising the frequency of molecular layer stimulation has been reported to cause both long-term increases (Salin et al., 1996) and decreases (Schreurs and Alkon, 1993; Hartell, 1996b) in the synaptic strength at PF to Purkinje cell synapses. As described already in both the general introduction and chapter 3, in the absence of Ca^{2+} chelators raising the frequency and intensity of PF stimulation was sufficient to produce a LTD of PF-EPSPs (Hartell, 1996b). In contrast, when a postsynaptic Ca^{2+} chelator was included in the intracellular pipette solution, in whole cell recordings, a LTP of PF-EPSCs was induced by a 15 second 8Hz tetanus (Salin et al., 1996). In the same study, extracellular FP recordings (where no manipulations were made to the level of either extracellular or intracellular Ca^{2+}) revealed that a brief tetanus also resulted in large synaptic enhancement of FP responses. The LTP was accompanied by a decrease in the PPR suggesting a presynaptic origin and application of a blocker of the regulatory site of PKA (Rp-8-CPT-cAMPs) was found to prevent the LTP. In addition, the cAMP activator forskolin mimicked the potentiation (Salin et al., 1996). The key components of the cAMP signalling cascade that might be necessary for a cAMP-mediated form of LTP and the site of action of the inhibitors used in this chapter are illustrated in figure 5.1.1.

As outlined in the general introduction it is generally agreed that mGluR activation is necessary for the induction of LTD (see for example, Shigemoto et al., 1994; Conquet et al., 1994; Aiba et al., 1994). mGluRs are reported to be abundant in Purkinje cells (Martin et al., 1992; Gorcs et al., 1993). It was suggested that mGluRs could mediate the slow depolarising synaptic potential recorded from biplanar cerebellar slices that was produced by a brief tetanic stimulation. This potential was resistant to ionotropic glutamate receptor and GABAR antagonists (Batchelor and Garthwaite, 1993). It has since been shown that the mGluR antagonist MCPG could antagonise this slow syanptic potential (Batchelor et al., 1994). MCPG also blocked the LTD of PF-EPSPs that was observed when an injection of 8-Br-cGMP was paired with PF stimulation (Hartell, 1994b). It was suggested that mGluRs were located perisynaptically on somatic membranes of Purkinje cells and were likely to be activated by high frequency stimuli (Baude et al., 1994). These pieces of evidence imply that raised frequency activation of the cerebellar molecular layer could activate mGluRs.

As discussed previously, studies with an electrochemical NO probe revealed that high frequency molecular layer activation could trigger a cAMP-mediated potentiated release of NO (Kimura et al., 1998). It is also known that strong activation of PFs can initiate an influx of Ca^{2+} (Eilers et al., 1995; Hartell, 1996b; Eilers et al., 1997b).

Stimulation of PFs by raised frequency molecular layer activation has been suggested to:
a) activate mGluRs (Batchelor and Garthwaite, 1993; Batchelor et al., 1994; Hartell, 1994b)
b) trigger localised increases in Ca^{2+} (Eilers et al., 1995; Hartell, 1996b; Eilers et al., 1997b)
c) cause release of NO (Shibuki and Kimura, 1997; Kimura et al., 1998).
Therefore, we anticipated that 8Hz molecular layer stimulation could not only fulfil the requirements for LTP, but also some of the prerequisites for LTD. In this chapter the possible interaction between LTP and LTD at PF to Purkinje cell synapses was examined using the extracellular FP recording technique.

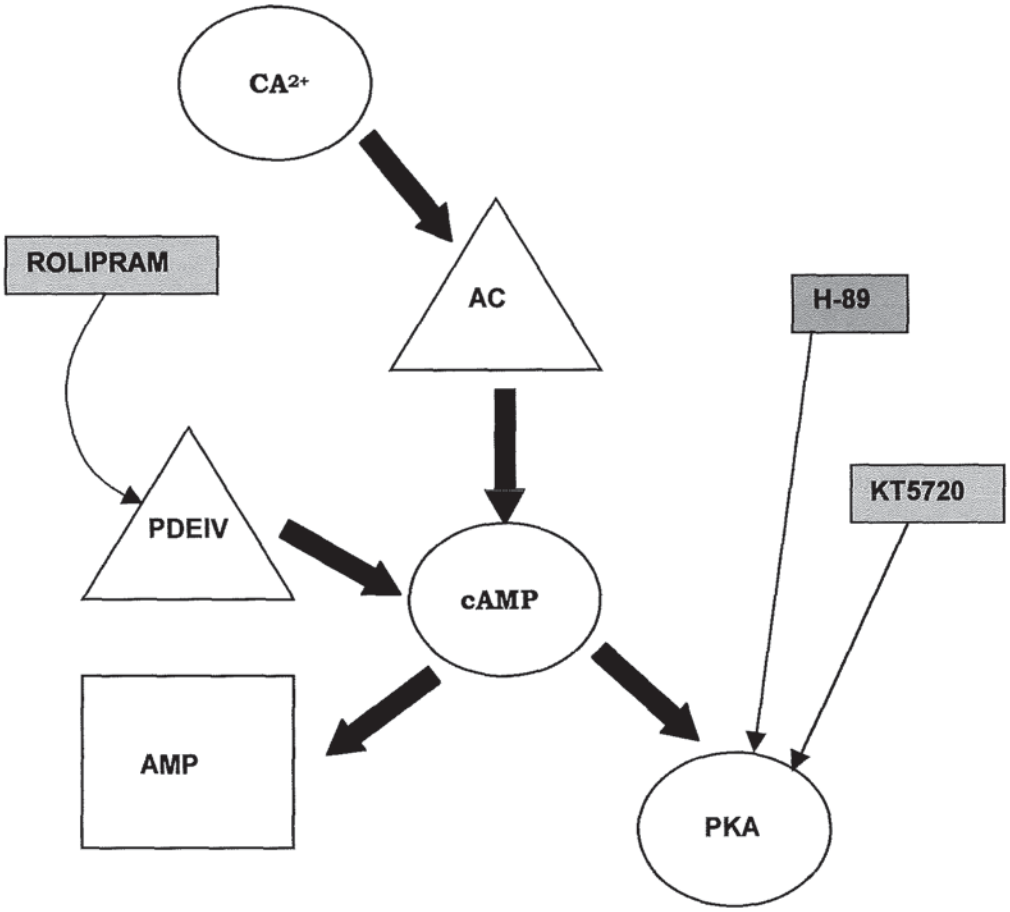

Figure 5.1.1 An illustration of the key components of the cAMP cell signalling cascade
Ca^{2+} activates adenylate cyclase (AC). AC stimulates the formation of cAMP from adenosine triphosphate (ATP). cAMP can be degraded by cAMP-specific type IV phosphodiesterases (PDEIV) into adenosine-5'-monophosphate (5'-AMP). cAMP activates protein kinase A which in turn regulates the level of protein phosphorylation. The grey boxes and narrow lines show the site of action of rolipram, H-89 and KT5720 that were used to inhibit type IV PDEs, and PKA respectively.

5.2 METHODS

5.2.1 SLICE PREPARATION

The majority of experiments were performed using sagittal slices prepared from 14-21 day old rats as described in chapter 2.2.1. In one set of experiments sagittal slices were prepared from 28-35 day old rats using the same method. Transverse slices were used in some experiments and these were prepared according to the methods described in chapter 3.2.1.

5.2.2 FIELD POTENTIAL RECORDING

In sagittal and transverse slices FP responses were obtained using the same method described in chapter 2.2.2.

5.2.3 APPLICATION OF DRUGS

For bath perfusion 7-NI, ODQ and KT5823 were made up as described in chapter 4.2.3. The cell permeable, selective and potent inhibitor of protein kinase A N-[2-bromocinnamyl(amino)ethyl]-5-isoquinolinesulfonamide (H-89, Calbiochem, Geilen et al., 1992) and the type IV cAMP-specific phosphodiesterase inhibitor 4-[3-(Cyclopentyloxy)-4-methoxyphenyl]-2-pyrrolidinone (rolipram, Sigma, Beavo, 1988) were made up as concentrated stock solutions of 2mM and 50mM respectively in DMSO. They were then diluted in the ACSF solution prior to perfusion to a final concentration of less than 0.1% DMSO.

5.3 RESULTS

5.3.1 EFFECT OF 8HZ STIMULATION FOR 15 SECONDS (BRF) ON EXTRACELLULAR FIELD POTENTIAL RESPONSES IN SAGITTAL SLICES OF CEREBELLAR VERMIS

In these experiments we set out to try to reproduce the LTP previously described in sagittal slices by activating the molecular layer at a raised frequency (Salin et al., 1996). Sagittal slices were prepared from the brains of 14-21 day old rats and perfused in ACSF containing 20μM picrotoxin to block $GABA_AR$ activation. After a suitable baseline period the stimulation to one of the two molecular layer stimulation pathways, designated the 'test' pathway, was increased from 0.2 to 8Hz for 15 seconds. The other 'control' pathway was not stimulated. This protocol was termed brief raised frequency (BRF) stimulation. As shown in figure 5.3.1 and 5.3.2 BRF stimulation had very little effect on the N2 amplitude, slope or on the amplitude of the N1 component of FP responses. After 45 minutes the average N2 amplitude (mean % $\pm$ S.E.M) for the test and control pathways were not significantly different 101.0 $\pm$ 8.6 and 92.7 $\pm$ 7.8% of baseline levels, respectively (N = 6, Wilcoxon Matched-Pairs test, $p>0.05$). In one recording in the test pathway a potentiation emerged in the amplitude of the N2 component but in the remaining 5 cases there was no change.

We modified the experimental conditions in line with the method described by (Salin et al., 1996) in an attempt to produce a similar form of LTP. Firstly, a higher than normal concentration of picrotoxin was incorporated into the ACSF and then BRF stimulation was repeated. Secondly, the molecular layer was activated by BRF in slices prepared from the brains of 4-5 instead of 2-3 week old rats. The results of these experiments are summarised in figure 5.3.2. Despite altering the conditions under which BRF was applied we were not able to induce LTP consistently.

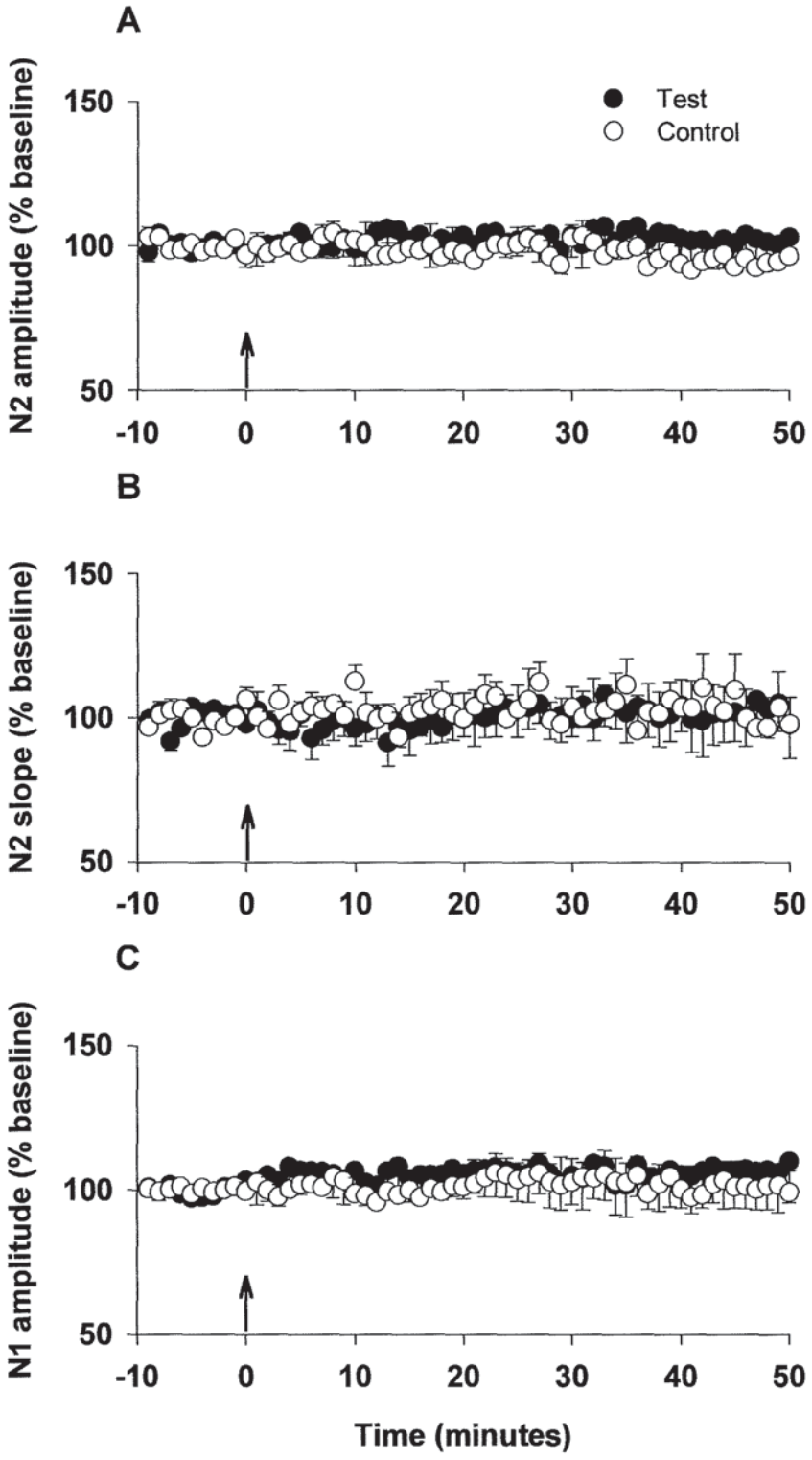

Figure 5.3.1 Effects of a 15 second period of 8Hz stimulation to the test pathway in the presence of 20μM picrotoxin

Graphs A - C illustrate the FP N2 amplitude, slope and N1 amplitude, respectively. Data are expressed as the mean % ± S.E.M. of 10 responses collected during a 10 minute baseline period. N = 6 paired recordings. Closed circles, test pathway stimulated at 8Hz for 15 seconds; open circles, control pathway. Arrow indicates the start of the 8Hz stimulation.

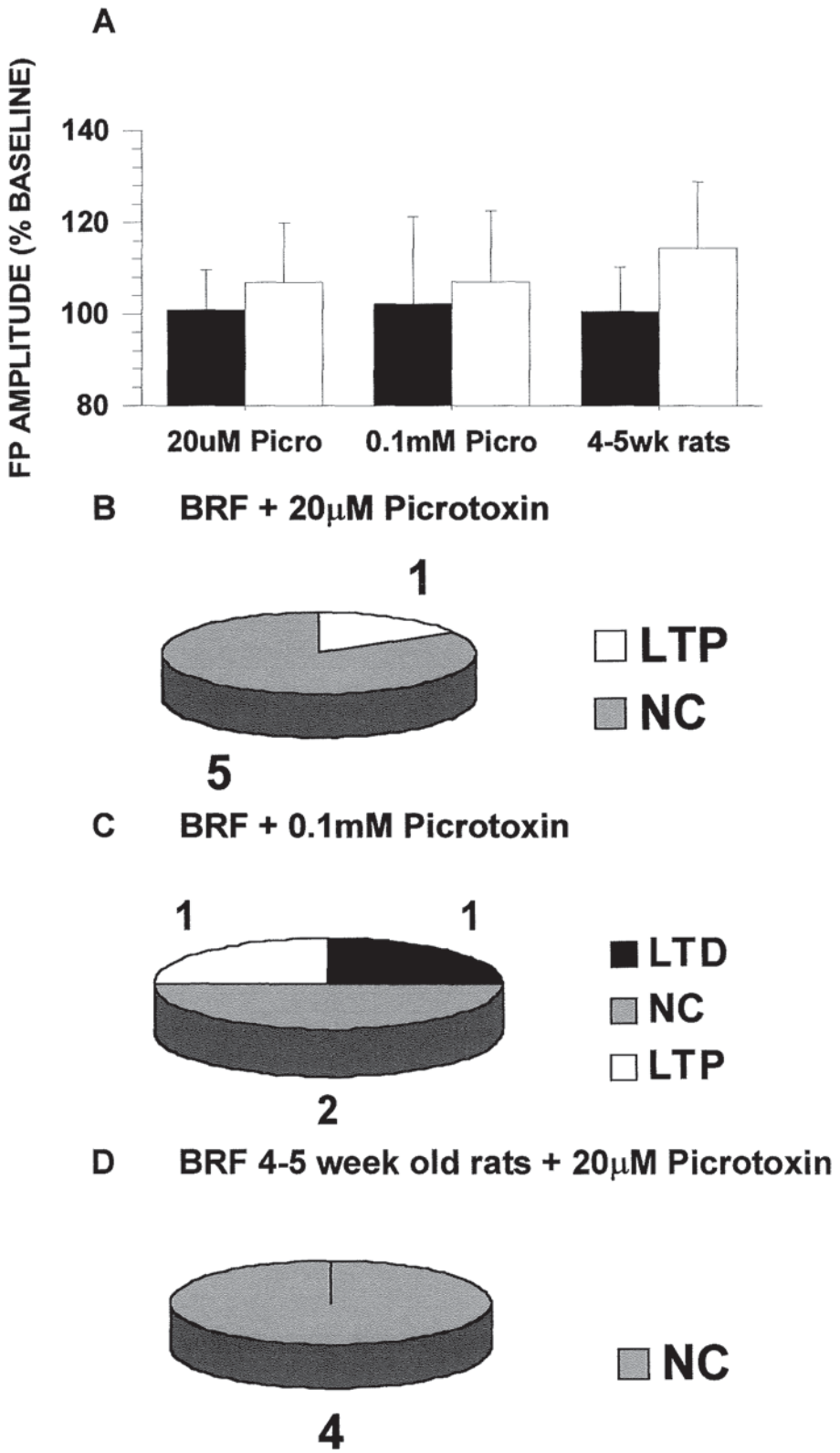

Figure 5.3.2 Bar chart and pie charts to show the effect of brief raised stimulation
Bar chart A shows the average N2 amplitude mean ± S.E.M measured 45 minutes after BRF stimulation. Black bars; test pathway stimulated at 8Hz for 15 seconds, white bars; control pathway that was not stimulated. Both the bar chart from left to right and the pie charts B and C represent BRF stimulation in sagittal slices from i) 14-21 day old rats perfused in ACSF with 20μM picrotoxin, ii) 14-21 day old rats perfused in a higher than normal concentration of ACSF (0.1mM) and iii) older than usual rats (4–5 weeks old) perfused in 'normal' ACSF (20μM picrotoxin). Pie charts represent the incidence of LTD, LTP and no change in the test pathway N2 amplitude measured 45 minutes after BRF stimulation.

5.3.2 EFFECT OF 8HZ STIMULATION FOR 2 MINUTES (RF STIMULATION) ON EXTRACELLULAR FIELD POTENTIAL RESPONSES IN SAGITTAL SLICES OF CEREBELLAR VERMIS

Since neither the level of picrotoxin nor the age of rats that we used led to a change in the strength of synaptic plasticity the duration of 8Hz stimulation applied to the test pathway was increased to 2 minutes this was termed the 8Hz pathway. The other pathway was activated at a lower rate of 1Hz and this was referred to as the 1Hz pathway. This was called the raised frequency (RF) paradigm. Using the criteria outlined in chapter 3.3.2, these experiments were grouped according to the incidences of LTD, LTP and no change in the N2 amplitude of the 8Hz pathway measured at 45 minutes after RF stimulation. Grouping the data in this way made it possible to observe changes in the 8Hz pathway and relate this to any alteration in the synaptic efficacy in the 1Hz pathway. In the 8Hz pathway, LTD was induced in 5 recordings, in 2 LTP was observed and in the remaining 3 cases there was no change.

Figures 5.3.3 and 5.3.4 illustrate the group of data in which a slowly emerging depression was observed. During the period of RF stimulation, the N2 amplitude and slope and the amplitude of N1 in the 8Hz pathway dropped dramatically below baseline levels. Within 45 minutes a LTD of the N2 component slowly emerged in the 8Hz pathway reaching 55.4 $\pm$ 3.8% of the baseline level (N = 5) in the N2 amplitude. The amplitude of N1 in the 8Hz pathway was slightly decreased after RF stimulation. The depression was accompanied by a slight and gradual increase in the amplitude of the PPR. RF stimulation also caused a transient reduction in the N2 amplitude and slope and the N1 amplitude in the 1Hz pathway. In the 1Hz pathway the amplitude of N2 after 45 minutes was 74.2 $\pm$ 9.5% of the baseline level (N = 5). The 8Hz and 1Hz pathways were not significantly different 45 minutes after raising the stimulation frequency (N = 5, Wilcoxon Matched-Pairs test, $p>0.05$). However, in both pathways the N2 amplitudes which were 104.5 $\pm$ 1.9 and 103.2 $\pm$ 7.8% of the baseline level were significantly depressed when compared to a separate group of control data activated at 0.2Hz throughout as shown in figure 3.3.1 (N = 6, Mann-Whitney U test $p<0.01$

and $p<0.05$, respectively). The amplitude of N1 in the 1Hz pathway remained slightly reduced after stimulation.

Figures 5.3.5 and 5.3.6 show the 2 recordings in which an average LTP of 122.8% was observed in the 8Hz pathway N2 amplitude within 45 minutes of RF stimulation. For the duration of the RF stimulation both the N2 and N1 components of FPs dropped below baseline levels. After stimulation there was an increase in N1 in the 8Hz pathway which reached 120.5% of the baseline level. This potentiation was accompanied by a decrease in the amplitude of the PPR. In the 1Hz pathway the amplitudes of N2 and N1 also increased above baseline levels and reached 107.5% and 111.8% of baseline levels, respectively, within 45 minutes. There was also a small decrease observed in the amplitude of the PPR after stimulation in the 1Hz pathway.

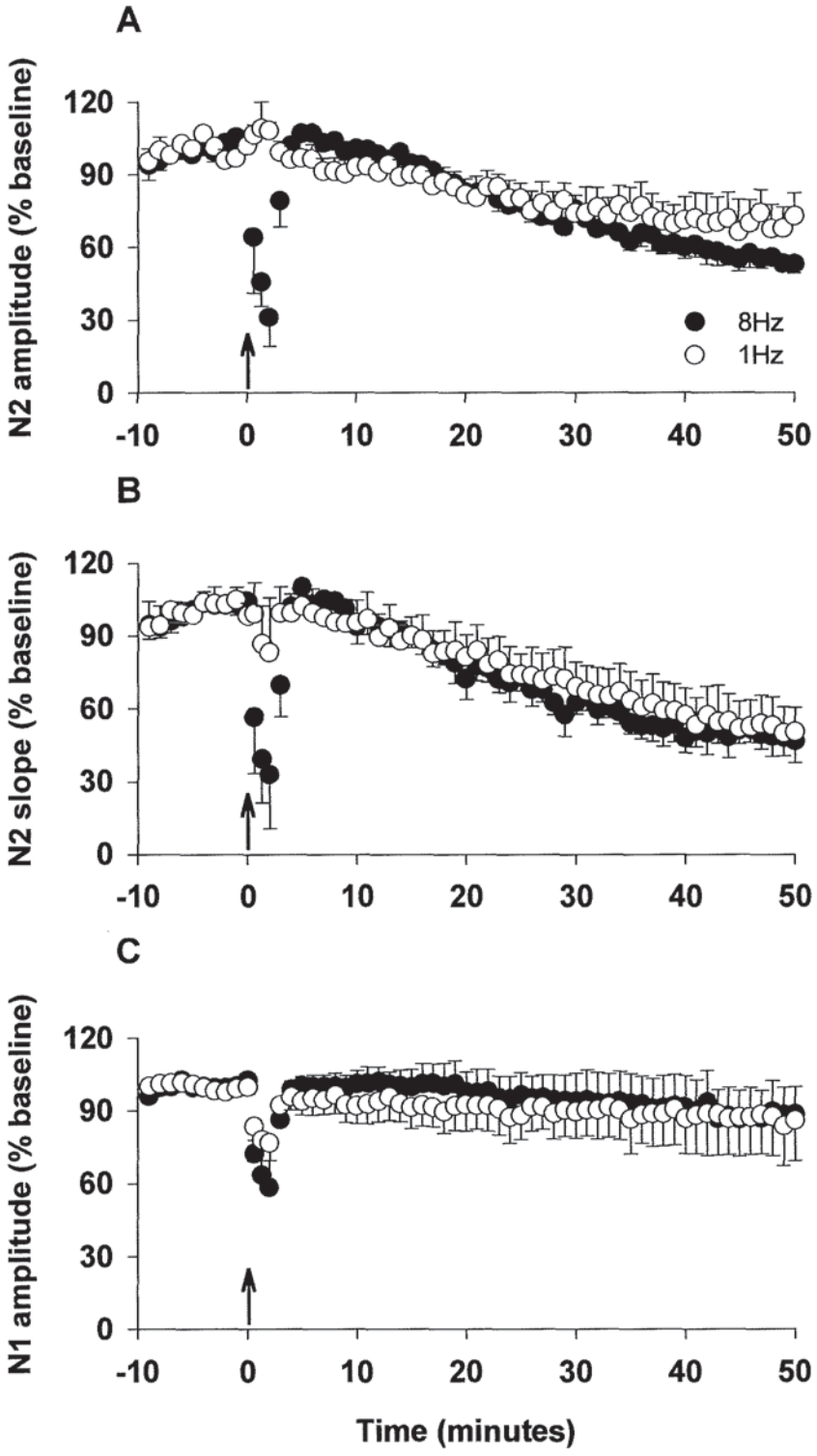

Figure 5.3.3 Graphs show the group of data in which a slowly emerging long term depression was observed in the 8Hz pathway after stimulation

Graphs A - C illustrate the FP N2 amplitude, N2 slope and N1 amplitude, respectively. Data are expressed as the mean % ± S.E.M. of 10 responses collected during a 10 minute baseline period. N = 5 paired recordings. Closed circles, pathway stimulated at 8Hz for 2 minutes; open circles, pathway stimulated at 1Hz for 2 minutes. Arrow indicates the start of the 1 or 8Hz stimulation period.

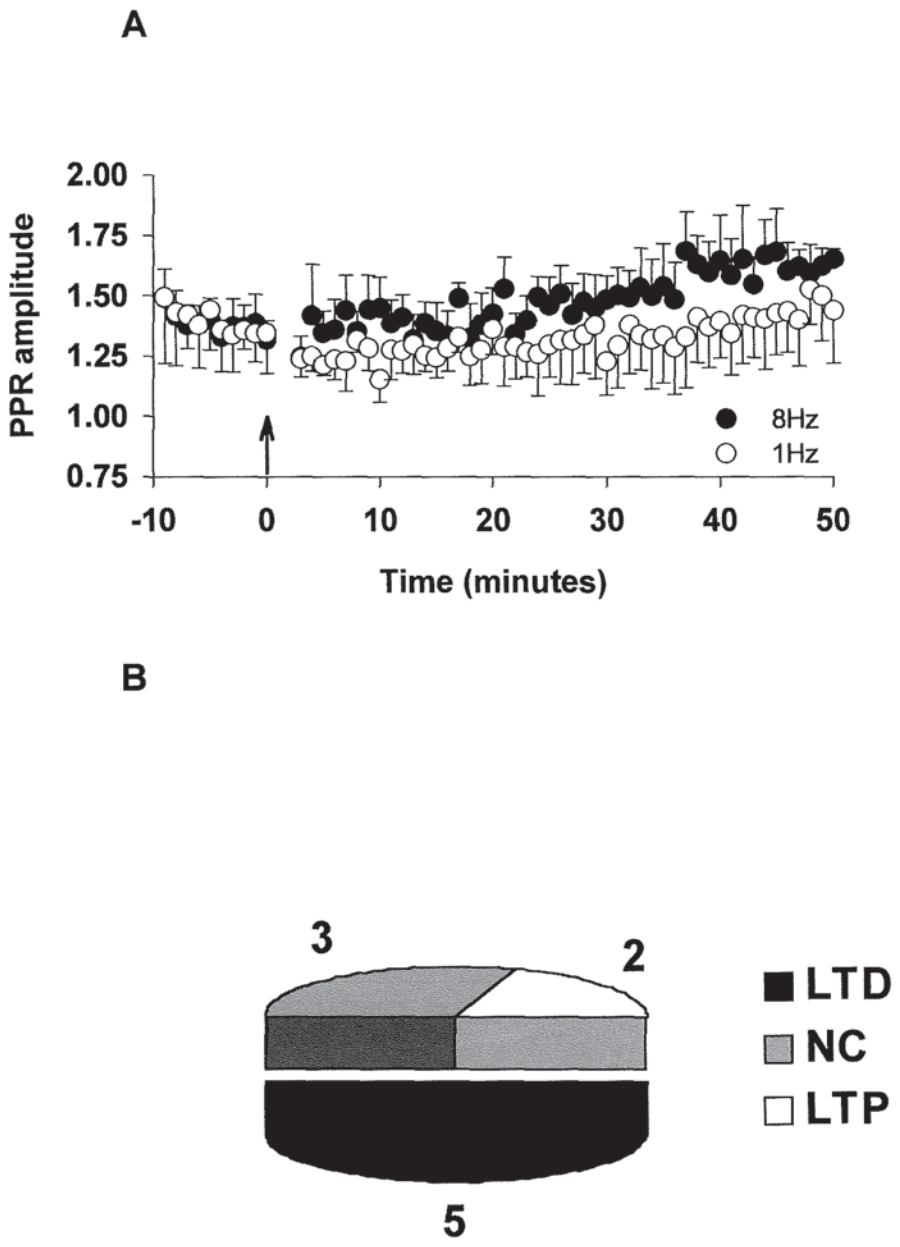

Figure 5.3.4 Graph represents the group of data in which a slowly emerging long term depression was observed in the 8Hz pathway after stimulation, pie chart represents the incidence of synaptic change for the whole set of data as measured 45 minutes after RF stimulation

Graph A illustrates the amplitude of the PPR. Data are expressed as the mean % ± S.E.M. of 10 responses collected during a 10 minute baseline period. N = 5 paired recordings. Closed circles, pathway stimulated at 8Hz for 2 minutes; open circles, pathway stimulated at 1Hz for 2 minutes. Arrow indicates the start of the 1 or 8Hz stimulation period. Pie chart B represents the incidence of LTD, LTP and no change in the test N2 amplitude measured at 45 minutes after stimulation in the whole set of data (10 experiments).

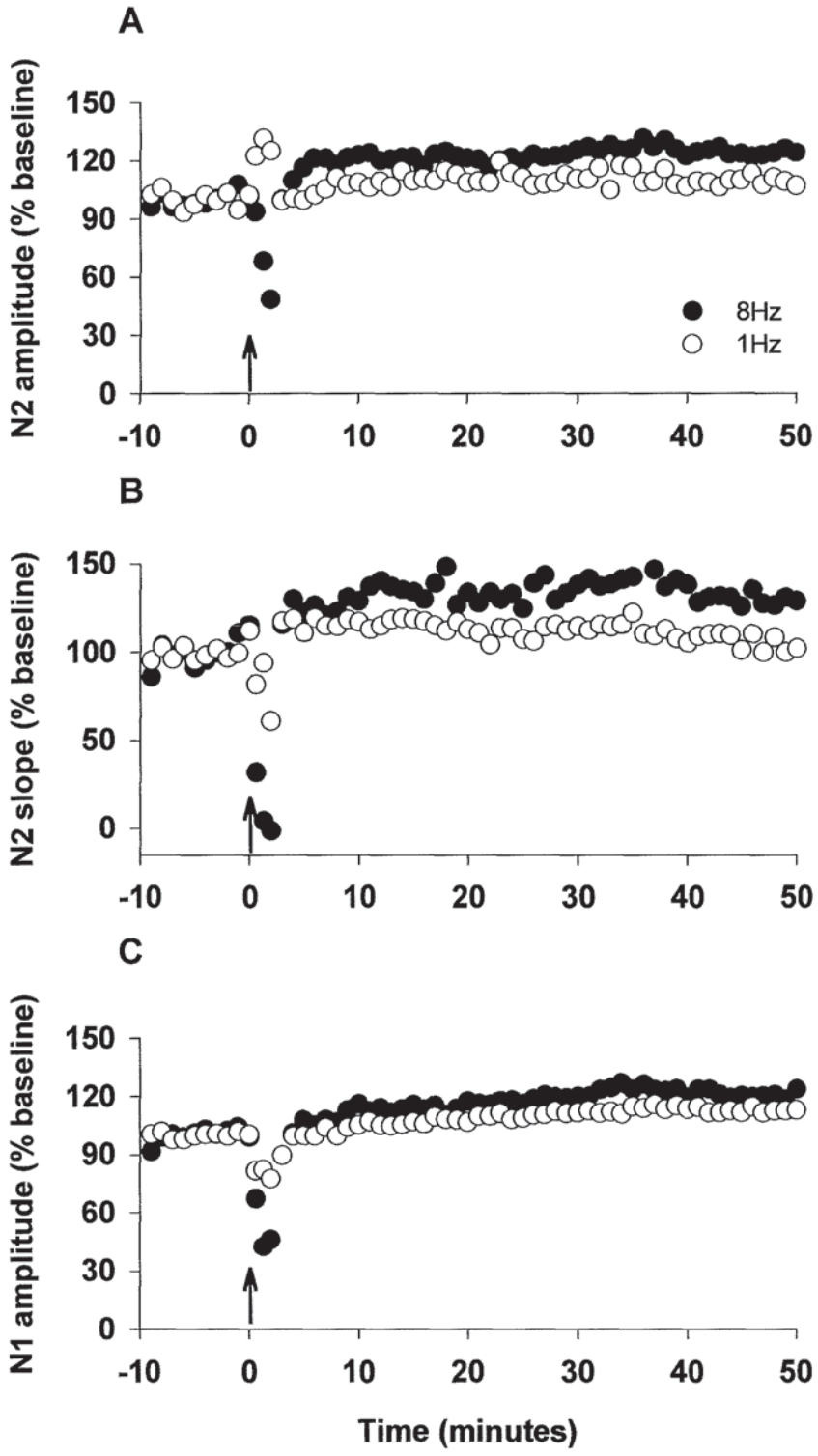

Figure 5.3.5 Graphs represent the average of the 2 recordings in which a long term potentiation was observed in the 8Hz pathway after stimulation
Graphs A - C are as shown in figure 5.3.3. N = 2 paired recordings.

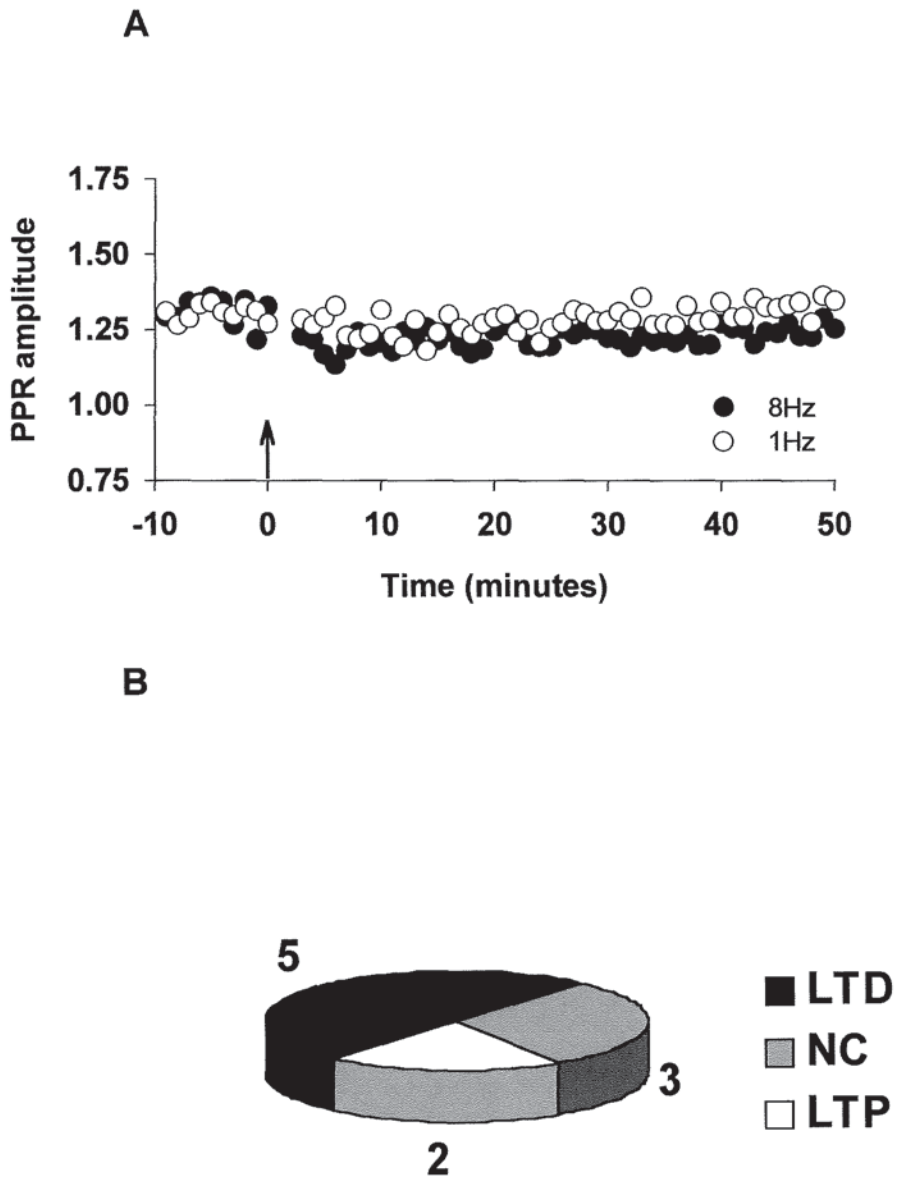

Figure 5.3.6 Graph represents the 2 recordings in which a long term potentiation was observed in the 8Hz pathway after stimulation, pie chart represents the incidence of synaptic change for the whole set of data as measured 45 minutes after RF stimulation

Graphs A and pie chart B are as shown in figure 5.3.4. N = 2 paired recordings.

5.3.3 EFFECT OF RF STIMULATION ON EXTRACELLULAR FIELD POTENTIAL RESPONSES IN THE PRESENCE OF INHIBITORS OF NITRIC OXIDE SYNTHASE, GUANYLATE CYCLASE OR PROTEIN KINASE G IN SAGITTAL SLICES OF CEREBELLAR VERMIS

Since RF stimulation tended to produce a LTD of N2 responses in 50% of recordings this protocol was repeated in the presence of inhibitors of cGMP signalling. To examine the roles of NO, GC and PKG in the induction of LTD rather than the continued expression of LTD the inhibitors were applied for at least 10 minutes prior to RF stimulation and were washed off within 5 minutes after the cessation of the RF paradigm. The effects of RF stimulation in the presence of 5μM of the NOS inhibitor 7-NI are shown in figures 5.3.7 and 5.3.8. During RF stimulation a decrease in both the N2 and N1 components of FPs was observed that was comparable to the effect seen in drug-free ASCF. This decrease was most prominent in the 8Hz pathway. After RF stimulation there was a small increase in the N2 amplitude and slope and the N1 amplitude in the 8Hz pathway. This effect was accompanied by a reduction in the amplitude of the PPR. The potentiation of the N2 component was not large enough to be classed as LTP. The incidences of LTD, LTP and no change in the N2 amplitude were determined 45 minutes after stimulation according to the criteria outlined in chapter 3, in 1 recording LTD was observed and in the remaining 5 cases there was no change. The N2 amplitudes in the 8Hz and 1Hz pathways showed no significant difference 45 minutes after stimulation with levels of 109.5 $\pm$ 7.8 and 98.8 $\pm$ 7.3% of baseline, respectively, ($N = 6$; Wilcoxon Matched-Pairs test $p>0.05$). The N2 slope showed a gradual reduction in the 1Hz pathway and reached levels of 67.5 $\pm$ 9.2% of baseline. In the 1Hz pathway no change was noted in N1 after stimulation but there was a transient increase in the amplitude of the PPR. At 45 minutes after stimulation the N2 slope measurement in the 8Hz and 1Hz pathways were significantly different (Wilcoxon Matched-Pairs test $p<0.05$).

Figures 5.3.9 and 5.3.10 show the effects of RF stimulation in the presence of 10 μM of the GC inhibitor ODQ. 45 minutes after stimulation in the 8Hz pathway a LTD of the N2 amplitude was observed in 1 recording but in the remaining 5 experiments there was no

change. No marked change was noted in the N1 amplitude in the 8Hz pathway after stimulation. In the 8Hz pathway there was a transient decrease in the amplitude of the PPR after stimulation. 45 minutes after stimulation the 8Hz and 1Hz pathway N2 amplitudes were not significantly different with values of 91.0 $\pm$ 5.6 and 100.0 $\pm$ 6.5% of baseline, respectively (N=6, Wilcoxon Matched-Pairs test $p>0.05$). Overall, little or no change was observed in the N2 component, the N1 amplitude or the amplitude of the PPR in the 1Hz pathway for the duration of the recording.

RF stimulation failed to induce LTD of the N2 component in the 8Hz pathway in the presence of KT5823 as shown in figures 5.3.11 and 5.3.12. The effects of RF stimulation in the presence of KT5823 were similar to those observed in the presence of 7-NI. There was a slight increase in the N2 and N1 components in the 8Hz pathway after RF stimulation and this was accompanied by a slight reduction in the amplitude of the PPR. This potentiation of the N2 component was not large enough to be classed as LTP. There were no incidences of LTD or LTP 45 minutes after stimulation according to the criteria outlined in chapter 3. 45 minutes after stimulation the 8Hz and 1Hz pathway N2 amplitudes were 107.9 $\pm$ 4.0 and 92.2 $\pm$ 8.4 % of baseline, respectively. There was a noticeable difference between the slope and amplitude of the N2 component in the 8Hz and 1Hz pathways but this did not achieve statistical significance (N =6, Wilcoxon Matched-Pairs test $p>0.05$). However, there was a statistical difference between the N1 amplitude in the 8Hz and 1Hz pathways which were 92.0 $\pm$ 6.2 and 118.1 $\pm$ 13.9 % of baseline levels, respectively (N = 6, Wilcoxon Matched-Pairs test $p<0.05$). In the 1Hz pathway the N1 amplitude showed a gradual decline but no change was observed in the amplitude of the PPR.

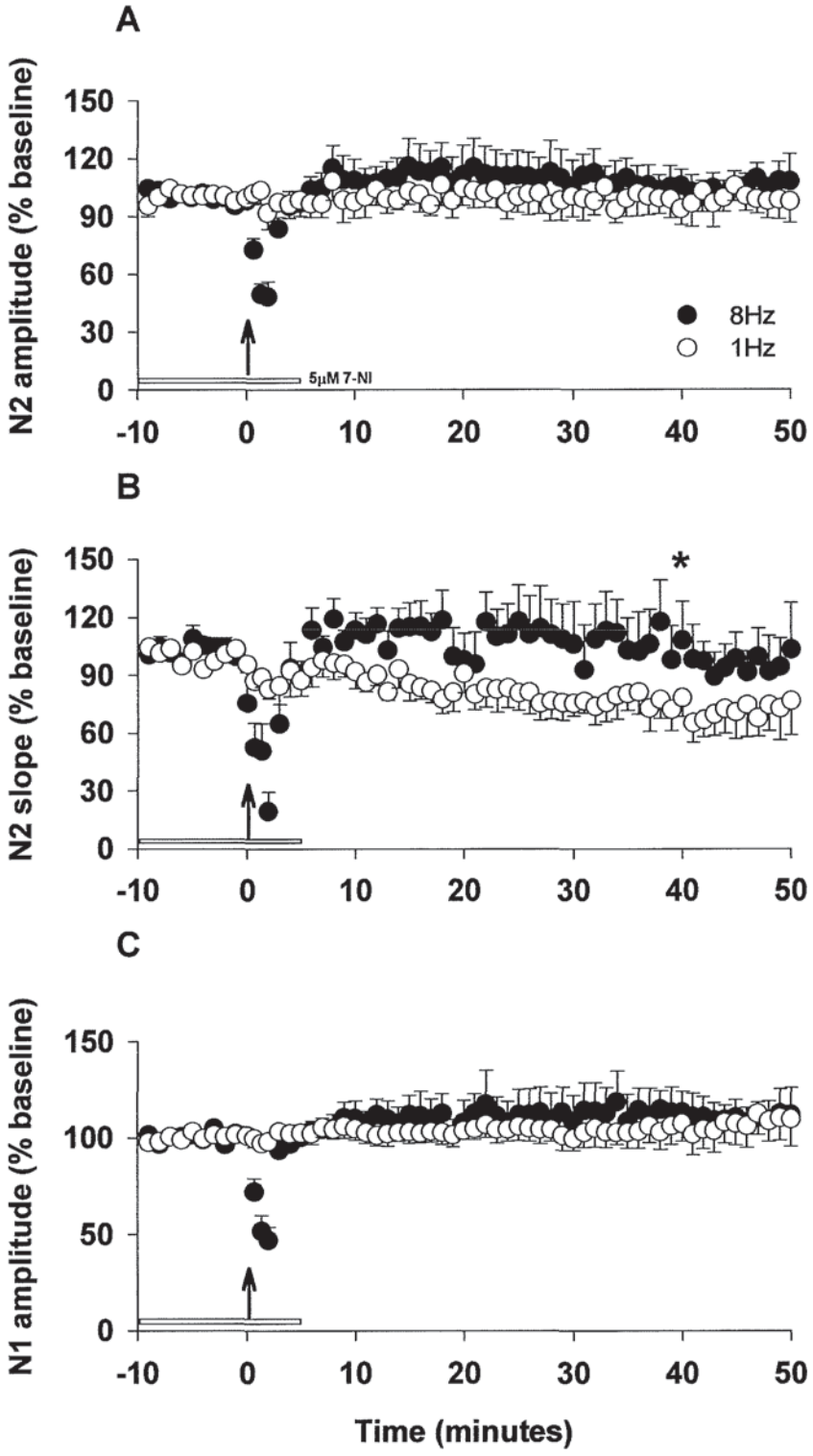

Figure 5.3.7 Effects of RF stimulation on field potential responses in the presence of 5μM 7-NI

Graphs A -C illustrate the FP N2 amplitude, N2 slope and N1 amplitude, respectively. Data are expressed as the mean % ± S.E.M. of 10 responses collected during a 10 minute baseline period. N = 6 paired recordings. Closed circles, pathway stimulated at 8Hz for 2 minutes; open circles, pathway stimulated at 1Hz for 2 minutes. Arrow indicates the start of RF stimulation. Horizontal white bar represents the application of 5μM 7-NI. Asterisk indicates where a significant difference was observed between the 1Hz and 8Hz pathways (Wilcoxon Matched-Pairs test $p<0.05$).

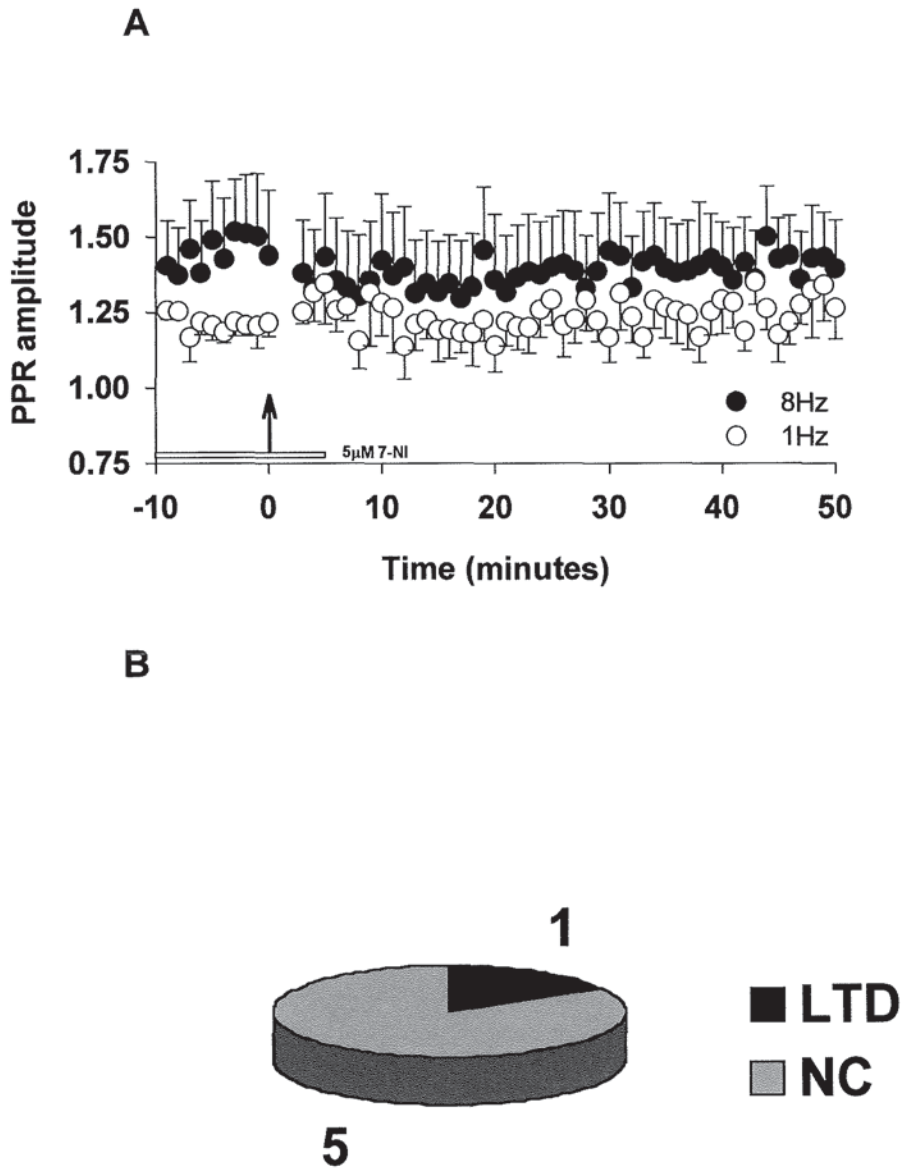

Figure 5.3.8 Effects of RF stimulation on field potential responses in the presence of 5μM 7-NI

Graph A illustrates the amplitude of the PPR. Data are expressed as the mean % ± S.E.M. of 10 responses collected during a 10 minute baseline period. N = 6 paired recordings. Closed circles, pathway stimulated at 8Hz for 2 minutes; open circles, pathway stimulated at 1Hz for 2 minutes. Arrow indicates the start of the RF stimulation. Horizontal white bar represents the application of 5μM 7-NI. Pie chart B shows the incidence of LTD, LTP and no change in the 8Hz pathway N2 amplitude 45 minutes after stimulation.

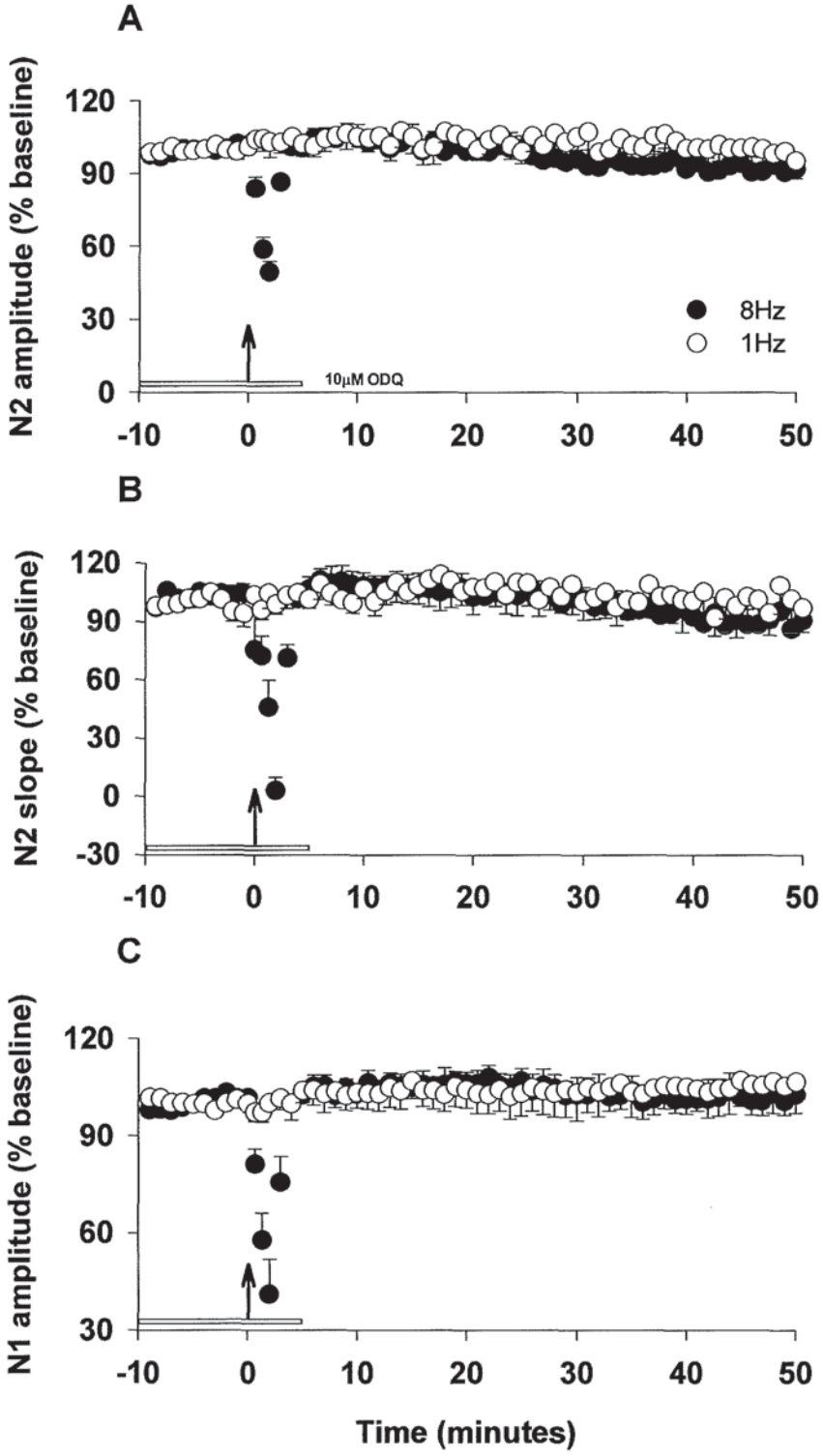

Figure 5.3.9 Effects of RF stimulation on field potential responses in the presence of 10μM ODQ

Graphs A - C are as shown in figure 5.3.7. N = 6 paired recordings. Horizontal white bar represents the application of 10μM ODQ.

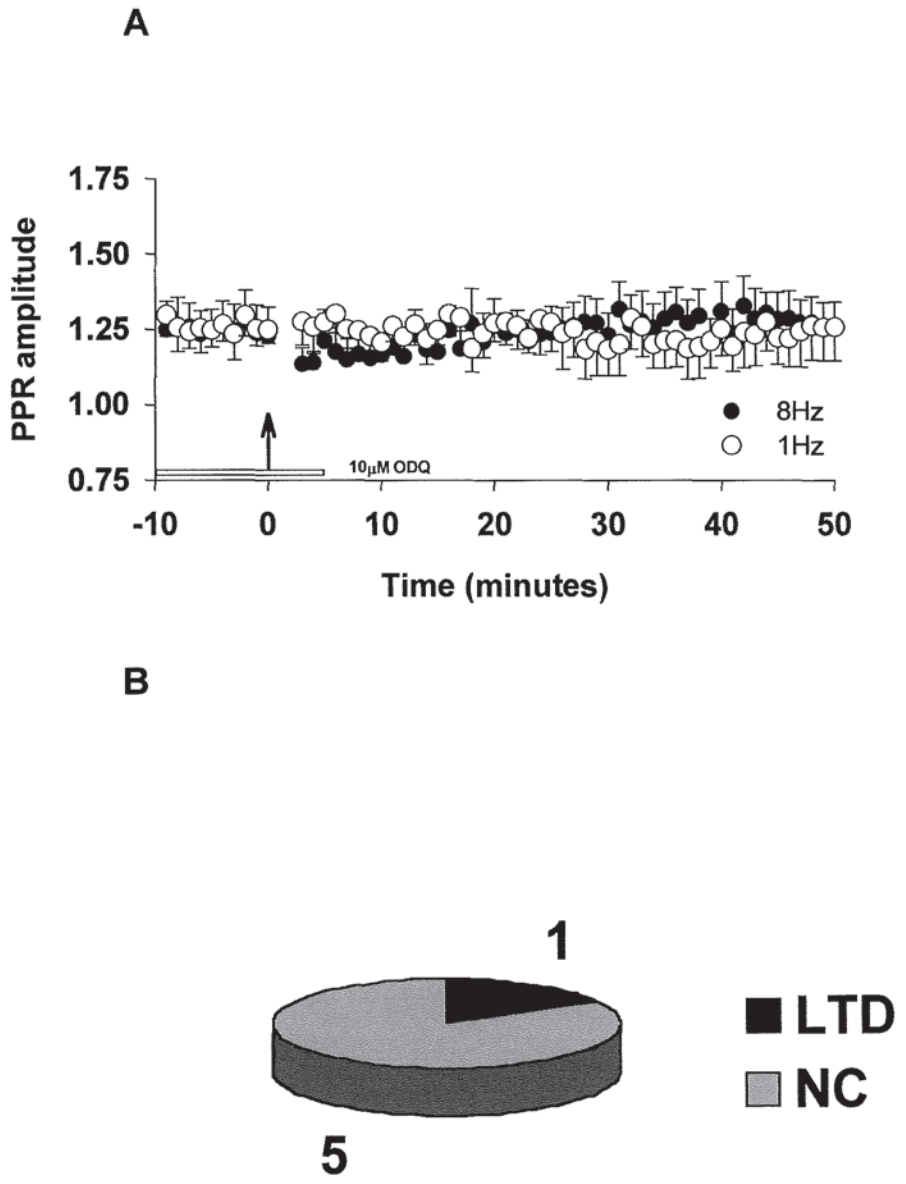

Figure 5.3.10 Effects of RF stimulation on field potential responses in the presence of 10μM ODQ

Graph A and pie chart B as shown in figure 5.3.8. N = 6 paired recordings. Horizontal white bar represents the application of 10μM ODQ.

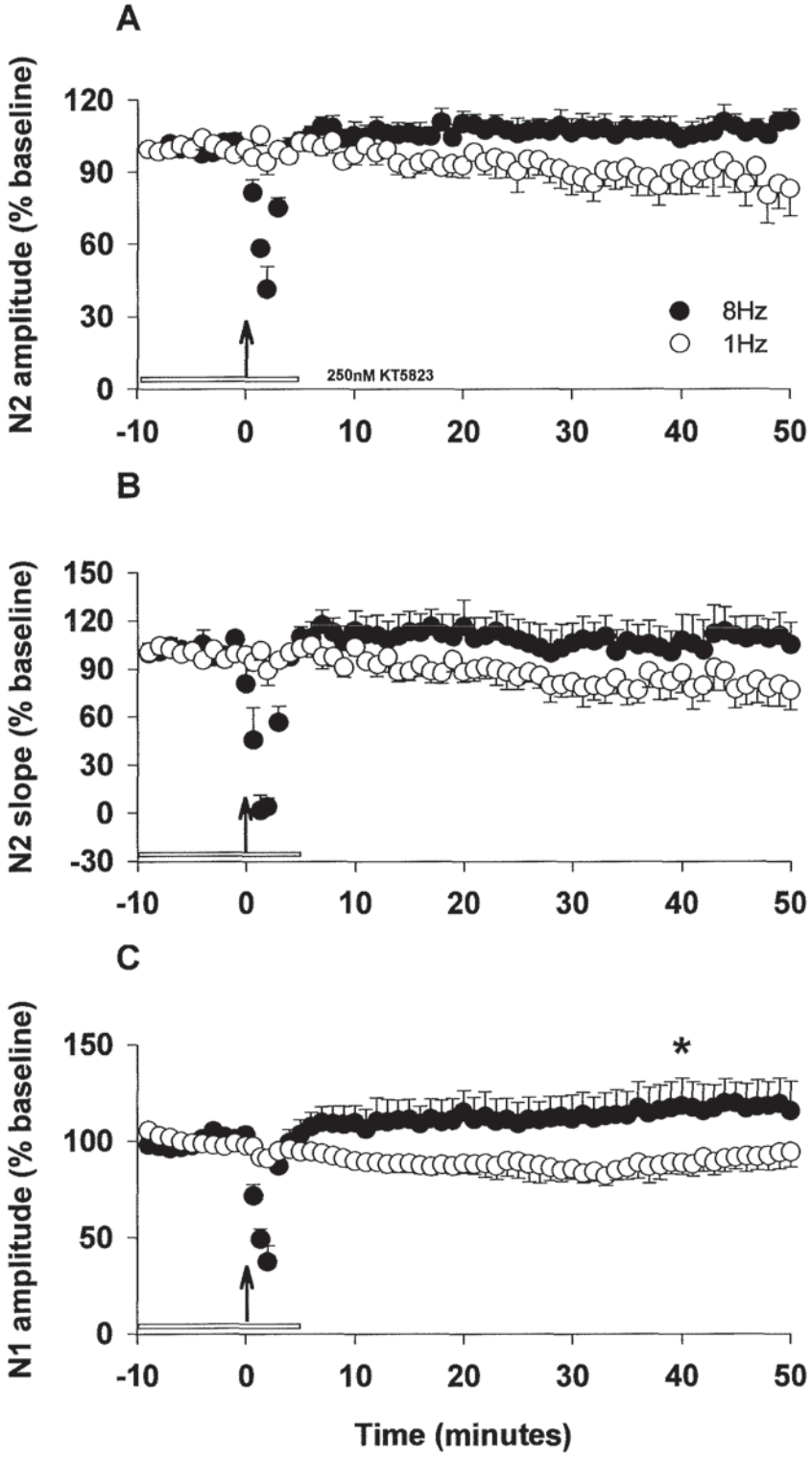

Figure 5.3.11 Effects of RF stimulation on field potential responses in the presence of 250nM KT5823

Graphs A - C are as shown in figure 5.3.7. N = 6 paired recordings. Horizontal white bar represents the application of 250 nM KT5823. Asterisk indicates where a significant difference was found between the 8Hz and 1Hz pathway at 45 minutes after RF stimulation (Wilcoxon Matched-Pairs test $p<0.05$).

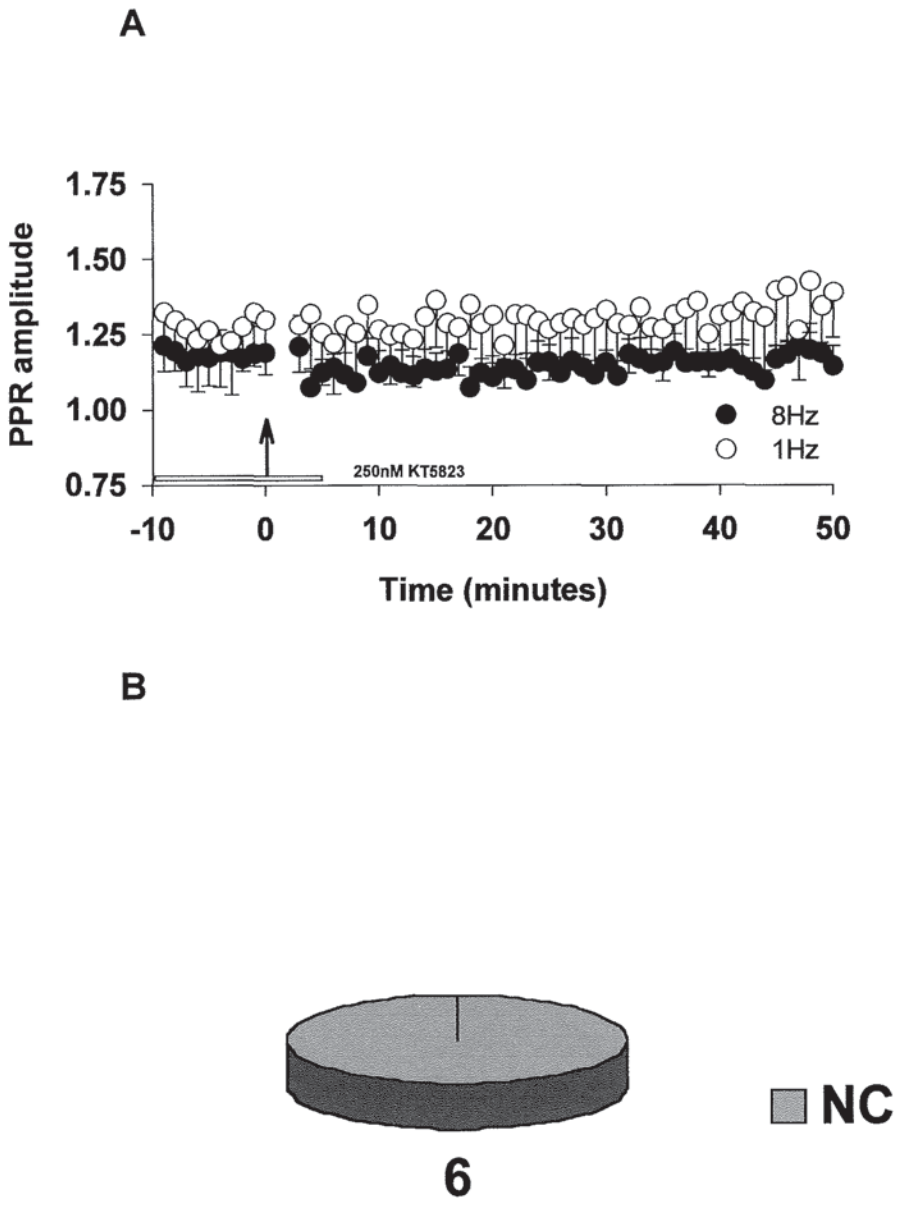

Figure 5.3.12 Effects of RF stimulation on field potential responses in the presence of 250nM KT5823

Graph A and pie chart B are as shown in figure 5.3.8. N = 6 paired recordings. Horizontal white bar represents the application of 250nM KT5823.

As described previously in chapter 4.3.1 the data from each of the RF experiments was summarised in the form of pie charts. The data were grouped according to the amplitude of the N2 component measured at 45 minutes after stimulation. Due to the variation within groups of data it was not valid to perform statistical comparisons between groups of pooled data and so pie charts were generated to compare the incidences of LTD, LTP and no change under different experimental conditions. As summarised in figure 5.3.13 a marked reduction in the incidence of LTD in the N2 component in the 8Hz pathway measured at 45 minutes after stimulation was observed when NOS, GC or PKG were inhibited, compared to that seen in control conditions.

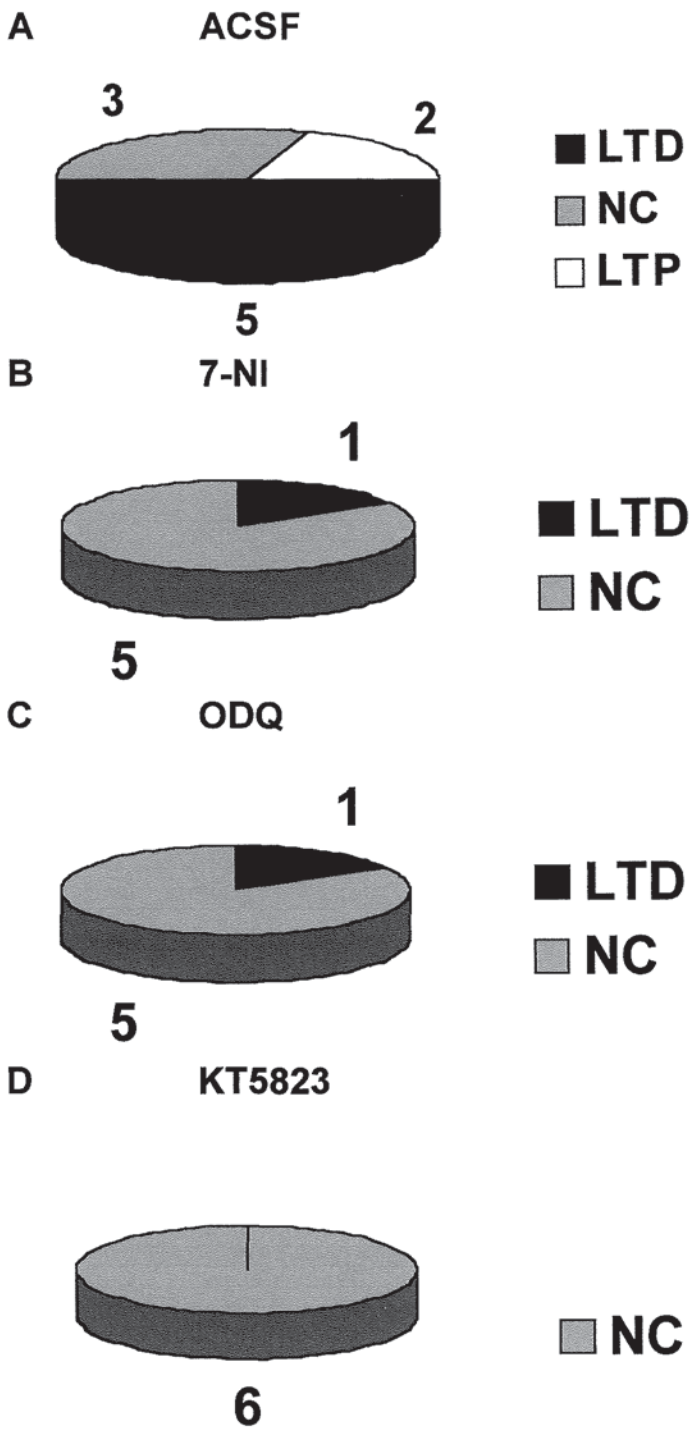

Figure 5.3.13 Effects of RF stimulation, alone or in the presence of inhibitors of nitric oxide synthase (5μM 7-NI), guanylate cyclase (10μM ODQ) or protein kinase G (250nM KT5823)

Pie charts represent the incidence of LTD, LTP and no change in the test pathway N2 amplitude as measured 45 minutes after the RF stimulation period. Pie charts A – D show the effect of RF stimulation in drug free ACSF and in the presence of 5μM 7-NI, 10μM ODQ or 250nM KT5823.

5.3.4 EFFECT OF RF STIMULATION ON EXTRACELLULAR FIELD POTENTIAL RESPONSES IN THE PRESENCE OF AN INHIBITOR OF TYPE IV SPECIFIC PHOSPHODIESTERASES IN SAGITTAL SLICES OF CEREBELLAR VERMIS

In sagittal slices, a depression of synaptic transmission predominated following a 2 minute period of RF stimulation. Under conditions of NOS or PKG inhibition, however, an underlying potentiation emerged suggesting that under certain conditions cGMP signalling leading to LTD prevails over the effects of cAMP signalling leading to potentiation. The idea that the inhibition of cGMP signalling might unmask an underling potentiation was also considered in chapter 4. It was postulated that raising the level of cAMP might therefore push the plasticity in this system towards the direction of LTP. Therefore in the next set of experiments, rolipram, which is an inhibitor of type IV cAMP-specific PDE (Beavo, 1988) was added to the perfusion medium before and during RF stimulation. In the presence of 50μM rolipram, raising the frequency of molecular layer stimulation from 0.2 to 8Hz induced a clear, input-specific LTP of the N2 and N1 components of FP responses as shown in figures 5.3.14 and 5.3.15. The LTP was accompanied by a small, sustained decrease in the amplitude of the PPR. After stimulation there was no change in the amplitude of N2 or N1 or the amplitude of the PPR in the 1Hz pathway. The N2 slope in the 1Hz pathway was below baseline levels for the remainder of the experiment. The N2 amplitudes for 8Hz and 1Hz pathways were 128.5 $\pm$ 12.8 and 96.4 $\pm$ 12.7 (N = 5), respectively 20 minutes after stimulation. A Wilcoxon Matched-Pairs test showed that there was a significant difference between the N2 amplitude and slope in the 8Hz and 1Hz pathways 20 minutes after stimulation ($p<0.01$). This experiment was also repeated using a lower concentration of rolipram. A comparison between the effect of RF stimulation in the presence of 5 or 50μM rolipram is shown in the bar chart figure 5.3.15.

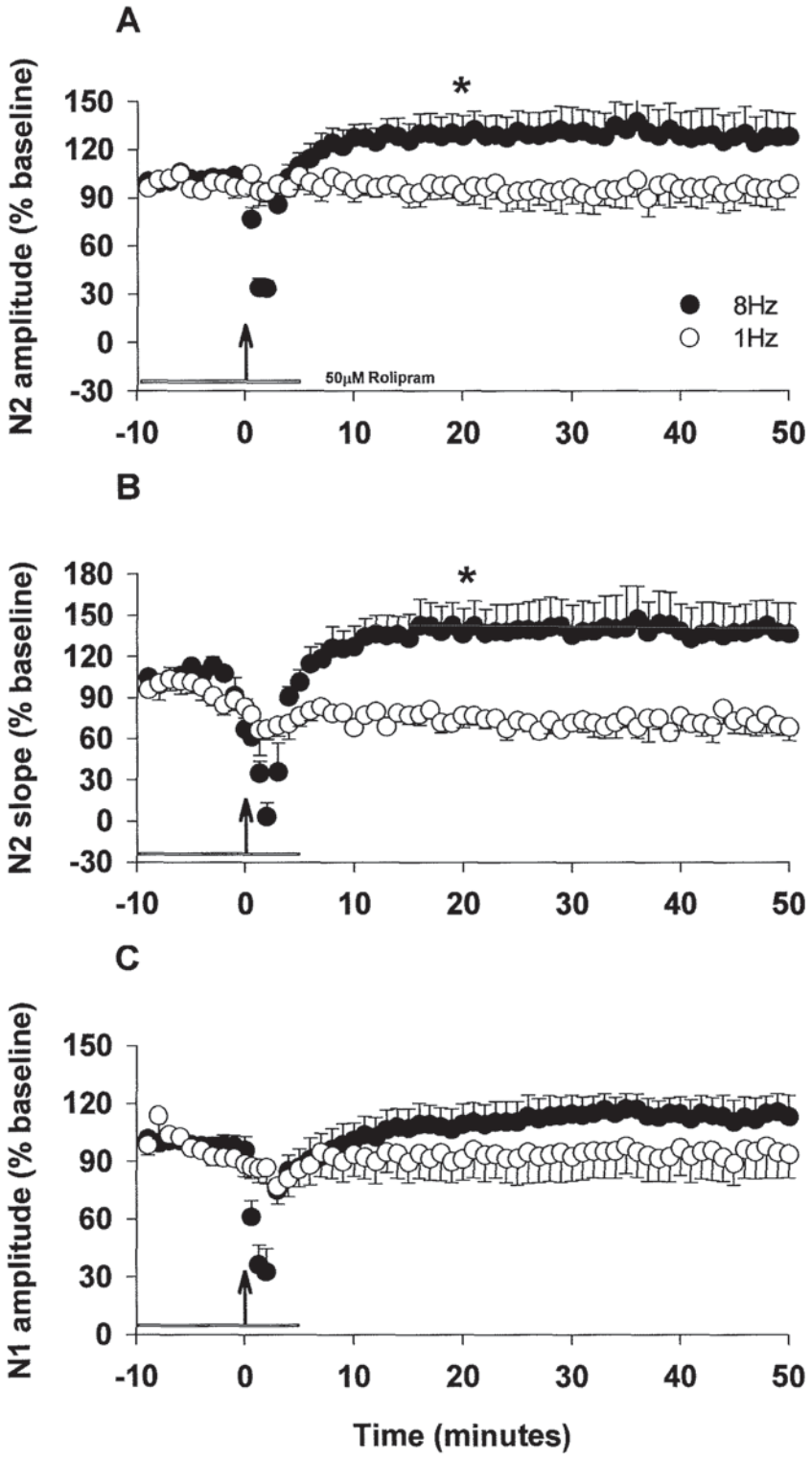

Figure 5.3.14 Effects of RF stimulation on field potential responses in the presence of 50μM rolipram

Graphs A - C are as shown in figure 5.3.7. N = 5 paired recordings. Horizontal white bar represents the application of 50μM rolipram. Asterisks indicate where a significant difference was observed between the 1Hz and 8Hz pathways (Wilcoxon Matched-Pair test $p<0.05$).

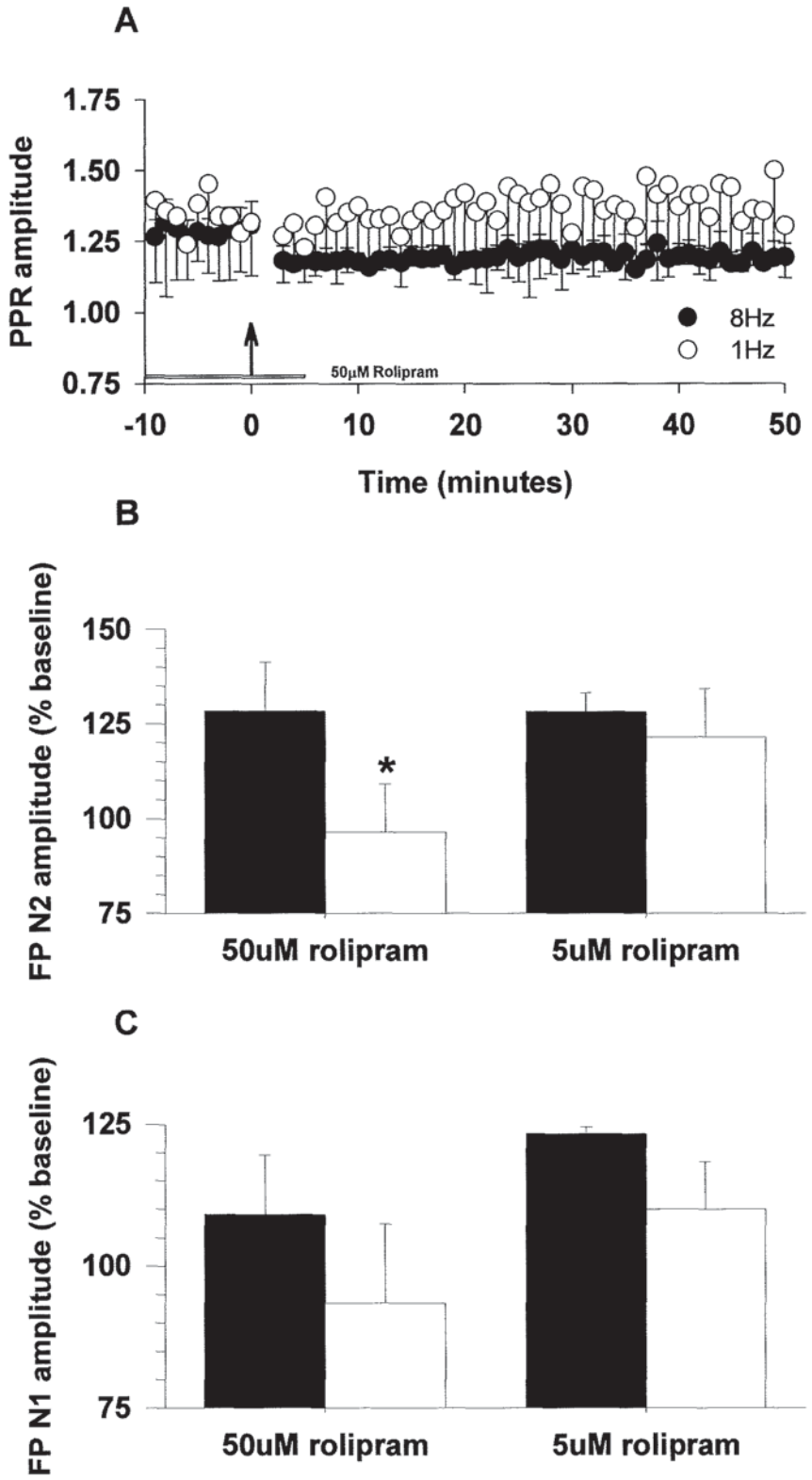

Figure 5.3.15 Effects of RF stimulation on field potential responses in the presence of 5 or 50μM rolipram

Graph A shows the effect of RF stimulation on the amplitude of the paired pulse ratio in the presence of 50μM rolipram and is as shown in figure 5.3.8. N = 5 paired recordings. Horizontal white bar represents the application of 50μM rolipram. Bar charts B and C compare the effect of RF stimulation during the application of 5 or 50μM rolipram on the N2 and N1 amplitudes, respectively. Asterisk indicates where a significant difference was observed between the 1Hz and 8Hz pathway (Wilcoxon Matched-Pairs test $p<0.05$).

5.3.5 EFFECT OF RF STIMULATION ON EXTRACELLULAR FIELD POTENTIAL RESPONSES IN TRANSVERSE SLICES OF CEREBELLAR VERMIS

In chapter 4 differences were noted in the incidence of LTD, LTP and no change between transverse and sagittal slices following RSIF stimulation. Therefore RF stimulation was performed in transverse slices in drug-free ACSF as shown in figures 5.3.16 and 5.3.17. A clear LTP of the amplitude and slope of the N2 component was observed in all recordings in the 8Hz pathway after RF stimulation. According to the amplitude measurement of N2 there was also a potentiation in 3 recordings in the control pathway. The N2 amplitude reached 149.6 $\pm$ 9.3% of baseline (N = 6) in the 8Hz pathway and 126.8 $\pm$ 22.6% of baseline (N = 6) in the 1Hz pathway within 30 minutes of stimulation. Neither the amplitude nor the slope of the N2 component in the 8Hz and 1Hz pathways were significantly different 30 minutes after stimulation (Wilcoxon Matched-Pairs test $p>0.05$). In addition, a marked increase in the amplitude of N1 was observed in both pathways which reached levels of 144.7 $\pm$ 9.7 and 134.9 $\pm$ 21.9% of baseline levels, respectively (N = 6). In the 8Hz pathway the increase in N1 coincided with an obvious drop in the amplitude of the PPR. There was a small increase noted in the amplitude of the PPR immediately after stimulation in the 1Hz pathway.

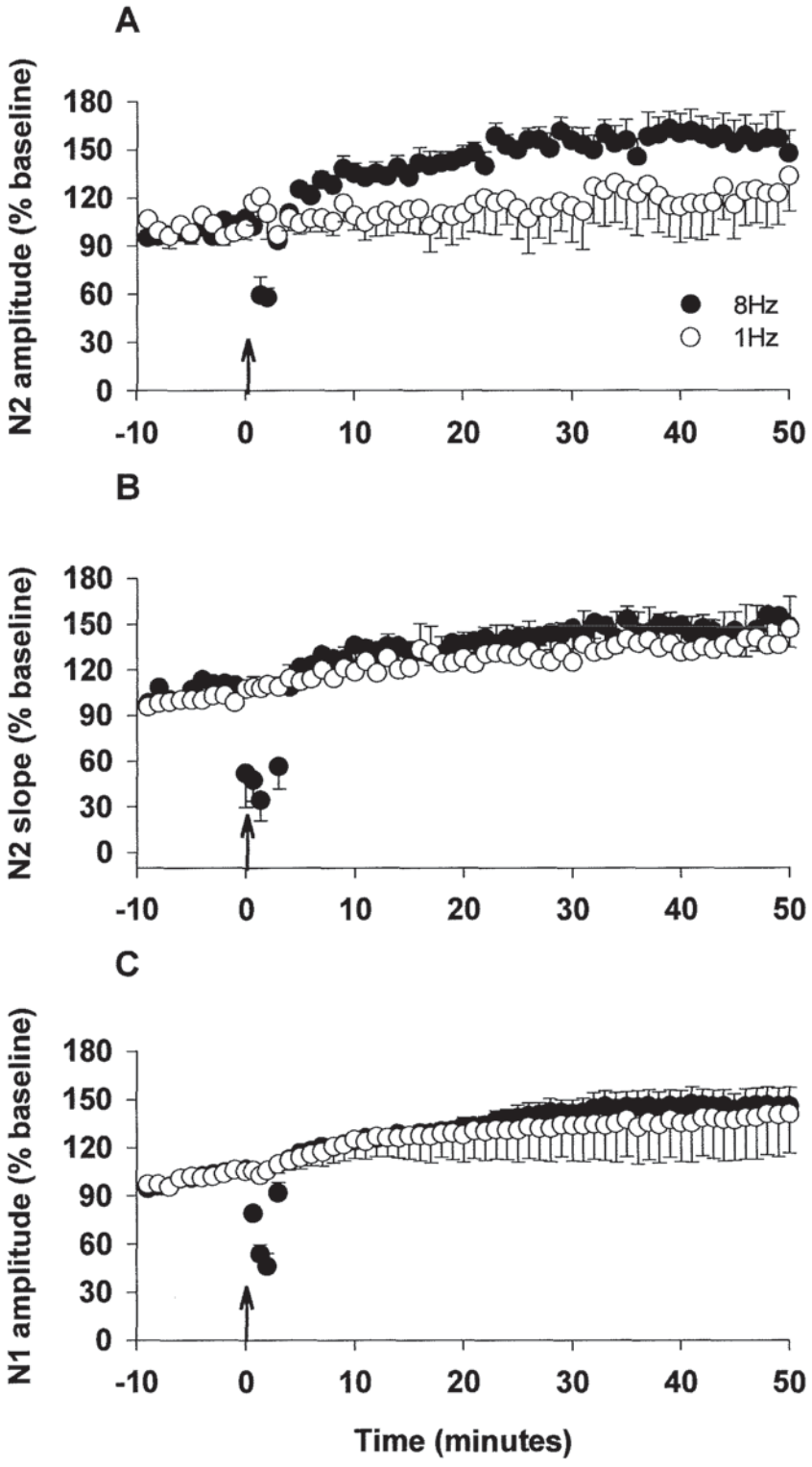

Figure 5.3.16 Effects of RF stimulation on field potential responses in a transverse slice of cerebellar vermis

Graphs A – C are as shown in figure 5.3.3. N = 6 paired recordings.

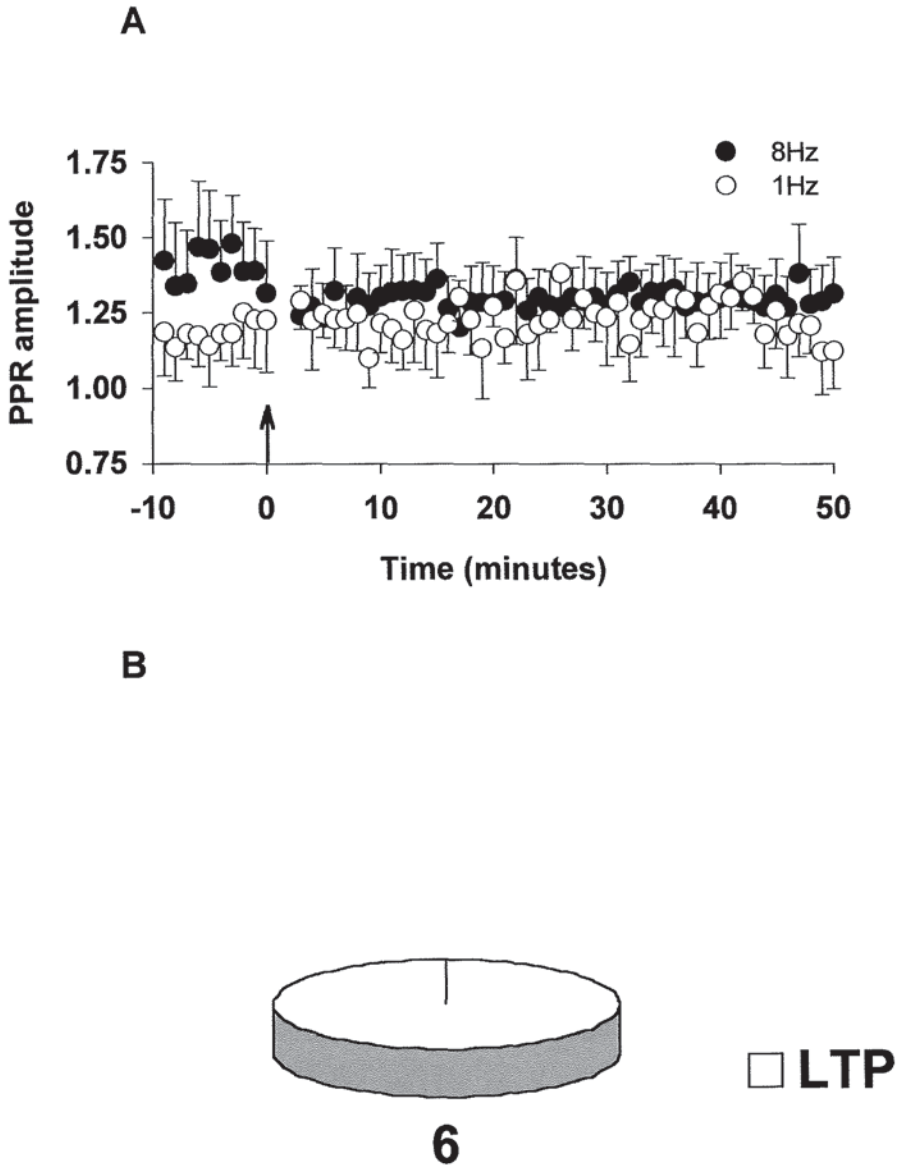

Figure 5.3.17 Effects of RF stimulation on field potential responses in a transverse slice of cerebellar vermis

Graph A and pie chart B are as shown in figure 5.3.4. N = 6 paired recordings. Pie chart shows the incidence of LTD, LTP and no change in the 8Hz pathway measured 30 minutes after RF stimulation.

5.3.6 EFFECT OF RF STIMULATION ON EXTRACELLULAR FIELD POTENTIAL RESPONSES IN THE PRESENCE OF INHIBITORS OF NITRIC OXIDE SYNTHASE OR PROTEIN KINASE A IN TRANSVERSE SLICES OF CEREBELLAR VERMIS

In separate groups of experiments the RF paradigm was repeated in transverse slices in the presence of inhibitors of PKA and NOS. The effect of 1 or 8Hz stimulation in the presence of 0.2 μM H-89 a selective and potent inhibitor of PKA is shown in figures 5.3.19 and 5.3.20. There was no obvious change in the N2 or N1 components of FPs for the duration of the experiment. After stimulation a gradual increase in the amplitude of the PPR was observed in the 8Hz pathway but no change was noted in the 1Hz pathway. Within 30 minutes of stimulation there was no significant difference between the N2 amplitudes in the 8Hz and 1Hz pathways which were 97.9 ± 5.4 and 102.4 ± 7.6% of baseline levels, respectively (N = 6, Wilcoxon Matched-Pairs test $p>0.05$). A statistical difference was found between the N2 amplitudes measured at 30 minutes after RF stimulation in the 8Hz pathway in drug-free ACSF when compared to the amplitude in the presence of H-89 (Mann-Whitney U test $p<0.01$). These data confirmed that the LTP that was induced in transverse slices by RF stimulation showed similarities to the cAMP-mediated LTP observed by Salin *et al.,* 1996.

As shown in figures 5.3.21 and 5.3.22 the inhibition of NOS also reduced the incidence of LTP induced by RF stimulation in transverse slices. The data were grouped according to the incidence of LTD, LTP and no change in the N2 amplitude of the 8Hz pathway measured at 30 minutes after stimulation. In 4 recordings there was no change, 1 recording was depressed and in the remaining 2 cases LTP could still be detected. After stimulation there was no change in the N1 amplitude in the 8Hz pathway, but there was a suggestion of a transient decrease in the amplitude of the PPR. The amplitudes of N2 in the 8Hz and 1Hz pathways were 101.1 ± 8.9 and 105.3 ± 3.2% of baseline levels, respectively (N = 7) within 30 minutes of stimulation. In the 1Hz pathway there was a suggestion that N1 increased after stimulation but little or no change was noted in the amplitude of the PPR. In the 8Hz pathway the N2 amplitude of FPs recorded in the presence of 7-NI were significantly different to those recorded in drug-free ACSF 30 minutes after RF stimulation (Mann-Whitney U test $p<0.01$). The incidences of LTD, LTP and no change in the N2 component

were noted at 30 minutes after stimulation. As summarised in the bar chart in figure 5.3.18 below and in the pie charts in figure 5.3.23 in the presence of an inhibitor of PKA or NOS there was a considerable reduction in the incidence of LTP in the N2 component in the 8Hz pathway recorded at 45 minutes after stimulation. This was most apparent when RF stimulation was performed in the presence of H-89.

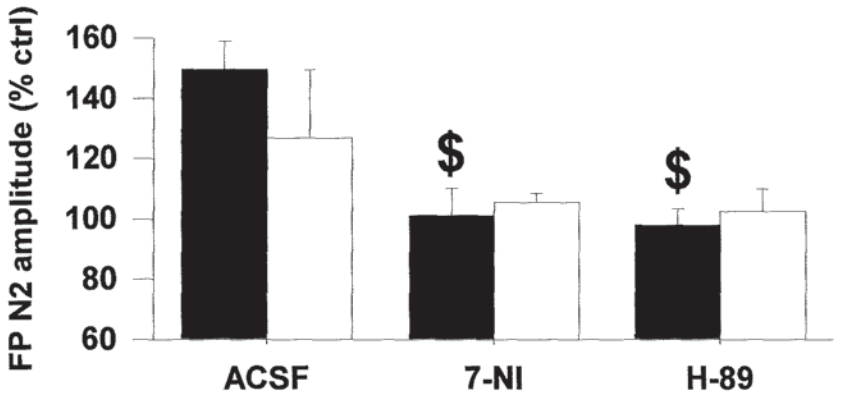

Figure 5.3.18 Effects of RF stimulation in drug-free ACSF or in the presence of an inhibitor or protein kinase A (0.2 μM H-89) or nitric oxide synthase (5μM 7-NI) in transverse slices of cerebellar vermis

Bar chart represents the N2 amplitude in the 8Hz (black) and 1Hz (white) pathway measured 30 minutes after the RF stimulation period. From left to right RF stimulation in drug-free ACSF and in the presence of 0.2μM H-89 or 5μM 7-NI. Dollar signs ($) indicate where a significant difference was observed between the amplitude of N2 in the 8Hz pathway after RF stimulation in the presence of an inhibitor of PKA or 7-NI when compared to the amplitude under control conditions (Mann-Whitney U test $p<0.01$).

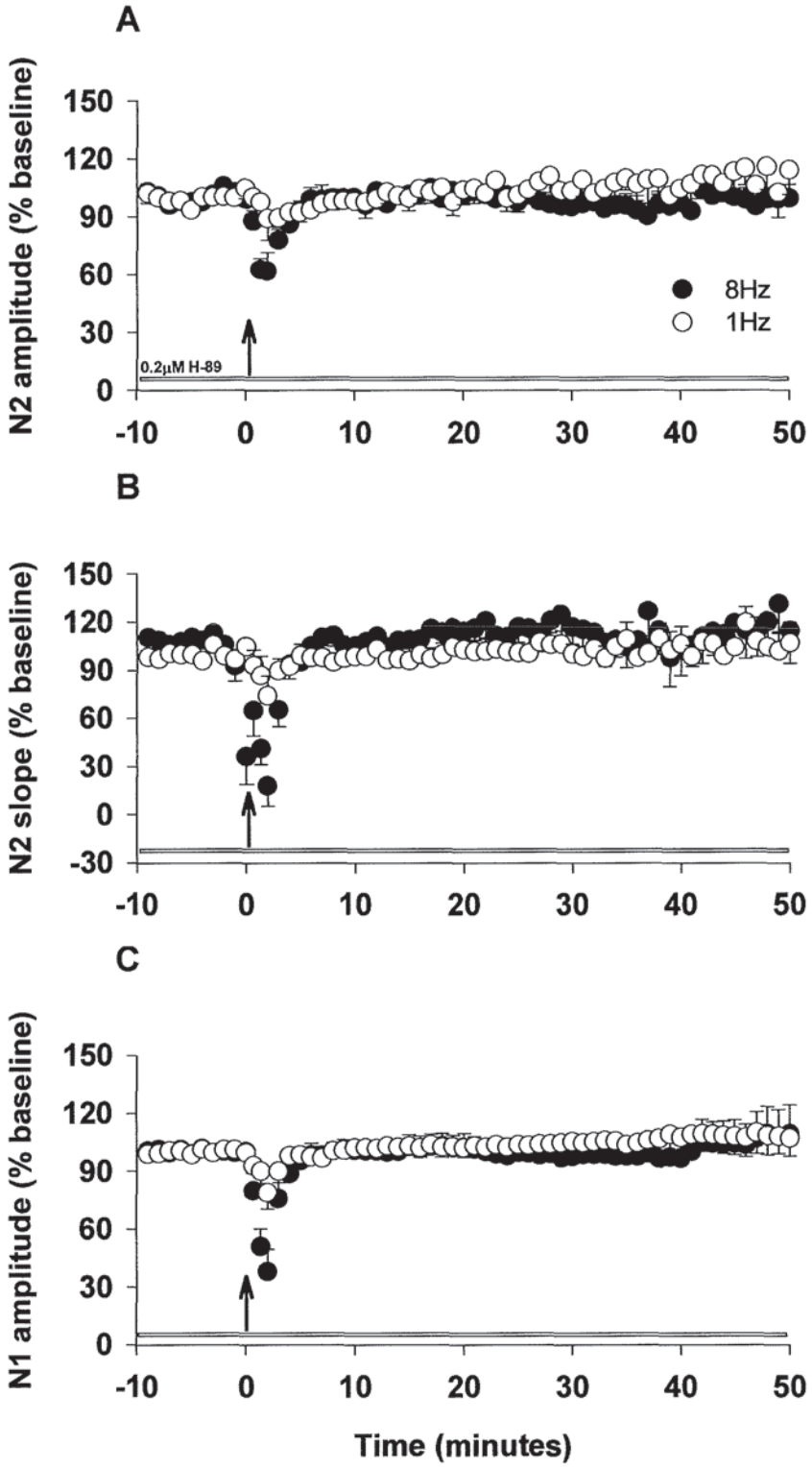

Figure 5.3.19 Effects of RF stimulation on field potential responses in the presence of 0.2μM H-89 in transverse slices of cerebellar vermis

Graphs A – C are as shown in figure 5.3.7. N = 6 paired recordings. Horizontal white bar represents the application of 0.2μM H-89.

A

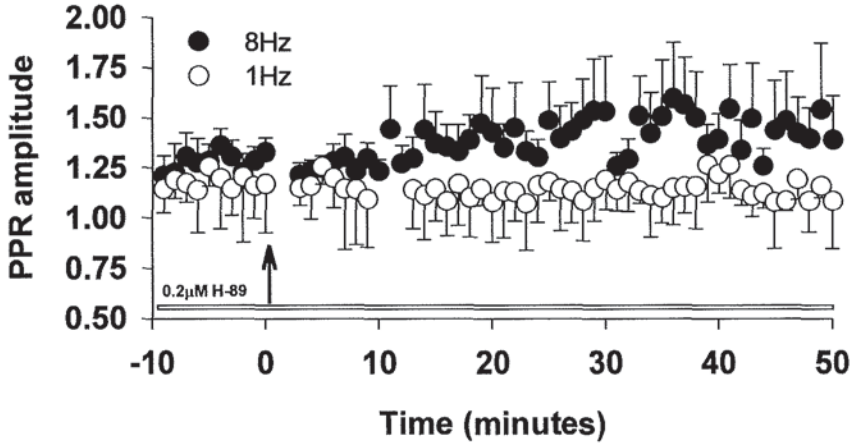

B

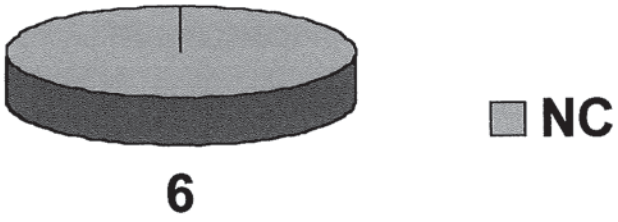

Figure 5.3.20 Effects of RF stimulation on field potential responses in the presence of 0.2μM H-89 in transverse slices of cerebellar vermis

Graphs A and B are as shown in figure 5.3.8. N = 6 paired recordings. Horizontal white bar represents the application of 0.2μM H-89.

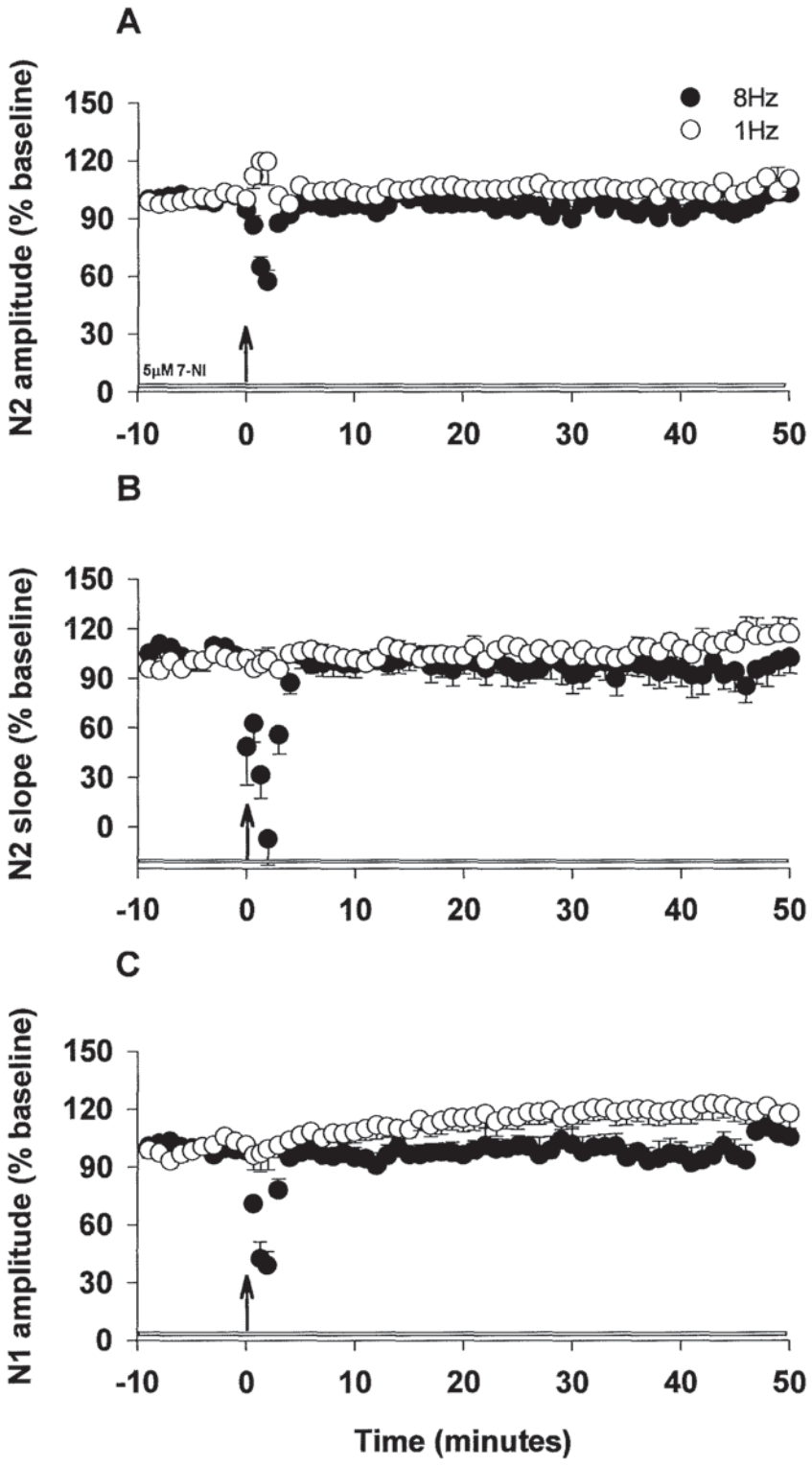

Figure 5.3.21 Effects of RF stimulation on field potential responses in the presence of 5μM 7-NI in transverse slices of cerebellar vermis

Graphs A – C are as shown in figure 5.3.7. N = 7 paired recordings. Horizontal white bar represents the application of 5μM 7-NI.

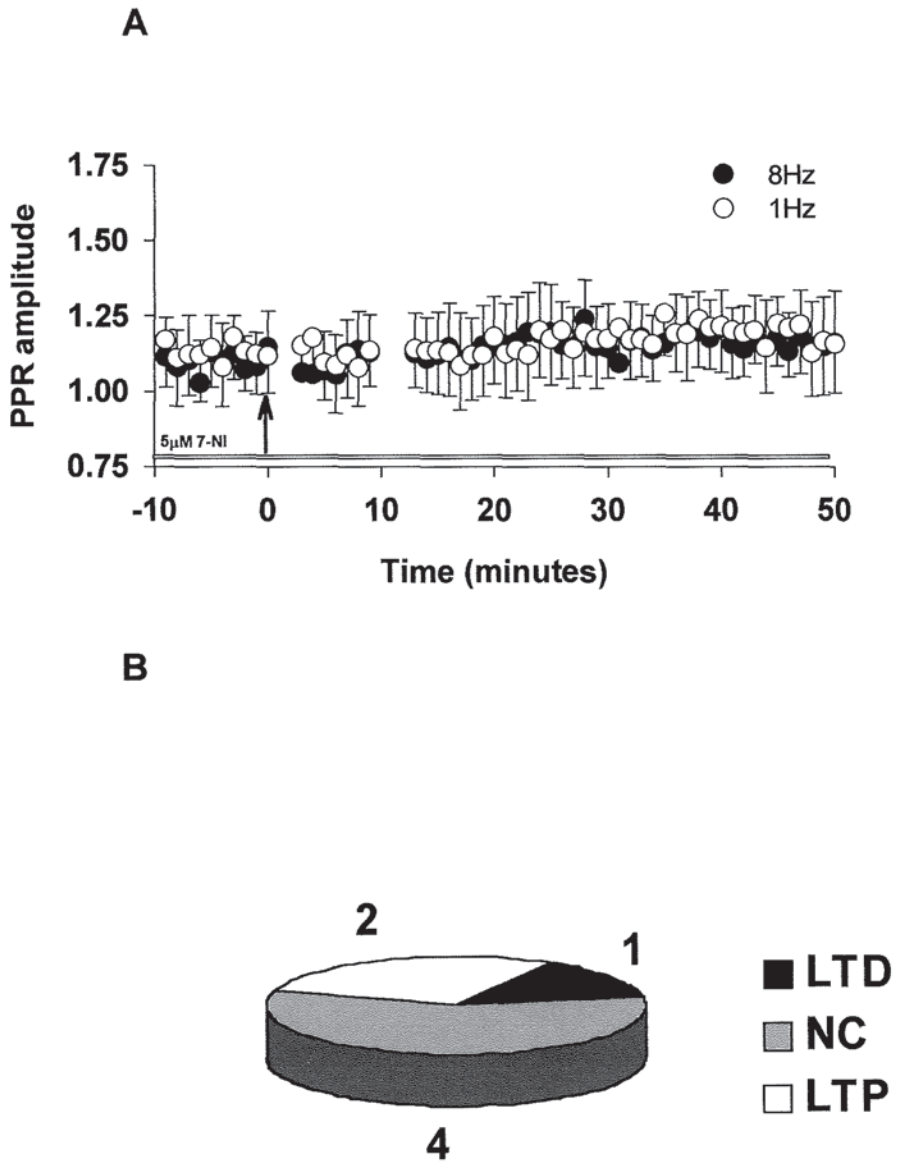

Figure 5.3.22 Effects of RF stimulation on field potential respones in the presence of 5μM 7-NI in a transverse slice of cerebellar vermis

Graph A and pie chart B are as shown in figure 5.3.8. N = 7 paired recordings. Horizontal white bar represents the application of 5μM 7-NI.

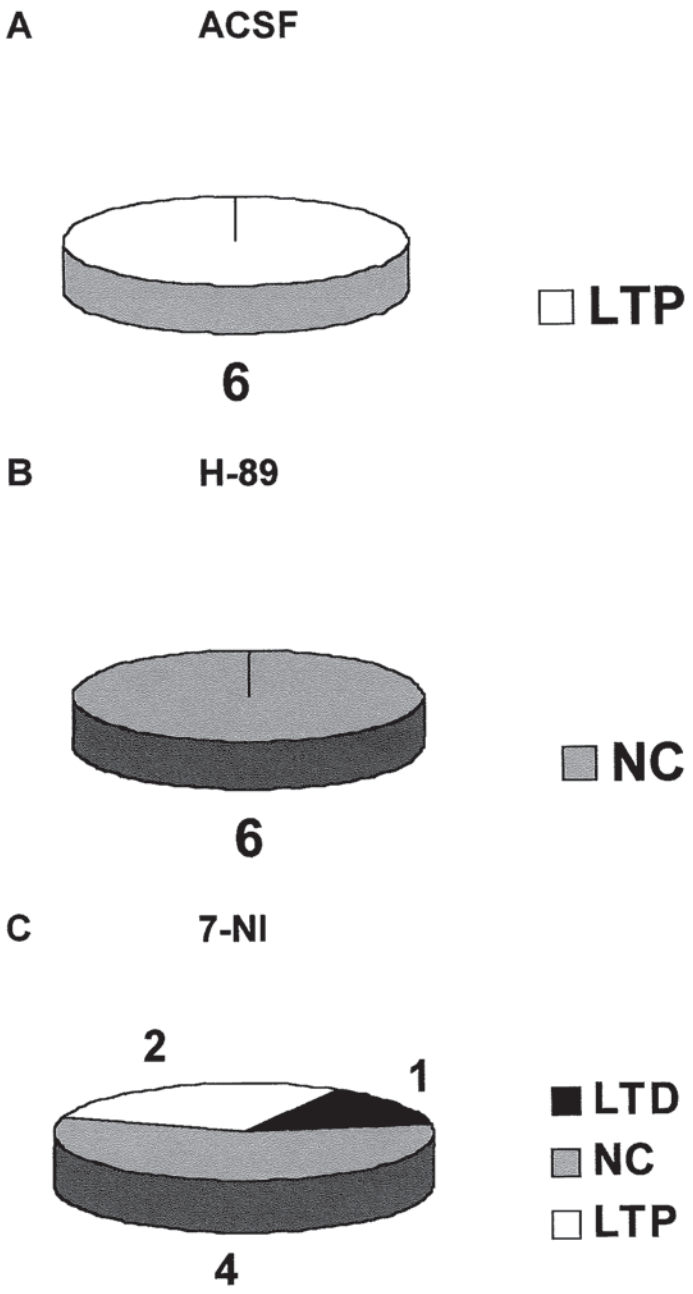

Figure 5.3.23 Effects of RF stimulation, alone or in the presence of inhibitors of protein kinase A (0.2 μM H-89) or nitric oxide synthase (5μM 7-NI) in transverse slices of cerebellar vermis

Pie charts represent the incidence of LTP, LTD and no change in the test pathway N2 amplitude 30 minutes after the stimulation period. Pie charts A – C show the effect of RF stimulation in drug-free ACSF and in the presence of 0.2μM H-89 or 5μM 7-NI, respectively.

5.4 DISCUSSION

In the presence of 20μM or 0.1mM picrotoxin, increasing the frequency of molecular layer stimulation from 0.2 to 8Hz for 15 seconds did not produce an obvious effect on the extracellular FP responses recorded in sagittal slices of cerebellar vermis prepared from either 14 -21 or 28-35 day old rats. BRF stimulation was not sufficient for the induction of LTD or LTP that could be detected in this extracellular model. This finding was in contrast to the report that a brief 15 second period of 8Hz stimulation could induce a LTP of FP responses (Salin et al., 1996).

In sagittal slices a LTD emerged within 45 minutes of stimulation in 5/10 or 50% of the field potential recordings when the frequency of molecular layer activation was raised to 8Hz in one pathway and to a lower rate of 1Hz in the other pathway for 2 minutes. In those recordings in which a LTD was observed in the 8Hz pathway the FP responses in the 1Hz pathway were also depressed. The depression in the 8Hz pathway was accompanied by a small decrease in N1 and a gradual increase in the amplitude of the PPR. This suggested that the mechanism for the slowly emerging depression could involve a presynaptic decrease in the probability of vesicular release of glutamate from PF terminals.

NO has a short biological half life, therefore the actions of NO are likely to be confined to the vicinity of its production site. NO has the ability to diffuse from the site where it is produced to act on neighbouring cells because of its lipid solubility. The exact distances NO can travel is still a matter of debate. In organotypic slice cultures of rat hippocampus it was proposed that LTP might not be spatially restricted at distances of less than 70μm (Engert and Bonhoeffer, 1997). Fluorescent imaging of the stimulating electrode positions in the sagittal slice described in chapter 3 showed that test and control pathways ranged between 40 and 100μm apart. The LTD described in this experiment in the 1Hz pathway could therefore possibly be explained by the diffusion of NO released by 8Hz stimulation to distant synapses at the control site inducing a form of LTD similar to the NO-LTD which has been described by other groups (DeSchutter, 1995; Hartell, 1996b).

The inhibition of NOS, GC or PKG appeared to reduce the incidence of LTD of the N2 component of FP responses following RF stimulation suggesting that key components in the cGMP-signalling cascade might be important for the induction of LTD in 50% of FP responses by the RF stimulation method.

Pairing RF stimulation with inhibition of cAMP-specific type IV PDEs led to a frequency-dependent potentiation of the N2 component of FP responses, which was accompanied by an increase in N1 and a decrease in the PPR. Therefore there could be a presynaptic mechanism underlying this effect. The increase in N1 suggests an increase in the number of PFs that were recruited by molecular layer stimulation. The decrease in the amplitude of the PPR is indicative of an increase in the probability of neurotransmitter release. These data suggest that under conditions of raised cAMP RF stimulation can induce a cAMP-mediated form of LTP of presynaptic origin and supports the findings of (Salin et al., 1996). Perhaps the balance between postsynaptic LTD and presynaptic LTP of FP responses in this extracellular model depends on the respective activities of cAMP and cGMP pathways. This hypothesis is supported by the finding that in the presence of an inhibitor of cGMP specific type V PDEs, PF stimulation induced a robust LTD of PF to Purkinje cell synaptic transmission (Hartell, 1996a). Under conditions of raised cAMP activity there appears to be an increased likelihood of inducing LTP whereas if breakdown of cGMP is prevented the conditions favour LTD.

A number of studies have investigated what synaptic events lead to the cAMP mediated LTP that has been observed at PF-Purkinje cell synapses. Changes in the excitability of PFs and an enhancement of Ca^{2+} influx and neurotransmitter release have been proposed as effects of cAMP activation (Chen and Regehr, 1997). A change in the waveform of the action potential volley that was termed 'spike broadening' was also proposed as a possible mechanism for LTP at PF-Purkinje cell synapses. The spike broadening was reported to cause not a larger Ca^{2+} signal but a longer lasting Ca^{2+} influx that could contribute to LTP (Sabatini and Regehr, 1997).

In transverse slices RF stimulation in 6 experiments produced an activity-dependent LTP of FP responses in the 8Hz pathway within 30 minutes. This was accompanied by an increase in N1 and a decrease in the amplitude of the PPR suggesting that this potentiation was mediated presynaptically. This result was in complete contrast to the induction of a small potentiation in only 2 recordings by RF stimulation in sagittal slices.

There are anatomical differences between sagittal and transverse slices of cerebellar vermis:-

i) Transverse slices are cut in the plane of PFs and therefore incorporate intact PFs whereas in sagittal slices the PFs are truncated to the thickness of the slice.

ii) Sagittal slices are cut in the plane of CFs, Purkinje cell axons and dendritic trees therefore, molecular layer stimulation might activate Purkinje cells or climbing fibres directly.

iii) In sagittal slices there could be additional NO release from basket cells situated adjacent to Purkinje cells, this is less likely in transverse slices because of the distance of electrodes from the recording site.

iv) Intact inhibitory interneurons are likely to be included in transverse slices of cerebellar vermis. The presence of picrotoxin in the ACSF should eliminate the contribution of inhibitory $GABA_AR$. However, activation of $GABA_BR$ could influence the accumulation of cAMP in presynaptic terminals.

Changes in synaptic efficacy were dramatically altered by subtle changes in the conditions under which RF stimulation was performed. For example, increasing the availability of cAMP by preventing its breakdown with an inhibitor of type IV cAMP-specific PDEs was sufficient to tip the balance in favour of LTP. In sagittal slices LTD was induced in only 50% of recordings following RF stimulation. In transverse slices RF stimulation consistently produced a clear, presynaptic potentiation. Using an electrochemical probe similar to that described by (Kimura et al., 1998) it would be interesting to compare the levels of NO release elicited by RF stimulation in sagittal slices cut perpendicular to the PFs and in transverse slices cut in the plane of PFs. The LTP in transverse slices was partially blocked

by a NOS inhibitor suggesting that NO may influence the production of LTP as well as LTD in the cerebellar cortex.

In transverse slices there were no incidences of potentiation after RF stimulation was applied in ACSF that contained the selective cAMP-dependent PKA inhibitor, H-89. This provided strong evidence that the cAMP signalling pathway was required for the induction of this form of LTP and was consistent with previous reports that raised frequency activation of the molecular layer could produce a LTP of FP responses (Salin et al., 1996).

CHAPTER 6

DO $GABA_B$ RECEPTORS CONTRIBUTE TO THE FIELD POTENTIAL RESPONSES EVOKED BY MOLECULAR LAYER STIMULATION?

6.1 INTRODUCTION

The inhibitory neurotransmitter GABA is found throughout the nervous system. GABA was found to act at a group of receptors named $GABA_AR$ following studies with the competitive GABAR antagonist bicuculline (Curtis and Johnson, 1974). Later a second novel inhibitory GABAR was identified which elicited a GABA-mediated response but was insensitive to block by bicuculline. These receptors known as $GABA_BR$ were first recognised in 1981 on peripheral autonomic nerve terminals (Hill and Bowery, 1981). Autoradiographic localisation studies using the GABA analogue baclofen, which has a high affinity for $GABA_BR$ sites showed that in the cerebellum the $GABA_BR$ sites were confined to the molecular layer (Wilkin et al., 1981).

Data from native receptor studies suggested that as many as 5 $GABA_BR$ subtypes could exist (Gemignani et al., 1994). Two $GABA_BR$ proteins termed $GABA_BR1$ and $GABA_BR2$ have now been cloned. These proteins have seven transmembrane domains and couple to G-proteins. *In situ* hybridisation studies reported that the messenger RNA for $GABA_BR1$ was found in abundance in Purkinje cells and also at moderate levels in the molecular layer (Kaupmann et al., 1997). More recently it has been discovered that functional $GABA_BR$ exist as heterodimers formed from the two closely related $GABA_BR1$ and $GABA_BR2$ subunits that interact at the C-terminus. $GABA_BR2$ corresponds in both size and distribution to $GABA_BR1$ and has a sequence homology of approximately 35% (Möhler and Fritschy, 1999).

It is thought that presynaptic $GABA_BR$ diminish the evoked release of neurotransmitter through inhibition of an inward Ca^{2+} conductance. This effect explains the ability of the GABA analogue (-) baclofen to suppress neurotransmitter release (Bowery et al., 1981). Postsynaptically $GABA_BR$ activation initiates an increase in K^+ conductance that produces membrane hyperpolarisation. This hyperpolarisation triggers inhibitory postsynaptic potentials and a reduced responsiveness of postsynaptic membranes to excitatory neurotransmitters (Bowery, 1993). Further studies are necessary to investigate the coupling of the newly identified $GABA_BR$ heterodimers to K^+ and Ca^{2+} channels.

There is evidence that the $GABA_BR$ is coupled to G-proteins of the Gi and Go type (Morishita and Sastry, 1995). Pertussis toxin inactivates G-proteins by catalysing the transfer of an adenosine diphosphate-ribose group from nicotinamide adenine dinucleotide to a cysteine residue which interacts with the guanosine triphosphate binding site of the G-protein (Dolphin, 1987). In HEK cells which are deficient in Go $GABA_BR$-mediated modulation of AC is sensitive to pertussis toxin suggesting that in these cells the receptors couple to Gi proteins (Kaupmann et al., 1997).

AC is a key component of the cAMP signalling cascade. It catalyses the production of cAMP that in turn stimulates the cAMP-dependent PKA as shown in figure 5.1.1. $GABA_BR$ can regulate cAMP production in the brain. It was reported that (-) baclofen inhibits cAMP production when the production of the second messenger is stimulated by forskolin which is a potent activator of AC (Wojcik and Neff, 1984; Knight and Bowery, 1996; Cunningham and Enna, 1996; Kaupmann et al., 1997). The data suggests that $GABA_BR$ are negatively coupled to AC. In contradiction to this, another study reported that $GABA_BR$ can increase cAMP levels by activation of receptors positively coupled to AC (Karbon and Enna, 1985).

In the cerebellar cortex anatomical (Bowery and Pratt, 1992) and pharmacological studies (Batchelor and Garthwaite, 1992; Vigot and Batini, 1997) suggest both presynaptic and postsynaptic roles for $GABA_BR$ at the PF to Purkinje cell synapse. There is some evidence for a postsynaptic location for $GABA_BR$ on the dendrites of Purkinje cells and a presynaptic site on the terminals of PFs. The neurotransmitter of basket and stellate cells is GABA.

These interneurons synapse with the Purkinje cell body and dendrites respectively, indicating that $GABA_BR$ could be postsynaptically located. A slow $GABA_BR$-mediated potential was identified at the synapse between PFs and Purkinje cells in a biplanar cerebellar slice preparation. This indicated that there were functional $GABA_BR$ on Purkinje cells (Batchelor and Garthwaite, 1992). There is also some indirect evidence for presynaptic $GABA_BR$ on glutamatergic terminals (Wojcik and Neff, 1984). An investigation into the role of presynaptic $GABA_BR$ suggested that the extent of inhibitory action of these receptors was dependent on the level of activity of their target synapses (Brenowitz et al., 1998). The $GABA_BR$ agonist baclofen has been used extensively in the treatment of spasticity. It was noted that it produced a loss of memory in animal models. This observation suggests that $GABA_BR$ could have implications in learning and memory processes and therefore possibly in synaptic plasticity (as discussed by, Bowery and Pratt, 1992). In the hippocampus, LTP that is associated with memory retention is facilitated by baclofen (Davies et al., 1990).

The possibility that $GABA_AR$ influence synaptic transmission at PF-Purkinje cell synapses in our FP recording experiments can largely be excluded because the Cl^- channel blocker picrotoxin was routinely included in the ACSF to antagonise $GABA_AR$. The aim of this chapter was to investigate the possible contribution of $GABA_BR$ to the FP responses evoked by molecular layer stimulation. In addition, the possibility that activation of $GABA_BR$ could modify the incidence or the direction of plasticity was considered.

6.2 METHODS

6.2.1 SLICE PREPARATION

The experiments were performed using sagittal slices prepared from 14-21 day old rats as described in chapter 2.2.1.

6.2.2 FIELD POTENTIAL RECORDING

In sagittal slices FP responses were obtained using the same method described in chapter 2.2.2.

6.2.3 INTRACELLULAR PIPETTE SOLUTION

Whole cell patch-clamp recording electrodes, were filled with an intracellular pipette solution of the following composition (mM) KGluconate, 132; NaCl, 8; $MgCl_2$, 2; HEPES, 30; Na_2ATP, 4; BAPTA; 0.5; GTP, 0.3; adjusted to pH 7.3.

6.2.4 WHOLE CELL PATCH-CLAMP RECORDING

Whole cell patch-clamp recordings of EPSCs were made from Purkinje cells visualised using a 40 X water immersion lens. For recording, patch electrodes with resistances of 2-4 MΩ, were filled with a potassium gluconate-based intracellular pipette solution. A second patch electrode was filled with ACSF and placed on the surface of the molecular layer to activate PFs. Cells were held in voltage clamp mode at a holding potential of -70mV. After entering the whole cell recording mode a PF input to the Purkinje cell was activated for 100μs at a rate of 0.2Hz with a stimulus intensity of between 1 and 10 Volts. Pairs of stimuli were delivered at 40ms intervals and the PPR was calculated. Data were stored and analysed on-line using custom written software (Anderson and Collingridge, 1999).

6.2.5 APPLICATION OF DRUGS

The $GABA_BR$ agonist (-) β-p-chlorophenyl GABA (baclofen), its inactive isomer (+) baclofen and the specific $GABA_BR$ antagonists CGP55845 and CGP62349 were made up as concentrated stock solutions of 2mM and 1mM respectively, dissolved in distilled water and then diluted in the ACSF solution prior to bath perfusion. The (-) / (+) baclofen, CGP55845 and CGP62349 were kindly supplied by Professor Wolfgang Froestl.

6.3 RESULTS

6.3.1 EFFECT OF THE $GABA_B$ RECEPTOR AGONIST 2μM (-) BACLOFEN OR ITS INACTIVE ISOMER (+) BACLOFEN ON BOTH EXTRACELLULAR FIELD POTENTIAL RESPONSES AND PARALLEL FIBRE EXCITATORY POSTSYNAPTIC CURRENTS RECORDED IN SAGITTAL SLICES OF CEREBELLAR VERMIS

$GABA_BR$ are thought to cause a reduction in neurotransmitter release by initiating a decrease in Ca^{2+} conductance (Bowery, 1993). Although the actions of $GABA_BR$ agonists on synaptic transmission are already well established it was necessary to examine what effect the $GABA_BR$ agonist (-) baclofen had on the FP responses detected using this extracellular recording system. Bath perfusion of the $GABA_BR$ agonist 2μM (-) baclofen for 8 minutes produced a pronounced decrease in the amplitude and slope of the N2 component of FP responses as shown in figure 6.3.1. Within 3 minutes of application of (-) baclofen the mean N2 amplitude was depressed to 51.2 ± 5.5% of the baseline level, (N = 11 pathways taken from 9 recordings). As shown in figure 6.3.2, this depression was coincident with a partially reversible increase in the amplitude of the PPR. The N2 component did not completely recover and 32 minutes after application of (-) baclofen the amplitude was still below baseline levels at 85.7 ± 5.6% of baseline. Also shown in figure 6.3.1 are the effects of application of inactive isomer 2μM (+) baclofen for 8 minutes. Paired pulse data was not collected for these experiments. There was no obvious change in the N2 or N1 components of FP responses in the presence of (+) baclofen. The peak depression of N2 induced by (-) baclofen (51.2 ± 5.5%) was statistically greater than that observed with (+) baclofen which was 100.6 ± 2.5% of baseline (N = 7 pathways taken from 4 paired recordings, Mann-Whitney U test $p<0.001$).

Whole cell recordings revealed that PF-EPSCs were similarly reduced in amplitude in the presence of 2μM (-) baclofen. The maximum depression of the PF-EPSC amplitudes reached 32.6 ± 2.2% of baseline levels (N = 5) as shown in graph B in figure 6.3.2. An

increase in the PPR accompanied the depression. By vertically expanding the amplitude of the PF-EPSC recorded 4 minutes after the application of (-) baclofen it was possible to compare the time course of the reduced response with that of the baseline response. In the example traces shown in figure 6.3.3C there did appear to be a change in the time course of the PF-EPSC after the application of (-) baclofen.

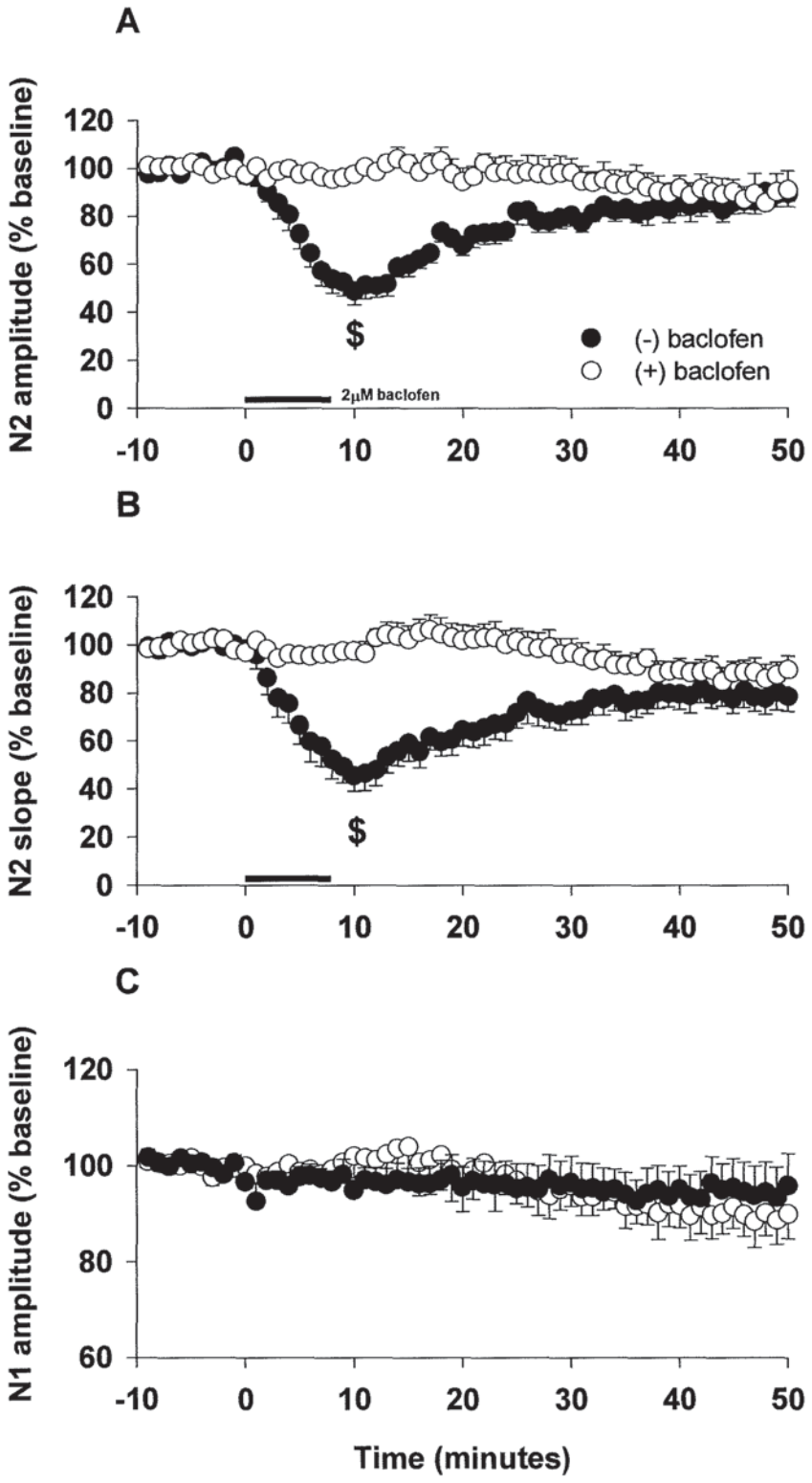

Figure 6.3.1 Effect of 2μM of the $GABA_B$ receptor agonist (-) baclofen and its inactive isomer (+) baclofen on field potential responses

Graphs A - C illustrate the FP N2 amplitude and slope and the N1 amplitude, respectively. Data are expressed as the mean % ± S.E.M. of 10 responses collected during a 10 minute baseline period. Closed circles, (-) baclofen, N = 11 pathways taken from 9 recordings; open circles, (+) baclofen, N = 7 pathways taken from 4 recordings. Horizontal black bar represents the application of 2μM (-) or (+) baclofen. Dollar signs ($) indicate where the peak depression induced by (-) baclofen was significantly greater than that observed with (+) baclofen Mann-Whitney U test $p<0.001$.

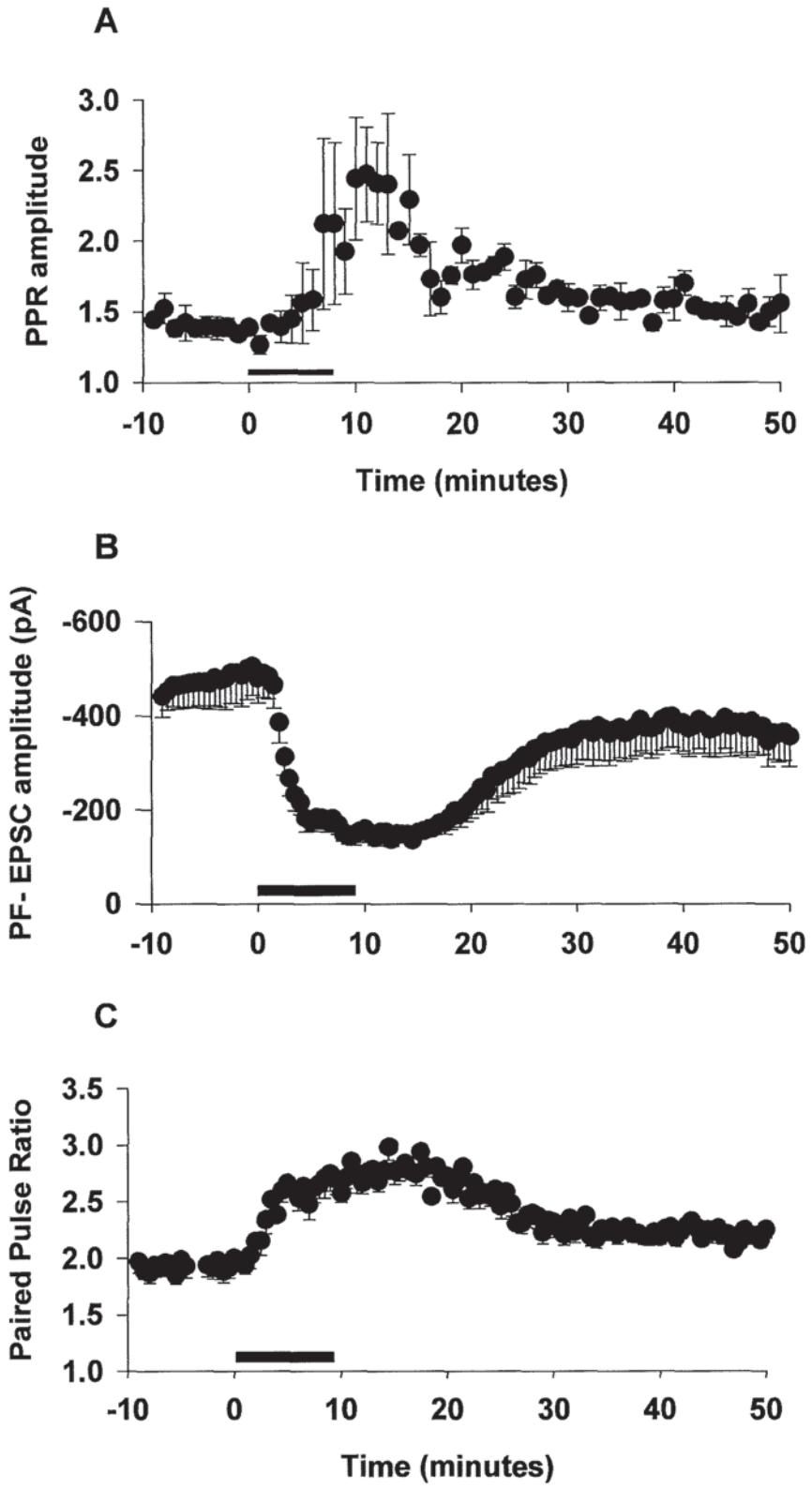

Figure 6.3.2 Effect of the $GABA_B$ receptor agonist 2μM (-) baclofen
Graph A illustrates the amplitude of the PPR of FPs. Data are expressed as the mean % ± S.E.M. of 10 responses collected during a 10 minute baseline period. Closed circles, (-) baclofen, N = 11 pathways taken from 9 recordings; closed circles (+) baclofen, N = 7 pathways taken from 4 paired recordings. Horizontal black bar represents the application of 2μM (-) or (+) baclofen. No paired pulse data was collected for (+) baclofen. Also shown in graphs B and C are the effects of (-) baclofen on the amplitude and PPR of PF-EPSCs.

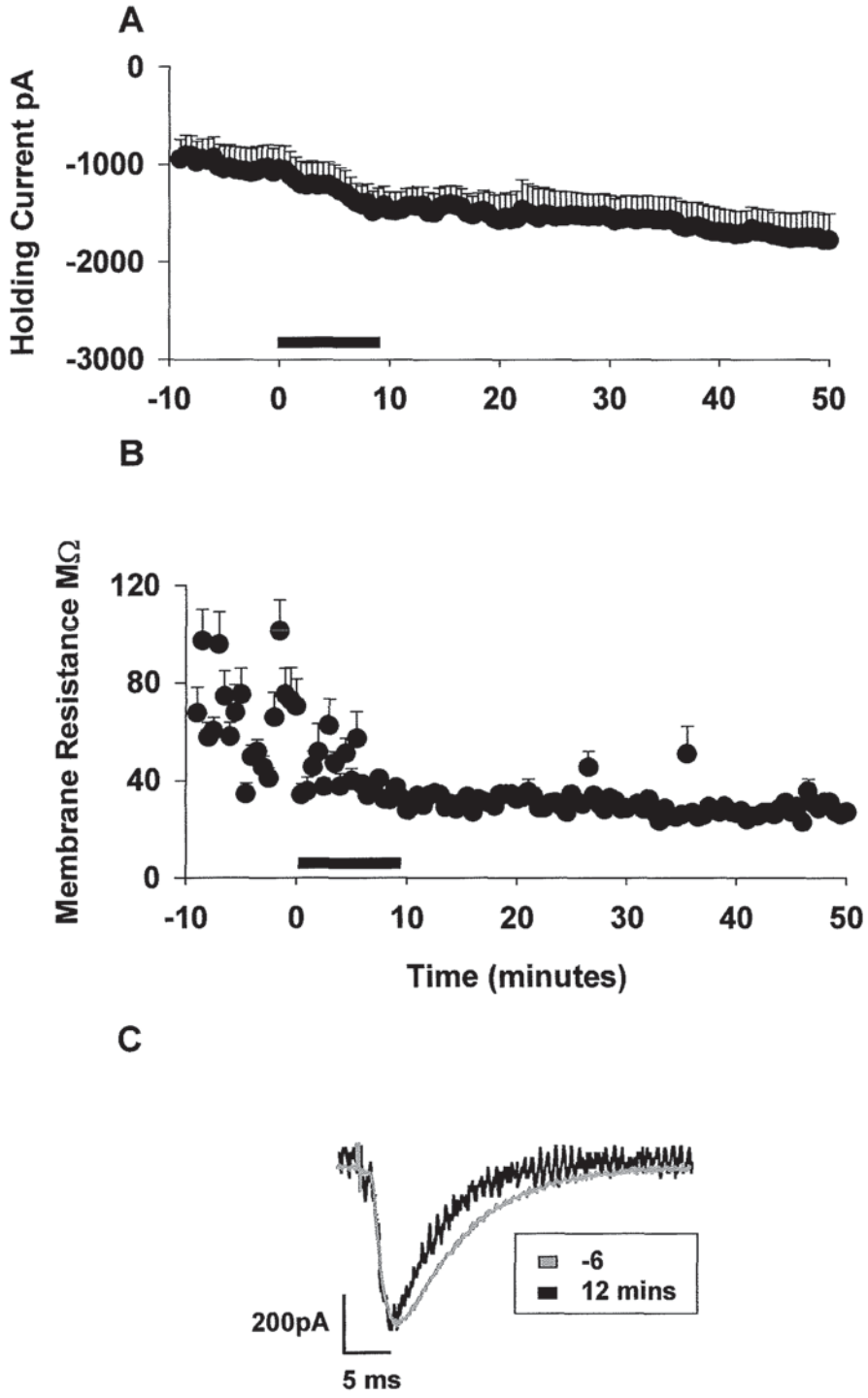

Figure 6.3.3 Effect of the $GABA_B$ receptor agonist 2μM (-) baclofen on PF-EPSCs
Graphs A and B illustrate the effect of (-) baclofen on the holding current and the input resistance during the recording of PF-EPSCs. Black horizontal bar indicates the period of (-) 2μM baclofen application. Panel C illustrates PF-EPSCs recorded 5 minutes prior to (grey) and 4 minutes after the application of (-) baclofen (black). Scale bar 200pA, 5ms, the vertical scale relates to the grey trace only since the black trace was expanded vertically in order to compare the time course of the EPSCs prior to and after the application of (-) baclofen.

6.3.2 EFFECT OF THE $GABA_B$ RECEPTOR AGONIST 2μM (-) BACLOFEN ON EXTRACELLULAR FIELD POTENTIAL RESPONSES IN THE PRESENCE OF THE SELECTIVE $GABA_B$ RECEPTOR ANTAGONISTS 1μM CGP55845 OR 1μM CGP62349 IN SAGITTAL SLICES OF CEREBELLAR VERMIS

In a further set of experiments (-) baclofen was applied in the presence of the $GABA_BR$ antagonists CGP55845 and CGP62349 to ensure that these compounds could block the effects of baclofen in this system. CGP55845 or CGP62349, at a concentration of 1μM, were applied for 20-30 minutes prior to the application of (-) baclofen. As shown in figure 6.3.4 the effects of (-) baclofen on the N1 and N2 components of FP responses were blocked by the selective $GABA_BR$ antagonist 1μM CGP55845. The N2 amplitude was 98.7 ± 6.2% of baseline (N = 7 pathways taken from 4 paired recordings) which was significantly different from 51.2 ± 5.5% of baseline in the absence of a $GABA_BR$ antagonist (Mann-Whitney U test $p<0.001$) as measured 3 minutes after the application of 2μM baclofen.

As shown in figure 6.3.5 similar effects on the N1 and N2 components of FPs were observed with the selective $GABA_BR$ antagonist 1μM CGP 62349, which significantly blocked the effects of 2μM (-) baclofen. The amplitude of the N2 component was 101.5 ± 4.5 (N = 8 pathways taken from 5 recordings) 3 minutes after the application of (-) baclofen which was significantly different to 51.2 ± 5.5 in the absence of CGP62349 (Mann-Whitney U test $p<0.001$). The N1 amplitude showed no obvious change for the duration of the recording.

As shown in figure 6.3.6 at the start of the CGP55845 or CGP62349 perfusions there was a hint of a potentiation in the N2 component of FP responses. This potentiation was not large enough to be classed as LTP. However, this observation raised the possibility that in drug-free ACSF there could be endogenous GABAergic tone that could activate $GABA_BR$ and contribute to the FP responses evoked by stimulation of the molecular layer. To further investigate this hypothesis CGP62349 was then applied at a higher concentration of 5μM for 30 minutes. It was no longer possible to detect a small potentiation of the FP responses at this concentration. Curiously, there were signs of a depression in both the amplitude and slope of N2. This reduction did not fall below 80% of baseline levels and therefore was not

considered to be LTD. In future experiments it might be interesting to observe the effects of lower concentrations of CGP55845 and CGP62349.

Bar charts were constructed to compare the acute and long-term effects of (-) or (+) baclofen alone or in the presence of CGP55845 or CGP62349 as shown in figure 6.3.7. Mann Whitney U tests highlighted the significant differences in the peak depression induced by (-) baclofen compared to that observed with its inactive isomer (+) baclofen or in the presence of the $GABA_BR$ antagonists ($p<0.05$).

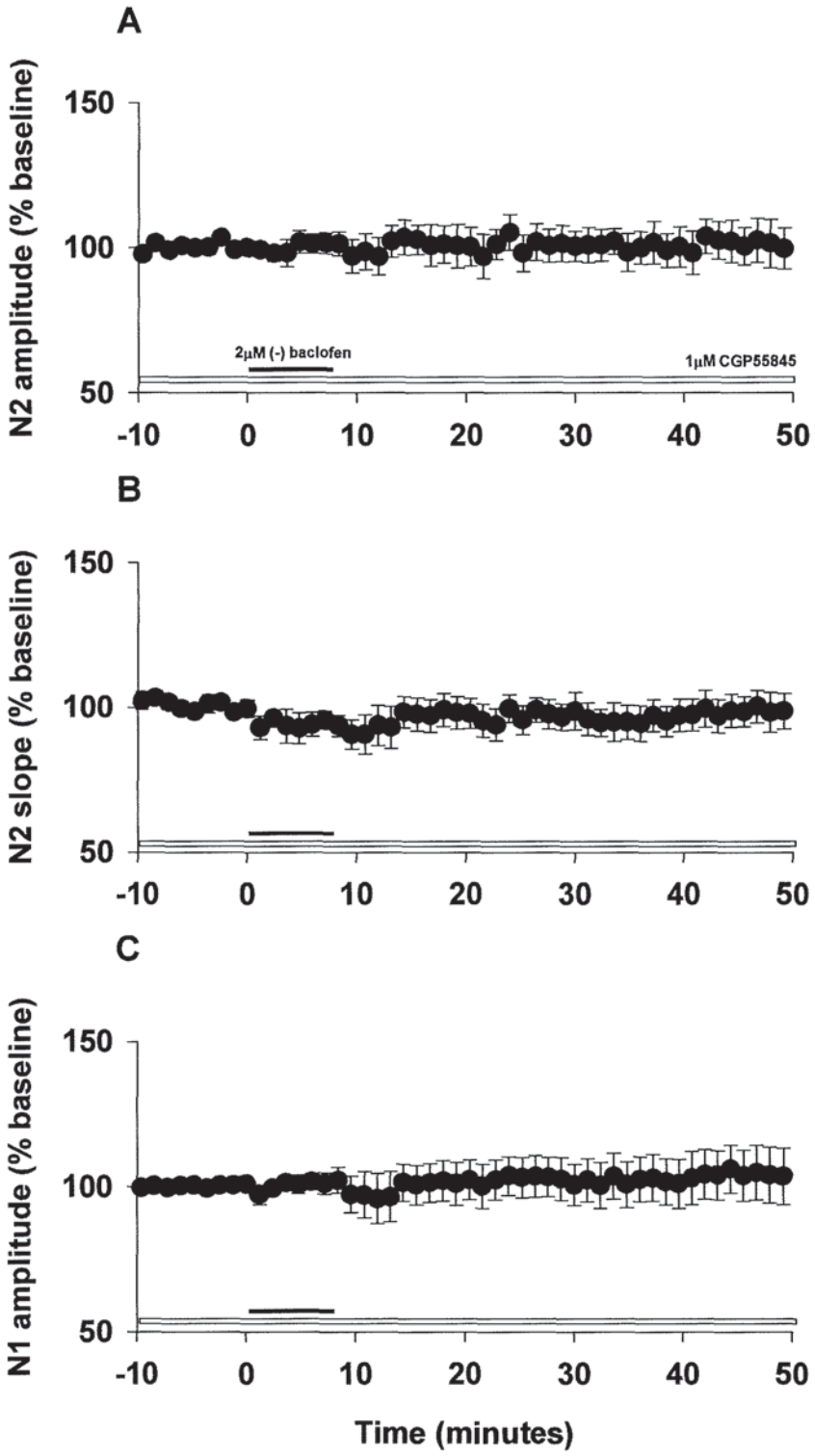

Figure 6.3.4 Effect of the $GABA_B$ receptor agonist 2μM (-) baclofen on field potential responses in the presence of the $GABA_B$ receptor antagonist 1μM CGP 55845
Graphs A and B illustrate the FP N2 amplitude and slope, respectively. Data are expressed as the mean % ± S.E.M. of 10 responses collected during a 10 minute baseline period. N = 7 pathways taken from 4 paired recordings. Horizontal black bar indicates the perfusion of 2μM (-) baclofen. Horizontal white bar represents the application of 1μM CGP55845.

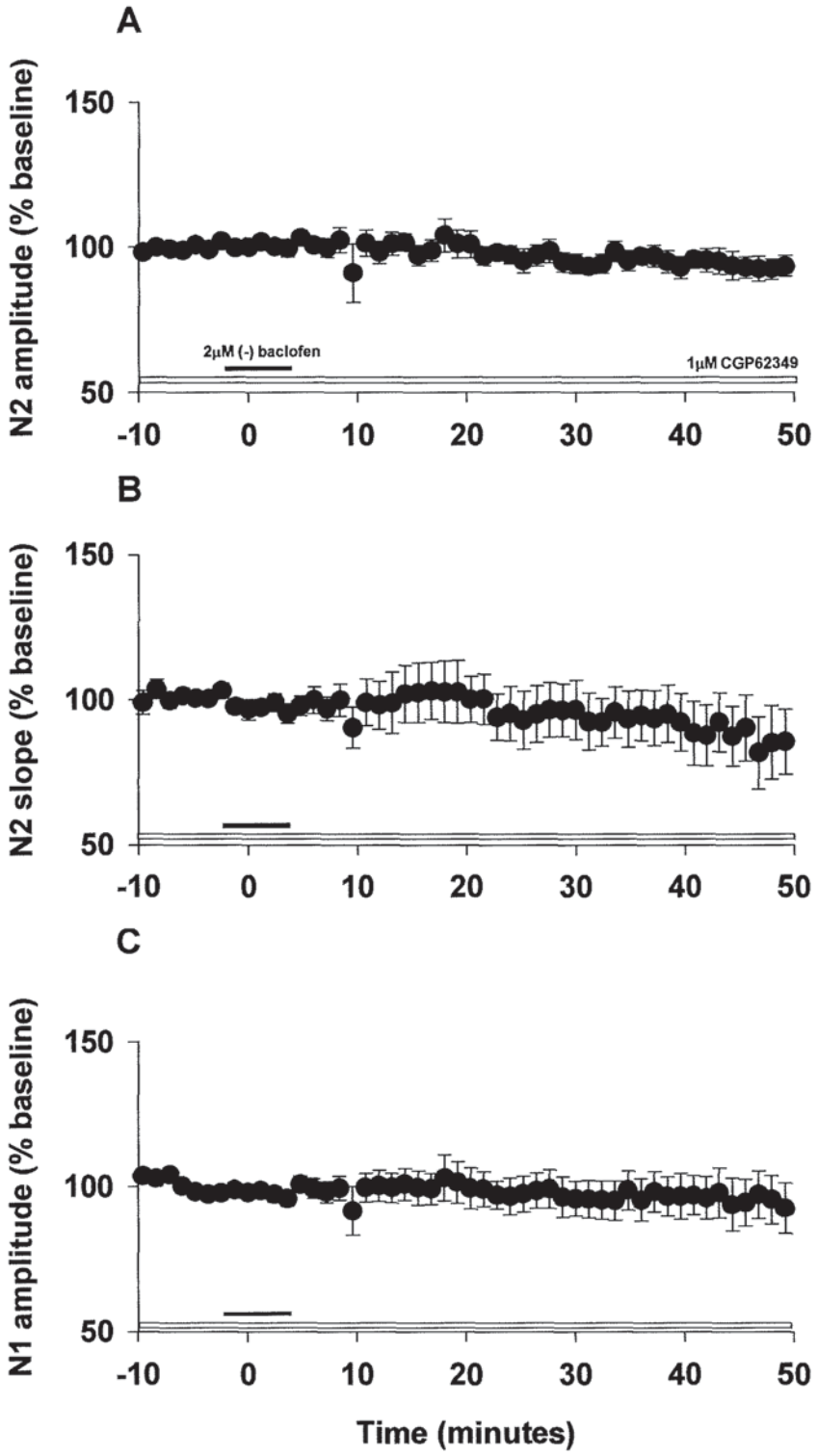

Figure 6.3.5 Effect of the $GABA_B$ receptor agonist 2μM (-) baclofen on field potential responses in the presence of the $GABA_B$ receptor antagonist 1μM CGP62349

Graphs A -C illustrate the FP N2 amplitude slope and N1 amplitude, respectively. Data are expressed as the mean % ± S.E.M. of 10 responses during a 10 minute baseline period. N = 8 pathways taken from 5 paired recordings. Horizontal black bar indicates the application of 2μM (-) baclofen. Horizontal white bar represents the application of 1μM CGP62349.

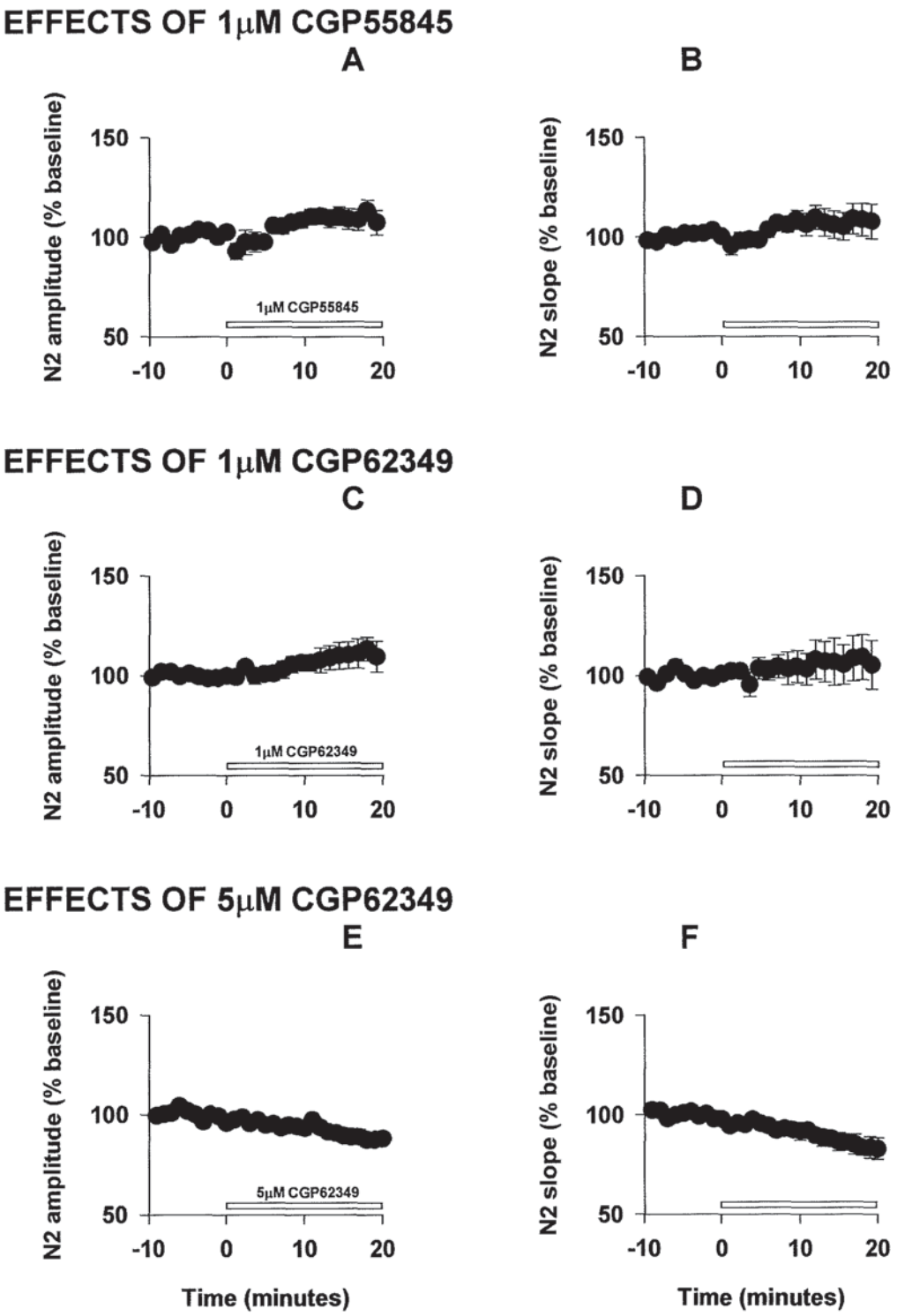

Figure 6.3.6 Effect of the $GABA_B$ receptor antagonists 1μM CGP55845 and 1 or 5μM CGP62349 on field potential responses

Graphs A and B illustrate the effect of 1μM CGP55845 on the N2 amplitude and slope of FPs. Graphs C and D and show the effect of 1μM CGP62349 on the N2 component of FPs and graphs E and F represent the effects of 5μM CGP62349. Data are expressed as the mean % ± S.E.M of 10 responses collected during a 10 minute baseline period. N = 7 pathways taken from 4 paired recordings. Horizontal white bars indicate the perfusion of CGP55845 or CGP62349 application.

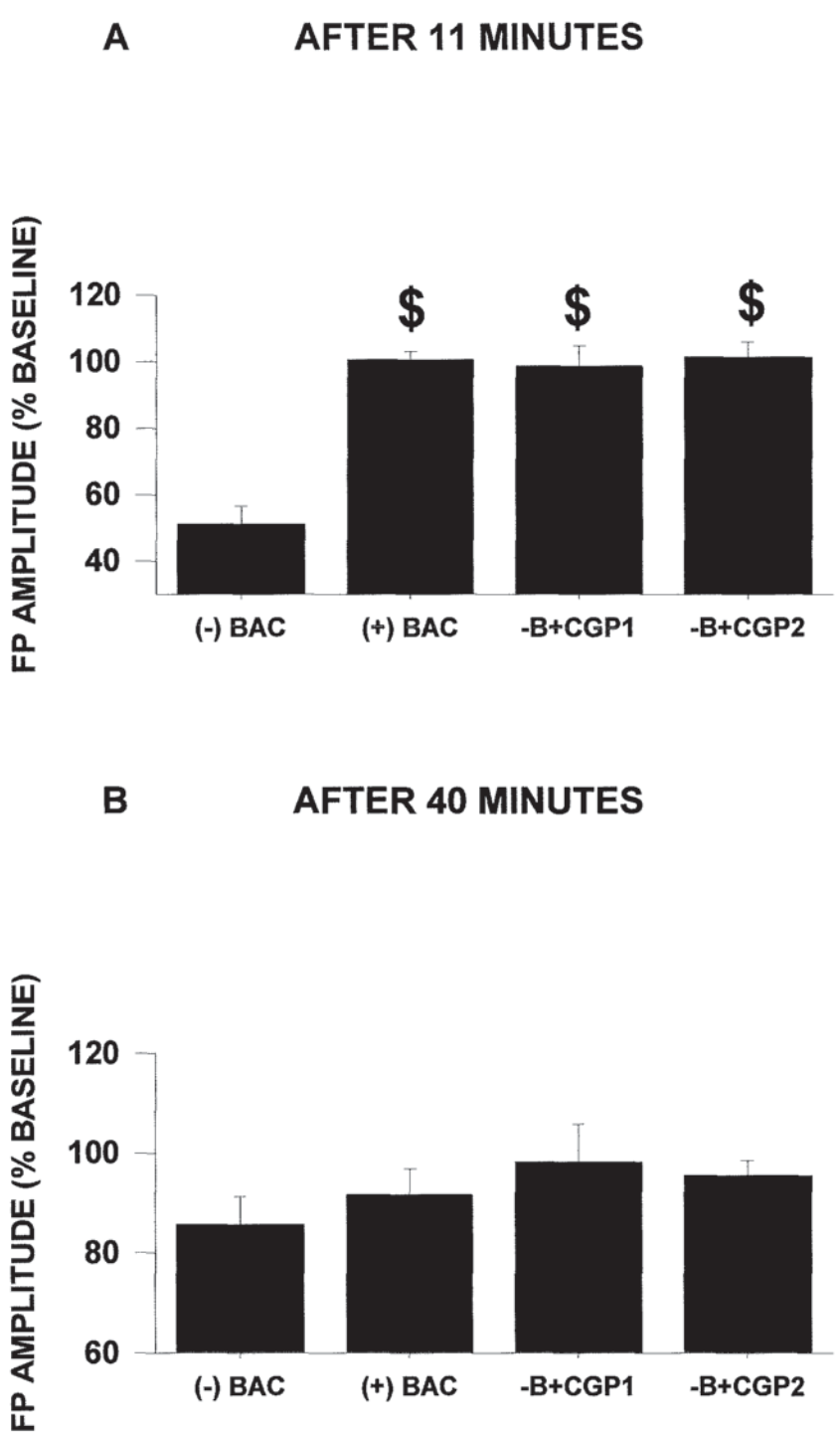

Figure 6.3.7 A summary of the effects of (-) or (+) baclofen alone or in the presence of $GABA_B$ receptor antagonist

Bar charts A and B represent the amplitude of the N2 component measured at 11 and 40 minutes, respectively after the application of (-) baclofen. Dollar signs ($) indicate where the peak depression induced by (-) baclofen was significantly greater than that observed with its inactive isomer (+) baclofen or in the presence of CG55845 (CGP1) or CGP62349 (CGP2, Mann-Whitney U test $p<0.01$).

6.3.3 EFFECT OF DELAYED APPLICATIONS OF THE SELECTIVE $GABA_B$ RECEPTOR ANTAGONIST 1μM CGP62349 ON THE RECOVERY OF EXTRACELLULAR FIELD POTENTIAL RESPONSES AFTER APPLICATION OF THE $GABA_B$ RECEPTOR AGONIST 2μM (-) BACLOFEN IN SAGITTAL SLICES OF CEREBELLAR VERMIS

A further set of experiments were designed to see if the long-term decrease of FP responses that was observed after the application of (-) baclofen was due to the incomplete washout of (-) baclofen or to a long-term modification of synaptic transmission. Delayed applications of CGP62349 were made at 20 or 30 minutes after the perfusion of (-) baclofen. The rationale behind this approach was to establish if the remaining depression was rapidly reversed upon wash-out of the antagonist. Bath perfusion of (-) baclofen produced a pronounced depression of the N2 component of FP responses. Application of CGP62349 20 minutes after the application of (-) baclofen produced a significantly faster recovery of the N2 component of FP responses 114.9 $\pm$ 9.3% of baseline (N = 7 pathways taken from 4 paired recordings) than at 30 minutes, 77.1 $\pm$ 8.4% of baseline (N = 7 pathways taken from 4 paired recordings, Mann-Whitney U test $p<0.05$). The extent of recovery when CGP62349 was applied 20 minutes after (-) baclofen application was also significantly different from the recovery of the FP N2 amplitude in slices perfused with normal ACSF (Mann-Whitney U test $p<0.05$). The acute effect of (-) baclofen was accompanied by a partially reversible increase in the amplitude of the PPR. A long-term decrease in the N1 amplitude was apparent in the FP recordings in which CGP62349 was applied 30 minutes after the perfusion of (-) baclofen. There was no obvious change in N1 for the duration of the recording for the other two experiments. These data are summarised in the graphs in figures 6.3.8 and 6.3.9. It was difficult to interpret the greater extent of recovery of the FP responses that was noted when CGP62349 was applied 20 minutes after (-) baclofen application. This will be dealt with in more detail in the discussion.

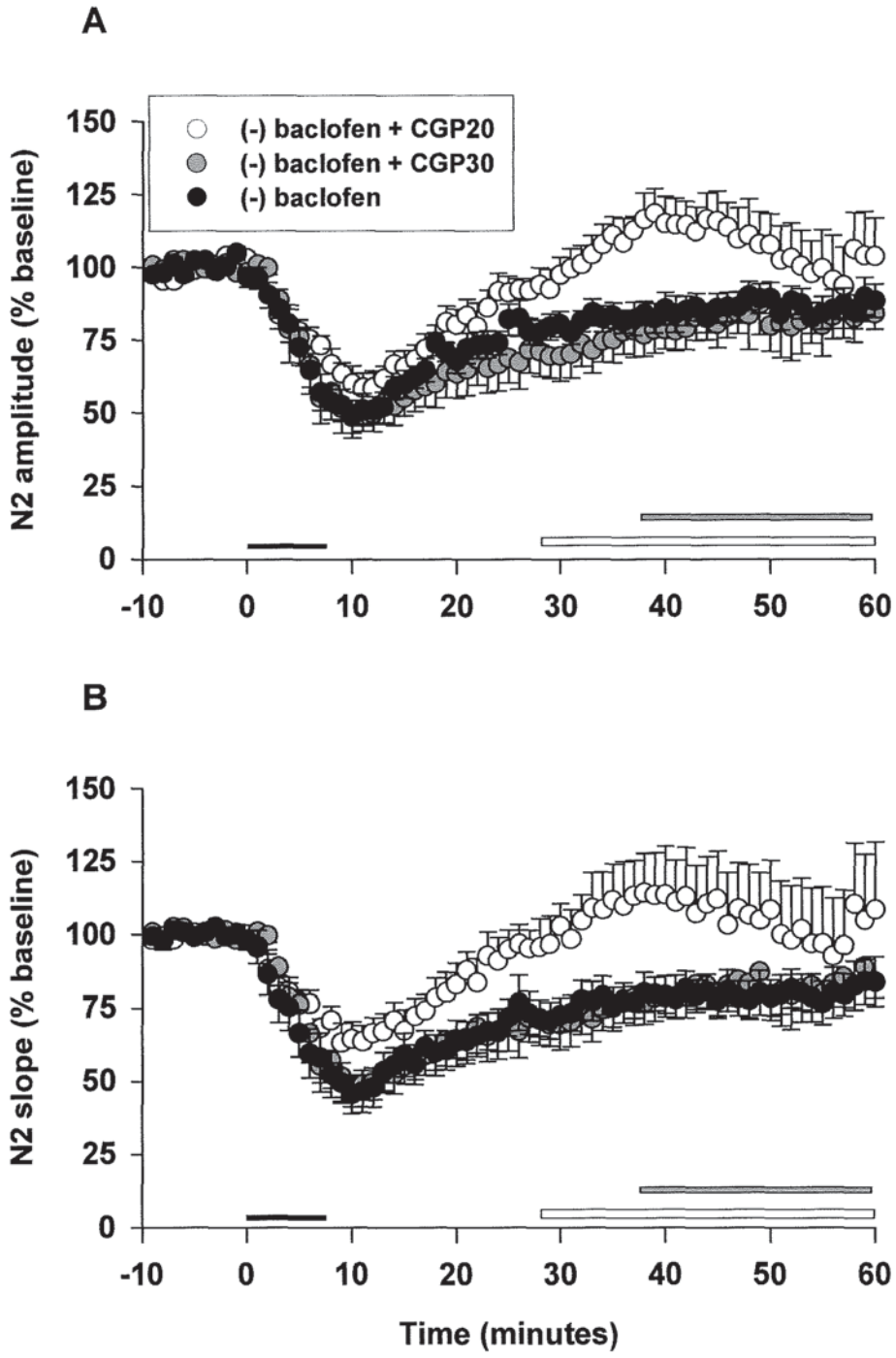

Figure 6.3.8 Effect of delayed applications of 1μM of the $GABA_B$ receptor antagonist CGP62349 on field potential responses after bath perfusion of 2μM (-) baclofen

Graphs A and B illustrate the FP N2 amplitude and slope respectively. Data are expressed as the mean % ± S.E.M. of 10 responses collected during a 10 minute baseline period. Black circles, (-) baclofen alone, N = 11 pathways taken from 9 recordings; white circles, CGP62349 applied after 20 minutes, N = 7 pathways taken from 4 recordings; grey circles, CGP62349 applied after 30 minutes , N = 7 pathways taken from 4 recordings. Horizontal black bar represents the application of 2μM (-)baclofen. The start of the applications of CGP62349 at 20 and 30 minutes after the perfusion of (-) baclofen are annotated with the white and grey horizontal bars, respectively.

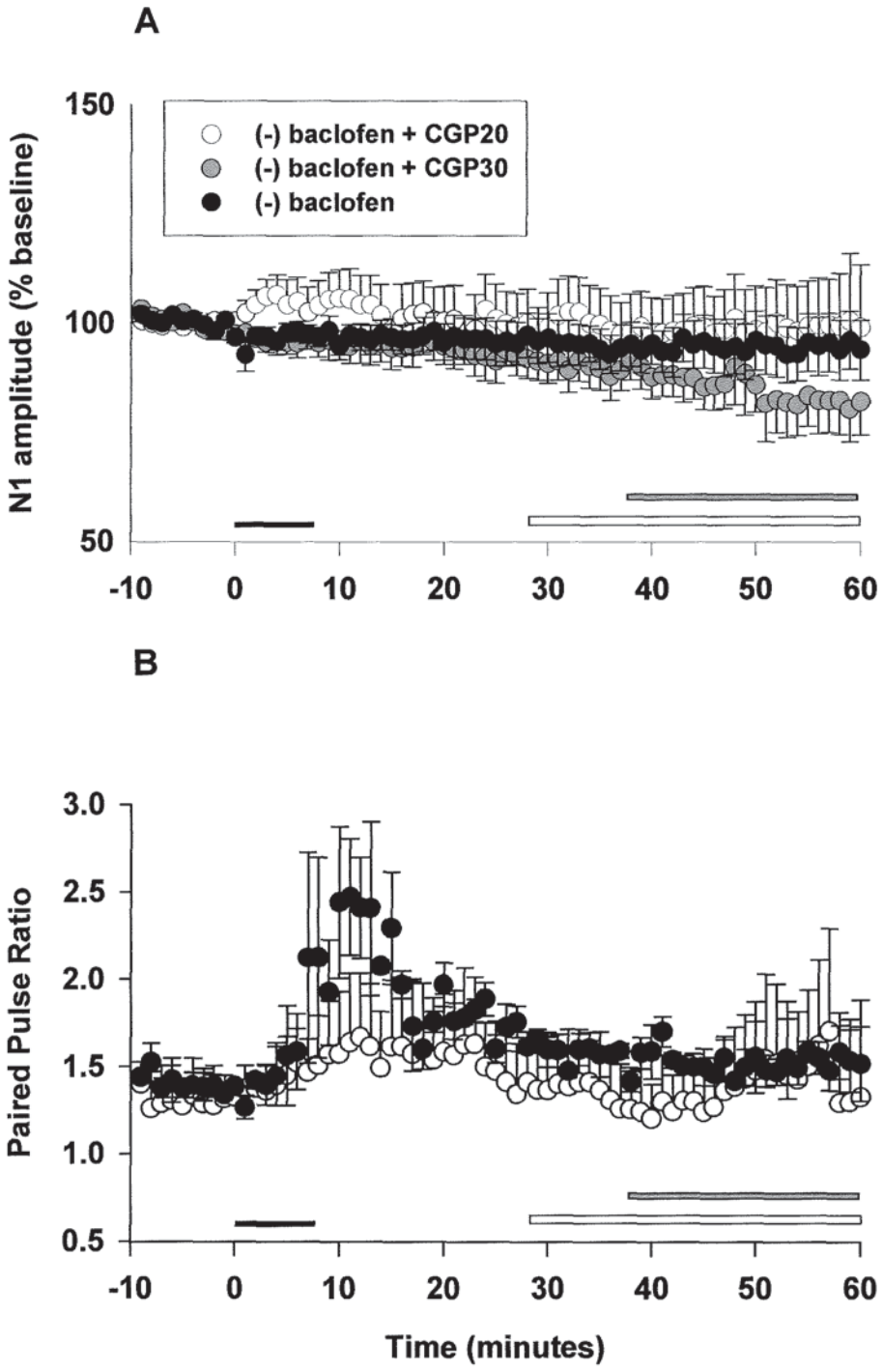

Figure 6.3.9 Effect of delayed applications of 1μM of the $GABA_B$ receptor antagonist CGP62349 on field potential responses after bath perfusion of 2μM (-) baclofen
Graphs A and B illustrate the FP N1 amplitude and the amplitude of the PPR respectively. Graphs are as shown in figure 6.3.7. PPR data was not collected for the experiment when CGP62349 was applied 30 minutes after the application of (-) baclofen.

6.3.4 EFFECT OF RAISED STIMULUS INTENSITY AND INCREASED FREQUENCY STIMULATION FOR 5 MINUTES IN SAGITTAL SLICES OF CEREBELLAR VERMIS IN THE PRESENCE OF THE $GABA_B$ RECEPTOR ANTAGONIST CGP62349

Once we had established that the concentrations of CGP62349 used were effective in blocking $GABA_B$Rs, the effect of $GABA_B$R blockade on synaptic plasticity following RSIF was examined. The effects of RSIF stimulation on FP responses in the presence of 1μM of the $GABA_B$R antagonist CGP62349 are shown in figure 6.3.11. There was no obvious change in the N2 or N1 components of the FP waveform in either pathway after stimulation for the remainder of the recording. The test and control pathway N2 amplitudes were not significantly different 35 minutes after stimulation 96.6 ± 4.6 and 101.5 ± 5.2 (N = 7 paired recordings, Wilcoxon Matched-Pairs test P>0.05), respectively. The incidences of LTD, LTP and no change 35 minutes after RSIF stimulation in drug-free ACSF and in the presence of CGP62349 are summarised in the pie charts in figure 6.3.11 below.

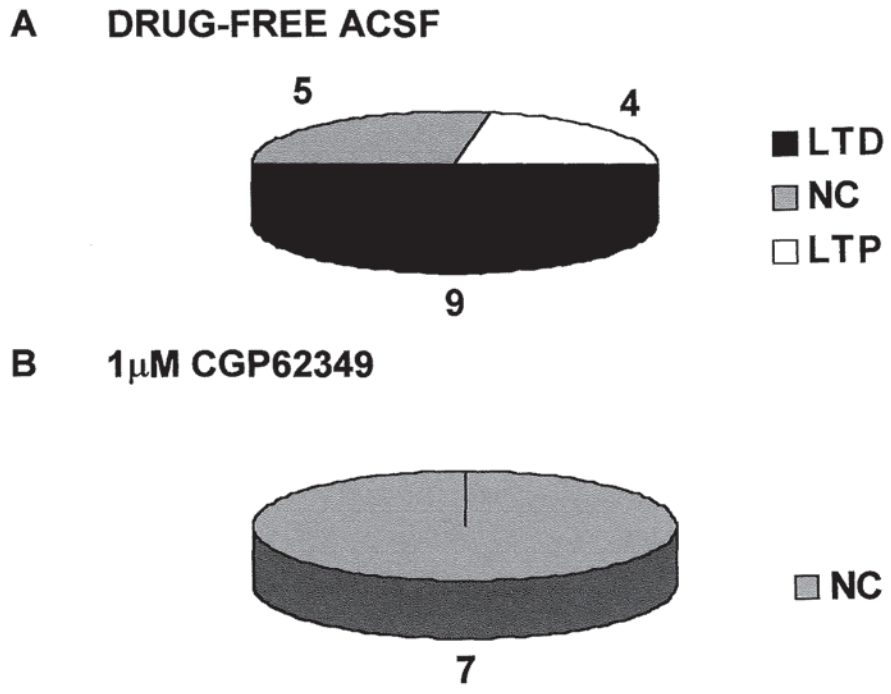

Figure 6.3.10 Effect of RSIF stimulation under control conditions or in the presence of the $GABA_B$ receptor antagonist 1μM CGP62349
Pie charts represent the incidence of LTD, LTP and no change in the test pathway N2 amplitude measured at 35 minutes after the stimulation period. Pie charts A and B show the effect of RSIF stimulation in drug-free ACSF and in the presence of 1μM CGP62349, respectively.

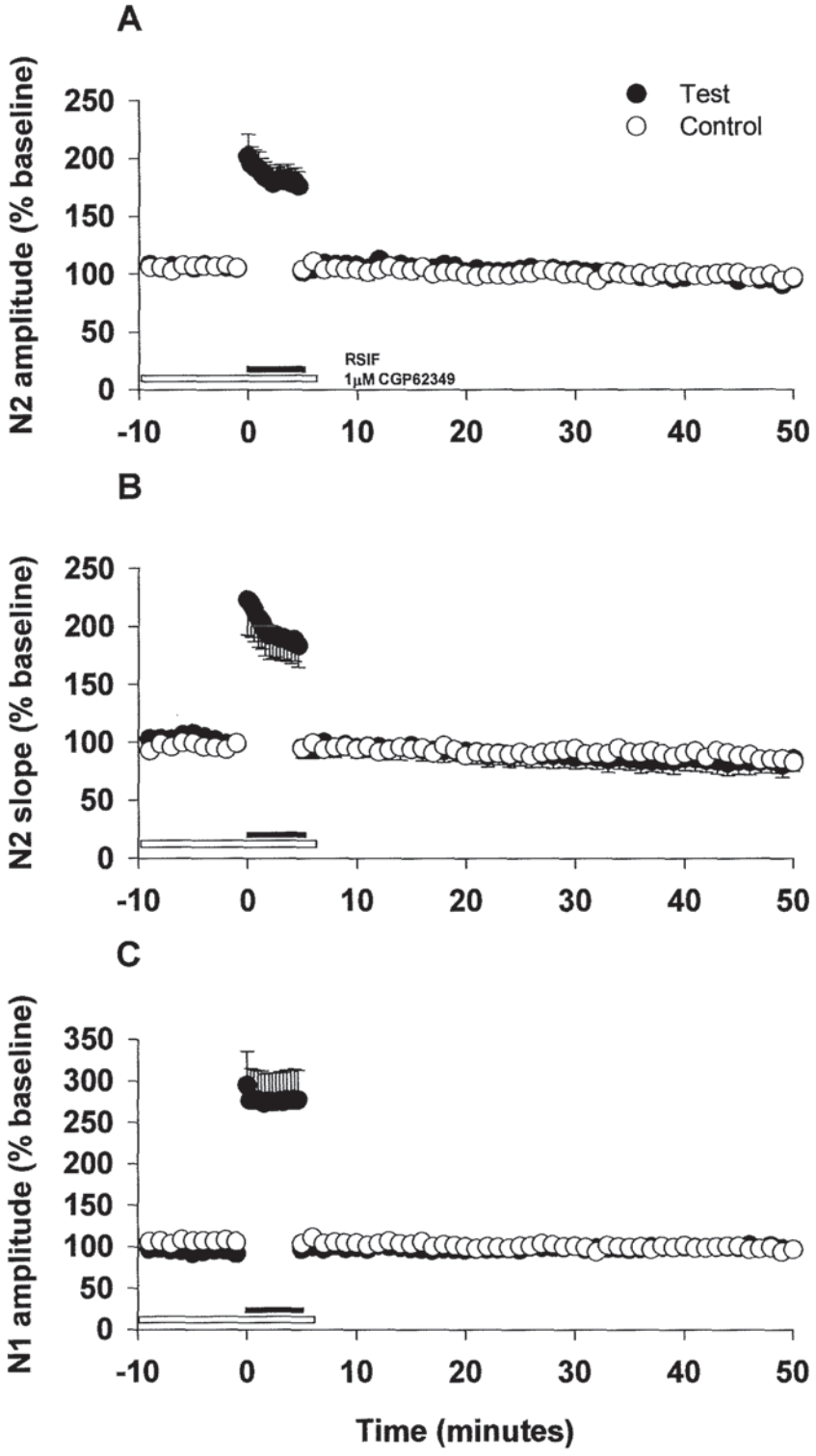

Figure 6.3.11 Effect of a 5 minute period of RSIF stimulation on field potential responses in the presence of the $GABA_B$ receptor antagonist 1μM CGP62349

Graphs A -C illustrate the FP N2 amplitude, slope and N1 amplitude, respectively. Data are expressed as the mean % ± S.E.M. of 10 responses collected during a 10 minute baseline period. N = 7 paired recordings. Closed circles, test pathway that underwent RSIF stimulation for 5 minutes; open circles, control pathway. Horizontal black bar indicates the period of RSIF stimulation. Horizontal white bar represents the application of 1μM CGP62349.

6.3.5 EFFECT OF RAISED FREQUENCY (RF) STIMULATION ON EXTRACELLULAR FIELD POTENTIAL RESPONSES IN THE PRESENCE OF THE $GABA_B$ RECEPTOR ANTAGONIST CGP62349

The effects of RF stimulation in the presence of 1μM CGP62349 are shown in figures 6.3.12 and 6.3.13. During stimulation the N2 and N1 components were briefly reduced in the test pathway. After RF stimulation there was an indication of a small increase in the N2 amplitude and slope in some recordings in the test pathway which was accompanied by a reduction in the amplitude of the PPR. This brief potentiation of the N2 component was not large enough to be classed as LTP. In the 8Hz pathway the brief potentiation in the N2 slope reached 115.9 ± 8.5 (N = 7) 5 minutes after stimulation. According to the criteria outlined in chapter 3 in section 3.3.2 the incidence of LTD, LTP and no change in the amplitude of the N2 component was observed 45 minutes after RF stimulation. In 3 recordings LTD was observed and in the remaining 4 cases there was no change. The 8Hz and 1Hz N2 amplitudes showed no significant difference 45 minutes after stimulation with levels of 86.3 ± 5.5 (N = 7) and 77.7 ± 9.7 (N = 5, Wilcoxon Matched-Pairs test $P>0.05$), respectively. In the 1Hz pathway no apparent change was noted in N1 after stimulation. The amplitude of the PPR was transiently reduced after stimulation and gradually returned to pre-stimulation levels.

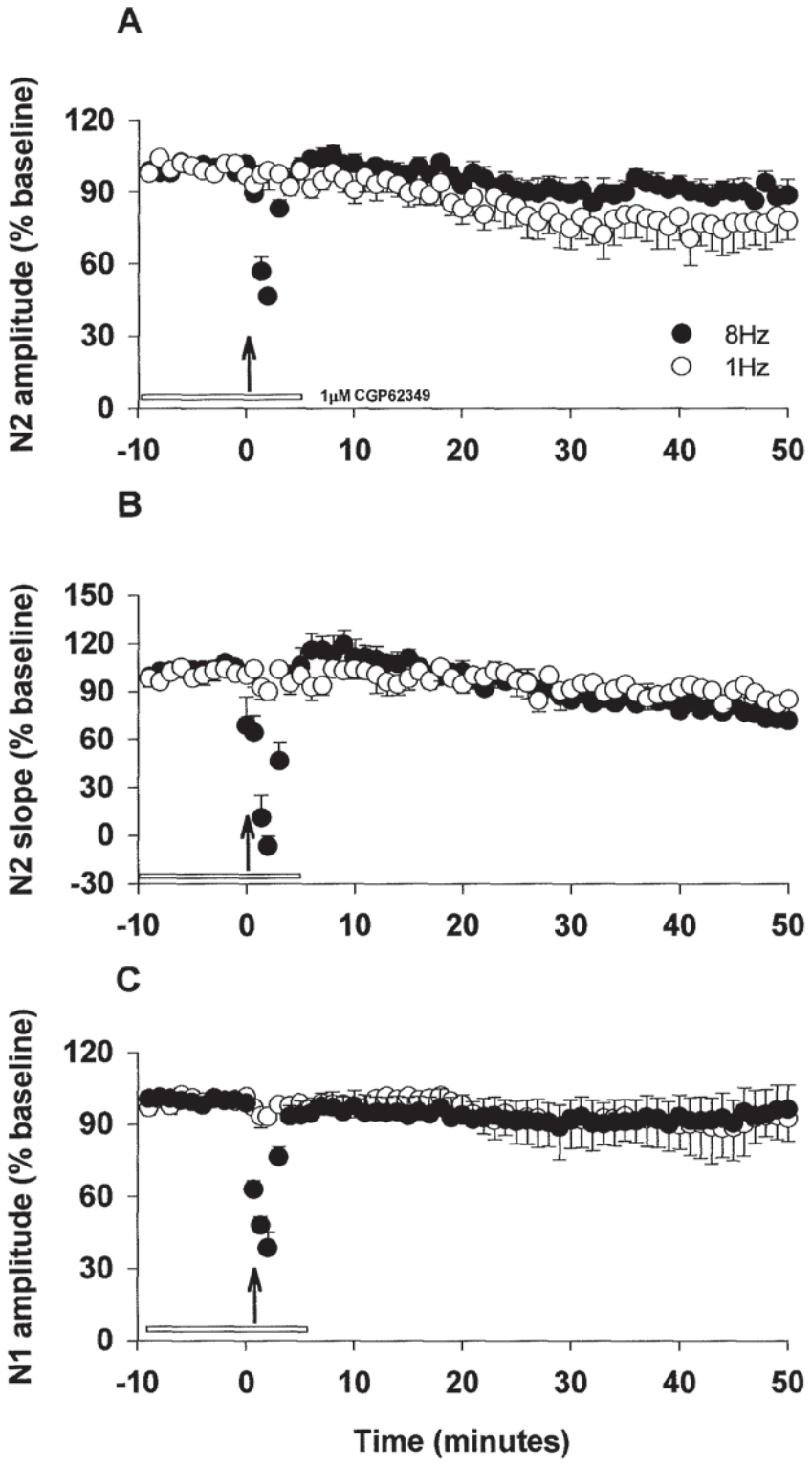

Figure 6.3.12 Effect of a 2 minute period of RF stimulation on field potential responses in the presence of the $GABA_B$ receptor antagonist 1μM CGP62349

Graphs A - C illustrate the FP N2 amplitude, N2 slope and N1 amplitude, respectively. Data are expressed as the mean % ± S.E.M. of 10 responses collected during a 10 minute baseline period. N = 4 paired recordings 7 pathways 8Hz, 5 pathways 1Hz. Closed circles, pathway stimulated at 8Hz for 2 minutes; open circles, pathway stimulated at 1Hz for 2 minutes. The arrow indicates the start of RF stimulation. Horizontal white bar represents the application of 1μM CGP62349.

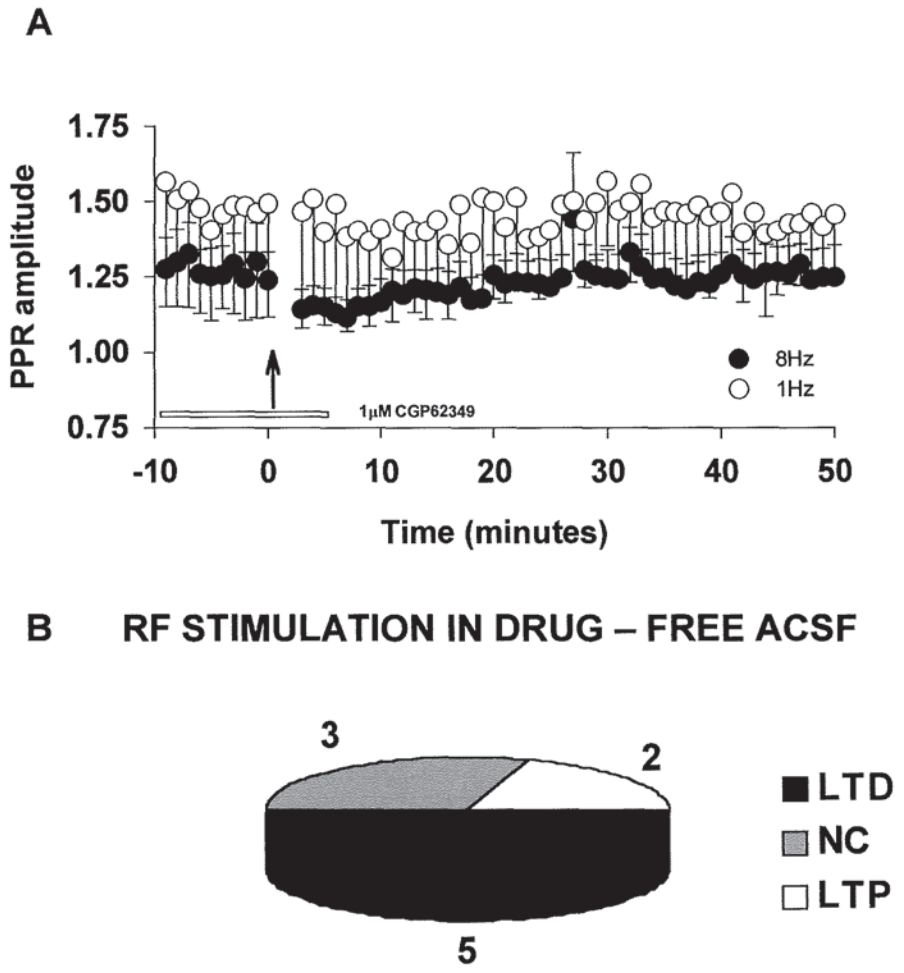

Figure 6.3.13 Effects of a 2 minute period of RF stimulation on field potential responses in the presence of the $GABA_B$ receptor antagonist 1μM CGP62349
Graph A illustrates the amplitude of the PPR. Data are expressed as the mean % ± S.E.M. of 10 responses collected during a 10 minute baseline period. N = 4 paired recordings, 7 pathways 8Hz, 5 pathways 1Hz. Closed circles, pathway stimulated at 8Hz for 2 minutes; open circles, pathway stimulated at 1Hz for 2 minutes. The arrow indicates the start of RF stimulation. Horizontal white bar represents the application of 1μM CGP62349. Pie charts B and C represent the incidences of LTD, LTP and no change in the 8Hz pathway 45 minutes after stimulation in drug-free ACSF and in the presence of CGP62349, respectively.

6.4 DISCUSSION

Consistent with previous reports (-) baclofen produced an acute depression of the N2 component of FP responses which partially recovered on washout. This depression was coincident with a partially reversible increase in the amplitude of the PPR. PF-EPSCs were also attenuated in the presence of (-) baclofen and were accompanied by an increase in the PPR which partially recovered on washout and an increase in the rate of decay of the PF-EPSCs. Together these data support earlier studies and indicate that the principle effects of baclofen on synaptic transmission are largely presynaptic (Bowery, 1993).

We found no clear evidence for tonic $GABA_BR$-mediated activity at PF-Purkinje cell synapses. CGP55845 and CGP62349 were effective at antagonising the activity of $GABA_BR$ at a concentration of 1μM but had no obvious effect on basal FP responses. Interestingly when CGP62349 was applied 20 minutes after application of (-) baclofen there was a faster recovery of the N2 component of FP responses and some indication that the response was actually above baseline levels. It is difficult to account for the difference in the extent of recovery of the FP responses when CGP62349 was applied 20 or 30 minutes after the end of the perfusion of baclofen. This discrepancy could relate to differences in the perfusion rate and the amount of time the drugs were in contact with the slice. However, it is likely that the long-term decrease in the N2 component of FPs that was noted after the application of (-) baclofen was simply due to incomplete washout of the agonist.

In chapter 3 RSIF stimulation was reported to induce an input-specific LTD of FP responses in 9/18 recordings. To investigate if the presence of an antagonist of $GABA_BR$ could modify the incidence or direction of synaptic plasticity. The RSIF stimulation method was repeated in the presence of 1μM CGP62349. In 7 recordings, no incidences of LTD were observed 35 minutes after RSIF stimulation. This data suggested that $GABA_BR$ could have a role in the induction of this form of input-specific LTD of FP responses. Inhibitory $GABA_BR$ are thought to modulate synaptic transmission by presynaptic inhibition of transmitter release or by an

increase in K^+ conductance triggering a hyperpolarisation and therefore a reduced excitability of the postsynaptic cells to excitatory neurotransmitter (Bowery, 1993).

In drug-free ACSF, a 2 minute period of 1 or 8Hz stimulation produced a slowly emerging depression in both test and control pathways within 45 minutes of stimulation in 50% of the FP recordings (chapter 5). The depression in the 8Hz pathway was more prominent than that seen in the 1Hz pathway. The effects of RF stimulation in the presence of 1μM CGP62349 were not conclusive. In the presence of the $GABA_BR$ antagonist in 3 recordings there was a LTD observed and in the remaining 4 recordings there was no change 45 minutes after stimulation.

In summary, the $GABA_BR$ agonist (-) baclofen produces an acute depression of the FPs evoked by molecular layer stimulation and of PF-EPSCs. The depression of FPs can be blocked by the perfusion of $GABA_BR$ antagonists CGP55845 and CGP62349. In drug-free ACSF a LTD of FP responses was induced in 50% of cases by either RSIF stimulation or RF stimulation. In the presence of CGP62349 there was some evidence that the number of incidences of LTD was reduced. This was particularly noticeable in the RSIF experiments where there were no incidences of LTD out of the total group of 7 recordings. These findings indicate that activating $GABA_BR$ might not only influence the strength of synaptic transmission at PF to Purkinje cell synapses but they may also serve a role in plasticity. Further experiments are necessary to investigate this possibility.

CHAPTER 7

GENERAL DISCUSSION

The initial aim of this PhD project was to set-up an *in vitro* extracellular system for recording population responses from the Purkinje cell layer in slices of cerebellar vermis. The intention was to characterise and identify the components of FP waveforms that were evoked by activation of the molecular layer. The challenge then was to use this electrophysiological technique to investigate what conditions were necessary to induce long-term alterations in the strength of transmission at the synapse between Purkinje cells and PFs. Initially the experiments focused on determining which parameters of stimulation could lead to LTD. Data from these studies in turn suggested that under certain conditions LTD could mask an underlying potentiation. This therefore led to an investigation into the synaptic conditions required for cerebellar form LTP.

Sagittal or transverse slices of cerebellar vermis were prepared from the brains of 14-21 day old male Wistar rats for the purpose of recording extracellular FP responses from the cerebellar molecular layer. In chapter 2 the activation of the molecular layer was found to evoke FP responses with two characteristic negative-going components that were termed N2 and N1. The properties of these FP responses were consistent with responses that were mediated by PF stimulation and shared properties with PF-mediated EPSCs (Konnerth et al., 1990). The FP responses were smoothly graded with stimulus intensity and the second response to paired pulses delivered at 40ms intervals was facilitated. Unfortunately because the experiments with 3-AP in sagittal slices proved unsuccessful we were unable to completely eliminate the possibility that there could be a CF contribution to the FP responses.

The sodium channel blocker TTX and the AMPA receptor antagonist CNQX were used to examine the synaptic contributions to the N2 and N1 components of the FP waveforms in the

sagittal slice preparation. TTX was found to block both the N1 and N2 components, the N2 component was additionally sensitive to CNQX. This data indicated that the N1 component of the waveform related to the PF volley and the N2 component related to the synaptic excitation of AMPA receptors at PF to Purkinje cell synapses. The waveform of the FPs was similar to the monosynaptic population responses previously described by Chen & Thompson, 1995 and more recently by Salin *et al.,* 1996. The waveforms showed some similarities to the FPs interpreted by Eccles *et al.,* 1967 but had fewer components because molecular layer stimulation activated solely PF to Purkinje cell synapses and not the mossy fibre to granule cell synapse as well.

Control experiments were made in sagittal slices to confirm that the N2 and N1 components of FP responses could be recorded for 1 hour and to check that paired stimuli delivered at 40ms intervals did not affect the baseline stability. In chapter 3 the stability of the system was established and then attempts were made to induce a LTD of the FP responses evoked by molecular layer stimulation. Strong activation of PFs was previously reported to be sufficient to induce a LTD of PF-EPSPs (Hartell, 1996b). Based on this finding the frequency of molecular layer activation and the stimulus intensity were systematically altered to determine if similar parameters of stimulation could also produce a long-term attenuation of cerebellar FPs.

Firstly the frequency of activation of the molecular layer was increased from 0.2 to 1Hz for 5 minutes. In separate experiments the stimulus intensity was raised to approximately 50% above the baseline stimulus level for 5 minutes. Neither of these parameters was sufficient to induce a robust LTD of the N2 component of FPs but when they were combined an input-specific LTD was observed in 50% of FP recordings. This LTD was not associated with a long-term decrease in the N1 component. There was a transient reduction in the PPR but this was only apparent during the RSIF paradigm. This observation suggested that the mechanism for this form of LTD was entirely postsynaptic. In the remaining 50% of the recordings there was a near equal split of incidences of LTP or no change. Therefore, the combined RS and IF parameters could provide the necessary elements for LTD. However,

clearly the RSIF did not always produce the optimal conditions for LTD since only 50% of the recordings were depressed.

The RSIF stimulation method was also repeated in transverse slices and was found to induce LTD in the N2 component more successfully. This effect was most prominently detected as a change in the slope of the N2 component. We speculate that there could be a difference in the nature of the synaptic contacts between PF and Purkinje cells. The extent of NO release, Ca^{2+} release and mGluR and AMPAR activation initiated by molecular layer stimulation may not be the same in transverse and sagittal slices.

The inability to induce LTD in 100% of recordings in either type of slice preparation could relate to the sources of variation that are inherent in this FP recording technique. It is known that certain parameters of PF stimulation can induce localised increases in Ca^{2+} (Eilers et al., 1995; Hartell, 1996b; Eilers et al., 1997b). A number of reports have also indicated that raising the frequency of molecular layer activation can increase the release of NO (Shibuki and Kimura, 1997; Kimura et al., 1998). It is probable that the amount of NO release and the level of Ca^{2+} influx initiated by stimulation of the molecular layer will be sensitive to the extent of PF activation. Therefore the stimulus intensity and size of the FP at the start of the experiment and during the period of RSIF stimulation could influence the probability of inducing LTD.

A number of studies have already concentrated on establishing that AMPAR activation (Linden et al., 1993; Batchelor et al., 1994; Hemart et al., 1995), mGluR activation (Linden and Connor, 1991; Shigemoto et al., 1994; Conquet et al., 1994; Aiba et al., 1994; Hartell, 1994b; DeZeeuw et al., 1998) and an influx of Ca^{2+} through voltage-gated ion channels (Crepel and Krupa, 1988; Sakurai, 1990; Konnerth et al., 1990; Linden et al., 1991; Shibuki and Okada, 1992a; Kasono and Hirano, 1994) are necessary for the induction of LTD. It was not feasible to investigate what effect buffering calcium levels might have on the induction of this extracellular form of LTD. Inclusion of a Ca^{2+} chelator into the ACSF would disturb the cerebellar slice by preventing calcium-dependent neurotransmitter release. Therefore it was decided to concentrate on looking at the possible involvement of the cGMP

cell-signalling cascade in the induction of LTD in this extracellular FP model. Support for a role for NO/cGMP/PKG signalling in the induction of LTD is controversial but it has been reported in a number of laboratories (Shibuki and Okada, 1991; Ito and Karachot, 1992; Daniel et al., 1993; Hartell, 1994a; Hartell, 1996a).

Three compounds were used to investigate the possible role of cGMP signalling in the form of LTD that was induced in 50% of FP responses by RSIF stimulation in chapter 4. At 35 minutes after RSIF stimulation the incidences of LTD, LTP and no change in the amplitude of the N2 component of FP responses were recorded and expressed in the form of pie charts. These comparisons were certainly an indication that in the presence of 7-NI, ODQ or KT5823 there were fewer incidences of LTD after RSIF stimulation when compared to drug-free ACSF. In addition there was an indication that blocking the cGMP signalling process through inhibition of NOS, GC or PKG could reveal an underlying potentiation. This effect was most apparent when the RSIF stimulation paradigm was applied in the presence of ODQ or KT5823. This observation raised the possibility that cGMP activity might normally mask the effects of cAMP and therefore cAMP-mediated actions would become more prominent under conditions of reduced cGMP activity. Fewer incidences of LTD were observed when the RSIF method of molecular layer activation was repeated in the presence of 7-NI in transverse slices.

The inhibitors were only applied before and during the stimulation period. The interpretation of these results could therefore be criticised because there is the chance that the washout of the drugs might have affected the FP waveforms. It is not possible to be sure how long the drugs are likely to take to washout of the brain slice, therefore, we do not know if this is an issue or not. To eliminate the possibility that the results were merely an artefact of washout perhaps in future experiments the inhibitors could be applied for a longer period. Longer applications of the drugs would have made it possible to observe the effect of NOS, GC or PKG inhibition on the maintenance as well as the induction of LTD. However, the data did suggest that these enzymes may be important for the form of LTD that was observed in 50% of FPs in this extracellular model.

In separate experiments in chapter 4 the hypothesis that an increase in the level of available NO or cGMP paired with stimulation of the molecular layer at a raised frequency could provide the conditions for the induction of LTD in sagittal slices was investigated. When paired with IF stimulation both SNP and 8-Br-cGMP produced an acute depression of the N2 and N1 components of the FP responses in sagittal slices. This effect began at the start of IF stimulation. After the application of SNP a more sustained reduction in the N2 amplitude was apparent in 4 out of 9 recordings 25 minutes after IF stimulation. A long-lasting depression was observed in 1 out of 6 recordings after perfusion with 8-Br-cGMP.

Preventing the breakdown of cGMP by the application of the cGMP-specific type V PDE inhibitor UK 114 542-27 produced an acute depression. In over 50% of recordings a long-term attenuation of the FP responses emerged within 25 minutes of IF molecular layer activation. Inhibition of NOS by 7-NI prevented both the acute and long-lasting depression of the FP responses. Under these conditions a potentiation was evident.

In chapter 5 the nature of the synaptic plasticity that followed a period of raised frequency molecular layer stimulation was investigated in both sagittal and transverse slices. In cerebellar slices cut in a sagittal orientation BRF activation was not sufficient to induce a change in the strength of PF to Purkinje cell synaptic transmission. However, when the period of 8Hz activation was increased to 2 minutes in these slices LTD was observed in 50% of recordings within 45 minutes. This observation showed similarities to the findings of (Schreurs and Alkon, 1993) namely that the activation of PFs alone at a raised frequency could induce LTD. In contrast in transverse slices RF stimulation induced a clear LTP of the 8Hz pathway within 30 minutes. Some potentiation was also apparent in the 1Hz pathway. The potentiation was accompanied by an increase in N1 and a reduction of the amplitude of the PPR. These findings were in agreement with the reports that RF activation of the molecular layer can induce a LTP of FP responses (Salin et al., 1996).

Similar results to those described in chapter 4 were obtained when the RF stimulation paradigm was repeated during the bath application of 7-NI, ODQ and KT5823. The inhibition of NOS, GC or PKG paired with RF stimulation led to fewer cases of the slowly emerging

LTD than in drug-free ACSF and an underlying LTP also emerged. As has already been mentioned, in hindsight it would perhaps have been more sensible to apply the inhibitors for the duration of the recordings to rule out the idea that the washout of the drugs affected the FP responses.

Inhibition of cGMP signalling consistently revealed a potentiation suggesting that there might be an interaction between cGMP and cAMP. Type IV and V PDEs are reported to be specific for the breakdown of cAMP and cGMP, respectively. There are thought to be 20 or more other PDE isozymes that catalyse the breakdown of cyclic nucleotides, therefore there is the possibility that another cGMP-stimulated PDE isozyme could exist (Beavo, 1988). The hydrolysis of cAMP might be catalysed by a PDE that is stimulated by cGMP activity. This could be the mechanism for how cAMP signalling can predominate when NOS, GC or PKG, and hence cGMP signalling is inhibited. Figure 7.1.1C suggests how the binding of cGMP to an allosteric site on the cGMP-stimulated PDE molecule might enhance the probability of cAMP hydrolysis. Whether or not the cAMP-specific type IV PDEs in addition to cGMP-stimulated PDEs catalyse the hydrolysis of cAMP is unknown. The nature of the interaction between the different PDEs remains to be established.

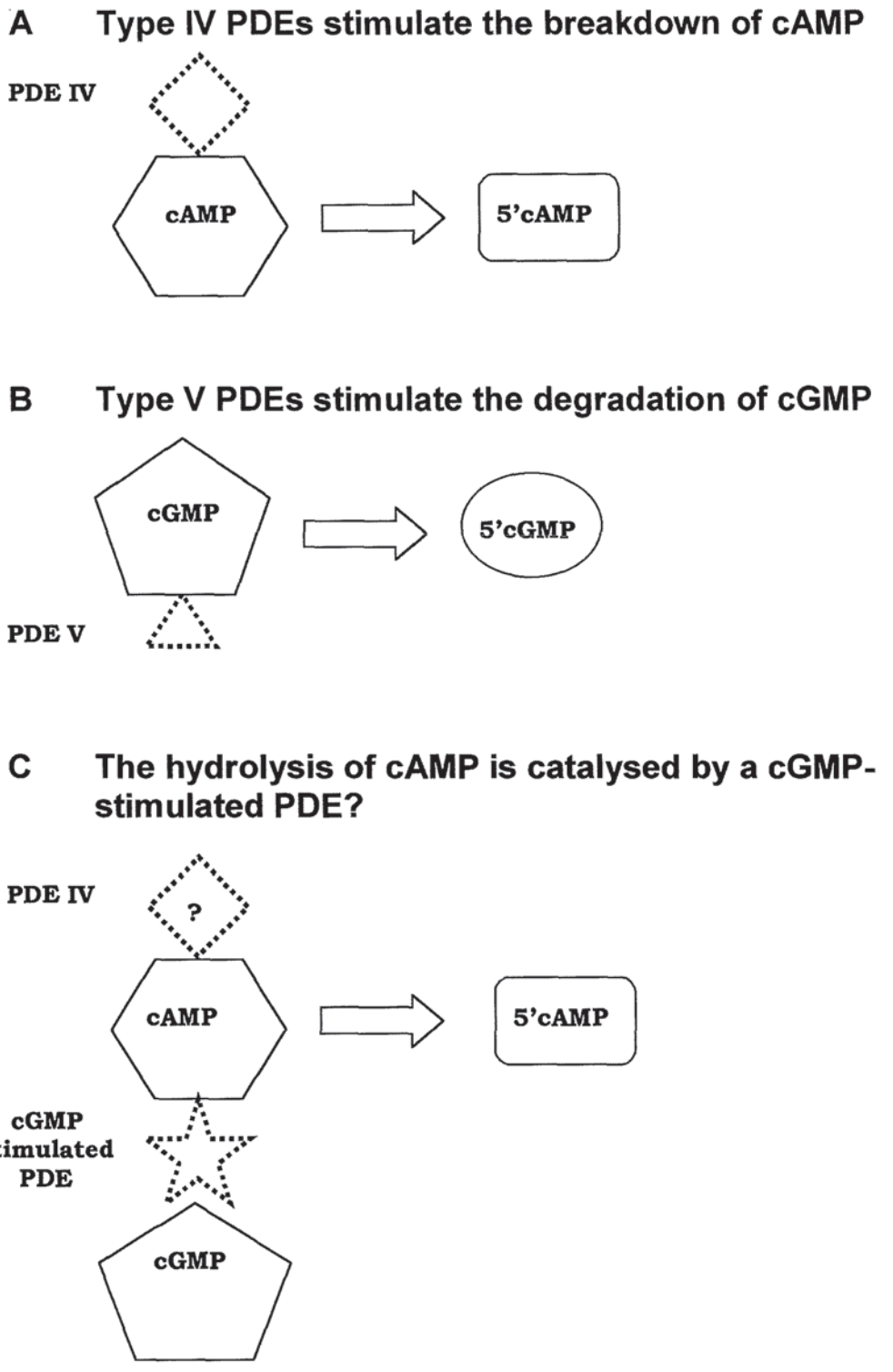

Figure 7.1.1 An illustration of the possible interaction between cGMP and the phosphodiesterases responsible for the breakdown of cAMP

Diagrams A and B represent the breakdown of cAMP (hexagon) to 5'AMP (rectangle) by type IV cAMP-specific PDEs (diamond) and the conversion of cGMP (pentagon) to 5'GMP (oval) by cGMP-specific type V PDEs (triangle), respectively. Diagram C suggests how a cGMP-stimulated PDE isozyme (star) could promote the hydrolysis of cAMP. Shapes with the dotted lines relate to PDEs and those with solid lines are the cyclic nucleotides and their breakdown products.

We discovered that if an inhibitor of cAMP breakdown was applied during the RF stimulation paradigm in sagittal slices it was then possible to induce a clear input-specific LTP of FP responses. This enhancement was comparable to the presynaptic cAMP-mediated potentiation that was reported in FP recordings following brief repetitive stimulation of the molecular layer (Salin et al., 1996). In summary, by modifying the conditions under which RF stimulation was performed it was possible to induce LTD or LTP. This data supports the theory that the induction of LTD depends on the level of cGMP and that raised cAMP levels are necessary for LTP. In addition it is likely that the activity of cGMP and cAMP-specific phosphodiesterases responsible for the breakdown of the two cyclic nucleotides might be crucially important in determining the direction of plasticity.

The LTP of the N2 and N1 components of the FP waveforms and the decrease of the amplitude of the PPR that was observed in transverse slices in drug-free ACSF was no longer apparent in the presence of H-89 or 7-NI to inhibit PKA or NO, respectively. Firstly these observations confirmed those findings of (Salin et al., 1996), namely that a presynaptic cAMP-mediated form of LTP could be produced in FPs by RF stimulation. Secondly the data raised the possibility that NO might also be required for the induction of LTP in the cerebellar cortex.

$GABA_BR$ have been localised in the cerebellar molecular layer (Wilkin et al., 1981). It was reported that $GABA_BR$ mediated potentials could be recorded at the synapse between PF and Purkinje cells in biplanar slices of cerebellar vermis (Batchelor and Garthwaite, 1992). These discoveries raise the possibility that the activation of $GABA_BR$ could influence the plasticity at these synapses. In chapter 6 a limited number of experiments were performed to examine the actions of the $GABA_BR$ agonist (-) baclofen and its inactive isomer (+) baclofen on FP responses. The effect of (-) baclofen on PF-EPSCs was also examined. These experiments confirmed the effects of baclofen on synaptic transmission that have already been established (Bowery, 1993). After the period of (-) baclofen application a residual depression of FP responses remained. Delayed applications of the $GABA_BR$ antagonist CGP62349 indicated that this depression could be accounted for by incomplete washout of (-) baclofen.

In separate experiments the RSIF paradigm was repeated in the presence of 1μM CGP62349. In all 7 experiments there were no incidences of LTD following RSIF activation of the molecular layer. This observation raised the possibility that the LTD that was observed in 50% of FP responses in drug-free ACSF might involve $GABA_BR$ activation. In contrast the induction of a slowly emerging LTD did not appear to be dramatically altered by RF stimulation in the presence of the $GABA_BR$ antagonist. More studies are necessary to investigate more fully the possible role of $GABA_BR$ in the induction of LTD of FP responses.

The extracellular FP recording technique was performed to observe the concerted behaviour of populations of Purkinje cells. As outlined in chapter 2 extracellular electrophysiological recording has a number of advantages over whole cell patch-clamp methods. To a certain extent it was a benefit that the technique was non-invasive to the cells. However, because it was not possible to inject drugs into the Purkinje cells via a patch pipette sometimes the choice of inhibitors was limited because cell permeable compounds had to be chosen. In addition from a practical point of view it proved to be quite expensive to bath perfuse drugs.

Positive aspects of this PhD research were that an extracellular FP recording system was set-up and the waveforms of the population responses evoked by stimulation of the molecular layer were successfully characterised. The system was sufficiently sensitive to be able to detect long-term alterations in the FP waveforms. Furthermore it was possible to modify the parameters of stimulation in favour of the induction of either LTD or LTP. A number of difficulties were encountered in trying to induce LTD in this extracellular FP recording system however it was possible to induce LTD of the N2 component in 50% of FP responses by:-

i) RSIF stimulation in sagittal or transverse slices

ii) RF molecular layer activation in sagittal slices or

iii) IF stimulation paired with the application of an inhibitor of cGMP-specific type V PDEs in the sagittal slice preparation.

Therefore this research supports the hypothesis that PF activation alone can satisfy the requirements for LTD (Eilers et al., 1995; DeSchutter, 1995; Hartell, 1996b; Eilers et al., 1997b). However, we cannot be entirely sure that only PFs were activated.

In addition a LTP of the N2 component of FP responses was demonstrated in the transverse slice preparation following RF stimulation. This potentiation was associated with an increase in the amplitude of N1 and a decrease in the amplitude of the PPR. In the slices of cerebellar vermis cut in a sagittal orientation it was also possible to produce LTP by RF stimulation but only when cAMP degradation was prevented by the inhibition of cAMP-specific PDEs. An increase in N1 and a reduction in the amplitude of the PPR was also evident in these experiments. These data strengthen the idea that LTP in the cerebellar cortex requires cAMP and is presynaptically mediated (Salin et al., 1996; Kimura et al., 1998).

The preliminary finding that RSIF stimulation failed to produce any incidences of LTD in the presence of a $GABA_BR$ antagonist suggested that $GABA_BR$ might in some way contribute to the transmission at PF to Purkinje cell synapses. In future experiments it would be interesting to:-

i) investigate further the possible interaction between cGMP and cAMP and the mechanism for the hydrolysis of these cyclic nucleotides by PDEs

ii) bath perfuse the mGluR or AMPAR antagonists MCPG or CNQX, respectively during RSIF or RF stimulation to examine the possible role of mGluR and AMPAR in the induction and maintenance of this extracellular form of LTD

iii) to investigate more fully the nature of the synaptic plasticity evoked by RSIF and RF stimulation in transverse slices of cerebellar vermis

iv) to utilise specific inhibitors to establish if protein tyrosine kinase (Boxall et al., 1996b) or phospholipase A_2 for which roles in cerebellar LTD have been proposed are necessary for the induction of LTD in an extracellular model (Linden, 1995).

v) to discover if $GABA_BR$ influence the direction or extent of the synaptic plasticity in the cerebellar cortex

An illustration of the synaptic events that may be necessary for the LTD observed in this extracellular FP recording system is proposed in figure 7.1.2. Some of the experiments outlined above would help to confirm or challenge this mechanism.

Adaption of the VOR is thought to represent a form of motor learning (Ito, 1982; DuLac et al., 1995; Lisberger, 1998). Behavioural responses to head movement have been shown to exhibit short and long-term plasticity (DuLac et al., 1995). The expression of an inhibitor of PKC in Purkinje cells was found to block the adaption of the VOR and cerebellar LTD (DeZeeuw et al., 1998). In the cerebellum the induction of LTD was disturbed and EBC was impaired in GFAP mutant mice (Shibuki et al., 1996). In addition motor co-ordination and LTD in the cerebellum were also disrupted in GluRδ2 mutant mice (Kashiwabuchi et al., 1995). The findings of this PhD research are another step towards a greater understanding of how alterations in synaptic efficacy at PF to Purkinje cell synapses might underlie learning and memory processes.

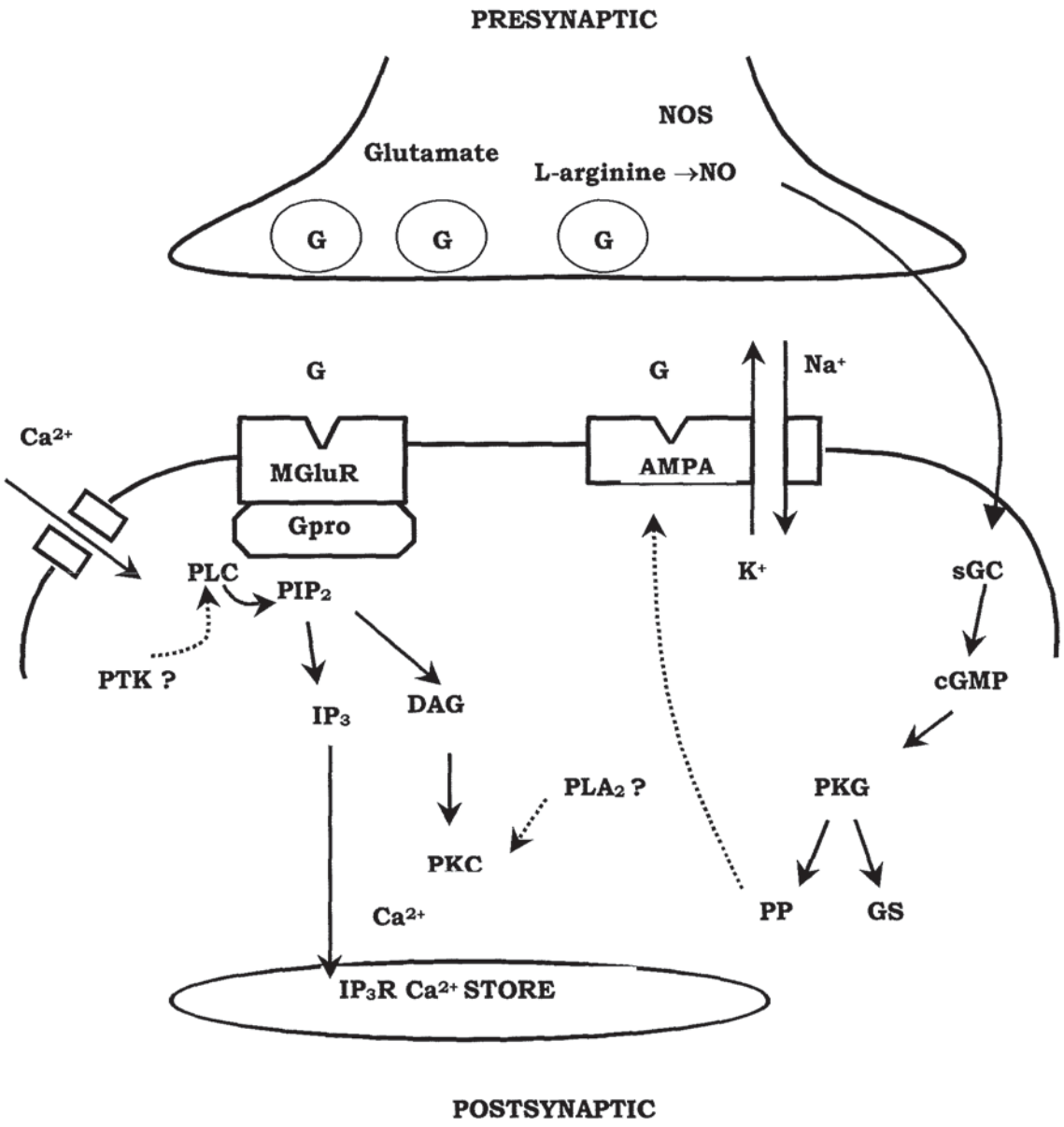

Figure 7.1.2 A possible mechanism for the induction of LTD in an extracellular field potential recording model

The diagram represents the three basic requirements for LTD: a rise in Ca^{2+} influx through voltage gated Ca^{2+} channels and release from intracellular stores triggered by the activation of AMPAR and mGluR, respectively. Activation of PIP_2 by PLC generates the second messenger molecules IP_3 and DAG. IP_3 and DAG are thought to initiate Ca^{2+} release from intracellular stores and activation of PKC, respectively. Also shown is the mechanism by which cGMP signalling might contribute to the induction of LTD. NO release could be triggered by activation of the cerebellar molecular layer. NO stimulates cGMP via GC. cGMP in turn activates PKG. PP stimulated by PKG would influence the extent of AMPAR phosphorylation. PTK and PLA_2 may also be important for LTD via interactions with PKC and PLC, respectively.

REFERENCE LIST

Ahn, S., Ginty, D.D., and Linden, D.J. (1999). A late phase of cerebellar long-term depression requires activation of CaMKIV and CREB. Neuron *23*, 559-568.

Aiba, A., Kano, M., Chen, C., Stanton, M.E., Fox, G.D., Herrup, K., Zwingman, T.A., and Tonegawa, S. (1994). Deficient cerebellar long-term depression and impaired motor learning in mGluR1 mutant mice. Cell *79*, 377-388.

Ajima, A. and Ito, M. (1995). A unique role of protein phosphatase in cerebellar long-term depression. NeuroReport *6*, 297-300.

Alberts, B., Bray, D., Lewis, J., Raff, M., Roberts, K., and Watson, J.D. (1994). Molecular Biology of the Cell (New York: Garland Publishing, Inc).

Albus, J.S. (1971). A theory of cerebellar function. Math.Biosci. *28*, 167-171.

Anderson, W.W. and Collingridge, G.L. (1999). A data acquisition program for on-line analysis of long-term potentiation and long-term depression. Soc.Neurosci.Abstr *23*, 665

Andersson, G. and Oscarsson, O. (1978). Climbing fiber microzones in cerebellar vermis and their projection to different groups of cells in the lateral vestibular nucleus. Exp.Brain Res. *32*, 565-579.

Ariano, M.A., Lewicki, J.A., Brandwein, H.J., and Murad, F. (1982). Immunohistochemical localization of guanylate cyclase within neurons of rat brain. Proc.Natl.Acad.Sci.USA *79*, 1316-1320.

Babbedge, R.C., Blandward, P.A., Hart, S.L., and Moore, P.K. (1993). Inhibition of rat cerebellar nitric oxide synthase by 7-nitro indazole and related substituted indazoles. Brit.J.Pharmacol. *110*, 225-228.

Bandle, E. and Guidotti, A. (1978). Studies on the cell location of cyclic 3',5'-guanosine monophosphate. Brain Res. *156*, 412-416.

Batchelor, A.M. and Garthwaite, J. (1992). GABA(B) receptors in the parallel fiber pathway of rat cerebellum. Eur.J.Neurosci. *4*, 1059-1064.

Batchelor, A.M. and Garthwaite, J. (1993). Novel synaptic potentials in cerebellar Purkinje cells; probable mediation by metabotropic glutamate receptors. Neuropharm. *32*, 44136-44136.

Batchelor, A.M., Madge, D.J., and Garthwaite, J. (1994). Synaptic activation of metabotropic glutamate receptors in the parallel fibre-Purkinje cell pathway in rat cerebellar slices. Neurosci. *63*, 911-915.

Baude, A., Molnar, E., Latawiek, D., McIlhinney, and Somogyi, P. (1994). Synaptic and nonsynaptic localization of the GluR1 subunit of the AMPA-type excitatory amino acid receptor in the rat cerebellum. J.Neurosci. *14*, 2830-2843.

Baude, A., Nusser, Z., Roberts, J.D.B., Mulvihill, E., McIlhinney, R.A.J., and Somogyi, P. (1993). The metabotropic glutamate receptor (mGluR1a) is concentrated at perisynaptic membrane of neuronal subpopulations as detected by immunogold reaction. Neuron *11*, 771-787.

Beavo, J.A. (1988). Multiple isozymes of cyclic nucleotide phosphodiesterase. Adv.Second Messenger Phosphoprotein Res. *22*, 1-38.

Bladen, C., Loewen, D., and Vincent, S.R. (1996). Autoradiographic localization of [3H]-cyclic GMP binding sites in the rat brain. J.Chem.Neuroanat. *10*, 287-293.

Bliss, T.V.P. and Collingridge, G.L. (1993). A synaptic model of memory: long term potentiation in the hippocampus. Nature *361*, 31-39.

Bliss, T.V.P. and Lomo, T. (1973). Long-lasting potentiation of synaptic transmission in the dentate area of the anaesthetized rabbit following stimulation of the perforant path. J.Physiol.(Lond.) *232*, 331-356.

Blond, O., Daniel, H., Otani, S., Jaillard, D., and Crepel, F. (1997). Presynaptic and postsynaptic effects of nitric oxide donors at synapses between parallel fibres and Purkinje cells: Involvement in cerebellar long-term depression. Neurosci. *77*, 945-954.

Bowery, N.G. (1993). GABA(B) receptor pharmacology. Ann.Rev.Pharmacol.Toxicol. *33*, 109-147.

Bowery, N.G., Doble, A., Hill, D.R., Hudson, A.L., Shaw, J.S., Turnbull, M.J., and Warrington, R. (1981). Bicuculline-insensitive GABA receptors on peripheral autonomic nerve-terminals. Eur.J.Pharm. *71*, 53-70.

Bowery, N.G. and Pratt, G.D. (1992). GABA(B) Receptors as targets for drug-action. Drug Res. *42-1*, 215-223.

Boxall, A.R. and Garthwaite, J. (1996a). Long-term depression in rat cerebellum requires both NO synthase and NO-sensitive guanylyl cyclase. Eur.J.Neurosci. *8*, 2209-2212.

Boxall, A.R., Lancaster, B., and Garthwaite, J. (1996b). Tyrosine kinase is required for long-term depression in the cerebellum. Neuron *16*, 805-813.

Bramham, C.R., Alkon, D.L., and Lester, D.S. (1994). Arachidonic acid and diacylglycerol act synergistically through protein kinase C to persistently enhance synaptic transmission in the hippocampus. Neurosci. *603*, 737-743.

Bredt, D.S., Hwang, P.M., and Snyder, S.H. (1990). Localization of nitric oxide synthase indicating a neural role for nitric oxide. Nature *347*, 3768-3770.

Brenowitz, S., David, J., and Trussell, L. (1998). Enhancement of synaptic efficacy by presynaptic GABA(B) receptors. Neuron *20*, 135-141.

Brown, T.H., Kairiss, E.W., and Keenan, C.L. (1990). Hebbian synapses: Biophysical mechanisms and algorithms. Annu Rev.Neurosci. *13*, 475-511.

Butler, A.R., Flitney, F.W., and Williams, D.H. (1995). NO, nitrosonium ions, nitroxide ions, nitrosothiols and iron- nitrosyls in biology - a chemists perspective. Trends Pharmacol.Sci. *16*, 18-22.

Butt, E., Pohler, D., Genieser, H.-G., Huggins, J.P., and Bucher, B. (1995). Inhibition of cyclic GMP-dependent protein kinase-mediated effects by (Rp)-8-bromo-PET-cyclic GMPS. Br.J.Pharmacol. *116*, 3110-3116.

Calabresi, P., Gubellini, P., Centonze, D., Sancesario, G., Morello, M., Giorgi, M., Pisani, A., and Bernardi, G. (1999). A critical role of the nitric oxide/cGMP pathway in corticostriatal long-term depression. J.Neurosci. *19*, 2489-2499.

Catterall, W.A. (1992). Cellular and molecular-biology of voltage-gated sodium channels. Physiol.Rev. *72*, S15-S48

Chen, C. and Thompson, R.F. (1995). Temporal specificity of long-term depression in parallel fiber-Purkinje synapses in rat cerebellar slice. Learning and Memory *2*, 185-198.

Chen, C.F. and Regehr, W.G. (1997). The mechanism of cAMP-mediated enhancement at a cerebellar synapse. J.Neurosci. *17*, 8687-8694.

Conquet, F., Bashir, Z.I., Davies, C.H., Daniel, H., Ferraguti, F., Bordi, F., Franz-Bacon, K., Reggiani, A., Matarese, V., Conde, F., Collingridge, G.L., and Crepel, F. (1994). Motor deficit and impairment of synaptic plasticity in mice lacking mGluR1. Nature *372*, 237-243.

Conti, M. and Catherine-Jin, S.L. (1999). The molecular biology of cyclic nucleotide phosphodiesterases. Prog.Nucleic Acid Res.Molec.Biol. *63*, 1-38.

Crepel, F. and Audinat, E. (1991). Excitatory amino acid receptors of cerebellar Purkinje cells; development and plasticity. Prog.Biophys.and Mol.Biol. *55*, 31-46.

Crepel, F., Audinat, E., Daniel, H., Hemart, N., Jaillard, D., Rossier, J., and Lambolez, B. (1994). Cellular locus of the nitric oxide-synthase involved in cerebellar long-term depression induced by high external potassium concentration. Neuropharm. *33*, 1399-1405.

Crepel, F. and Jaillard, D. (1990). Protein kinases, nitric oxide and long-term depression of synapses in the cerebellum. NeuroReport *1*, 133-136.

Crepel, F. and Krupa, M. (1988). Activation of protein kinase C induces a long-term depression of glutamate sensitivity of cerebellar Purkinje cells. An in vitro study. Brain Res. *458*, 397-401.

Cunningham, M.D. and Enna, S.J. (1996). Evidence for pharmacologically distinct GABA(B) receptors associated with cAMP production in rat brain. Brain Res. *720*, 220-224.

Curtis, D.R. and Johnson, G.A.R. (1974). Amino acid transmitters in the mammalian central nervous system. Ergeb.Physiol.Biochem.Exp.Pharmacol. *69*, 97-118.

Daniel, H., Hemart, N., Jaillard, D., and Crepel, F. (1992). Coactivation of metabotropic glutamate receptors and of voltage-gated calcium channels induces long-term depression in cerebellar Purkinje cells in vitro. Exp.Brain Res. *90*, 327-331.

Daniel, H., Hemart, N., Jaillard, D., and Crepel, F. (1993). Long-term depression requires nitric oxide and guanosine 3':5'cyclic monophosphate production in rat cerebellar Purkinje cells. Eur.J.Neurosci. *5*, 1079-1082.

Daniel, H., Levenes, C., and Crepel, F. (1998). Cellular mechanisms of cerebellar LTD. Trends Neurosci. *21*, 401-407.

Davies, C.H., Davies, S.N., and Collingridge, G.L. (1990). Paired-pulse depression of monosynaptic GABA-mediated inhibitory postsynaptic responses in rat hippocampus. J.Physiol.(Lond.) *424*, 513-531.

Debanne, D., Guerineau, N.C., Gahwiler, B.H., and Thompson, S.M. (1996). Paired-pulse facilitation and depression at unitary synapses in rat hippocampus - quantal fluctuation affects subsequent release. J.Physiol.(Lond.) *491*, 163-176.

DeSchutter, E. (1995). Cerebellar long-term depression might normalize excitation of Purkinje cells, a hypothesis. Trends Neurosci. *18*, 291-295.

DeZeeuw, C.I., Hansel, C., Bian, F., Koekkoek, S.E., VanAlphen, A.M., Linden, D.J., and Oberdick, J. (1998). Expression of a protein kinase C inhibitor in Purkinje cells

blocks cerebellar LTD and adaptation of the vestibulo-ocular reflex. Neuron *20*, 495-508.

Dolphin, A.C. (1987). Nucleotide binding-proteins in signal transduction and disease. Trends Neurosci. *10*, 53-57.

DuLac, S., Raymond, J.L., Sejnowski, T.J., and Lisberger, S. (1995). Learning and memory in the vestibular-ocular reflex. Annu.Rev.Neurosci. *18*, 409-441.

Eaton, S.A., Jane, D.E., Jones, P.J., Porter, R.P., Pook, P.C., Sunter, D.C., Udvarhelyi, P.M., Salt, T.E., and Watkins, J.C. (1993). Competitive antagonism at metabotropic receptors by (S)-4-carboxyphynylglycine and (RS)-alpha-methyl-4-carboxyphynylglycine. Eur.J.Pharmacol. *244*, 195-197.

Eccles, J.C., Ito M, and Szentagothai, J. (1967a). The Cerebellum as a Neuronal Machine (New York: Springer Verlag).

Eccles, J.C., Sasaki, K., and Strata, P. (1967b). Interpretation of the potential fields generated in the cerebellar cortex by a mossy fibre volley. Exp.Brain Res. *3*, 58-80.

Eilers, J., Augustine, G.J., and Konnerth, A. (1995). Subthreshold synaptic Ca^{2+} signalling in fine dendrites and spines of cerebellar Purkinje neurons. Nature *373*, 155-158.

Eilers, J. and Konnerth, A. (1997a). Dendritic signal integration. Curr.Opin.Neurobiol. *7*, 385-390.

Eilers, J., Takechi, H., Finch, E.A., Augustine, G.J., and Konnerth, A. (1997b). Local dendritic Ca^{2+} signaling induces cerebellar long-term depression. Learning & Memory *4*, 159-168.

Ekerot, C.F. and Kano, M. (1985). Long-term depression of parallel fiber synapses following stimulation of climbing fibers. Brain Res. *342*, 357-360.

Engert, F. and Bonhoeffer, T. (1997). Synapse specificity of long-term potentiation breaks down at short distances. Nature *388*, 279-284.

Ferrendelli, JA. (1978). Distribution and regulation of cyclic GMP in the central nervous system. Adv.Cyclic Nucleotide Res. *9*, 453-464.

Finch, E.A. and Augustine, G.J. (1998). Local calcium signalling by inositol-1,4, 5-trisphosphate in Purkinje cell dendrites. Nature *396*, 753-756.

Fitzsimonds, R.M., Song, H., and Poo, M. (1997). Propagation of activity-dependent synaptic depression in simple neural networks. Nature *388*, 439-448.

Freeman, J.H., Shi, T., and Schreurs, B.G. (1998). Pairing-specific long-term depression prevented by blockade of PKC or intracellular Ca^{2+}. NeuroReport *9*, 2237-2241.

Fukuto, J.M. and Mayer, B. (1996). The Enzymology of Nitric Oxide Synthase. In Methods in Nitric Oxide Research. M. Feelisch and J.S. Stamler, eds. (USA: John Wiley & Sons Ltd), pp. 147-160.

Furuichi, T., Yoshikawa, S., Miyawaki, A., Wada, K., Maeda, N., and Mikoshiba, K. (1989). Primary structure and functional expression of the inositol 1,4,5- trisphosphate-binding protein-p400. Nature *342* , 32-38.

Garthwaite, J. and Batchelor, J.M. (1996). A biplanar slice preparation for studying cerebellar synaptic transmission. J.Neurosci.Methods. *64*, 189-197.

Garthwaite, J. and Beaumont, P.S. (1989). Excitatory amino-acid receptors in the parallel fiber pathway in rat cerebellar slices. Neurosci.Lett. *107*, 151-156.

Garthwaite, J., Southam, E., Boulton, C.L., Nielson, E.B., Schmidt, K., and Mayer, B. (1995). Potent and selective-inhibition of nitric oxide-sensitive guanylyl cyclase by 1h-[1,2,4]oxadiazolo[4,3-a]quinoxalin-1-one. Mol.Pharmacol. *48*, 184-188.

Geilen, C.C., Wieprecht, M., Wieder, T., and Reutter, W. (1992). A selective inhibitor of cyclic amp-dependent protein-kinase, n-[2- Bromocinnamyl(Amino)Ethyl]-5-Isoquinolinesulfonamide (H-89), Inhibits phosphatidylcholine biosynthesis in hela-cells. FEBS Lett. *309*, 381-384.

Gemignani, A., Paudice, P., Bonanno, G., and Raiteri, M. (1994). Pharmacological discrimination between gamma-aminobutyric-acid type-B receptors regulating cholecystokinin and somatostatin release from rat neocortex synaptosomes. Mol.Pharmacol. *46*, 558-562.

Glaum, S.R., Traverse, S.N., Rossi, D.J., and Millar, R.J. (1992). Role of metabotropic glutamate (t-ACPD) receptors at the parallel fiber-Purkinje cell synapse. J.Neurophysiol. *64*, 1453-1462.

Gorcs, T.J., Penke, B., Boti, Z., Katarova, Z., and Hamori, J. (1993). Immunohistochemical visualization of metabotropic glutamate receptor. NeuroReport *4*, 283-286.

Hall, K.U., Collins, S.P., Gamm, D.M., Massa, E., DePaoliRoach, A.A., and Uhler, M.D. (1999). Phosphorylation-dependent inhibition of protein phosphatase-1 by G-substrate - A Purkinje cell substrate of the cyclic GMP-dependent protein kinase. J.Biol.Chem. *274*, 3485-3495.

Hamill, O.P., Marty, A., Neher, E., Sakmann, B., and Sigworth, F.J. (1981). Improved patch-clamp techniques for high-resolution current recording from cells and cell-free membrane patches. Pflugers Arch. *391*, 85-100.

Hartell, N.A. (1994a). cGMP acts within cerebellar Purkinje cells to produce long term depression via mechanisms involving PKC and PKG. NeuroReport *5*, 833-836.

Hartell, N.A. (1994b). Induction of cerebellar long term depression requires activation of glutamate metabotropic receptors. NeuroReport *5*, 913-916.

Hartell, N.A. (1996a). Inhibition of cGMP breakdown promotes the induction of cerebellar long-term depression. J.Neurosci. *16*, 2881-2890.

Hartell, N.A. (1996b). Strong activation of parallel fibers produces localized calcium transients and a form of LTD that spreads to distant synapses. Neuron *16*, 601-610.

Hashikawa, T., Nakazawa, K., Mikawa, S., Shima, H., and Nagao, M. (1995). Immunohistochemical localization of protein phosphatase isoforms in the rat cerebellum. Neurosci. *22*, 133-136.

Hashimoto, T. and Kuriyama, K. (1997). In vivo evidence that GABA(B) receptors are negatively coupled to adenylate cyclase in rat striatum. J.Neurochem. *69*, 365-370.

Hebb, D. (1949). The first stage of perception: Growth of the assembly. In The organisation of behaviour: A Neuropsychological theory. AnonymousUSA: John Wiley & Sons), pp. 60-78.

Hemart, N., Daniel, H., Jaillard, D., and Crepel, F. (1994). Properties of glutamate receptors are modified during long-term depression in rat cerebellar Purkinje cells. Neurosci. *19*, 213-221.

Hemart, N., Daniel, H., Jaillard, D., and Crepel, F. (1995). Receptors and second messengers involved in long-term depression in rat cerebellar slices in vita reappraisal. Eur.J.Neurosci. *7*, 45-53.

Hill, D.R. and Bowery, N.G. (1981). Baclofen-H-3 and H-3-GABA bind to bicuculline-insensitive GABA(B) sites in rat-brain. Nature *290*, 149-152.

Hirano, T. (1990). Synaptic transmission between rat inferior olivary neurones and cerebellar Purkinje cells in culture. J.Neurophysiol. *63*, 181-189.

Holscher, C. (1997). Nitric oxide, the enigmatic neuronal messenger: Its role in synaptic plasticity. Trends Neurosci. *20*, 298-303.

Honore, T., Davies, S.N., Drejer, J., Fletcher, E.J., Jacobsen, P., Lodge, D., and Nielsen, F.E. (1988). Quinoxalinediones - potent competitive non-NMDA glutamate receptor antagonists. Science *241*, 701-703.

Horn, R. and Marty, A. (1988). Muscarinic activation of ionic currents measured by a new whole-cell recording method. J.Gen.Physiol. *92*, 145-159.

Houk, J.C., Buckingham, J.T., and Barto, A.G. (1996). Models of the cerebellum and motor learning. Behav.Brain Sci. *19*, 368

Inoue, T., Kato, K., Kohda, K., and Mikoshiba, K. (1998). Type 1 inositol 1,4,5-trisphosphate receptor is required for induction of long-term depression in cerebellar Purkinje neurons. J.Neurosci. *18*, 5366-5373.

Ito, M. (1982). Cerebellar control of the vestibulo-ocular reflex around the flocculus hypothesis. Annu.Rev.Neurosci. *5*, 0-96.

Ito, M. (1989). Long-term depression. Annu.Rev.Neurosci. *12*, 85-102.

Ito, M. and Kano, M. (1982). Long-lasting depression of parallel fiber-Purjkinje cell transmission induced by conjunctive stimulation of parallel fibres and climbing fibers in the cerebellar cortex. Neurosci.Lett. *33*, 253-258.

Ito, M. and Karachot, L. (1992). Protein kinases and phosphatase inhibitors mediating long-term desensitization of glutamate receptors in cerebellar Purkinje cells. Neurosci. *14*, 27-38.

Ito, M., Sakurai, M., and Tongroach, P. (1982). Climbing fiber induced depression of both mossy fiber responsiveness and glutamate sensitivity of cerebellar Purkinje cells. J.Physiol.(Lond.) *324*, 113-134.

Kano, M. and Kato, M. (1987). Quisqualate receptors are specifically involved in cerebellar synaptic plasticity. Nature *325* , 276-279.

Kano, M. and Konnerth, A. (1992). Cerebellar Slices for Patch Clamp Recording. In Practical Electrophysiological Methods. H. Kettenmann and R. Grantyn, eds. (New York: Wiley-Liss, Inc.), pp. 54-57.

Karachot, L., Kado, R.T., and Ito, M. (1995). Stimulus parameters for induction of long-term depression in in vitro rat Purkinje cells. Neurosci.Res. *21*, 161-168.

Karbon, E.W. and Enna, S.J. (1985). Characterisation of the relationship between gamma-aminobutyric acid-B agonists and transmitter-coupled cyclic nucleotide-generating systems in rat-brain. Mol.Pharmacol. *27*, 53-59.

Kase, H., Iwahashi, K., Nakanishi, S., Matsuda, Y., Yamada, K., Takahashi, M., Murakata, C., Sato, A., and Kaneko, M. (1987). K-252 compounds, novel and potent inhibitors of protein-kinase-C and cyclic nucleotide-dependent protein-kinases. Biochem.Biophys.Res.Commun. *142*, 436-440.

Kashiwabuchi, N., Ikeda, K., Araki, Hirano, T., Shibuki, K., Takayama, C., Inoue, Y., Kutsuwasa, T., Yagi, T., Kang, Y., Aizawa, S., and Mishina, M. (1995). Impairment of

motor coordination, Purkinje cell synapse formation, and cerebellar long-term depression in GluRd2 mutant mice. Cell *91*, 43831-43831.

Kasono, K. and Hirano, T. (1994). Critical role of postsynaptic calium in cerebellar long-term depression. NeuroReport *6*, 17-20.

Kasono, K. and Hirano, T. (1995). Involvement of inositol trisphosphate in cerebellar long-term depression. NeuroReport *6*, 569-572.

Katz, B. and Miledi, R. (1968). The role of calcium in neuromuscular facilitation. J.Physiol.(Lond.) *195*, 481-492.

Kaupmann, K., Huggel, K., Heid, J., Flor, P.J., Bischoff, S., Mickel, S.J., McMaster, G., Angst, C., Bittiger, H., Froestl, W., and Bettler, B. (1997). Expression cloning of GABA(B) receptors uncovers similarity to metabotropic glutamate receptors. Nature *386*, 239-246.

Kelm, M. and Yoshida, K. (1996). Metabolic Fate of Nitric Oxide and Related N-oxides. In Methods in Nitric Oxide Research. M. Feelisch and J.S. Stamler, eds. (John Wiley & Sons Ltd), pp. 47-58.

Kimura, S., Uchiyama, S., Takahashi, H.E., and Shibuki, K. (1998). cAMP-dependent long-term potentiation of nitric oxide release from cerebellar parallel fibers in rats. J.Neurosci. *18*, 8551-8558.

Knight, A.R. and Bowery, N.G. (1996). The pharmacology of adenylyl-cyclase modulation by GABA(B) Receptors in rat-brain slices. Neuropharm. *35*, 703-712.

Konnerth, A., Dreessen, J., and Augustine, G.J. (1992). Brief dendritic calcium signals initiate long-lasting synaptic depression in cerebellar Purkinje cells. Proc.Natl.Acad.Sci.USA *89*, 7051-7055.

Konnerth, A., Llano, I., and Armstrong, C.M. (1990). Synaptic currents in cerebellar Purkinje cells. Proc.Natl.Acad.Sci.USA *87*, 2662-2665.

Kose, A., Saito, N., Ito, H., Kikkawa, U., Nishizuka, Y., and Tanaka, C. (1988). Electron microscopic localization of type I protein kinase C in rat Purkinje cells. J.Neurosci. *8*, 4262-4268.

Lambolez, B., Audinat, E., Bochet, P., Crepel, F., and Rossier, J. (1992). AMPA receptor subunits expressed by single Purkinje cells. Neuron *9*, 247-258.

Lechner, H.A. and Byrne, J.H. (1998). New perspectives on classical conditioning: A synthesis of Hebbian and non-Hebbian mechanisms. Neuron *20*, 355-358.

Lev Ram, V., Jiang, T., Wood, J., Lawrence, D.S., and Tsien, R. (1997). Synergies and coincidence requirements between NO, cGMP, and Ca^{2+} in the induction of cerebellar long-term depression. Neuron *18*, 1025-1038.

Lev Ram, V., Makings, L.R., Keitz, P.F., Kao, J.Y., and Tsien, R.Y. (1995). Long-term depression in cerebellar Purkinje neurons results from coincidence of nitric oxide and depolarization-induced Ca^{2+} transients. Neuron *15*, 407-415.

Li, C. and McIlwain, H. (1957). Maintenance of resting membrane potentials in slices of mammalian cerebral cortex and other tissues *in vitro*. J.Physiol.(Lond.) *139*, 178-190.

Liljelund, P. and Levine, J.M. (1998). Dynamic behavior of the ends of growing parallel fibers in early postnatal rat cerebellum. J.Neurobiol. *36*, 91-104.

Linden, D.J. (1994a). Input-specific induction of cerebellar Long-term depression does not require presynaptic alteration. Learning and Memory *1*, 121-128.

Linden, D.J. (1994b). Long-term synaptic depression in the mammalian brain. Neuron *12*, 457-472.

Linden, D.J. (1995). Phospholipase A2 controls the induction of short-term versus long-term depression in the cerebellar Purkinje neuron in culture. Neuron *15*, 1393-1401.

Linden, D.J. (1996). A protein synthesis-dependent late phase of cerebellar long-term depression. Neuron *17*, 483-490.

Linden, D.J. and Connor, J.A. (1991). Participation of postsynaptic PKC in cerebellar long-term depression in culture. Science *254*, 1656-1659.

Linden, D.J. and Connor, J.A. (1992). Long-term depression of glutamate currents in cultured cerebellar Purkinje neurons does not require nitric oxide signalling. Eur.J.Neurosci. *4*, 10-15.

Linden, D.J. and Connor, J.A. (1995a). Long-term synaptic depression. Annu.Rev.Neurosci. *18*, 319-357.

Linden, D.J., Dawson, T.M., and Dawson, V.L. (1995b). An evaluation of the nitric oxide/cGMP-dependent protein kinase cascade in the induction of cerebellar long-term depression in culture. J.Neurosci. *15*, 5098-5105.

Linden, D.J., Dickenson, M.H., Smeyne, M., and Connor, J.A. (1991). A long-term depression of AMPA currents in cultured cerebellar Purkinje neurons. Neuron *7*, 81-89.

Linden, D.J., Smeyne, M., and Connor, J.A. (1993). Induction of cerebellar long-term depression in culture requires postsynaptic action of sodium ions. Neuron *11*, 1093-1110.

Lisberger, S.G. (1998). Physiologic basis for motor learning in the vestibulo-ocular reflex. Otolaryngol.Head Neck Surg. *119*, 43-48.

Llano, I., DiPolo, R., and Marty, A. (1994). Calcium-induced calcium release in cerebellar Purkinje cells. Neuron *12*, 663-673.

Llinas, R., Walton, K., Hillman, D.E., and Sotelo, C. (1975). Inferior Olive; its role in motor learning. Science *190*, 1230-1231.

Maren, S. and Baudry, M. (1995). Properties and mechanisms of long-term synaptic plasticity in the mammalian brain - relationships to learning and memory. Neurobiol.Learn.Mem. *63*, 1-18.

Marr, D. (1969). A theory of cerebellar cortex. J.Physiol.(Lond.) *202*, 437-470.

Martin, L.J., Blackstone, C.D., Huganir, R.L., and Price, D.L. (1992). Cellular localization of a metabotropic glutamate receptor in rat brain. Neuron *9*, 259-270.

Matsuoka, I., Giulli, G., Poyard, M., Stengel, D., Parma, J., Guallaen, G., and Hanoune, J. (1992). Localization of adenyl and guanylyle cyclase in rat brain by *in situ* hybridization: Comparison with calmodulin mRNA distribution. J.Neurosci. *12*, 3350-3360.

Mikoshiba, K. (1997). The InsP(3) receptor and intracellular Ca^{2+} signaling. Curr.Opin.Neurobiol. *7*, 339-345.

Milner, B., Squire, L.R., and Kandel, E.R. (1998). Cognitive neuroscience and the study of memory. Neuron *20*, 445-468.

Möhler, H. and Fritschy, J-M. (1999). $GABA_B$ receptors make it to the top – as dimers. Trends Pharmacol. Sci *20,* 87-89.

Moore, P.K. and Handy, R.C. (1997). Selective inhibitors of neuronal nitric oxide synthase - Is no NOS really good NOS for the nervous system? Trends Pharmacol.Sci *18*, 204-211.

Morishita, W. and Sastry, B.R. (1995). Pharmacological characterization of pre-and postsynaptic GABA(B) Receptors in the deep nuclei of rat cerebellar slices. Neurosci. *68*, 1127-1137.

Nairn, A.C., Hemmings, H.C., and Greengard, P. (1985). Protein kinases in the brain. Annu.Rev.Biochem. *54*, 931-976.

Nakanishi, S. (1989). K-252-derivatives - K252a, K252b, KT5720, KT5962, KT5823. Seitaino-Kagaku *40*, 364-365.

Nakanishi, S. (1994). Metabotropic glutamate receptors - synaptic transmission, modulation, and plasticity. Neuron *13*, 1031-1037.

Nakazawa, K., Mikawa, S., and Ito, M. (1998). Persistent phosphorylation parallels long-term desensitization of cerebellar Purkinje cell AMPA-type glutamate receptors. Learning & Memory *3*, 578-591.

Neher, E. (1992). Ion channels for communication between and within cells (Nobel lecture). Neuron *8*, 605-612.

Nicholson, C. and Freeman, J.A. (1974). Theory of current source-density analysis and determination of conductivity tensor for anuran cerebellum. J.Neurophysiol. *38*, 356-368.

Nicholson, C. and Llinas, R. (1975). Real time current source-density analysis using multi-electrode array in cat cerebellum. Brain Res. *100*, 418-424.

Nolte, J. (1988). Cerebellum. In The Human Brain. S. Bircher, ed. (St Louis: The C.V. Mosby Company), pp. 313-334.

Oscarsson, O. (1979). Functional units of the cerebellum - sagittal zones and microzones. Trends Neurosci. *2*, 143-145.

Palay, S.L. and Chan-Palay, V. (1974). Cerebellar cortex: Cytology and organization (New York: Springer Verlag).

Plant, T., Eilers, J., and Konnerth, A. (1996). Ca^{2+} signals underlying synaptic plasticity in cerebellar Purkinje cells. Semin.Neurosci. *8*, 271-279.

Qian, H.H. and Dowling, J.E. (1994). Pharmacology of novel GABA receptors found on rod horizontal cells of the white perch retina. J.Neurosci. *14*, 4299-4307.

Rae, J., Cooper, K., Gates, P., and Watsky, M. (1991). Low access resistance perforated patch recordings using amphotericin B. J.Neurosci.Methods. *37*, 15-26.

Rosemund, C., Legendre, P., and Westbrook, G.L. (1992). Expression of NMDA channels on cerebellar purkinje-cells acutely dissociated from newborn rats. J.Neurophysiol. *68*, 1901-1905.

Ross, W.N. and Werman, R. (1987). Mapping calcium transients in the dendrites of purkinje-cells from the guinea-pig cerebellum invitro. J.Physiol.(Lond.) *389*, 319-336.

Sabatini, B.L. and Regehr, W.G. (1997). Control of neurotransmitter release by presynaptic waveform at the granule cell to Purkinje cell synapse. J.Neurosci. *17*, 3425-3435.

Saito, N., Kikkawa, U., Nishizuka, Y., and Tanaka, C. (1988). Distribution of protein kinase C-like immunoreactive neurons in rat brain. J.Neurosci. *8*, 369-382.

Sakurai, M. (1990). Calcium is an intracellular mediator of the climbing fibre induction of cerebellar long-term depression. Proc.Natl.Acad.Sci.USA *87*, 3383-3385.

Salin, P.A., Malenka, R.C., and Nicoll, R.A. (1996). Cyclic-AMP mediates a presynaptic form of LTP at cerebellar parallel fiber synapses. Neuron *16*, 797-803.

Schoepp, D.D. and Conn, P.J. (1993). Metabotropic glutamate receptors in brain function and pathology. Trends Pharmacol.Sci. *14*, 13-20.

Schreurs, B.G. and Alkon, D.L. (1993). Rabbit cerebellar slice analysis of long-term depression and its role in classical conditioning. Brain Res. *631*, 23-240.

Schulz, S., Yuen, P.T., and Garbers, D.L. (1991). The expanding family of guanylyl cyclases. Trends Pharmacol.Sci. *12*, 116-120.

Sejnowski, T.J. (1999). The book of Hebb. Neuron *24*, 773-776.

Shibuki, K., Gomi, H., Chen, L., Bao, S.W., Kim, J.K., Wakatsuki, H., Fujisaki, T., Fujimoto, J., Katoh, A., Ikeda, T., Chen, C., Thompson, R.F., and Itohara, S. (1996). Deficient cerebellar long-term depression, impaired eyeblink conditioning, and normal motor coordination in GFAP mutant mice. Neuron *16*, 587-599.

Shibuki, K. and Kimura, S. (1997). Dynamic properties of nitric oxide release from parallel fibres in rat cerebellar slices. J.Physiol.(Lond) *498*, 443-452.

Shibuki, K. and Okada, D. (1991). Endogenous nitric oxide release required for long-term synaptic depression in the cerebellum. Nature *349*, 326-328.

Shibuki, K. and Okada, D. (1992a). Cerebellar long-term potentiation under surpressed postsynaptic Ca^{2+} activity. NeuroReport *3*, 231-234.

Shibuki, K. and Okada, D. (1992b). Roles of nitric oxide in cerebellar synaptic plasticity. In Neuroreceptors, Ion channels and the brain. N. Kawai, ed. (Elsevier Science), pp. 161-169.

Shigemoto, R., Abe, T., Nomura, S., Nakanishi, S., and Hirano, T. (1994). Antibodies inactivating mGluR1 metabotropic glutamate receptor block long-term depression in cultured Purkinje cells. Neuron *12*, 1245-1255.

Simpson, J.I., Wylie, D.R., and DeZeeuw, C.I. (1996). On climbing fiber signals and their consequence(s). Behav.Brain Sci. *19*, 384

Sitsapesan, R., Mcgarry, S.J., and Williams, A.J. (1995). Cyclic ADP-ribose, the ryanodine receptor and Ca^{2+} release. Trends Pharmacol.Sci. *16*, 386-391.

Sotelo, C., Hillman, D.E., Zamora, A.J., and Llinas, R. (1975). Climbing fiber deafferentation; its action on Purkinje cell dendritic spines. Brain Res. *98*, 574-581.

Southam, E. and Garthwaite, J. (1991). Climbing fibres as a source of nitric oxide in the cerebellum. Eur.J.Neurosci. *3*, 379-382.

Southam, E., Morris, R., and Garthwaite, J. (1992). Sources and targets of nitric oxide in rat cerebellum. Neurosci. *137*, 241-244.

Sutton, N.G. (1971). The Cerebellum. In Anatomy of the Brain and Spinal Medulla: a manual for students. N.G. Sutton, ed. (London: Butterworth & Co. Publishers Ltd.), pp. 85-97.

Takechi, H., Eilers, J., and Konnerth, A. (1998). A new class of synaptic response involving calcium release in dendritic spines. Nature *396*, 757-760.

Thompson, J.W. (1991). Cyclic nucleotide phosphodiesterases: Pharmacology, biochemistry and function. Pharmac.Ther. *51*, 13-33.

Thompson, R.F. (1986). The neurobiology of learning and memory. Science *233*, 941-947.

Thompson, R.F., Bao, S., Chen, L., Cipriano, B.D., Grethe, J.S., Kim, J.J., Thompson, J.K., Tracy, J.A., Weninger, M.S., and Krupa, D.J. (1997). Associative Learning. Int.Rev.Neurobiol. *41*, 151-189.

Usowicz, M.M., Sugimori, M., Chersky, B., and Llinas, R. (1992). P-type calcium channels in the somata and dendrites of adult cerebellar Purkinje cells. Neuron *9*, 1185-1199.

Vigot, R. and Batini, C. (1997). GABA(B) receptor activation of Purkinje cells in cerebellar slices. Neurosci.Res. *29*, 151-160.

Vigot, R., Billard, J.M., and Batini, C. (1993). Reduction of GABA inhibition in Purkinje and cerebellar nuclei neurons in climbing fiber deafferented cerebella of rat. Neurosci.Res. *17*, 249-255.

Vincent, S.R. (1996). Nitric oxide and synaptic plasticity: NO news from the cerebellum. Behav.Brain Sci. *19*, 362

Vincent, S.R. and Kimura, H. (1992). Histochemical mapping of nitric-oxide synthase in the rat-brain. Neurosci. *46*, 755-784.

Voogd, J. (1992). The morphology of the cerebellum; the last 25 years. Eur.J.Morphology *30*, 81-96.

Voogd, J. and Glickstein, M. (1998). The anatomy of the cerebellum. Trends Neurosci. *21*, 370-375.

Wagemann, E., Schmidtkastner, R., Block, F., and Sontag, K.H. (1995). Altered pattern of immunohistochemical staining for glial fibrillary acidic protein (GFAP) in the forebrain and cerebellum of the mutant spastic rat. J.Chem.Neuroanat. *8*, 151-163.

Walter, U. and Greengard, P. (1981). Cyclic AMP-dependent and cyclic GMP-dependent protein kinases of nervous tissues. Curr.Topics Cell.Reg. *19*, 219-256.

Walton, P.D., Airey, J.A., Sutko, J.L., Beck, C.F., Mignery, G.A., Sudhof, T.C., Deerinck, T.J., and Ellisman, M.H. (1991). Ryanodine and inositol trisphosphate receptors coexist in avian cerebellar Purkinje neurons. J.Cell Biol. *113*, 1145-1157.

Wang, X. and Robinson, P.J. (1997). Cyclic GMP-dependent protein kinase and cellular signaling in the nervous system. J.Neurochem. *68*, 443-456.

Wilkin, G.P., Hudson, A.L., Hill, D.R., and Bowery, N.G. (1981). Autoradiographic localization of GABA(B) receptors in rat cerebellum. Nature *294*, 584-587.

Willmott, N., Sethi, J.K., Walseth, T.F., Lee, H.C., White, A.M., and Galione, A. (1996). Nitric oxide-induced mobilization of intracellular calcium via the cyclic ADP-ribose signaling pathway. J.Biol.Chem. *271*, 3699-3705.

Wojcik, W.J. and Neff, N.H. (1984). Gamma-aminobutyric acid B-receptors are negatively coupled to adenylate-cyclase in brain, and in the cerebellum these receptors may be associated with granule cells. Mol.Pharmacol. *25*, 24-28.

Wood, J.S., Yan, X.W., Mendelow, M., Corbin, J.D., Francis, S.H., and Lawrence, D.S. (1996). Precision substrate targeting of protein-kinases - the cGMP- and cAMP-dependent protein-kinases. J.Biol.Chem. *271*, 174-179.

Yoon, K.W., Covey, D.F., and Rothman, S.M. (1993). Multiple mechanisms of picrotoxin block of GABA-induced currents in rat hippocampal-neurons. J.Physiol.(Lond.) *464*, 423-439.

Zagrebelsky, M., Strata, P., Hawkes, R., and Rossi, F. (1997). Reestablishment of the olivocerebellar projection map by compensatory transcommissural reinnervation following unilateral transection of the inferior cerebellar peduncle in the newborn rat. J.Comp.Neurol. *379*, 283-299.

Zhuo, M. and Hawkins, R.D. (1995). Long-term depression a learning-related type of synaptic plasticity in the mammalian central nervous system. Rev.Neurosci. *6*, 259-277.